



# UNIVERSITÀ DEGLI STUDI DI TRIESTE

## XXVIII CICLO DEL DOTTORATO DI RICERCA IN INGEGNERIA E ARCHITETTURA INDIRIZZO IN INGEGNERIA DELL'INFORMAZIONE

### VOLTAGE CONTROL SYSTEMS FOR TRANSMISSION AND DISTRIBUTION GRIDS

Settore scientifico-disciplinare: ING-IND/32

DOTTORANDO  
**RICCARDO CAMPANER**

COORDINATORE  
**PROF. ROBERTO VESCOVO**

A handwritten signature in black ink that reads "Roberto Vescovo".

SUPERVISORE DI TESI  
**PROF. GIORGIO SULLIGOI**

A handwritten signature in black ink that reads "Giorgio Sulligoi".

CO-SUPERVISORE DI TESI  
**PROF. MASSIMILIANO CHIANDONE**

A handwritten signature in black ink that reads "Massimiliano Chiandone".

ANNO ACCADEMICO 2015/2016



*Dedicated to my family*



# Abstract

---

## ▪ *Sommario*

L'attività di ricerca condotta durante il Dottorato ha riguardato l'analisi delle sempre più evidenti e diffuse problematiche legate ai cospicui livelli di generazione distribuita (GD) connessa alle reti elettriche di trasmissione e distribuzione.

Essa ha anche incluso la proposta di tecniche di controllo performanti ed effettivamente applicabili, utili per accogliere la generazione da fonti energetiche rinnovabili (FER) e garantire al contempo il mantenimento di livelli adeguati di affidabilità e qualità del servizio.

In particolare gli studi si sono focalizzati sul tema del controllo della tensione per impianti di GD basati su FER, sia allacciati a reti di distribuzione in media (MT) e bassa tensione (BT) che connessi direttamente alla rete di trasmissione in alta tensione (AT).

Per fornire un quadro d'insieme, di seguito, si riporta una breve sintesi dei diversi capitoli di cui l'elaborato si compone:

- Nel 1° Capitolo si descrive l'architettura tipica dei sistemi elettrici di potenza, il relativo cambiamento in atto dal tradizionale paradigma di produzione dell'energia verso il modello a generazione distribuita e le problematiche che si stanno manifestando a causa di tale cambiamento. Per dare un'idea della dimensione del fenomeno si forniscono alcuni dati sulla quantità di GD installata negli ultimi anni a livello internazionale e nazionale nonché i risultati di studi sulla convenienza economica ed energetica della tecnologia fotovoltaica, condotti al fine di poterne valutare i futuri impatti sui sistemi di distribuzione dell'energia.
- Nel 2° Capitolo si tracciano le caratteristiche che deve presentare una "Smart Grid" (rete elettrica in cui vi è una forte integrazione di tecnologie di informazione e comunicazione – ICT), idonea ad accogliere la generazione da fonte rinnovabile e non programmabile e garantire al contempo il mantenimento di livelli adeguati di affidabilità e qualità del servizio. Nello stesso capitolo si sintetizza il panorama normativo europeo e italiano, regolante la connessione di generazione distribuita a reti di distribuzione e trasmissione elettrica.
- Nel 3° Capitolo si concentra l'attenzione sul tema del controllo della tensione per impianti di GD basati su FER. In tale capitolo si riporta una rassegna delle tecniche di controllo proposte in letteratura e dalle recenti regole di connessione, nonché le tecniche di controllo elaborate e proposte dal nostro gruppo di ricerca.
- Nel 4° Capitolo vengono presentati i risultati degli studi condotti su alcune reti elettriche di test sia presenti nella letteratura scientifica che realmente esistenti.

- Nel 5° Capitolo si riportano infine alcune considerazioni conclusive.
- L'Appendice A1 fornisce una descrizione degli strumenti informatici utilizzati per condurre le simulazioni. In particolare i test sono stati condotti con l'ausilio del software Matlab®, il toolbox open source PSAT ed il software DOME per la realizzazione di simulazioni a regime e in dinamica.

- *Summary*

The research activities carried out for the present PhD dissertation concerns the increasingly evident and widespread set of problems related to the remarkable levels of distributed generation (DG) connected to transmission and distribution grids.

It has also included the proposal of applicable and performing control techniques, suitable to allow new connection of Renewable Energy Sources (RES) generators, able to assure adequate reliability and quality of service.

The focus of the research activity was directed to voltage control of DG units based on RES, both connected to low voltage (LV) and medium voltage (MV) distribution networks and the ones directly connected to high voltage (HV) transmission system.

A short summary of the different chapters provides an overview of the present work:

- Chapter 1 describes the typical architecture of power electric systems, the on-going change from the traditional paradigm of energy production towards the DG model and the problems deriving from such change. To provide an idea of the dimension of the phenomenon some data about DG installed in the latest years both at international and national level are given, together with the results of studies on the economic and energetic advantage of photovoltaic technology carried out in view of a possible assessment of future impacts on energy distribution systems.
- Chapter 2 outlines the features of a Smart Grid (an electric network with a strong integration of Information and Communication Technologies - ICT), apt to receive RES generation, at the same time guaranteeing suitable levels of reliability and quality service. The chapter summarizes the European and Italian Regulatory Environment for the connection of DG to distribution networks and electric transmission.
- Chapter 3 concentrates on voltage control for DG plants based on RES. The chapter reports a review of the control techniques proposed by literature and by recent connection rules, together with the control techniques collected and proposed by our research group.
- Chapter 4 presents the results of the studies carried out on some test electric networks presented in scientific literature and some really existing ones.
- Chapter 5 reports some final considerations.
- Appendix A1 provides a description of the software tools used to carry out the simulations. More specifically tests have been conducted with the aid of Matlab@ software, the toolbox open source PSAT and DOME software for steady state and dynamic simulations.



# Index

---

INDEX	I
LIST OF FIGURES	V
LIST OF TABLES	XI
GLOSSARY	XV
INTRODUCTION	1
CHAPTER 1. POWER ELECTRIC SYSTEMS	5
1.1 TRANSMISSION NETWORKS (HV, VHV)	7
1.2 DISTRIBUTION NETWORKS (MV, LV)	8
1.2.1 <i>The fit &amp; forget approach in distribution networks</i>	8
1.3 DISTRIBUTED GENERATION AND ACTIVE NETWORKS	9
1.3.1 <i>RES in the World</i>	10
1.3.2 <i>RES in Europe</i>	12
1.3.3 <i>RES in Italy</i>	13
1.3.3.1 Hydroelectric Energy in Italy	14
1.3.3.2 Wind Energy in Italy	15
1.3.3.3 Photovoltaic Energy in Italy	16
1.3.3.3.1 Assessment of Photovoltaic Systems for Electric Power Generation using EROEI (Energy Return On Energy Investment)	19
1.3.3.3.2 Evolution of the main economic parameters for photovoltaic plants installed in Italy	21
1.4 RECENT CHANGES IN ELECTRICAL SYSTEMS	29
1.4.1 <i>Problems and open issues of DG</i>	29
1.4.1.1 Issues related to electrical markets and dispatching	30
1.4.1.2 Weakening of reactive power capability	32
1.4.1.3 Stability of power electric systems	33
1.4.1.4 Formation of undesired islands	33
1.4.1.5 Power flow inversion and voltage profile changes	35
1.4.1.6 Increase of fault currents	36

---

1.4.1.7	Selectivity of protections	36
1.4.2	<i>Positive aspects and opportunities related to DG</i>	37
1.4.2.1	Impact of DG on power losses on a real-world distribution network	39
<b>CHAPTER 2.</b>	<b>THE EVOLUTION OF THE NETWORK TOWARDS SMART GRIDS</b>	<b>43</b>
2.1	THE FUTURE OF THE DISTRIBUTION NETWORK – THE NEW ROLE OF DSO	46
2.2	REGULATORY ENVIRONMENT, OPERATION AND SECURITY OF THE ELECTRIC SYSTEMS WITH DG	48
2.2.1	<i>European regulatory environment</i>	48
2.2.1.1	Technical specifications regulating DG connections	53
2.2.2	<i>Italian regulatory environment</i>	56
2.2.2.1	Regulations for distribution networks	56
2.2.2.1.1	Interface Protection System in line with system requirements	58
2.2.2.1.2	Taking part in defense plans	60
2.2.2.1.3	LVFRT (Low Voltage Fault Ride Through)	62
2.2.2.1.4	Voltage control	63
2.2.2.1.5	Generated active power limitation	63
2.2.2.2	Regulations for HV transmission network	65
<b>CHAPTER 3.</b>	<b>VOLTAGE CONTROL OF DISTRIBUTED GENERATION</b>	<b>69</b>
3.1	QUALITATIVE CONSIDERATIONS FOR DIFFERENT VOLTAGE LEVELS	69
3.1.1	<i>HV transmission lines</i>	71
3.1.2	<i>MV and LV distribution lines</i>	72
3.1.3	<i>Quantitative considerations</i>	73
3.2	VOLTAGE CONTROL TECHNIQUES FOR DGs CONNECTED TO MV AND LV DISTRIBUTION NETWORKS	75
3.2.1	<i>The voltage rise phenomenon in distribution networks</i>	75
3.2.2	<i>Reduction of active power injected by DGs</i>	77
3.2.3	<i>Adaptation or reconfiguration of the distribution network</i>	77
3.2.4	<i>Voltage reduction in primary substation</i>	77
3.2.5	<i>DG reactive power regulation</i>	78

3.2.6	<i>Control techniques proposed in Italy by the recent connection rules (CEI 0-16 CEI 0-21)</i>	80
3.2.7	<i>A proposed control technique based on the network linearization</i>	82
3.2.7.1	Choice of control nodes	84
3.3	VOLTAGE CONTROL TECHNIQUES FOR RES PRODUCTION POWER PLANTS	
	DIRECTLY CONNECTED TO HV TRANSMISSION NETWORK	85
3.3.1	<i>HV voltage control in Italy</i>	86
3.3.2	<i>Proposed control technique</i>	90
3.3.2.1	Definition and calculation	90
3.3.2.2	Voltage control scheme	93
3.3.2.3	Dynamic Decoupling matrix	95
3.3.2.4	Traditional power plant	100
<b>CHAPTER 4. CASE STUDIES AND RESULTS</b>		<b>105</b>
4.1	CASE STUDIES FOR POWER GENERATION PLANTS CONNECTED TO THE MV AND LV DISTRIBUTION NETWORKS	105
4.1.1	<i>Application of control techniques proposed in Italy by the recent connection rules (CEI 0-16 CEI 0-21)</i>	105
4.1.1.1	IEEE 37-bus	105
4.1.1.2	Actual real-world distribution network	110
4.1.2	<i>Application of the centralized control technique proposed</i>	115
4.1.3	<i>Concluding considerations on voltage control techniques for DGs connected to MV and LV distribution networks</i>	119
4.2	CASE STUDIES OF POWER GENERATION PLANTS DIRECTLY CONNECTED TO THE HV TRANSMISSION NETWORK	120
4.2.1	<i>Photovoltaic case</i>	121
4.2.2	<i>Wind farm case</i>	125
4.2.3	<i>Hydroelectric case</i>	129
4.2.4	<i>Virtual Power Plant case: a MV distribution network with several generators types</i>	135
4.2.5	<i>Propaedeutic studies for the experimental implementation of the proposed control technique to a 72,6 MWp PV power plant</i>	139

---

4.2.6	<i>Concluding considerations on the proposed voltage control technique for RES production power plants directly connected to HV transmission network</i>	148
<b>CHAPTER 5.</b>	<b>CONCLUSIONS</b>	<b>149</b>
<b>APPENDIX A1.</b>	<b>SOFTWARE TOOLS USED</b>	<b>151</b>
A1.1	PSAT - POWER SYSTEM ANALYSIS TOOLBOX	151
A1.2	DOME	155
<b>BIBLIOGRAPHY</b>		<b>157</b>

# List of Figures

---

<i>Figure 1 - Centralized and Distributed Generation [16]</i>	3
<i>Figure 2 - Electrical System Architecture [18]</i>	5
<i>Figure 3 - Daily Electricity Demand - 02/01/2016 [19]</i>	6
<i>Figure 4 - Interconnected Network of Continental Europe [21]</i>	7
<i>Figure 5 - Power Flow Inversions Average in Enel Distribuzione's primary substations [25]</i>	10
<i>Figure 6 - World Final Energy Consumption by Region [Mtoe] [26]</i>	10
<i>Figure 7 - World Electricity Generation by Fuel (TWh) [26]</i>	11
<i>Figure 8 - Gross Electricity Generation By Fuel in EU-28 - 1990-2014 (TWh) [26]</i>	12
<i>Figure 9 - Gross RES Electricity Generation By Fuel in EU-28 - 1990-2014 (TWh) [26]</i>	12
<i>Figure 10 - Evolution of the installed RES power plants in Italy [27]</i>	13
<i>Figure 11 - Evolution of hydroelectric power plants in Italy [28] [29]</i>	14
<i>Figure 12 - Evolution of wind power plants in Italy [28] [29]</i>	15
<i>Figure 13 - Average size of wind farms from 2000 to 2014 [28] [29]</i>	15
<i>Figure 14 - Power of photovoltaic systems in main countries at the end of 2015 [31]</i>	16
<i>Figure 15 - Evolution of power and number of photovoltaic plants in Italy [31] [32]</i>	17
<i>Figure 16 - Evolution of the average power of photovoltaic plants in Italy [31] [32]</i>	17
<i>Figure 17 - Photovoltaic plants in Italy for voltage level at the end of 2015 [31]</i>	18
<i>Figure 18 - Production of photovoltaic plants in Italy [31] [32]</i>	18
<i>Figure 19 - Comparison of EROEI among new and traditional PV technologies [37]</i>	20
<i>Figure 20 - Yearly installed power in the Italian market</i>	21
<i>Figure 21 - Cash flow analysis over 30 years of operation for a 3kWp PV plant installed in 2014 in Rome (Grid parity scenario, NO incentives)</i>	26
<i>Figure 22 - Cash flow analysis over 30 years of operation for a 3kWp PV plant installed in 2014 in Rome (Grid parity scenario - 50% tax-deduction)</i>	26
<i>Figure 23 - Cash flow analysis over 30 years of operation for a 3kWp PV plant installed in 2014 in Rome (Grid parity scenario - 100% self-consumption - NO incentives)</i>	27
<i>Figure 24 - Evolution of the Levelized Cost Of Energy in the Italian market over the period 2003-2014</i>	28
<i>Figure 25 - Ratio between average hourly SNP and overall average SNP [24]</i>	30

---

<i>Figure 26 - Trend of the net efficiency of the Italian production power plants [24]</i>	31
<i>Figure 27 - Comparison between the situation in April 2010 and April 2015 (monthly average values) [24]</i>	32
<i>Figure 28 - SUD Zone in April 2015 (working days) [24]</i>	32
<i>Figure 29 - Distribution network operating in island [74]</i>	34
<i>Figure 30 - a) power flow goes from primary station towards passive users; b) in presence of DG the power flow may be inverted [74]</i>	35
<i>Figure 31 - Distribution network voltage profile with or without DG presence [74]</i>	35
<i>Figure 32 - Untimely disconnection on a safe line in DG presence</i>	36
<i>Figure 33 - Simple test network (i.e. generator in position 3)</i>	38
<i>Figure 34 - Power losses as a function of DG position.</i>	38
<i>Figure 35 - Actual LV distribution network used in the case study</i>	40
<i>Figure 36 - Change in the optimization paradigm of the whole electric system: generation and load controlled (orange) and uncontrolled (grey) [92]</i>	43
<i>Figure 37 - Smart Grid Model [93]</i>	44
<i>Figure 38 - Active power frequency response capability of power-generating modules [115]</i>	51
<i>Figure 39 - U-Q/Pmax-profile of a synchronous power-generating module [115]</i>	51
<i>Figure 40 - Fault-ride-through profile of a power-generating module [115]</i>	52
<i>Figure 41 - Sending of the signal from the primary station to users [74]</i>	58
<i>Figure 42 - Functioning logic for the activation of the threshold of relay [138]</i>	59
<i>Figure 43 - Logic Flow [140]</i>	60
<i>Figure 44 - System Architecture [140]</i>	61
<i>Figure 45 - LVFRT curve for LV distribution networks [137]</i>	62
<i>Figure 46 - Curve of active power reduction in over frequency for LV distribution networks [137]</i>	64
<i>Figure 47 - Curve of active power reduction in over frequency [133]</i>	65
<i>Figure 48 - LVFRT curve for PV power plants [133]</i>	66
<i>Figure 49 - LVFRT curve for wind power plants [142]</i>	66
<i>Figure 50 - Capability curve for PV inverters [133]</i>	67
<i>Figure 51 - Local logic Q=f(V) [133]</i>	67
<i>Figure 52 - Equivalent single-phase model</i>	69

---

<i>Figure 53 - Double Bipole Representation</i>	70
<i>Figure 54 – Perrine-Baum Diagram for a HV network</i>	71
<i>Figure 55 - Equivalent single-phase model for a MV or LV distribution network</i>	72
<i>Figure 56 - Perrine-Baum Diagram for a MV or LV distribution network</i>	72
<i>Figure 57 - Line connecting two buses [151]</i>	75
<i>Figure 58 - Voltage profiles for a MT grid with and without DG [152]</i>	76
<i>Figure 59 - Local Control [151]</i>	78
<i>Figure 60 - Centralized control [151]</i>	78
<i>Figure 61 - Power factor control law [138]</i>	80
<i>Figure 62 - Reactive power factor control [138]</i>	81
<i>Figure 63 - Schematic diagram of the voltage control hierarchical system [73]</i>	86
<i>Figure 64 - Identification of pilot nodes in Italy [185]</i>	87
<i>Figure 65 - Block Diagram of SART [73]</i>	88
<i>Figure 66 - Typical topology of a RES power plant connected to the HV level</i>	90
<i>Figure 67 - Synoptic schema of Secondary Voltage Control</i>	93
<i>Figure 68 - Distributed Generator model</i>	94
<i>Figure 69 - Topology of plant A</i>	95
<i>Figure 70 - Topology of plant B</i>	96
<i>Figure 71 - Reactive power response without Dynamic Decoupling matrix: network A</i>	98
<i>Figure 72 - Reactive power response with Dynamic Decoupling matrix: network A</i>	98
<i>Figure 73 - Voltage and reactive power response for a step in reference voltage without the Dynamic Decoupling matrix: network B</i>	99
<i>Figure 74 - Voltage and reactive power response for a step in reference voltage with the Dynamic Decoupling matrix: network B</i>	99
<i>Figure 75 - Typical topology of a traditional power plant</i>	100
<i>Figure 76 - Equivalent electrical model</i>	101
<i>Figure 77 - IEEE 37-bus MV test system [207]</i>	105
<i>Figure 78 - Model used for PV energy resources [210]</i>	107
<i>Figure 79 - Daily voltage profile at node 735 with unity power factor</i>	108
<i>Figure 80 - Daily voltage profile at node 735 with reactive power control</i>	108
<i>Figure 81 - Daily voltage profile at node 735 with power factor control</i>	108

---

<i>Figure 82 - Voltage profile for the test network IEEE 37-bus: radial branch to node 735 (DG1)</i>	108
<i>Figure 83 - Real-world grid used in the case study</i>	110
<i>Figure 84 - Voltage profiles for three branches: solid line (with DG), dashed lines (without DG)</i>	111
<i>Figure 85 - Voltage profile for maximum DG</i>	114
<i>Figure 86 - Diagram of the test network</i>	115
<i>Figure 87 - Voltage profile</i>	117
<i>Figure 88 - Plant topology</i>	121
<i>Figure 89 - Voltage profile at the point of delivery (in p.u.)</i>	124
<i>Figure 90 - Reactive power profile of generators (in p.u.)</i>	124
<i>Figure 91 - Plant topology</i>	125
<i>Figure 92 - Voltage profile at the point of delivery (in p.u.)</i>	128
<i>Figure 93 - Reactive power profile of generators (in p.u.)</i>	128
<i>Figure 94 - Reactive power profile of generators - second simulation (in p.u.)</i>	128
<i>Figure 95 - Plant topology</i>	130
<i>Figure 96 - Voltage profile at the point of delivery (in p.u.)</i>	132
<i>Figure 97 - Voltage profile at the different nodes of generation (in p.u.)</i>	133
<i>Figure 98 - Reactive power profile of generators (in p.u.)</i>	133
<i>Figure 99 - Reactive power profile of generators (MVAr)</i>	133
<i>Figure 100 - Reactive power profile of generators and voltage response at the point of delivery without Dynamic Decoupling matrix</i>	134
<i>Figure 101 - Reactive power profile of generators and voltage response at the point of delivery with Dynamic Decoupling matrix</i>	134
<i>Figure 102 - Primary substation</i>	135
<i>Figure 103 - Network topology</i>	136
<i>Figure 104 - Voltage profile at the point of connection (in p.u.)</i>	137
<i>Figure 105 - Reactive power profile of generators (MVAr)</i>	138
<i>Figure 106 - Aerial view of the PV plant [216]</i>	139
<i>Figure 107 - General layout of the electrical system infrastructure</i>	140
<i>Figure 108 - Detail of a MV section [217]</i>	140

---

<i>Figure 109 - Plant topology</i>	141
<i>Figure 110 - Scenario 1, Simulation 1: Voltage profile at the point of delivery and Reactive power profile of generators (in p.u.)</i>	143
<i>Figure 111 - Scenario 1, Simulation 2: Voltage profile at the point of delivery and Reactive power profile of generators (in p.u.)</i>	143
<i>Figure 112 - Scenario 2, Simulation 1: Voltage profile at the point of delivery and Reactive power profile of generators (in p.u.)</i>	144
<i>Figure 113 - Scenario 2, Simulation 2: Voltage profile at the point of delivery and Reactive power profile of generators (in p.u.)</i>	144
<i>Figure 114 – Detail of reactive power profile of generators (in p.u.): without Dynamic Decoupling matrix (in p.u.)</i>	145
<i>Figure 115 – Detail of reactive power profile of generators (in p.u.): with Dynamic Decoupling matrix (in p.u.)</i>	145
<i>Figure 116 - Scenario 3, Simulation 1: Voltage profile at the point of delivery and Reactive power profile of generators (in p.u.)</i>	146
<i>Figure 117 - Scenario 3, Simulation 2: Voltage profile at the point of delivery and Reactive power profile of generators (in p.u.)</i>	146
<i>Figure 118 - Electric network and its modelization in PSAT</i>	152
<i>Figure 119 - Simulink blocks used and example of setting mask for conductors</i>	153
<i>Figure 120 - Main graphical interface</i>	153
<i>Figure 121 - Visualization of time domain simulation results</i>	154
<i>Figure 122 - Representation of the structure of Dome</i>	155



# List of Tables

---

<i>Table 1 - Main national climate and energy targets [12]</i>	2
<i>Table 2 - Targets for RES in Italy [15]</i>	3
<i>Table 3 - World Final Energy Consumption by Region (Mtoe) [26]</i>	11
<i>Table 4 - World Electricity Generation by Fuel (TWh) [26]</i>	11
<i>Table 5 - Installed RES Electricity Capacity in EU-28 [26]</i>	12
<i>Table 6 - Evolution of RES power plants in Italy [27]</i>	13
<i>Table 7 - Overview of hydroelectric power plants at the end of 2014 in Italy [28]</i>	14
<i>Table 8 - Overview of the wind power plants at the end of 2014 in Italy [28]</i>	16
<i>Table 9 - Interests for Italian state bonds.</i>	22
<i>Table 10 - Prices of electricity in the Italian residential market - VAT included.</i>	22
<i>Table 11 - Mean and weighted yields for three representative cities in Italy</i>	22
<i>Table 12 - Overnight capital costs for a 3kWp PV plant installed in Italy over the period 2003-2014</i>	23
<i>Table 13 - Payback Time (PBT), Internal Rate of Return (IRR) and Levelized Costs of Energy (LCOE) for three different locations in Italy (Initial Capital Outlay)</i>	24
<i>Table 14 - Payback Time (PBT), Internal Rate of Return (IRR) and Levelized Costs of Energy (LCOE) for three different locations in Italy (Feed-in-tariff - “First feed-in scheme”)</i>	24
<i>Table 15 - Payback Time (PBT), Internal Rate of Return (IRR) and Levelized Costs of Energy (LCOE) for three different locations in Italy (Feed-in-tariff - “Fifth feed-in scheme”)</i>	25
<i>Table 16 - Payback Time (PBT), Internal Rate of Return (IRR) and Levelized Costs of Energy (LCOE) for three different locations in Italy (Grid parity scenario, NO incentives)</i>	25
<i>Table 17 - Payback Time (PBT), Internal Rate of Return (IRR) and Levelized Costs of Energy (LCOE) for three different locations in Italy (Grid parity scenario, 50% tax-deduction)</i>	26

---

<i>Table 18 - Payback Time (PBT), Internal Rate of Return (IRR) and Levelized Costs of Energy (LCOE) for three different locations in Italy (Grid parity scenario - 100% self-consumption - NO incentives)</i>	27
<i>Table 19 - Cable types and data</i>	39
<i>Table 20 - Energy flows</i>	41
<i>Table 21 - Results: Active power losses for each bus</i>	41
<i>Table 22 - Requirements of Smart Grid applications [97]</i>	44
<i>Table 23 - Comparison of communication technologies for Smart Grid [98]</i>	45
<i>Table 24 - Main national climate and energy targets [12]</i>	50
<i>Table 25 - Functions required for LV connections in Europe [125]</i>	54
<i>Table 26 - Functions required for MV connections in Europe [125]</i>	55
<i>Table 27 - Cable types</i>	96
<i>Table 28 - Line lengths - Plant A</i>	96
<i>Table 29 - Line lengths - Plant B</i>	96
<i>Table 30 - Characteristics of the generators - Plant A</i>	96
<i>Table 31 - Characteristics of the generators - Plant A</i>	97
<i>Table 32 - Sensitivity Coefficients - Plant A</i>	97
<i>Table 33 - Sensitivity Coefficients - Plant B</i>	97
<i>Table 34 - Dynamic Decoupling matrix - Plant A</i>	97
<i>Table 35 - Dynamic Decoupling matrix - Plant B</i>	97
<i>Table 36 - Cable data for the IEEE 37-bus network</i>	106
<i>Table 37 - Cable lengths</i>	106
<i>Table 38 - MV test network DGs data</i>	107
<i>Table 39 - Cable data for the Actual Real-World distribution network</i>	110
<i>Table 40 - DGs data for Scenario I</i>	111
<i>Table 41 - Loads data</i>	112
<i>Table 42 - DGs data for Scenario II</i>	114
<i>Table 43 - Generators data</i>	115
<i>Table 44 - Cable data</i>	116
<i>Table 45 - Original Condition</i>	117
<i>Table 46 - Perturbed Condition</i>	117

---

<i>Table 47 - Controlled Condition</i>	118
<i>Table 48 - Legend of symbols used</i>	120
<i>Table 49 - Cable types</i>	122
<i>Table 50 - Inverter Stations</i>	122
<i>Table 51 - Line lengths</i>	123
<i>Table 52 - Cable types</i>	126
<i>Table 53 - Line lengths</i>	126
<i>Table 54 - Characteristics of the transformers</i>	126
<i>Table 55 - Sensitivity Coefficients <math>dv/dq</math></i>	127
<i>Table 56 - Dynamic Decoupling matrix</i>	127
<i>Table 57 - Characteristics of the generators</i>	129
<i>Table 58 - Characteristics of the transformers</i>	129
<i>Table 59 - Cable types</i>	131
<i>Table 60 - Line lengths</i>	131
<i>Table 61 - Sensitivity Coefficients <math>dv/dq</math></i>	131
<i>Table 62 - Dynamic Decoupling matrix</i>	132
<i>Table 63 - Characteristics of the generators</i>	137



# Glossary

---

- ACER: Agency for the Cooperation of Energy Regulators
- AVR: Automatic Voltage Regulator
- BVR: Busbar Voltage Regulator
- DG: Distributed Generation
- DGs: Distributed Generators
- DMS: Distribution Management Systems
- DSO: Distribution System Operator
- EMS: Energy Management System
- ENTSO-E: European Network of Transmission System Operators for Electricity
- EROEI: Energy Return On Energy Investment
- GRPR: Group Reactive Power Regulator
- HV: High Voltage
- ICT: Information Communication Technology
- IEEE: Institute of Electrical and Electronics Engineers
- IPS: Interface Protection System
- ISO: International Organization for Standardization
- LCA: Life Cycle Analysis
- LV: Low Voltage
- MV: Medium Voltage
- OLTC: On-Load Tap Changer
- p.u.: Per Unit
- POC: Point of Connection
- POD: Point of Delivery
- PV: Photovoltaic
- QoS: Quality of Service
- RES: Renewable Energy Sources
- RPR: Reactive Power Regulator
- RVR: Regional Voltage Regulator
- SCADA: Supervisory Control & Data Acquisition
- SVR: Secondary Voltage Regulation

STATCOM: Static Synchronous Compensator

TCP/IP: Transmission Control Protocol/Internet Protocol

TSO: Transmission System Operator

TVR: Tertiary Voltage Regulator

VHV: Very High Voltage

$A_{bn}$ : Base power of the p.u.

$P_n$ : Nominal power

$P_{ref}$ : Active power reference

$Q_{ref}$ : Reactive power reference

$V_{bn}$ : Base voltage of the p.u.

$V_n$ : Nominal voltage

$q_{liv}$ : Reactive power level

# Introduction

---

On April 23rd 2009 the European Parliament approved the Directive 2009/28/EC [1] containing the climate & energy package (also known as "20-20-20" package), to ensure that the European Union will achieve its climate targets by 2020: a 20% reduction in greenhouse gas emissions, a 20% improvement in energy efficiency, and a 20% increase of the share of energy produced from renewable sources measured on final consumptions<sup>1</sup>.

The "package" took effect in June 2009 and is valid from January 2013 until 2020.

The national targets for 2020, expressed as percentage changes from 2005 levels, are differentiated according to EU countries relative wealth<sup>2</sup> (measured by Gross Domestic Product per capita) [2].

The breakdown of the targets among the different countries has given Italy the commitment to satisfy the 17% of national consumption through the exploitation of renewable energy by 2020<sup>3</sup> (Table 1).

In Italy, in June 2010 the Ministry for Economic Development presented "The National Renewable Energy Action Plan" to the EU Commission. The Action Plan establishes that renewable sources will have to sustain 28.97% gross final consumption in the electric section to balance the expected minor penetration in transportation and in thermal uses (heating and cooling) (Table 2). It is a matter of increasing the already meaningful 18% gained in 2010 [3] through direct incentive policies of renewable energies for the production of electricity such as Green Certificates [4], "Feed-in scheme" [5] [6] [7] [8] [9] [10], White Certificates [11] and so on.

The political scenario leads to an increase in the exploitation of renewable energy resources (photovoltaic, wind and others) and to a better utilization of fossil fuels resources through co-generative power plants that are often implemented with small and medium size generators located near the loads.

---

<sup>1</sup> Final consumption of energy comprises all forms of energy in the civic and industrial sector and in transportation.

<sup>2</sup> Less wealthy countries are allowed emission increases because their relatively higher economic growth is likely to be accompanied by higher emissions.

<sup>3</sup> Such share is to be allocated according to further specific objectives between the single Regions (according to "burden sharing").

Country	2020 target
Austria	34,00%
Belgium	13,00%
Bulgaria	16,00%
Cyprus	13,00%
Czech Republic	13,00%
Denmark	30,00%
Estonia	25,00%
Finland	38,00%
France	23,00%
Germany	18,00%
Greece	18,00%
Hungary	13,00%
Ireland	16,00%
Italy	17,00%
Latvia	40,00%
Lithuania	23,00%
Luxembourg	11,00%
Malta	10,00%
Netherlands	14,00%
Poland	15,00%
Portugal	31,00%
Romania	24,00%
Slovakia	14,00%
Slovenia	25,00%
Spain	20,00%
Sweden	49,00%
United	15,00%
Croatia	20,00%
EU-28	20,00%

**Table 1 - Main national climate and energy targets [12]**

Additional factors for such an increase are [13] [14]:

- the liberalization of electricity markets which augments the possibility for investments in the production of electrical energy also with small capitals and therefore small size generators;
- the steady increase in electrical energy consumption and in the costs for traditional fossil fuels.

	Consumptions from RES	Gross Final Consumption (GFC)	RES/GFC
	[Mtep]	[Mtep]	[%]
Electricity	9,112	31,448	28,97%
Heat	9,520	60,135	15,83%
Transports	2,530	39,630	6,38%
<b>TOTAL</b>	<b>22,306</b>	<b>131,214</b>	<b>17%</b>

Table 2 - Targets for RES in Italy [15]

The new paradigm for the generation and distribution of electrical energy is no longer based on big centralized power plants, it is rather characterized by a geographically distributed generation with small and medium sized generators (Figure 1).

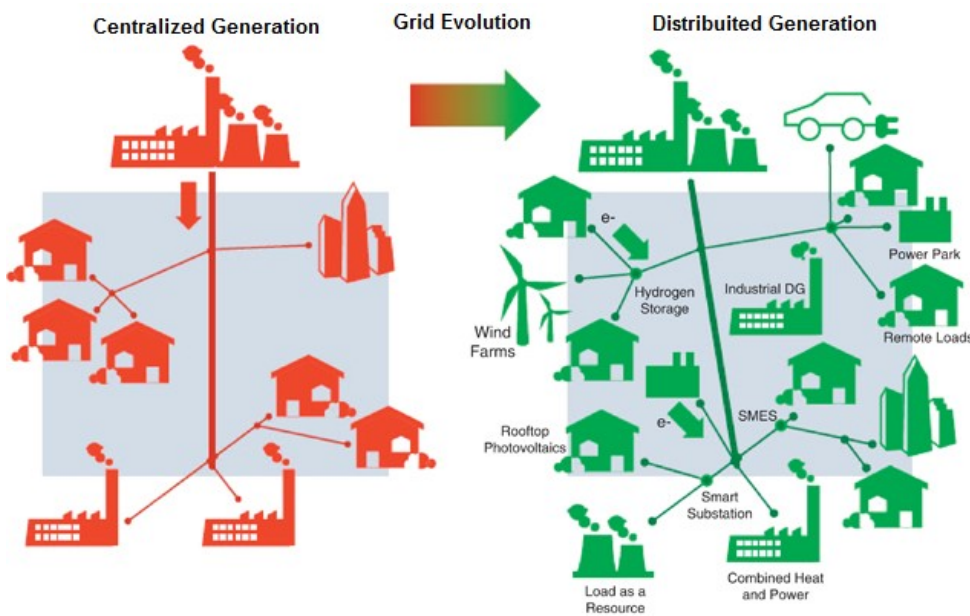


Figure 1 - Centralized and Distributed Generation [16]

The DG therefore guarantees the possibility to differentiate the energetic resources to be converted into electric energy thus allowing substantial increase of renewable sources exploitation.

It follows that on some portions of the electrical grid, nonprogrammable energy from renewable source will represent an ever-growing fraction of the total quantity transported by infrastructure. In addition, the start of electric mobility meant to improve transportation performances, will definitely affect distribution networks.

The first effects are already visible on distribution networks: in most cases a generation surplus rather than the absorption present on the same network can be observed. The consequences being the inversion of power flow in transformers and excessive variations of voltage profiles that may in turn result in undesirable disconnections of distributed generators (not linked to effective network disservice). Furthermore, one cannot forget

the possible phenomenon of the undesired island (when the generator keeps on injecting power even if the network is out of service) and the influences on the stability and the security of the whole electric system.

The first step for a correct management of a similar kind of network, with bi-directional flows of energy is real time knowledge of the power produced by DGs connected to MV and LV networks. The second step is its dispatch possibility.

In view of a total control of the electric network, a measurement apparatus supported by a bi-directional communication system in any node of the grid is needed. A concept of smart grid is then born implying innovative structures and procedures which besides keeping a high degree of security and reliability of the entire system, are also able to [17]:

- face the problems related to the management of DG;
- control system loads;
- promote energy efficiency and a higher involvement of active and passive end-users with reference to electric market.

The evolution from traditional network to smart grid is therefore essential to receive generation from a renewable source at the same time guaranteeing maintenance of suitable levels of service reliability and quality.

# Chapter 1.

## Power electric systems

Electrical systems are indeed complex realities, with wide geographic extensions and made up of generating plants, transformers, transmission and distribution networks to transport electric energy from the areas of production to those of use. They are structured in multiple layers:

- **Production:** electricity does not exist in nature and must therefore be produced starting from primary sources by means of specific power plants;
- **Transmission:** transport of electricity is carried out on all main connections at HV and VHV (380 kV- 220 kV - 150 kV), from production centers to transformer stations to lower voltage levels;
- **Distribution:** the last phase concluding the production chain of an electricity system is represented by distribution, that is the delivery of electricity at MV (15-20-23 kV) and LV (230-400 V) to end-users.

Electrical systems have been designed for a mono-directional power flow (Figure 2).

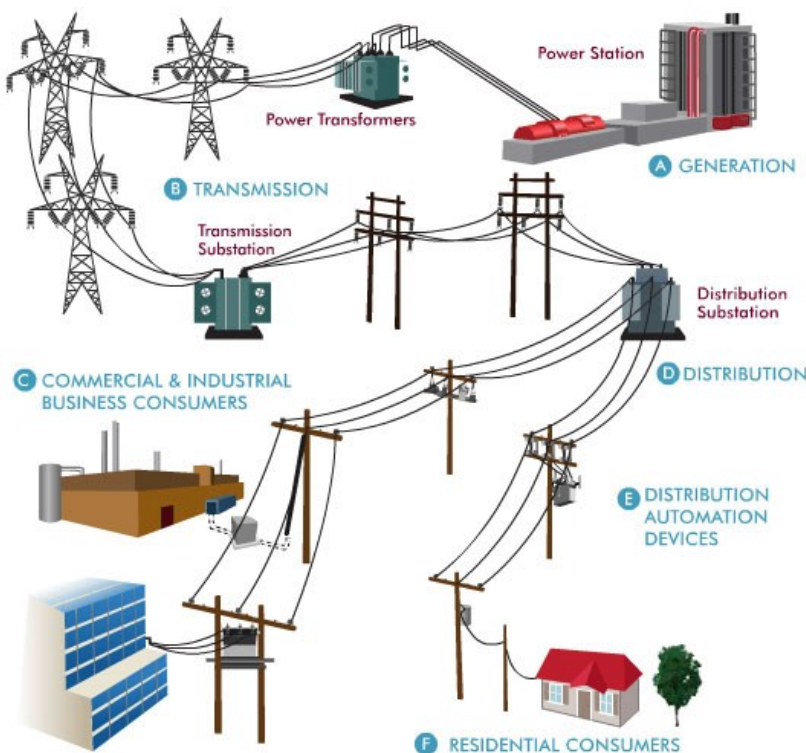


Figure 2 - Electrical System Architecture [18]

The correct operation of a power system requires frequency control (equal on all the whole system) and voltage control (that can be different at each node but needs to be

comprised on a valid range). While frequency is related to the correct balance of active power, voltage is mainly related to reactive power flows.

In order to fulfill such objectives one has to develop an adequate planning phase and also an on-going check in real time.

Planning is structured according to the following stages:

- Load Forecasting:** forecasting of short and medium term needs is made on the basis of time series of local area electric needs, taking into account the macroeconomic scenarios and the variable data on climate and weather according to the most updated available information at the moment of the analysis (Figure 3);

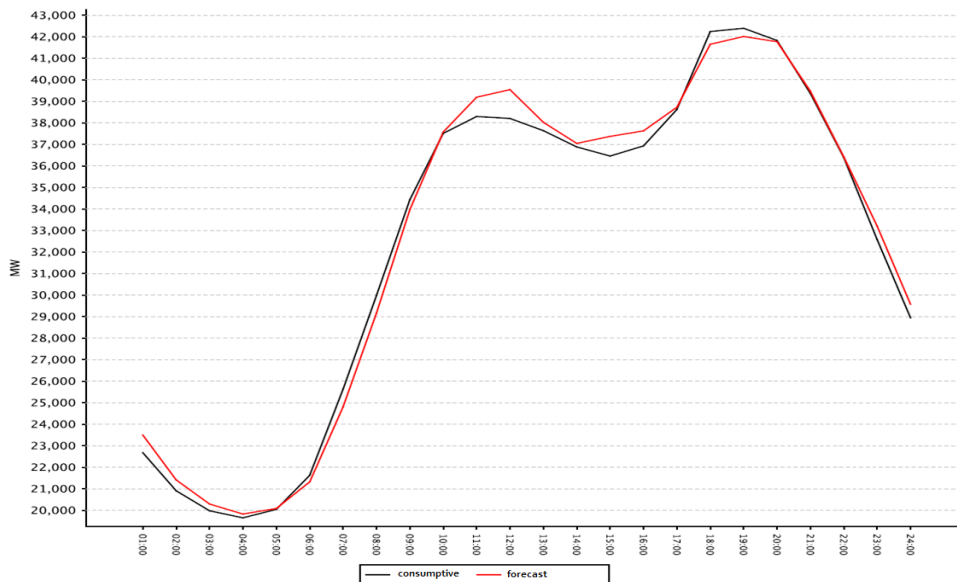


Figure 3 - Daily Electricity Demand - 02/01/2016 [19]

- Unit Commitment:** identification of the optimal set of generators suitable to satisfy the expected load;
- Dispatching:** for optimum partition of the total load between the identified set of generators.

During the real time control phase, the state of the electric system is analyzed intervening where appropriate on productions and on the structure of the network, so as to guarantee balance in respect of all system disturbances like:

- load slow fluctuations along the day;
- system contingencies due to a sudden unavailability of network elements (for examples lines and transformers) or big generators, as a result of short circuits or other faults that may put them out of service.

An inadequate management of contingencies may trigger domino effects up to (as extreme condition) instability of the electric system and to total black-out [20].

## 1.1 Transmission networks (HV, VHV)

Transmission grids are needed for electricity transmission in routes long even several hundred kilometers at high and very high voltage levels. They are operated in a meshed mode so as to make alternative paths available that can be used to distribute energy flows and to cope with unavailability of network components owing to maintenance operations or troubleshooting.

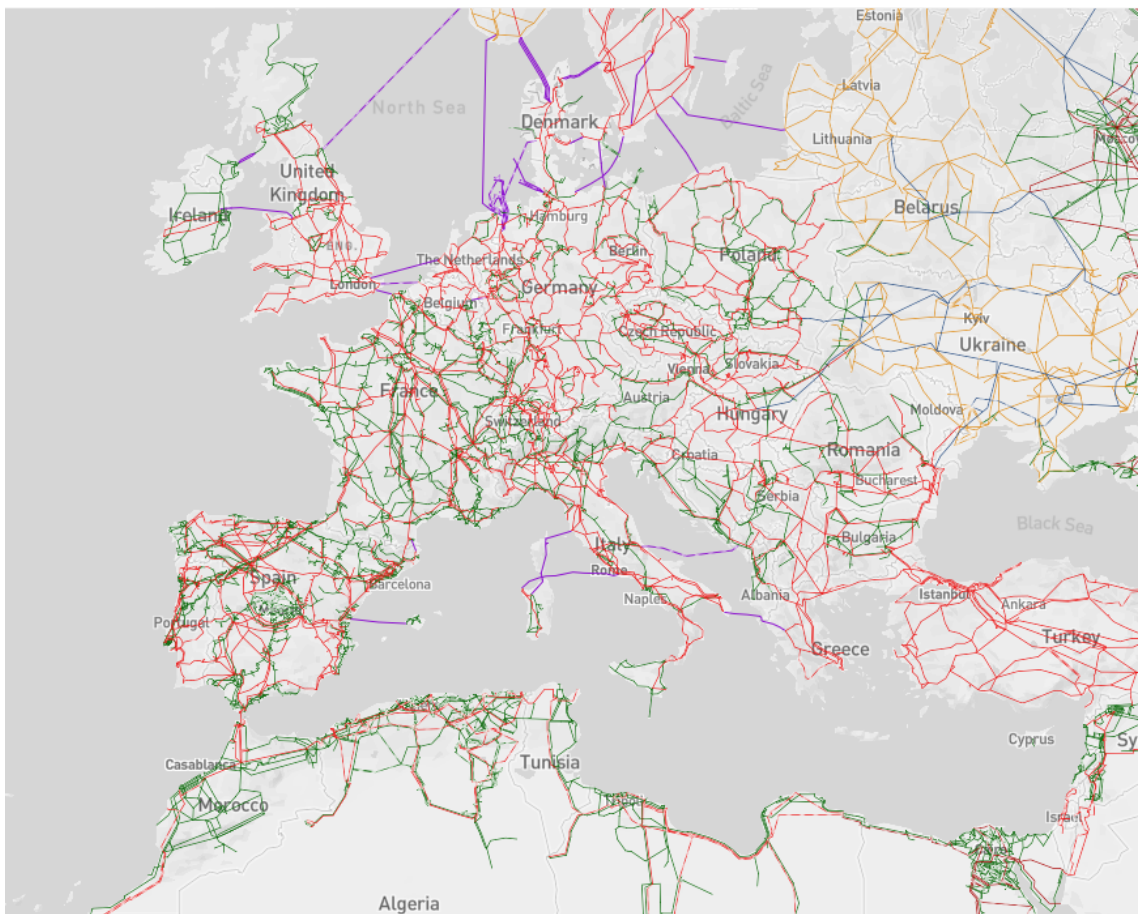


Figure 4 - Interconnected Network of Continental Europe [21]

Up to now electric transmission grids have reached a very high level of automation which generally guarantees high reliability and an optimum level of supply quality and continuity. Therefore, it can be said that the transmission grid, at least in our country, is already "Smart", and that the improvements and evolutions that will intervene integrate in an architecture that already allows the best control and management of network resources.

## **1.2 Distribution networks (MV, LV)**

Electric distribution networks are connected to the transmission network by means of primary substation that transform electric energy from HV to MV.

Such networks distribute energy for routes that may extend up to some kilometers:

- directly up to end-users with the Point of Delivery (POD) at MV level;
- up to secondary cabins which further lower the voltage level from MV to LV and thus to end-users with the Point of Delivery (POD) at LV level.

Differently from transmission networks, LV and MV distribution networks are generally operated in a radial configuration and have been conceived to operate with one-way power flows (from the transformation cabin connecting them to the HV network to the points of delivery) in order to satisfy end-users' electric stochastic demand.

### **1.2.1 The fit & forget approach in distribution networks**

At present generators are connected to the distribution network according to the *fit & forget* approach. Before connecting a generation plant to the related distribution network, the distributor ensures that at different possible load conditions, its operation may not cause problems to the network ("fit" phase), besides ensuring the plant complies with current connection technical rules.

Once the connection of the production plant to the distribution network has been made, the plant has the faculty to produce according to its capacity with the only constraint to respect technical rules and the value of maximum injected power. Since that moment the network operator may operates as if it forgot about its existence ("forget") [22].

The approach was generated because in the past the connection to the distribution network of small-size generators was considered a sporadic situation and as a result its operation was not foreseen for distributors.

### **1.3 Distributed Generation and active networks**

There are several different definitions of "Distributed Generation" in the international scientific literature and in the national regulations of several countries. Basically "Distributed Generation" consists of production units of small and medium size (i.e. from tens kW to some MW of nominal power) connected to distribution network.

These production units were installed in order to:

- feed electric loads mainly in the proximity of the electricity production site as in side industrial plants or buildings for commercial and residential activities, as well as to satisfy specific energy needs or of reliability;
- exploit primary energy sources, widespread on the territory and not differently exploitable through the traditional system of great size production including co-generative systems.

Even if relevant authors indicate nominal power as non-influential on the definition of DG, norm and practice show that DG plants have a nominal power lower than 10 MVA [23].

For what concerns "Active Network" it can be said that nowadays the concept is getting more and more widespread but literature has not yet reached a precise definition suitable to outline its meaning exactly. A possible definition of Active Distribution System could be the following: "A distribution network is active if it does not simply carry out the passive function feed end-users".

Essentially an "active electric network" is one that produces energy, that is a network where DG is present.

As the following paragraphs will highlight, the stock of national production based on Renewable Energy Sources (RES) has grown dramatically in the last years, thus becoming extremely important in terms of installed power.

The relevance of DG contribution is demonstrated by the increase of the energy flow inversion phenomena from the distribution network to the transmission system: the number of power flow inversions in primary stations HV/MV can be used as an indicator to assess the transformation state of electric networks.

For example, considering the Italian case, in Figure 5 it can be noticed that comparing the data of 2015 with the ones of the previous year, the percentage of HV/MV transformers with a power flow inversion towards HV Transmission Network for at least 5% of time (more than one hour a day) has risen from 252 of 2010 to 793 of 2015<sup>4</sup>. The graph also shows a substantial stabilization in the last two years [24] [25].

---

<sup>4</sup> In Italy the overall number of primary substations HV / MV is approximately 4000

It can therefore be assumed that most Italian distribution networks are getting more and more active.

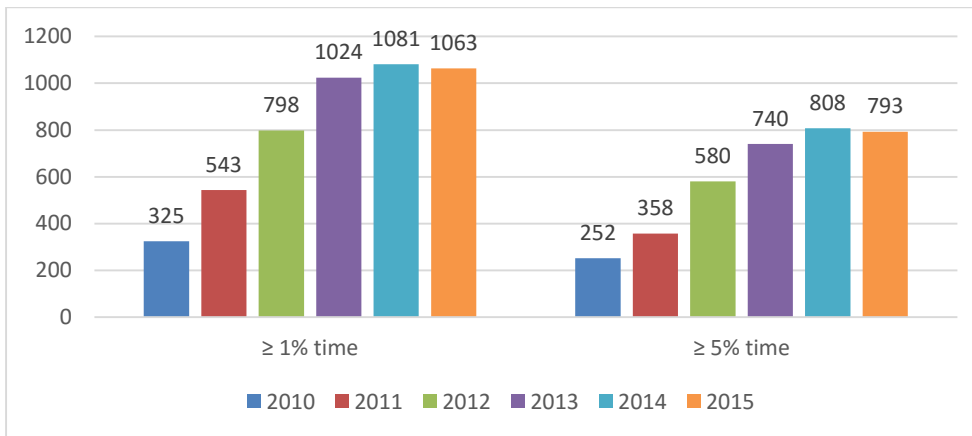


Figure 5 - Power Flow Inversions Average in Enel Distribuzione's primary substations [25]

In the following paragraphs, to provide an idea of the dimension of the phenomenon some data about DG installed in the latest years both at international and national level are given.

### 1.3.1 RES in the World

Over the past 20 years global energy consumption has increased almost constantly of about 50%: it has risen from 6539 Mtoe in 1995 to 9425 in 2014 (Figure 6 and Table 3).

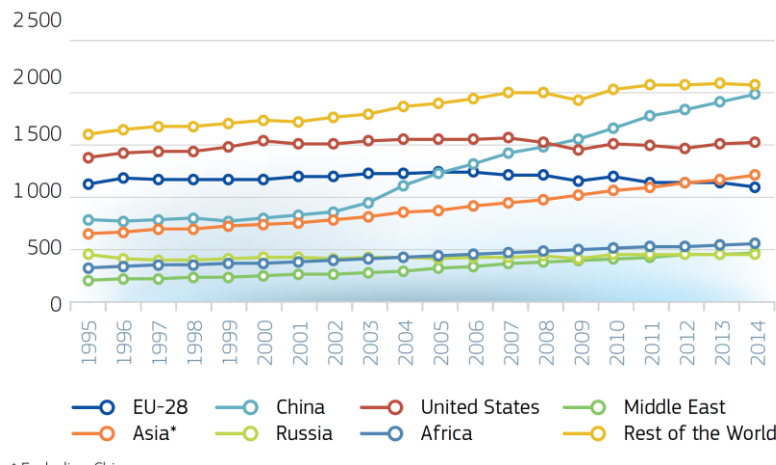


Figure 6 - World Final Energy Consumption by Region [Mtoe] [26]

It is interesting to note that:

- comparing to 1995, China has seen an increase in consumption of about 150%;
- the consumption of USA and Russia remained almost constant;
- EU-28 consumption has increased constantly until 2010, subsequently it decreased dramatically up to levels lower than those of 1995.

	<b>1995</b>	<b>2000</b>	<b>2005</b>	<b>2010</b>	<b>2014</b>	<b>2014(%)</b>
<b>EU-28</b>	1133	1180	1242	1208	1095	11.6%
<b>China</b>	788	796	1227	1667	1997	21.2%
<b>USA</b>	1378	1546	1563	1512	1538	16.3%
<b>Asia (without China)</b>	643	744	877	1073	1214	12.9%
<b>Africa</b>	324	369	437	508	559	5.9%
<b>Russia</b>	458	418	412	447	454	4.8%
<b>Middle East</b>	202	241	313	414	476	5.1%
<b>Rest of the World</b>	1613	1747	1905	2037	2092	22.2%
<b>Total</b>	<b>6539</b>	<b>7041</b>	<b>7977</b>	<b>8866</b>	<b>9425</b>	<b>100%</b>

**Table 3 - World Final Energy Consumption by Region (Mtoe) [26]**

Regarding electricity, the constant increase of consumption goes together with a steady increase of production. Energy sources that have recorded the largest increase are the Solid Fuels, Gas, and Renewable Energy. RES at the end of 2014 cover 22.3% of the total production (Table 4 and Figure 7).

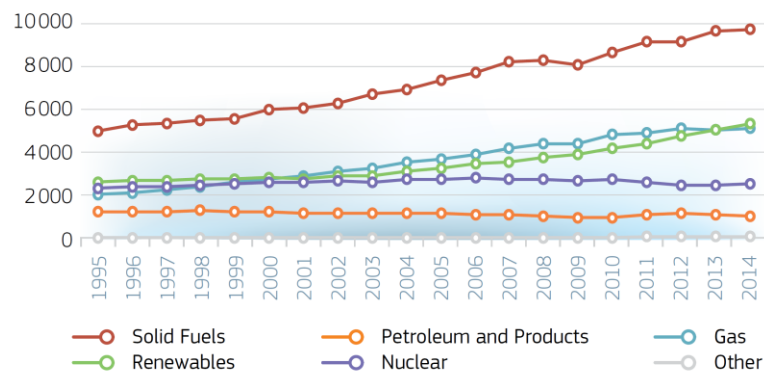


**Figure 7 - World Electricity Generation by Fuel (TWh) [26]**

	<b>1995</b>	<b>2000</b>	<b>2005</b>	<b>2010</b>	<b>2014</b>	<b>2014(%)</b>
<b>Solid Fuels</b>	4.992	6.005	7.335	8.665	9.707	40,8%
<b>Petroleum and Products</b>	1.279	1.251	1.178	982	1.023	4,3%
<b>Gas</b>	2.022	2.753	3.706	4.828	5.155	21,6%
<b>Renewables</b>	2.637	2.837	3.291	4.205	5.323	22,3%
<b>Hydro</b>	2.479	2.619	2.934	3.442	3.895	16,4%
<b>Solar/Wind/Other</b>	10	35	120	384	928	3,9%
<b>Biofuel and Waste</b>	131	164	223	367	493	2,1%
<b>Geothermal</b>	40	52	58	68	77	0,3%
<b>Nuclear</b>	2.332	2.591	2.768	2.756	2.535	10,6%
<b>Other</b>	24	34	46	58	72	0,3%
<b>Total</b>	<b>13.285</b>	<b>15.471</b>	<b>18.324</b>	<b>21.493</b>	<b>23.816</b>	<b>100%</b>

**Table 4 - World Electricity Generation by Fuel (TWh) [26]**

### 1.3.2 RES in Europe

In Europe, at the end of 2014, the installed production power plants based on RES is equal to 369,511 GW (37.8% of the total power installed) as shown in Table 5.

MW	TOTAL RES	Hydro	Wind	Solar PV	Solar Thermal	Geothermal	Tide, Wave and Ocean
EU-28	369.511	150.279	129.080	86.786	2.302	820	244
Share (%)	37,8%	15,4%	13,2	8,9%	0,2%	0,1%	0,0%

Table 5 - Installed RES Electricity Capacity in EU-28 [26]

RES power plants contribute to an energy production of about 930TWh (29.2% of total production). It is interesting to note that renewables are the only energy source that has recorded a positive growth rate in recent years (Figure 8).

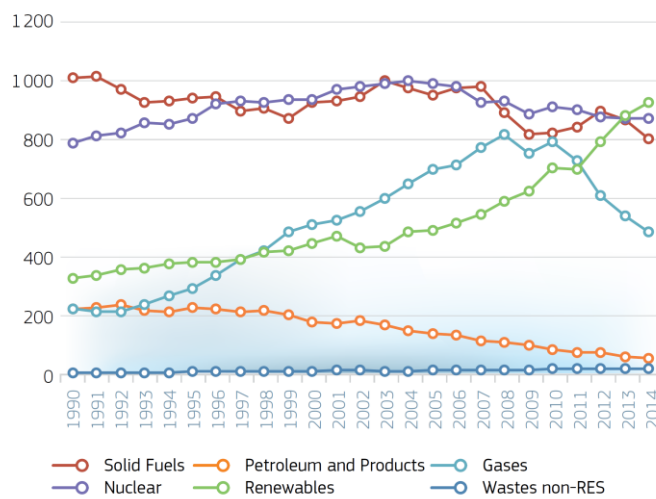


Figure 8 - Gross Electricity Generation By Fuel in EU-28 - 1990-2014 (TWh) [26]

Technologies that contribute most to renewable generation are in order: hydroelectric, wind, biomass and photovoltaic (here after PV) (Figure 9).

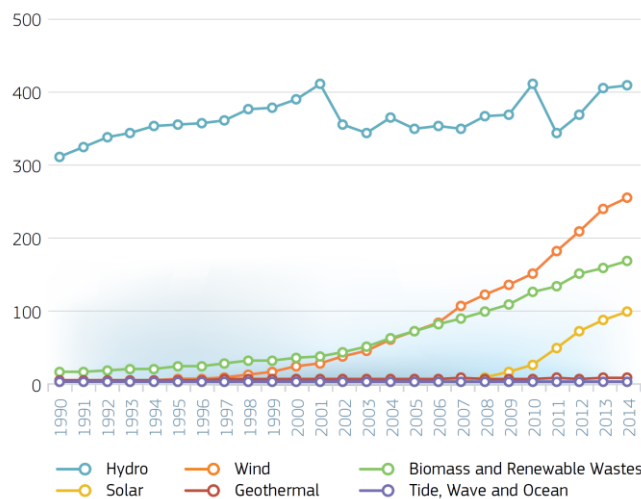


Figure 9 - Gross RES Electricity Generation By Fuel in EU-28 - 1990-2014 (TWh) [26]

### 1.3.3 RES in Italy

In the last years a significant change in the electric production mix have been recorded, due to the strong introduction of RES power plants (in particular the aleatory ones) [24].

Indeed it can be said that we are witnessing a real race to renewable sources: in the last five years the installed power of RES power plants in Italy has risen from 30.284MW of 2010 to 51.479MW<sup>5</sup> of 2015 (Figure 10) [27].

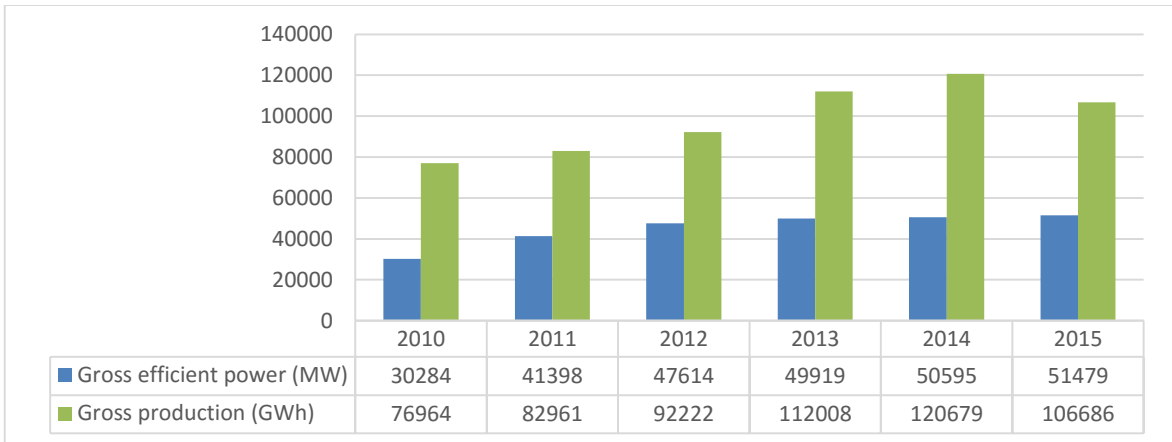


Figure 10 - Evolution of the installed RES power plants in Italy [27]

The growth is mainly due to the plants fed by bioenergy, but above all to new wind parks and to photovoltaic as shown in Table 6.

	2010	2011	2012	2013	2014	2015
<b>Gross efficient power (MW)</b>						
Hydraulic Energy	17.876	18.092	18.232	18.366	18.418	18.531
Wind Energy	5.814	6.936	8.119	8.561	8.703	9.126
Photovoltaic	3.470	12.773	16.690	18.185	18.609	18.910
Geothermal Energy	772	772	772	773	821	824
Bioenergies	2.352	2.825	3.802	4.033	4.044	4.087
<b>TOTAL</b>	<b>30.284</b>	<b>41.398</b>	<b>47.614</b>	<b>49.919</b>	<b>50.595</b>	<b>51.479</b>
<b>Gross production (GWh)</b>						
Hydraulic Energy	5.117	45.823	41.875	52.773	58.545	43.902
Wind Energy	9.126	9.856	13.407	14.897	15.178	14.883
Photovoltaic	1.906	10.796	18.862	21.589	22.306	22.847
Geothermal Energy	5.376	5.654	5.592	5.659	5.916	6.160
Bioenergies	9.440	10.832	12.487	17.090	18.732	18.894
<b>TOTAL</b>	<b>76.964</b>	<b>82.961</b>	<b>92.222</b>	<b>112.008</b>	<b>120.679</b>	<b>106.686</b>

Table 6 - Evolution of RES power plants in Italy [27]

<sup>5</sup> Preliminary estimates

### 1.3.3.1 Hydroelectric Energy in Italy

At the end of 2014, 3.432 hydroelectric power plants are operative in Italy. Most of them is of small size – with a total power lower than 1 MW (Table 7). Of the 18.418 MW installed in Italy at the end of 2014, the large majority refers to plants with a power above 10 MW [28].

During 2014 production from hydraulic source amounted to 58.545 GWh, 49% of total production from renewable sources. 76% of electricity generated by hydroelectric plants (44.404 GWh) was produced by plants of a power above 10 MW, 19% (10.993 GWh) by the ones with power between 1 and 10 MW and the remaining 5% (3.148 GWh) by small-size plants (lower than 1 MW) [28].

	n°	Power MW	Energy GWh
P ≤ 1 MW	2.304	678	3.148
1 MW < P ≤ 10 MW	825	2.494	10.993
P > 10 MW	303	15.245	44.404
<b>TOTAL</b>	<b>3.432</b>	<b>18.418</b>	<b>58.545</b>

Table 7 - Overview of hydroelectric power plants at the end of 2014 in Italy [28]

The period between 2001 and 2014 has been characterized mainly by the installation of small-size plants and installed power in Italy has grown at an average year rate of 0,7% (Figure 11). The natural consequence of such phenomenon is a progressive reduction of medium size power plants that has moved from 8,7 MW of 2001 to 5,4 MW in 2014.

The analysis of installed power and the number of plants over the last 10 years, shows that hydroelectric power has not changed considerably. The only relevant phenomenon is represented by the coming into operation of several small size flowing water hydro power plants.

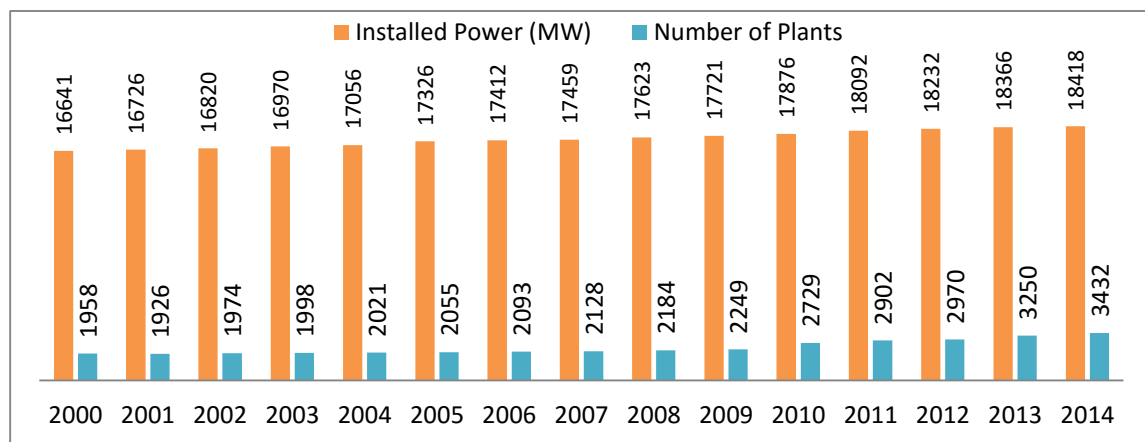


Figure 11 - Evolution of hydroelectric power plants in Italy [28] [29]

### 1.3.3.2 Wind Energy in Italy

From 2000 to 2014, in Italy, a strong development has been recorded also in wind farms (Figure 12). Indeed, at the end of 2000 installed plants were only 55 with a power equal to 363 MW, while at the end of 2014 installed wind power plants have reached a total power of 8.703 MW (1.847 plants), thus representing 17,2% of the one of the whole park of renewable energy plants [28] [29].

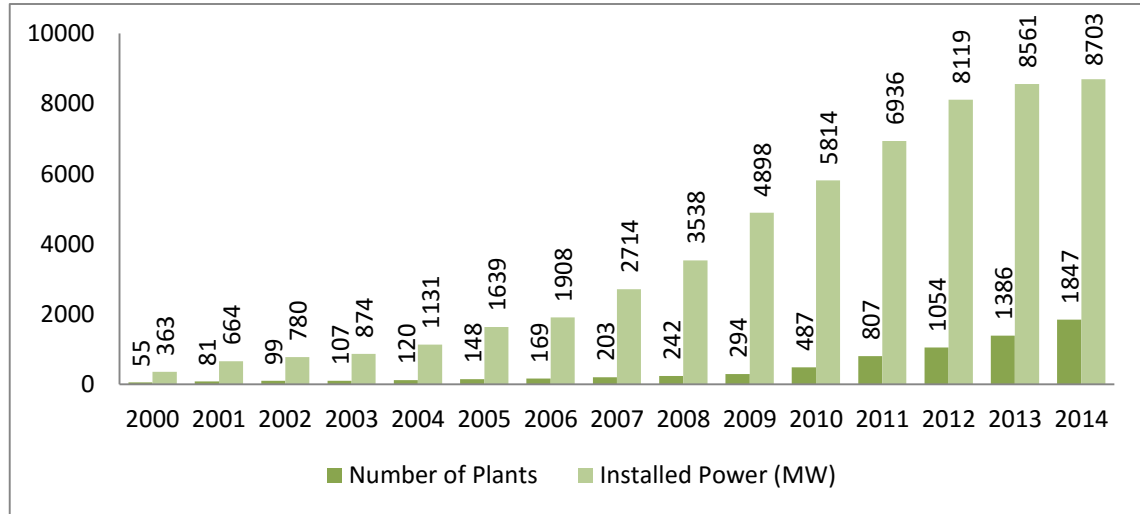


Figure 12 - Evolution of wind power plants in Italy [28] [29]

About 85% of installed plants is of small or middle size (power lower than 10 MW), and therefore commonly connected to MV and LV distribution networks. On the contrary, as for the level of installed power, 91% (7.933 MW) is concentrated in the 262 wind turbines of a power above 10 MW, generally connected directly in HV (Table 8).

From 2000 to 2009 the average power of wind farms has grown from 6.6 to 16.7 MW, while it has decreased in the following years (Figure 13).

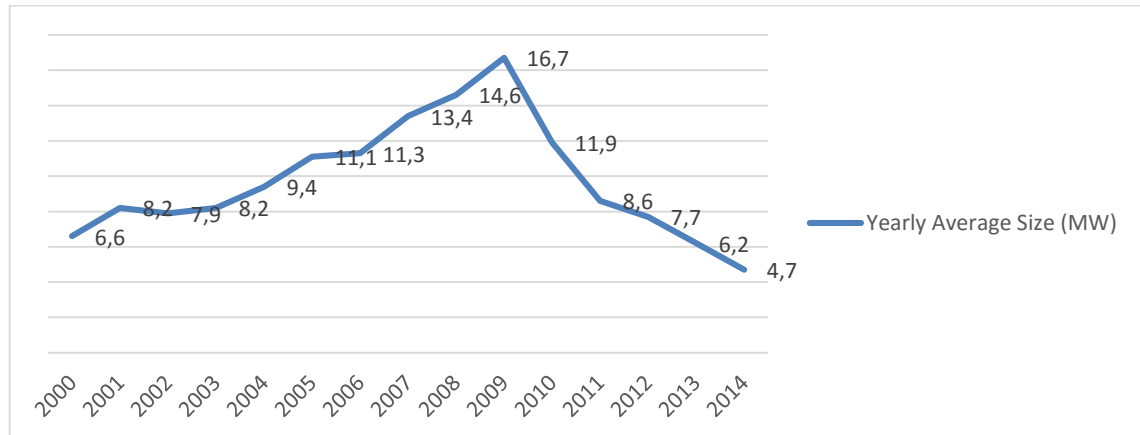


Figure 13 - Average size of wind farms from 2000 to 2014 [28] [29]

	n°	Power MW	Energy GWh
P ≤ 1 MW	1.477	233	338
1 MW < P ≤ 10 MW	108	536	915
P > 10 MW	262	7.933	13.926
<b>TOTAL</b>	<b>1.847</b>	<b>8.703</b>	<b>15.178</b>

**Table 8 - Overview of the wind power plants at the end of 2014 in Italy [28]**

During 2014 production from wind turbines was equal to 15.178 GWh, 13% of the total production from renewable sources. 92% of the electricity generated by wind turbine plants (13.926 GWh) was produced by plants with a power above 10 MW, 6% (915 GWh) by those with a power between 1 and 10 MW and the remaining 2% (338 GWh) by plants with a power lower than 1 MW (Table 8).

### 1.3.3.3 Photovoltaic Energy in Italy

In the last years, in Italy, the growth in number and power of photovoltaic plants has been very rapid [30]. Indeed, at the end of 2015 Italy ranked second behind Germany and fifth in the world for photovoltaic power installed [31].

Figure 14 reports the data concerning photovoltaic installed power at the end of 2015 for the first eight countries in the world.

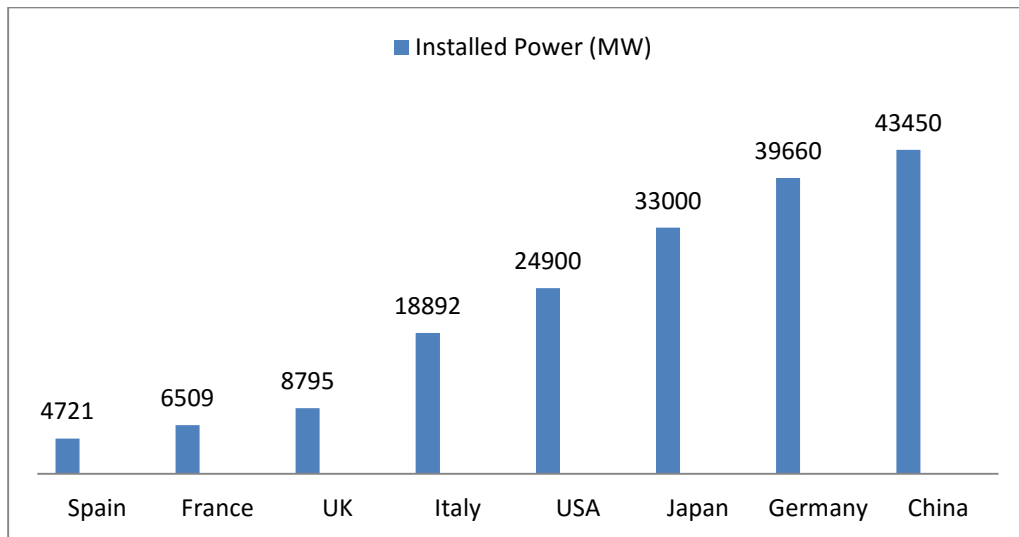


**Figure 14 - Power of photovoltaic systems in main countries at the end of 2015 [31]**

The world record belongs to China with more than 43 GW installed (among which 15.100 MW installed only in 2015), that has overtaken Germany where at the end of 2015 40 GW were installed. The increase of photovoltaic system installed in Japan and USA is considerable (respectively an additional power of about 9.700 MW and 6.600 MW).

As shown in Figure 15, in Italy:

- in 2009, 2010 and 2011 the number of plants more than doubled if compared with the previous year (at the end of 2011 about 330.200 plants were in operation while from 2012 to 2015 the rate of growth of plants diminished; at the end of 2015 the number of plants in operation amounted to 688.398);
- as for power, from 431 MW of 2008 it reached 18.892 MW in 2015 (with an increase of approximately 44 times).

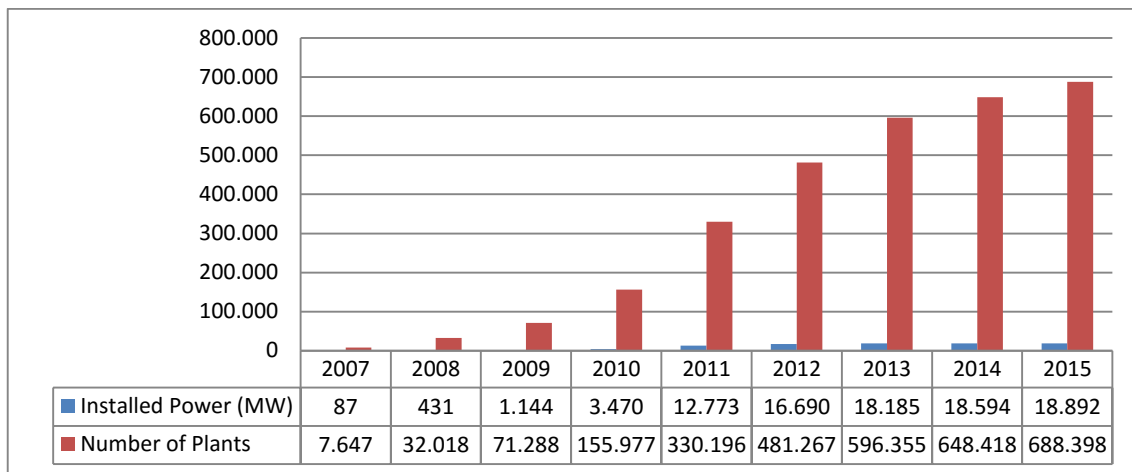


Figure 15 - Evolution of power and number of photovoltaic plants in Italy [31] [32]

Furthermore, interesting is to notice that the total power of the national photovoltaic park:

- from 2008 to 2011 has grown more than proportionally in comparison to the number of plants since plants of an ever-increasing dimension have come into operation: the phenomenon is particularly evident at the end of 2011 during which the average size of the park grew up to 53,4 kW (Figure 16);
- from 2012 to 2015 there has been a reversal of the trend with the installation of plants of increasingly lower power (mainly for household customers service). In 2015 the medium power installed was of 7,1 kW, with an average cumulative national size of about 27kW.

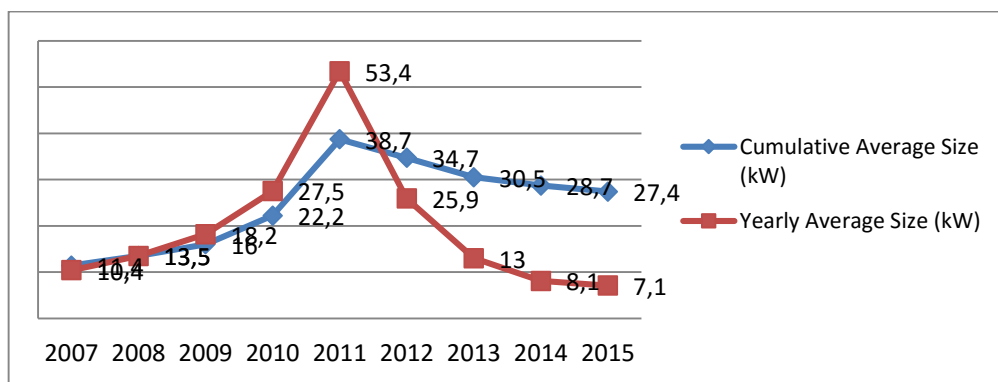


Figure 16 - Evolution of the average power of photovoltaic plants in Italy [31] [32]

As for the voltage level to which PV plants are connected it must be underlined that (Figure 17):

- almost the majority of installed plants in Italy (669.709 out of 688.398, amounting to 97,3%) are connected to LV distribution networks;
- the remaining part, consisting of fewer than 20.000 plants, are connected to MV distribution networks, represents however 58,4% of the installed power on the whole national territory;
- in the end a small number of plants is connected to HV network with a total power of about 1.176 MW (6,2% of the total amount).

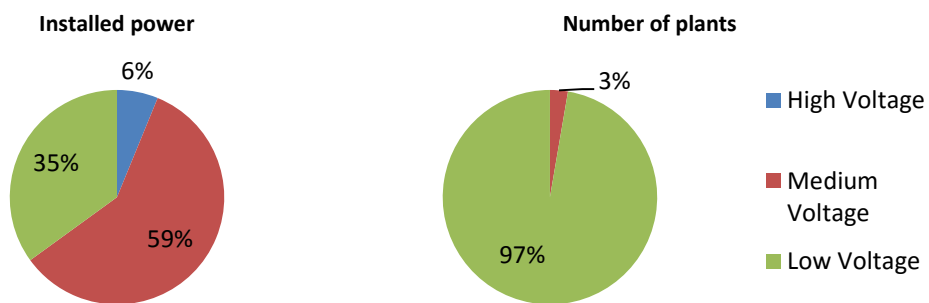


Figure 17 - Photovoltaic plants in Italy for voltage level at the end of 2015 [31]

Starting from very low values (39 GWh in 2007), PV energy production has increased of about 588 times in just nine years: in 2015 the production of photovoltaic plants in Italy reached 22.942 GWh (Figure 18).

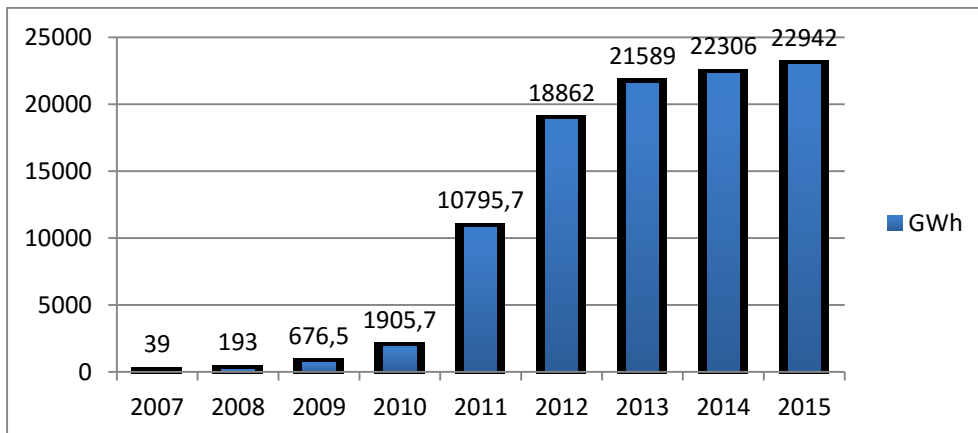


Figure 18 - Production of photovoltaic plants in Italy [31] [32]

As discussed above, in recent years the technologies that have recorded the highest increase of installed power are the photovoltaic and the wind power. It was therefore decided the phenomenon had to be investigated. To provide an idea of the possible future impact on energy distribution systems, studies on the energetic and economic advantages of photovoltaic technology have been conducted.

### **1.3.3.3.1 Assessment of Photovoltaic Systems for Electric Power Generation using EROEI (Energy Return On Energy Investment)**

In order to assess the actual yield of the plants and especially the sustainability of this technology, it is necessary to rely on indicators independent of economic fluctuations or political choices [33]. In this regard, some performance indices to assess the photovoltaic systems yield exclusively from an energetic point of view have been presented in literature. EROEI (Energy Return on Energy Investment) or sometimes EROI (Energy Return on Investment) [34], is the most complete indicator, which shows how many times a given energy production plant returns the expended energy throughout its complete life cycle.

In a perspective of energy investments sustainability, the repayment of the construction, functioning and decommissioning of a production plant in electricity, needs to be evaluated not only in economic terms, as it commonly happens, but also in terms of energy balance.

To this end, for a given source of energy, it is possible to calculate the ratio between the energy produced during the useful life of a production plant and the energy consumed to build, make it function and dismantle it. This ratio defines the Energy Return On Energy Investment:

$$\text{EROEI} = \frac{E_{\text{OUT}}}{E_{\text{IN}}} = \frac{\text{Usable Acquired Energy}}{\text{Energy Expended}}$$

When EROEI is less than 1, this means that the system delivers less energy than the one required to build it, make it function and dismantle it over its useful life. Therefore, the overall energy balance of the plant is negative. On the other hand, if the ratio is greater than 1, the power plant registers a positive net energy balance. It is worth noting that in systems where EROEI is less than about 2, the energetic convenience is only marginal, and so is also the economic convenience. It follows that such systems are of little practical use especially as long-term energy solutions. EROEI can be used to compare systems for the production of electricity based on different technologies and energy sources.

The energy contributions of all sources have to be considered in the calculation of EROEI:

- direct energy (used during the construction of the production plant);
- indirect energy (used to produce, deliver and assemble the materials during the building process) and
- the energy of raw materials (energy content of materials used in the building process, different from combustibles).

In the case of systems using fossil fuels, one must consider for example the energy expended for the primary source procurement (e.g., extraction from oilfield, transport to

the factory or to the plant, further treatments and processing, etc.). Similarly, the energy required to build the factory (e.g. for PV, the silicon factory, the cell and the module manufacturing plants, etc.), the energy required for all services (heating, power supply, etc.), and for the construction of all auxiliary facilities should be considered. Furthermore, the energy cost needed to dismantle the plant at the end of useful life and return the area used to its initial state, has to be taken into account.

The EROEI calculation requires a careful "lifecycle analysis" (Life Cycle Analysis, LCA), consisting of a technique, strictly defined by ISO (International Organization for Standardization), to assess the various aspects related to the development of a product and its potential impact on his life. In this regard, it must be noted that, despite the presence of rules, the EROEI calculation for an electric energy production plant is still a complex operation: it requires a large amount of input data and depends in part on estimable quantities that cannot be determined with absolute precision.

In literature, quite dispersed and variable values for EROEI of PV systems can be found for a number of different technologies and conditions of operation [35] [36] [37].

This is due to the influence of the large amount of variables that affect both the estimation of energy expended to build the panel, and the estimation of energy produced by the panel [38], such as the photovoltaic production technology used (Si-mono, poly Si-, Si-amorphous, CdTe, CIS, etc.) [37] [39] [40], the type of system (grid-connected, stand-alone) [41], the plant layout [42], its geographical location [43], positioning [44], etc. [45] [46] [47] [48].

As an example, Figure 19 depicts different values of EROEI for different technologies. Related indicators have also been used by some authors, such as ERF "Energy Return Factor", EYR "Energy Yield Return" or more frequently EPBT "Energy Payback Time", which is an extremely important index showing the time (measured in years) needed for the return on energy investment necessary to the constitution of the system [49] [50] [51].

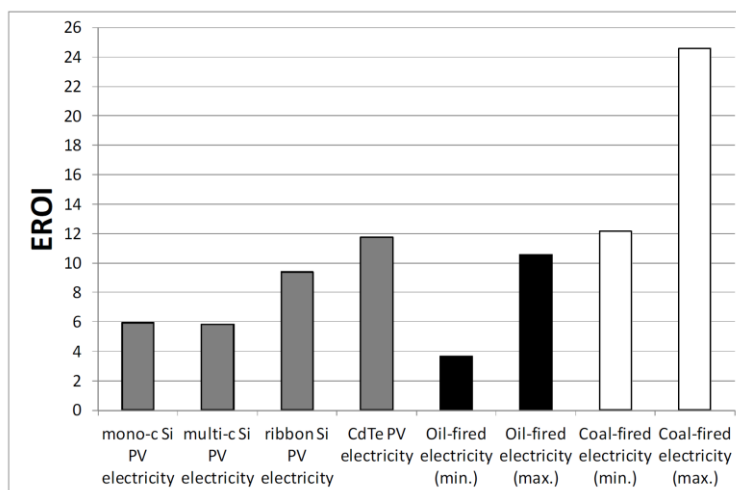


Figure 19 - Comparison of EROEI among new and traditional PV technologies [37]

### 1.3.3.3.2 Evolution of the main economic parameters for photovoltaic plants installed in Italy

Since 2001, the Italian photovoltaic market has been financially assisted with two main incentive schemes in order to support the growth of a niche industry that today shows its maturity being capable to survive without the need of subsidies [52] [53]:

- from 2001 to 2005 the incentive scheme was based on an initial investment of capital [54]: (here after ICO). The purchase cost for the investor was reduced by a government benefit (in many cases corresponding to the 75% of the cost of the plant);
- from 2005 to 2013 the incentive scheme was based on a feed-in-tariff mechanism [6] [7] [8] [9] [10] (here after FIT). The incentives were given on the basis of the energy produced and delivered to the electrical grid [55].

These incentive schemes have given remarkable results: as shown in Figure 20, between 2007 and 2011, the Italian installed PV capacity has grown up to more than 9GWp/year [56]. Cumulative installed power is today greater than 18GWp and PV is capable to guarantee almost the 10% of the total demand of electricity [57]. On 6th July 2013, the governmental incentive plan came to an end and therefore since that date the benefit for the owner of a PV system is represented by the only energy savings.

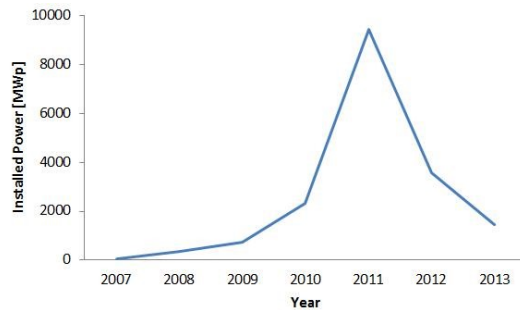


Figure 20 - Yearly installed power in the Italian market

In line with what described in [58] and [59], studies have been conducted in order to show how the main economic parameters involved in the installation of a PV plant - such as the Payback Time (PBT) and the Internal Rate of Return (IRR) - have not significantly changed during the last years even through the rather different regimes of incentives. Moreover, the PBT and the IRR remain unchanged even today considering only the energy savings that are bringing this solar market toward grid parity (i.e. the point where the price of electricity for the end consumer equals the generation cost from PV) for different types of customers. Finally, other two representative scenarios have also been studied and presented: the regime of grid parity associated to the 50% tax-deduction option offered today by the Italian law ("Detrazione IRPEF" [60]) and the regime of grid parity when the 100% of the produced energy is consumed in site.

- **Assumptions**

Below, the main assumptions adopted in the calculation of the PBTs, IRRs and LCOEs are described.

#### *A. Interest rate*

The interest rate represents the cost of the money for he who is going to invest in the installation of a PV plant. With reference to Table 9, the interest rate is set equal to the value of Italian state bonds [61] for the considered year.

Year	Bond interest [%]
2003	4,2
2006	3,6
2013	5,0
2014	3,6

**Table 9 - Interests for Italian state bonds.**

#### *B. Prices of electricity*

The study has been carried out considering the electricity price for a typical Italian family with a 3 kW contract and an electricity consumption not exceeding 2.700 kWh/year. With reference to Table 10, in Italy the end-customer price of electricity is provided by "Acquirente Unico" [62].

Year	Electricity Price [€]
2003	0,170
2006	0,198
2013	0,251
2014	0,253

**Table 10 - Prices of electricity in the Italian residential market - VAT included.**

#### *C. Yield of a photovoltaic plant*

The main economic parameters involved in the operation of the PV plants have been calculated considering different cities representing three representative case studies: Trieste in Northern Italy, Rome in Central Italy and Palermo in Southern Italy. Table 11 reports the mean electricity injected in the electrical grid by the PV plants installed in the considered area [63]. The corresponding weighted yields have been calculated considering a degradation rate of the PV modules equal to 0,68% (corresponding to a standard warranty on the power output for commercial PV modules - 17% of losses in 25 years of operations [64]).

City	Mean Yield [kWh/kWp/year]	Weighted Yield [kWh/kWp/year]
Trieste	1.139	1.027
Roma	1.278	1.152
Palermo	1.371	1.236

**Table 11 - Mean and weighted yields for three representative cities in Italy**

#### D. Photovoltaic plant overnight capital cost

The cost of a PV plant has considerably dropped during the last years. The considered overnight capital cost of a domestic 3 kWp PV plant over the period 2003-2014 is reported in Table 12, VAT included.

Year	Price [€/kWp]
2003	8.500
2006	7.000
2013	2.400
2014	2.200

Table 12 - Overnight capital costs for a 3kWp PV plant installed in Italy over the period 2003-2014

#### ▪ Models

For ICO scenario, the Internal Rate of Returns (*IRRs*) and Payback Times (*PBTs*) have been calculated as follows:

$$PBT = \frac{OCS}{CF_m} \quad (1.1)$$

$$IRR = \frac{CF_m}{OCS} \cdot 100 \quad (1.2)$$

Where *OCS* [€] is the overnight capital cost of the plant, and *CF<sub>m</sub>* [€] is the average cash flow calculated as the weighted yield times the electricity price.

For the FIT scenario, the different *IRRs* and *PBTs* have been calculated applying a cash flow analysis. The net present value *NPV* [€] of the cash flows generated over a period of 20 years has been calculated as:

$$NPV = -OCS + \sum_{k=1}^{20} ICF_k \cdot \frac{(1+g)^k \cdot (1+e)^k}{(1+i)^k} - \sum_{k=1}^{20} OCF_k \cdot (1+g)^k \quad (1.3)$$

Where *ICF<sub>k</sub>* and *OCF<sub>k</sub>* [€] are the incoming and out coming cash flows respectively, *g* and *e* [%] are the general and the energy inflation rates, while *i* [%] is the interest rate. The incoming and out coming cash flows, and the corresponding *IRRs* and *PBTs*, have been calculated as proposed in [58].

The LCOEs for the different years and locations have been calculated - without considering any incentive - with the models proposed in [52]:

$$LCOE = \frac{OCS \times CRF + FO\&MC}{\frac{E_0}{N} \times \sum_{k=1}^N \left( 1 - \frac{d_r \times (k-1)}{100} \right)} \quad (1.4)$$

Where  $CRF$  [%] is the capital recovery factor,  $FO\&MC$  [€] are the fixed operation and maintenance costs,  $E_0$  [kWh/kWp/year] is the mean yield of the plant,  $N$  [ ] is the number of annuities received, and  $d_r$  [%/year] is the degradation rate of the PV modules.

## ▪ Results

### A. Initial Capital Outlay

The Initial Capital Outlay (ICO) mechanism was introduced in 2001 by the Italian government (“Programma Tetti Fotovoltaici” [54]) in order to promote the installation of PV plants. The benefit given to the end-user was, in the most of the cases, a 75% of the overnight capital cost.

Table 13 reports the calculated economic parameters for a 3kWp PV plant installed in 2003 in the three considered locations.

City	PBT [year]	IRR [%]	LCOE [€/kWh]
Trieste	12,2	8,2	0,498
Roma	10,9	9,2	0,444
Palermo	10,1	9,9	0,414

**Table 13 - Payback Time (PBT), Internal Rate of Return (IRR) and Levelized Costs of Energy (LCOE) for three different locations in Italy (Initial Capital Outlay)**

The different LCOEs have been calculated considering the 100% of the overnight capital cost. The number of annuities is 30, that corresponds to widely accepted lifespan for a PV plant, and the FO&MC has been set to a 2%/year of the overnight capital cost.

### B. Feed-in-tariff - “First feed-in scheme”

The feed-in-tariff (FIT) mechanism was introduced in Italy in 2005 with the laws [5] [6] known as “First feed-in scheme” that - for a domestic 3kWp PV plant - guaranteed to the plant owners the following benefits:

- 0,445€/kWh for the produced energy over a period of 20 years;
- the net metering mechanism.

Table 14 reports the calculated economic parameters for a 3kWp PV plant installed in 2006 in the three considered locations.

City	PBT [year]	IRR [%]	LCOE [€/kWh]
Trieste	11,6	8,4	0,381
Roma	10,1	9,6	0,340
Palermo	9,3	10,4	0,317

**Table 14 - Payback Time (PBT), Internal Rate of Return (IRR) and Levelized Costs of Energy (LCOE) for three different locations in Italy (Feed-in-tariff - “First feed-in scheme”)**

Again, the LCOEs have been calculated assuming that no incentives were recognized to the plant owner. The number of annuities is 30 and the FO&MC is the 2% of the overnight capital cost.

### C. Feed-in-tariff - "Fifth feed-in scheme"

The last Italian FIT mechanism, known as "Fifth feed-in scheme" [10] ended in 2013 and, for a 3kWp PV plant connected to the electrical grid in July 2013, guaranteed to the plant owner a tariff of 0,182€/kWh for the energy injected into the grid over a period of 20 years.

Table 15 reports the calculated economic parameters for a 3kWp PV plant installed in 2013 in the three considered locations.

City	PBT [year]	IRR [%]	LCOE [€/kWh]
Trieste	10,1	8,9	0,154
Roma	8,7	10,2	0,138
Palermo	8,0	11,1	0,128

**Table 15 - Payback Time (PBT), Internal Rate of Return (IRR) and Levelized Costs of Energy (LCOE) for three different locations in Italy (Feed-in-tariff - "Fifth feed-in scheme")**

The LCOEs have been calculated assuming that no incentives were recognized to the plant owner. The number of annuities is 30 and the FO&MC is 2% of the overnight capital cost.

### D. Grid parity scenario - NO incentives

The Italian FIT ended in July 2013; after this date the only benefit for the owner of a PV plant is given by the energy savings.

Table 16 reports the calculated economic parameters for a 3kWp PV plant installed in 2014 in the three considered locations. With reference to the self-consumption, it is assumed that the 75% of the produced energy is consumed by the producer. The remaining 25% is collected by the grid operator at a conventional price set to 0,106€/kWh [65]<sup>6</sup>.

City	PBT [year]	IRR [%]	LCOE [€/kWh]
Trieste	10,6	9,1	0,120
Roma	9,3	10,4	0,107
Palermo	8,5	11,3	0,100

**Table 16 - Payback Time (PBT), Internal Rate of Return (IRR) and Levelized Costs of Energy (LCOE) for three different locations in Italy (Grid parity scenario, NO incentives)**

The LCOEs have been calculated assuming that no incentives were recognized to the plant owner. The number of annuities is 30 and the FO&MC is 2% of the overnight capital cost.

As an example, Figure 21 shows the cash flow analysis for a PV plant connected to the electrical grid in 2014 in Rome. After nine years, and for the entire lifespan of the system

---

<sup>6</sup>Data are referred to 2013.

(more than 30 years), the cost of electricity for the PV plant owner corresponds to the fixed operation and maintenance costs (i.e. circa the 10% of the original electricity bill).

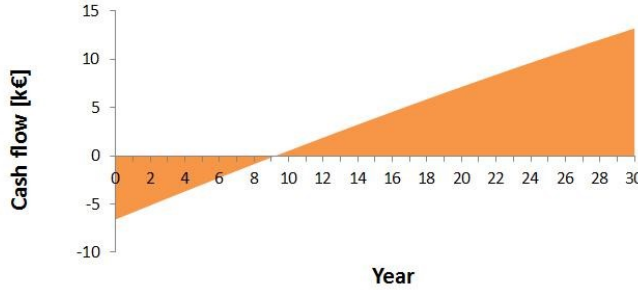


**Figure 21 - Cash flow analysis over 30 years of operation for a 3kWp PV plant installed in 2014 in Rome  
(Grid parity scenario, NO incentives)**

#### E. Grid parity scenario - 50% tax-deduction

Today, the 50% of the overnight cost of the PV plant is tax-deductible along 10 years [60]. This mechanism is known as “Detrazione IRPEF”. Considering this tax-deduction, Table 9 reports the payback times and the internal rates of return for a 3kWp PV plant installed in 2014. With reference to self-consumption, it is assumed that the 75% of the produced energy is consumed by the producer. The remaining 25% is collected by the grid operator at a conventional price set to 0,106€/kWh [65].

City	PBT [year]	IRR [%]
Trieste	6,9	11,6
Roma	6,4	12,9
Palermo	6,0	13,8

**Table 17 - Payback Time (PBT), Internal Rate of Return (IRR) and Levelized Costs of Energy (LCOE) for three different locations in Italy (Grid parity scenario, 50% tax-deduction)**

As an example, Figure 22 shows the cash flow analysis for a PV plant connected to the electrical grid in 2014 in Rome.

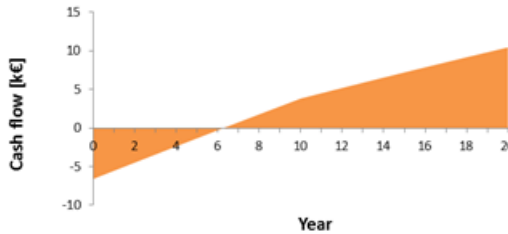


**Figure 22 - Cash flow analysis over 30 years of operation for a 3kWp PV plant installed in 2014 in Rome (Grid parity scenario - 50% tax-deduction)**

The tax-reduction guarantees to the owner of the PV plant very low electricity costs (circa the 10% of the original electricity bill) after only six years of operations.

#### D. Grid parity scenario - 100% self-consumption - NO incentives

In this case it is assumed that the 100% of the produced energy is consumed by the producer. This represents a common assumption for PV plants connected to electrical grids serving C&I size customers (such as, for example, an University campus [66] [67] or in general a public administration).

Table 18 reports the calculated economic parameters for a 3kWp PV plant installed in 2014 in the three considered locations.

City	PBT [year]	IRR [%]
Trieste	8,8	10,9
Roma	7,8	12,5
Palermo	7,1	13,5

**Table 18 - Payback Time (PBT), Internal Rate of Return (IRR) and Levelized Costs of Energy (LCOE) for three different locations in Italy (Grid parity scenario - 100% self-consumption - NO incentives)**

The LCOEs have been calculated assuming that no incentives were recognized to plant owners. The number of annuities is 30 and the FO&MC is 2% of the overnight capital cost.

As an example, Figure 23 shows the cash flow analysis for a PV plant connected to the electrical grid in 2014 in Rome.

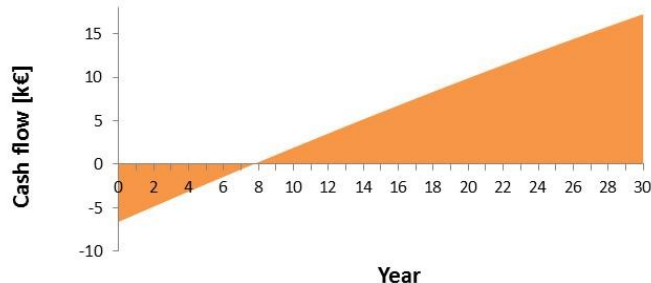


**Figure 23 - Cash flow analysis over 30 years of operation for a 3kWp PV plant installed in 2014 in Rome (Grid parity scenario - 100% self-consumption - NO incentives)**

In this case the capacity of using all the produced energy guarantee to the public administration/C&I size customer very low electricity costs (circa the 10% of the original electricity bill) after eight years of operations.

- **Conclusions**

The results show that the PBTs and the IRRs have remained more or less constant in the considered period and that today are even more attractive than in the past when the electricity produced by the PV plants was subsided by the government. This is mainly due to the cost of PV modules that have recently dropped tremendously (99% in the last thirty years). As a consequence, the Levelized Cost Of Energy (LCOE) shown in Figure

5 (one of the key indicators for comparison with other power generation technologies) is today still falling off. It is worth noting that no incentives have been considered in the results shown in Figure 24.

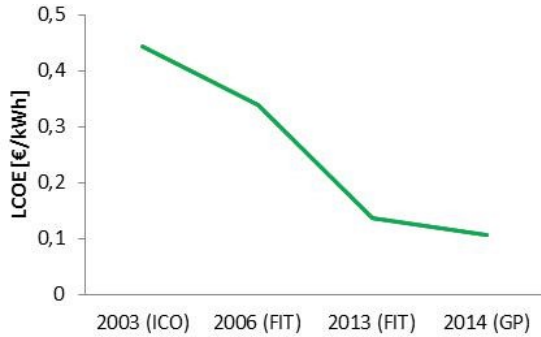


**Figure 24 - Evolution of the Levelized Cost Of Energy in the Italian market over the period 2003-2014**

Of particular interest are the cases considering the “Detrazione IRPEF” scheme and the 100% self-consumption scenario (C&I size customers like, for example, a University campus) that show very interesting opportunities for electricity costs savings.

For these reasons, the slowdown of the market shown in 2012 (Figure 20) does not seem to be directly related with economic factors and thus to be only indirectly connected with the end of the feed-in-tariff program.

Further studies involving non-technical and non-economic factors are needed to analyze the reasons behind such a discontinuity.

## **1.4 Recent changes in electrical systems**

From what described in previous paragraphs it can be said that in recent years several factors lead to an increase in the exploitation of renewable energy resources (PV, wind and others) and to a better utilization of fossil fuels resources through cogenerative power plants that are often implemented with small and medium size generators located near the loads:

- governments have enacted policies like the European climate and energy packet known as the 20-20-20 targets;
- the liberalization of electricity markets augments the possibility for investments in the production of electrical energy also with small capitals and therefore small size generators;
- the constant increase in electrical energy consumption and in the costs for traditional fossil fuels.

The new paradigm for the generation and distribution of electrical energy is no longer based on big centralized power plants but rather it is characterized by:

- geographically distributed generators;
- small and medium sized generators and
- generators mainly connected to LV and MV distribution networks.

### **1.4.1 Problems and open issues of DG**

The features of present electrical systems together with the rapid development of non-programmable renewable sources is implying economic and technical problems (that may affect the security of the electrical system) partly associated with the uncertainty of the sources. As seen in the previous paragraphs RES energy production is influenced by a multiplicity of factors (seasonality, diurnality, intermittence, anemometric conditions, technical problems like maintenance, the lack of production) that make power plants based on RES difficult to plan and dispatch.

The potentially more critical situations may present in the summer day periods in low load days (like holidays) when photovoltaic production is very high.

The main issues are described in following paragraphs.

#### 1.4.1.1 Issues related to electrical markets and dispatching

With reference to the Italian case, it is possible to observe that the spread of renewable energy plants, characterized by uncertainty of the source and virtually zero variable costs, has caused several problems related to electrical markets and dispatching:

- *Considerations on market prices*

The price profile of the Day Ahead Market has changed: until 2011 the highest prices were formed during the day - in correspondence with the maximum electricity demand in the network; currently the highest prices are formed in the early evening hours (17-21), or in the hours when photovoltaic production gradually ceases, compared to the hours when such production is present (Figure 25).

Thermal power plants must agree to produce at lower prices than the variable costs [24] [68] in order to:

- remain in operation during the day (due to their technical operating constraints) and
- be available to produce in the evening (where the PV production vanishes).

The share of variable costs not covered by daytime or early morning prices should therefore be covered by evening hours prices - this contributes to explain the increase in energy prices in those hours.

The overall average annual Single National Price (SNP) amounted to 64,12 €/MWh in 2010, 72,23 €/MWh in 2011, 75,47 €/MWh in 2012, 62,99 €/MWh in 2013, 52,08 €/MWh in 2014 and 52,31 €/MWh in 2015<sup>7</sup>.

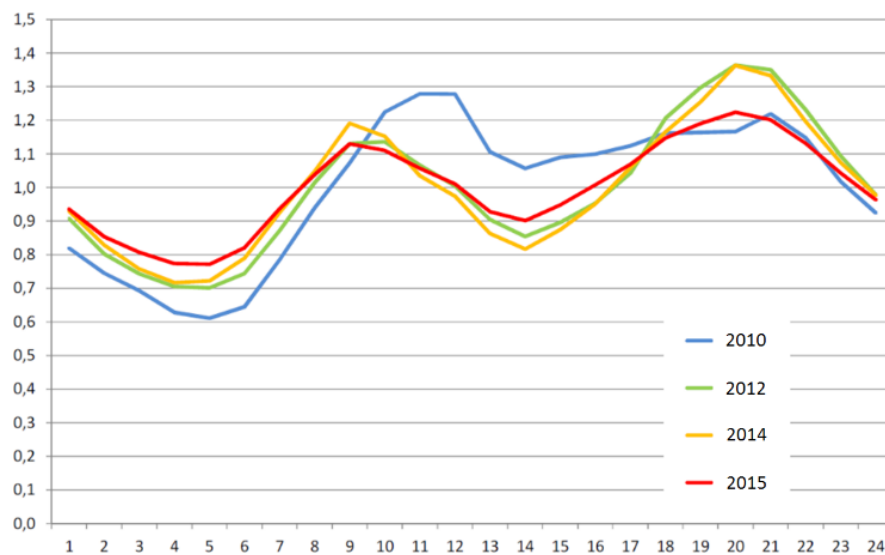


Figure 25 - Ratio between average hourly SNP and overall average SNP [24]

<sup>7</sup> In this regard, it must be remembered that the electricity market prices depend also on the trend of the natural gas price

- *Efficiency decrease of traditional power plants*

The programmable plants are used with an increasingly limited number of hours and with the purpose to cover load peaks.

As well known, thermal power plants are not characterized by flexibility in the modulation of the supplied power. The partial load operation and the continuous starts and stops (or load changes) lead an efficiency decrease, as shown in Figure 26 [24] [68].

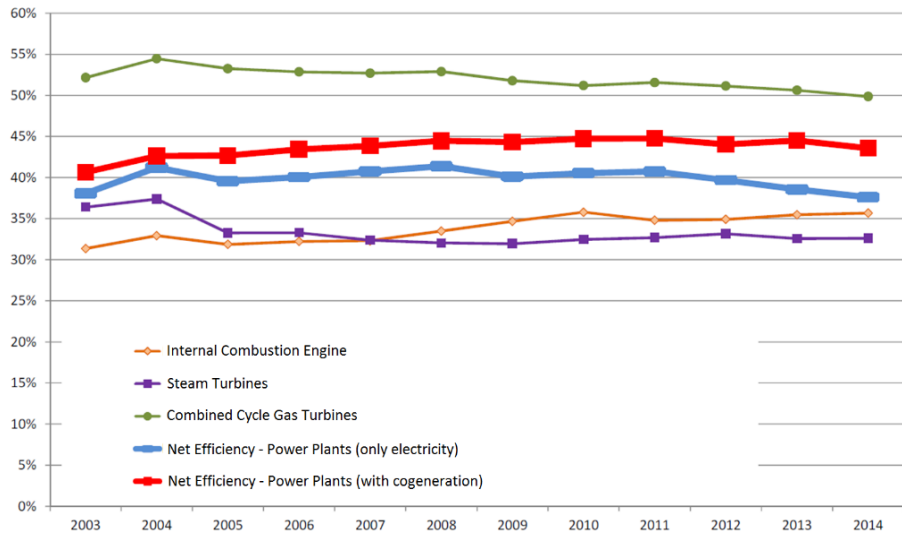


Figure 26 - Trend of the net efficiency of the Italian production power plants [24]

- *Difficulty in setting up reserve margins*

RES power plants influence both the phase of planning of the Dispatching Services Market and the real-time management of the same market - called "Balancing Market", mainly due to the fact that:

- the variability of the level of production of non-programmable plants creates great difficulties in the production forecasting of such plants;
- the trend of zonal time loads to be satisfied by means of generation from programmable plants are significantly modified by the production profiles of non-programmable renewable source plants.

The high penetration of plants fed by non-programmable renewable sources implies the reduction of residual loads to be satisfied by programmable plants, with the consequent need to increase the reserve capacity, to compensate the possible unavailability of RES [24].

Besides, in order to pursue the ramps (evening and morning) fast balancing actions are needed: actions made by programmable plants with high modulation skills, rapid response times and negligible permanence restrictions in day and night service [68] [69].

For example, Figure 27 shows the comparison between the situation in April 2010 and April 2015:

- The continuous curve represents the overall load profile;
- The yellow zone represents the energy injected by renewable energy plants;
- The dotted curve represents the residual load profile, to be satisfied by programmable plants.

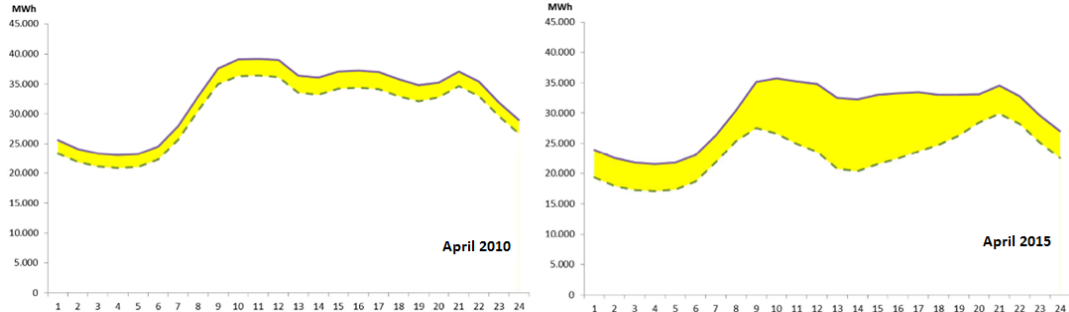


**Figure 27 - Comparison between the situation in April 2010 and April 2015 (monthly average values) [24]**

The shape of the load diagram is remarkably different, particularly on Saturday and Sunday in afternoon times. In the southern area (Figure 28), in some hours of the day, the production of photovoltaic and wind power plants results to be even higher than the total load (currently also on weekdays). Under such conditions, a reduction of the photovoltaic and wind power generation becomes necessary if such production cannot be transported elsewhere and if in the neighboring areas there are no sufficient plants for compensate the possible unavailability of the random sources [68] [69].

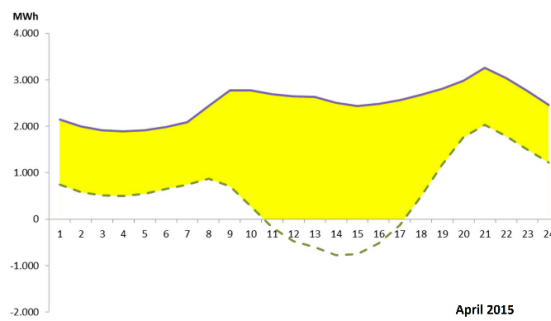


**Figure 28 - SUD Zone in April 2015 (working days) [24]**

#### 1.4.1.2 Weakening of reactive power capability

Currently, the Secondary Voltage Regulation (SVR) implemented in some countries in HV networks [70] [71] [72], involves traditional power stations (based on fossil fuels) and large hydroelectric power plants, while most of new renewable energy plants are not involved. Thus, existing voltage control systems decrease their controlling capability when new RES generators replace equivalent amounts of power of conventional thermal power plants [73].

#### **1.4.1.3 Stability of power electric systems**

The stability of power electric systems is influenced, at different levels by:

- ***Frequency transients due to events on HV network***

Frequency transients on the inter-connected transportation network (national and/or European), generated for example by load variations, disconnection of generators, lines disruptions, are generally compensated by generators having the necessary regulating capacities [74].

The wide spread generation units connected to the MV and LV distribution networks have not been asked such regulating services (and therefore they do not take part in frequency regulation). In addition, they gain the privilege of dispatch priority.

Under circumstances of minimum load such condition involves a deficit of regulating power with the risk of a stability loss of the network in case of transients and/or disservices on the interconnected transmission network.

Indeed, DG plants, in particular the photovoltaic, still present protection systems set so as to call for disconnection whenever frequency goes beyond the accepted interval. In case of a network accident with substantial frequency variations, a generation loss equal to the whole DG ("domino" effect) occurs, thus making the activation of the plan of load lightening necessary.

- ***Voltage dips due to events on HV***

Similarly to frequency transients, a voltage drop on HV network caused for example by a multiphase or single ground fault is transmitted on lower voltage networks. The Interface Protection System (IPS) of all distributed generators detects a voltage lower than the accepted limits thus causing the disconnection of the whole DG<sup>8</sup> [74].

The same phenomenon may occur on a MV network but with effects limited to the single fault and therefore negligible for the security of the global electric system.

#### **1.4.1.4 Formation of undesired islands**

When because of an ordinary power supply failure (because of the intervention of protections or maintenance operation) in a distribution network, DG could maintain the voltage of the same grid, an undesired island or *islanding* takes place [75].

For instance, taking into consideration the case reported in Figure 29, if for whatever reason the general control switch opens and PV plants are able to feed the load without provoking an appreciable variation of voltage and frequency, then the IPS of the DG does not intervene and as a result the system keeps functioning at nominal voltage and

---

<sup>8</sup> Such kind of faults on HV networks can be removed in 100-200 ms

frequency even if totally disconnected from the network and therefore out of the control of DSO.

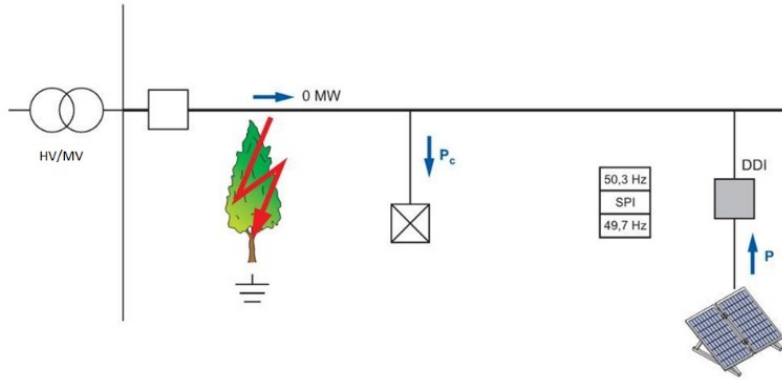


Figure 29 - Distribution network operating in island [74]

The formation of an island is an undesired phenomenon since it shows some inconveniences:

- The formation of an island is primarily a danger for they who have to intervene on the line considered out of voltage because the circuit breaker is open;
- The short circuit protection ceases to exist since in the island only the MV users' protective devices are present: the short circuit currents values are much lower than the ones present in ordinary power supply (for which the switches are sized); besides there does not exist any coordination between such protections;
- The same can be said for ground single-phase fault currents which may have too low values to determine the intervention of users' earth protections;
- Voltage and frequency control would be allocated to local generators, not mutually coordinated and not designed to the aim: in this respect it must be remembered that the island frequency will never be exactly the same to the one of the interconnected network and therefore a discrepancy between the network voltage and that of the island can occur. Such discrepancy may be very high<sup>9</sup> with possible damages to inverters, to synchronous generators, to distributor's switches and possible damages to users consuming appliances, on closing the distributor's switches [74].

---

<sup>9</sup> In some cases, it might even reach the so-called antiphase reclosure

#### 1.4.1.5 Power flow inversion and voltage profile changes

In some areas of distribution networks for some periods of time the produced energy which has not been consumed locally can be transmitted in the opposite direction to the traditional one, that is going back from LV towards MV and from MV towards HV (power flow inversion) [76].

Indeed a DG providing power higher than the one required locally determines a power flow inverted from the secondary winding to the primary winding of a transformer HV/MV or MV/LV (Figure 30).

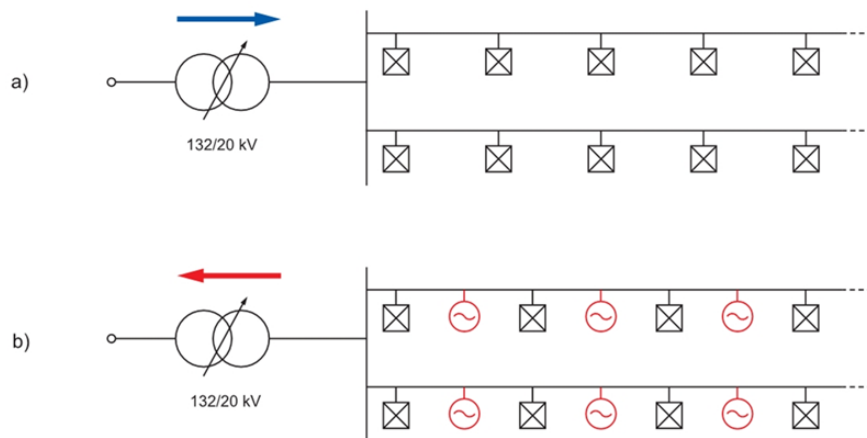


Figure 30 - a) power flow goes from primary station towards passive users; b) in presence of DG the power flow may be inverted [74]

In addition to this phenomenon, the active power injected by distributed generators determines the change to voltage profile in the distribution network (Figure 31) with voltage growth at the end of branches [77] [74]. The higher the ratio generation/load, the weaker the network and as a result the more frequent the phenomenon.

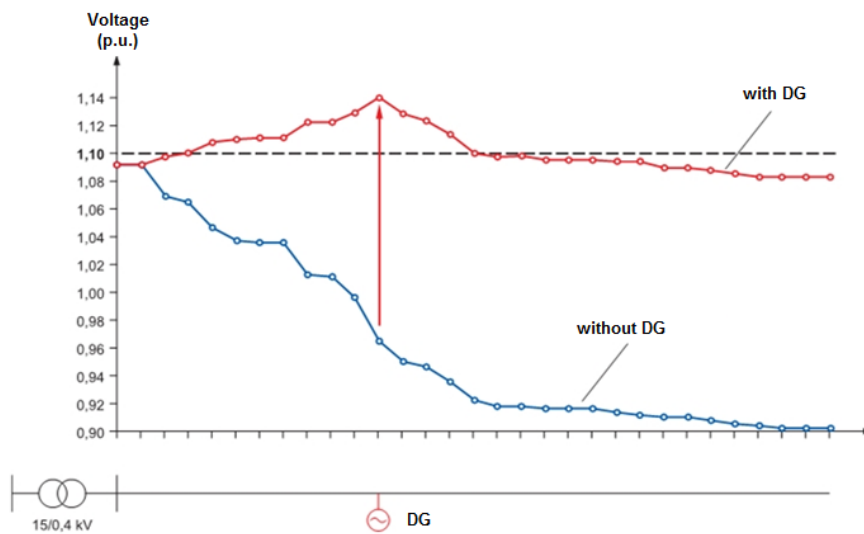


Figure 31 - Distribution network voltage profile with or without DG presence [74]

#### 1.4.1.6 Increase of fault currents

The connection of DG in distribution networks implies an increase of short circuit current (and therefore of short circuit power) in the same network. The installation of distributed generators in the network should therefore be coordinated to an updating of the short circuit current calculations [75].

This is required to ensure the short circuit currents do not exceed the network protection interruption power and the contribution of generators may not provoke the untimely intervention of the protections of maximum current set at the start of the lines [78].

#### 1.4.1.7 Selectivity of protections

The presence of DG on distribution networks creates a further problem of selectivity in the maximum current protection installed in primary substation to protect the various feeders [79].

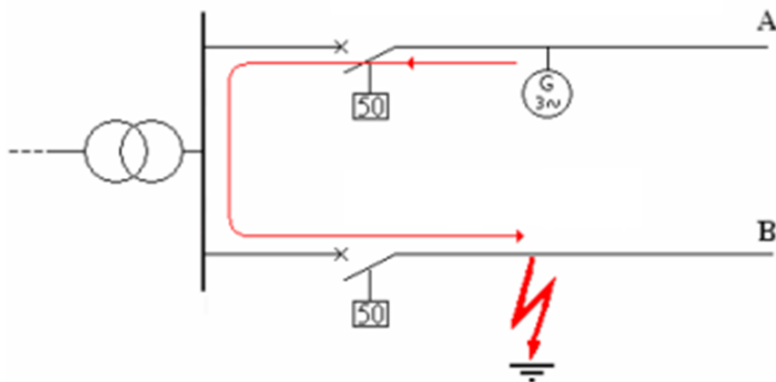


Figure 32 - Untimely disconnection on a safe line in DG presence

Considering for example the diagram of Figure 32, if a fault on line B is present, the DG present in line A will contribute to the same fault with a current that will be detected from the protection of maximum current of the same branch. If the level of the current supplied by DG of the safe line is such as to exceed the threshold of protection intervention the line switch will open even in absence of faults on the same line [78] [75].

### 1.4.2 Positive aspects and opportunities related to DG

In addition to the several problems introduced by the DG there are also some benefits. In fact, DG offers also several potential benefits that affect all of the energy sector, as for example:

- reduction of environmental impact and lower CO<sub>2</sub> emissions;
- possibility of producing energy close to load centers - savings in electricity transmission and distribution costs;
- the small size of generators guarantees modularity and flexibility in the choice of sites, which limit the risk of exposure of capital;
- attenuation of financial risk caused by the uncertainty of fuel costs and energy demand.

In particular the presence of generation in the distribution network can also lead to beneficial effects especially on the power losses in the distribution network, besides the various environmental advantages as described in [80] [81] [82] [83] [84] [85].

In general, the DG leads to a reduction of electricity transits in electric system [24], both in the distribution network to which the DG is connected and in the upper voltage network. This is true if [24]:

- there are not power flow inversions in transformation cabins;
- distributed generators are relatively close to load centers;
- the power injected into the grid, hour by hour, is less than the total absorbed by the loads fed by the line itself.

Power losses in electric grids are caused by active and reactive power flows through line resistances; the magnitude of the losses depends on the amount of current flow and the line resistance. This kind of losses can be called "Active Power Losses" (APL), and can be calculated as follow:

$$APL = R_{line} \cdot I_{load}^2 = \frac{R \cdot (P_{load}^2 + Q_{load}^2)}{3 \cdot V_n^2} \quad (1.5)$$

Where:

- $APL$ : Active Power Losses [W]
- $R_{line}$ : Line Resistance [ $\Omega$ ]
- $I_{load}$ : Load Current [A]
- $P_{load}$ : Load Real Power [W]
- $Q_{load}$ : Load Reactive Power [VAR]
- $V_n$  : Nominal Voltage [V]

Otherwise “Reactive Power Losses” (RPL) may be defined as the reactive power absorbed by the network components (line inductance, transformers, etc.).

For the simple network of Figure 33, the APL have been calculated varying the position and the power of a generator (while the loads are kept constant) and are shown in Figure 34.

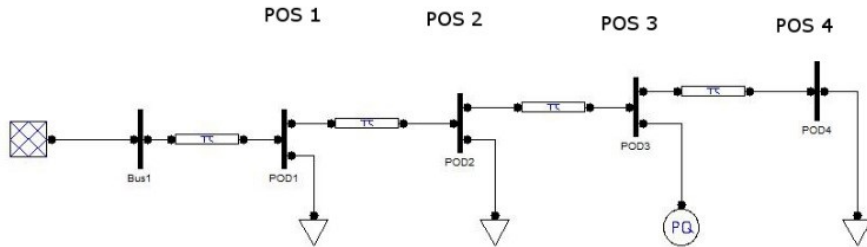


**Figure 33 - Simple test network (i.e. generator in position 3)**

From Figure 34, it can be stated that: APL are scarcely influenced by generated power when the generator is near the busbar. APL decrease when the generation is near the load, and under this condition, APL increase when production exceeds the load. Therefore, the optimal connecting point of a generator depends on the loads, on the generation levels and of course on the physical characteristics of the network.

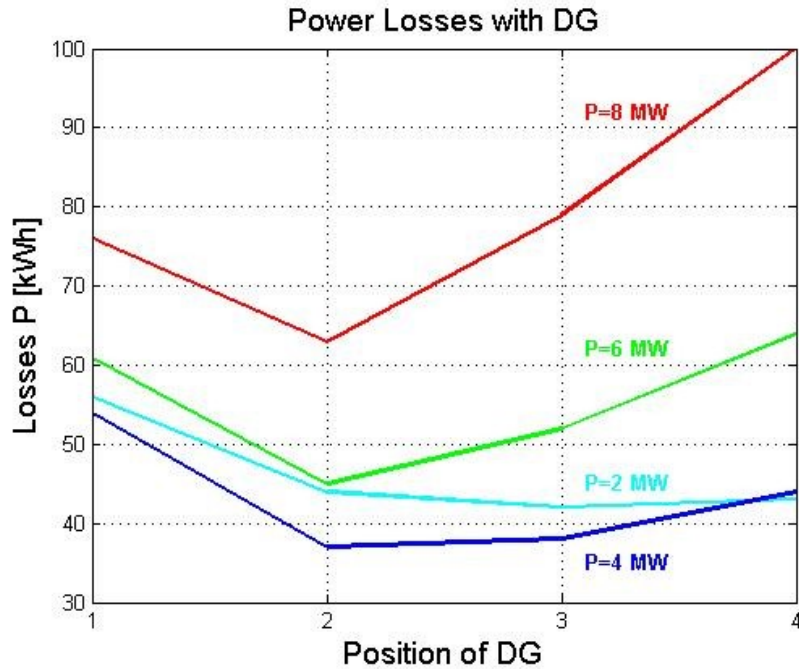


**Figure 34 - Power losses as a function of DG position.**

#### 1.4.2.1 Impact of DG on power losses on a real-world distribution network

In this paragraph are reported the studies conducted on the effects of the new connection of a generator to a real-world LV distribution network [86]. Such studies have been conducted to evaluate the losses of a real distribution network in order to satisfy the demands of the Italian Authority for Electricity and Gas<sup>10</sup> [87].

Furthermore, a new approach based also on minimizing active power losses when planning the connection of distributed generators is proposed.

- *Case Study*

An actual real-world LV distribution network has been considered to study the APL on different situations regarding the DG penetration. It is constituted by 125 Points Of Delivery (PODs), some of which are active. The data of the network, the loads and generators were provided by DSO.

In order to conduct such studies the model of the investigated network was first carried out and Figure 35 shows one of the four main feeders of this network.

Loads have been expressed using static PQ constant models. The model of the network takes into account neither the unbalanced loads nor the neutral conductor: i.e. the network has been modelled through its positive sequence single phase equivalent model.

The line styles used in in Figure 35 refer to the seven cable types illustrated in Table 19.

Line Type	Graphic symbol	R	I	c
		[Ohm/Km]	[mH/Km]	[μF/Km]
Type 1	 240 Cu	0,047	0,315	0,390
Type 2	 70 Al	0,075	0,350	0,320
Type 3	 35 Al	0,124	0,350	0,270
Type 4	 10 Cu	0,125	0,318	0,330
Type 5	 6 Cu	0,206	0,350	0,270

Table 19 - Cable types and data

---

<sup>10</sup> Between the end of 2013 and early 2014, the Italian Authority for Electricity and Gas has requested to the various Italian DSOs to evaluate the losses existing in their distribution networks. These studies, initially only required for HV and MV networks and further even for LV networks, allow the identification of areas with excessive losses, in order to plan corrective actions.

---

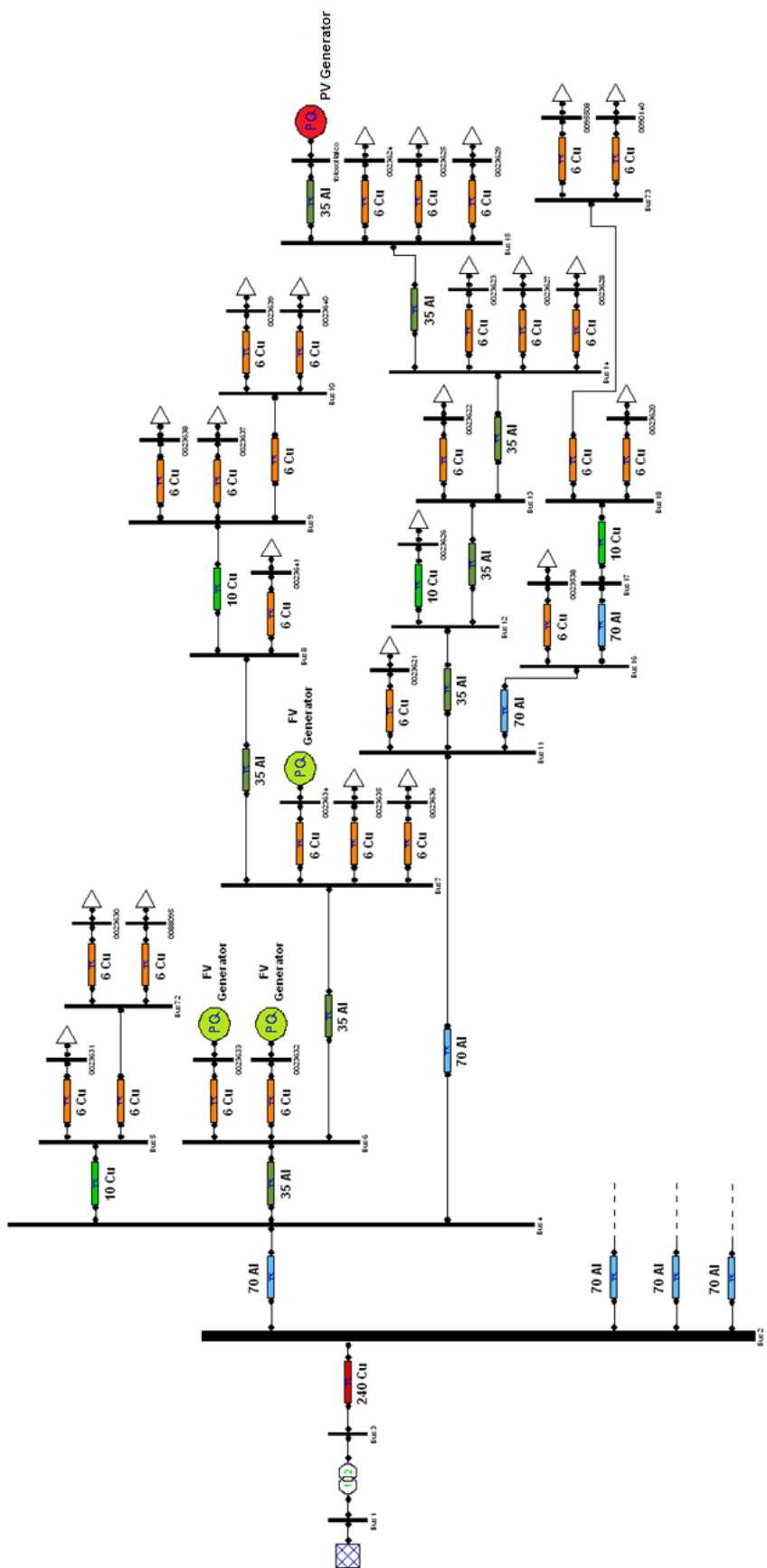


Figure 35 - Actual LV distribution network used in the case study

#### ▪ *Simulation Results*

Starting from this model, three main scenarios have been considered:

- scenario I: network feeding loads without presence of DG;
- scenario II: network feeding loads with DG connected to the network;
- scenario III: starting from scenario II, a new DG unit is connected in certain nodes indicated by the DSO. Simulations were therefore carried out to determine the best location for the new DG unit in terms of reduction of network losses.

All simulations have been carried out using DOME [88] - described in Appendix A1.2 - and network components have been modelled as shown in [89]. As an example, Table 20 reports the results of the simulations for one month - load data are sampled for each hour, therefore 720 load flow have been calculated. It can be inferred that in the month considered, the distributed production of 7961 kWh has brought to a decrease of active power losses by 20%.

	Scenario I (without DG)	Scenario II (with DG)
Total active energy through HV/MV Transf. [kWh]	20833	12765
Total active energy through HV/MV Transf. [kVARh]	9964	9935
Total active load [kWh]	20305	12344
Total reactive load [kVARh]	9847	9847
Total active losses [kWh]	528	421
Total reactive losses [kVAR]	116	87

Table 20 - Energy flows

#### ▪ *Optimal Placement*

Regarding the third scenario, although several algorithms have been presented for optimal allocation and sizing of DGs in distribution network (e.g. [90] [91]), a more practical approach has been followed in this study. From the knowledge of DSO, some possible points of connection have been identified. Among them, the connection point has been found simulating the network with the historical data of the loads (and of other generators) and the forecast of production of the new generator. As an example, the PV generator, represented by the red PQ block, can be connected to several other buses.

Iterating the multiple power flow (one for each hour) over the set of possible point of connection a table with the active power losses for each bus can be made:

Bus	Active power losses [kWh]
Bus 9	425,96
Bus 10	426,34
Bus 14	420,78
Bus 15	420,91
Bus 17	420,52
Bus 78	420,97

Table 21 - Results: Active power losses for each bus

From Table 21 it follows that the optimal position for the connection of a new generator is Bus 17. It is worth noting that networks in DOME are text files and can be modified with a simple shell script. Therefore, the iteration of the power flow over the buses of possible connection is a simple *for-cycle* in bash script.

- ***Concluding Considerations***

Studies carried out have confirmed the positive effect of DG in an actual real-world LV distribution network.

Furthermore, it has been shown that simulations with power flow software tools can greatly improve the design and management of such networks.

## Chapter 2.

# The evolution of the network towards Smart Grids

Considering what highlighted in the previous chapter it can be said that the wide spread generation has turned upside down the traditional scheme of electric energy distribution and posed a series of new problems. The features of the present MV and LV distribution networks, together with the application of the *fit & forget* criterion limit the possibility of a massive expansion of DG since, being DSO unable to control DGs, they are compelled to contain the quantity of generators to be installed in the same network [22].

Such limit might be enlarged if generators may be asked to modify their operation state according to the needs of the network thus collaborating to the operation of the same network. A DSO must therefore be able to reconfigure the networks and intervene in the operation of generators and their related loads however guaranteeing efficiency and the maximization of renewable sources.

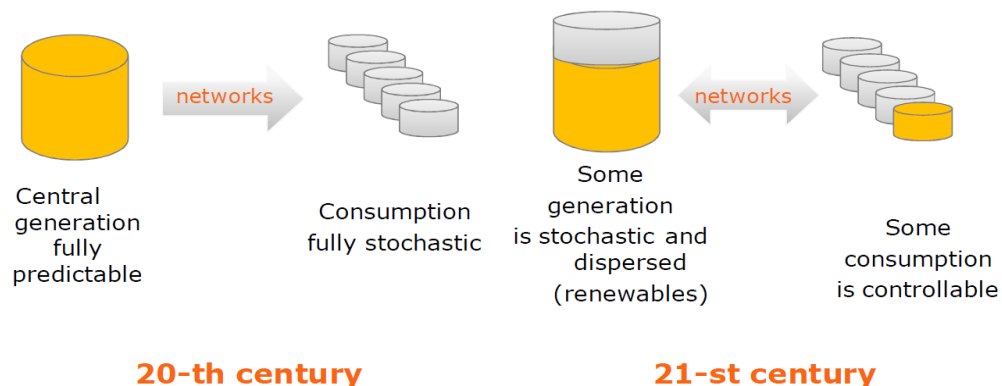


Figure 36 - Change in the optimization paradigm of the whole electric system: generation and load controlled (orange) and uncontrolled (grey) [92]

Figure 36 provides an insight of the way DG units can take part in the management of electric networks controlling the operative conditions of generation and load.

In order to carry out such paradigm, a grid development integrating ICT and a strong presence of distributed calculation systems is needed (Figure 37).

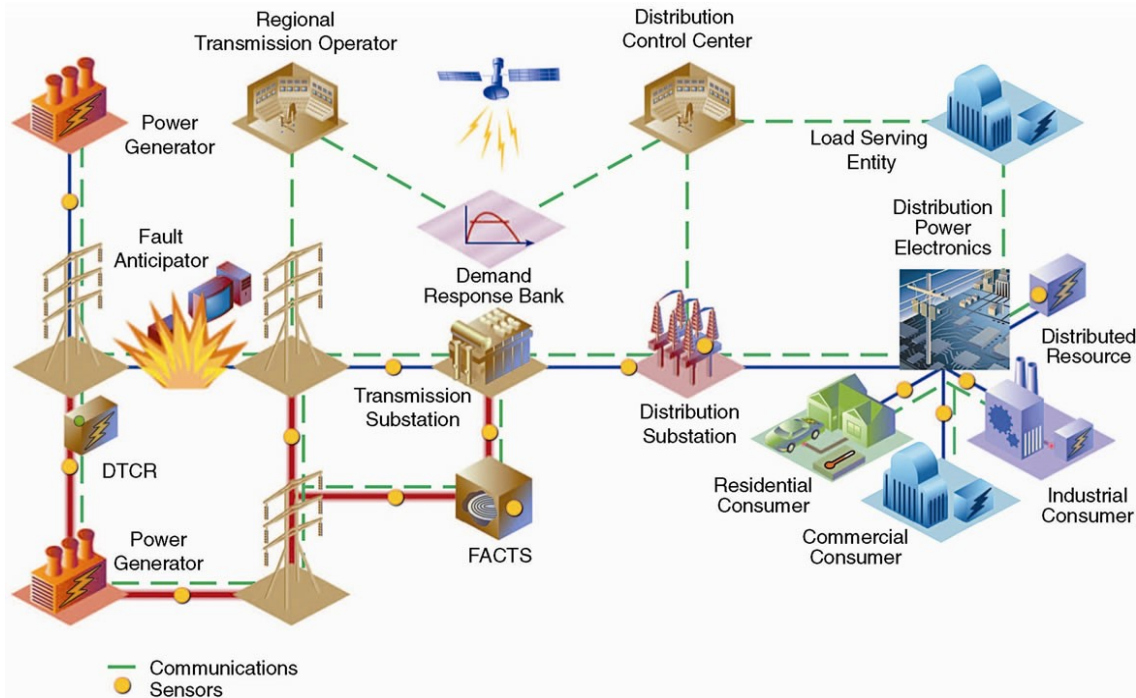


Figure 37 - Smart Grid Model [93]

The evolution towards "Smart Grids" is therefore essential to receive generation from renewable source and at the same time guarantee the maintenance of adequate levels of reliability and quality of service [94] [95]. This evolution requires information communication technologies as main ingredients: coordination between loads, generators and controls occurs through the communication of data.

The communication should often take place in real-time (where real-time here means with a delay superiorly limited, for interested readers more can be found in [96]).

Real-time constraints specifically for electric power systems have been detailed in [97]. In Table 22 some issue concerning DG are summarized.

Application	Bandwidth	Latency
Substation Automation	9.6-56 kbps	15-200 ms
Outage management	56 kbps	2000 ms
Distribution Automation	9.6-56 kbps	20-200 ms
Distribution Management	9.6-100 kbps	100 ms – 2 sec
Distribution Energy Resource Management	9.6-56 kbps	300 ms – 2 sec

Table 22 - Requirements of Smart Grid applications [97]

Such constraints depend on the type of application and the amount of data exchanged. Considering the latency as first issue, it can be said that the expected latency varies from tens of milliseconds to some seconds.

This order of magnitude in the delays can be satisfied with many of the communications technologies used in other areas (e.g. office automation, industrial automation, internet).

Therefore, in the last decade there is a growing use of protocols and technologies commonly used for local area network communication and wide area communication (i.e. the Internet network).

Concerning the physical layer, in the last years, there has been a development of several technologies [98]. Table 23 summarizes the ones that are relevant for power system and particularly for DG coordination.

Technology	Standard/protocol	Max data rate	Coverage range
Fiber optic	PON/WDM/SONET	2Gbps - 10Gbps	Up to 100 km
Ethernet	802.3x	10Mbps - 10 Gbps	Up to 100 m
PLC		10kbps - 200 Mbps	Up to 3 km
WiFi	802.11x	Up - 600 Mbps	Up to 100m
WiMax	802.16	75 Mbps	Up to 50 km
Cellular	2G to 4G	14.4 kbps - 100 Mbps	Up to 50 km
Satellite		1 Mbps	100 - 6000 km

**Table 23 - Comparison of communication technologies for Smart Grid [98]**

As an example in [99], measurements of a very common protocol used in power systems distributed network (DNP3), implemented on top of TCP/IP, are shown. In [100] it is shown how a secure and high performance communication service can be built on top of TCP/IP protocol stack to be used in Smart Grid applications.

Coordinated energy sources for voltage control on a regional scale have been studied also in [101] where a wireless technology for the communication has been proposed and tested (i.e. LTE) together with the application of QoS.

In particular, through some measurements latency has been attested to be around tens of milliseconds.

The algorithms that will be proposed in this work require a communication infrastructure with several characteristics. The analysis of the communication required for DG integration is out of the scope of the present thesis but, considered the cited examples, it can be argued that the implementation of such communications is already possible and technology is ready for that.

## **2.1 The future of the distribution network – the new role of DSO**

From what reported in the previous paragraphs, the increase of DG typically linked to renewable sources and therefore highly intermittent and scarcely predictable, implies related difficulties in a context of safe management of the electric system as well as the need of normative, regulatory and technical changes in transmission and distribution systems.

A condition shall be predicted in which on the local level DSO undertakes tasks and responsibilities of the assigned role that on a national scale are attributed to TSO. The operator of the distribution network will therefore turn into a kind of "local dispatcher" involving both active and passive users in the supply of services functional to the optimization of the operative conditions of the network, as for instance the voltage regulation, the supply of reactive power and the storage provision [102] [103].

Currently the SCADA systems installed in the DSO control centers supply - generally in real time - only information related to transformer cabins (active power, reactive power, voltage and current) and the condition of the maneuvering and protection devices upstream to each feeder. In the new role of "dispatcher" of the related distribution network, DSO will have to be able to manage and control the network in real time and consequently the interaction with the ICT world will be essential. It follows that the acquisition of dedicated information tools and the provision of suitable communicative channels with the network users play a fundamental role [102].

Also functions traditionally typical of EMS (Energy Management System) for transmission grids<sup>11</sup> like for example the evaluation of the condition and the analysis of contingencies will have to be integrated in DMS (Distribution Management System). Indeed, ahead of any calculation, analysis and commanding signal dispatch to the submitted system, a function of "state estimate" is required similar to the one suitable for transmission systems. Such estimate is similar to the one available for transmission systems that allow knowledge of the consistency and topology of the distribution network, the state of any switch and circuit breaker, the voltage on each bar of secondary cabins and the current on each *feeder* [102].

In transmission networks the algorithms of condition estimate are used to calculate the voltage at each node and as a result the current in each line and system transformer. For transition networks an adaptation of the algorithms of the condition estimate to applications for the distribution networks is surely necessary considered that such algorithms require a particularly high set of measures that make them unworkable to

---

<sup>11</sup> Along the years EMS and DMS have developed as two distinct branches of the control centers that make use of systems of acquisition and control of data (SCADA).

distribution networks, unless measuring and communication systems are deeply reconsidered and updated.

In this respect it is worth considering that rule IEC 61850 [104] is being researched for the definition of the communication systems and signal protocols to adapt for the data exchange between DSO and users of the distribution networks.

## **2.2 Regulatory environment, operation and security of the electric systems with DG**

The problems introduced by DG, analyzed in the previous chapter, were addressed by the regulatory bodies both at national and European level in order to achieve appropriate rules able to support the development of DG.

### **2.2.1 European regulatory environment**

Until now at European Level a lack of regulatory harmonization between EU Member States is confirmed. National initiatives have prevailed on those at EU level: the change of the paradigm of production has required the introduction of new specific connection rules for DG systems and the adaptation of grid codes in several European countries [105] [106] [107].

However, considering the urgency of the situation, the European Parliament with Regulation EC n. 714/2009 has required all Transmission System Operators (TSO) to collaborate through the European Network of Transmission System Operators for Electricity (ENTSOE [108]) for the definition of a new European Network Code based on a list of yearly priorities defined by ACER<sup>12</sup> (Agency for the Cooperation of Energy Regulators [109]) that will become a supranational legal act and will consequently prevail over the national ones<sup>13</sup> [110] [111].

The Agency's overall mission, as stated in its founding regulation, is to complement and coordinate the work of national energy regulators at EU level, and to work towards the completion of the single EU energy market for electricity and natural gas.

ACER develops a vision on changes needed on a particular energy subject. This results in ACER issuing a framework guideline, after which ENTSO-E is invited to draft a related network code<sup>14</sup>. The network codes are then assessed by ACER to ensure they are in line with the framework guidelines: if ACER deems that the code fulfils its framework guidelines and the EU's internal market objectives, and is fair and balanced, it recommends that the Commission adopt the code. Finally, the network codes go through the Comitology procedure, where they are scrutinized and agreed by Member States, before becoming directly applicable legislation across the EU.

---

<sup>12</sup> ACER's missions and tasks are defined by the Directives and Regulations of the Third Energy Package, especially Regulation (EC) 713/2009 establishing the Agency.

<sup>13</sup> National network codes will however be valid compatible with the requirements of the European Network code.

<sup>14</sup> In order to ensure the support of all branches of the energy sector, ENTSO-E works in close cooperation with stakeholders.

In particular ACER has issued 10 framework guidelines that have conducted ENTSO-E to the publication of new 10 European Network Codes and its implementation guidelines [112], as follows.

- *Entered into force:*

1. **Capacity Allocation & Congestion Management (CACM)** [113]: Entered into force on 15 August 2015. The provisions of CACM govern the establishment of cross-border EU electricity markets in the day-ahead and intraday timeframes, as well as methods for the calculation of interconnection capacity.
2. **Requirements for Generators (RfG)** [114] [115]: Entered into force on 17 May 2016. Provide a set of coherent requirements for generators (of all sizes) in order to meet the future power system challenges.
3. **Demand Connection (DCC)** [116] [117]: Entered into force on 7 September 2016. The provisions of Demand Connection (DCC) set requirements for new demand users and DSO connections and to outline demand side response requirements related to system frequency.
4. **High Voltage Direct Current Connections (HVDC)** [118]: Entered into force on 28 September 2016. Sets requirements for HVDC connections and offshore DC connected generation.
5. **Forward Capacity Allocation (FCA)** [119]: Entered into force on 17 October 2016. Set rules for calculating and buying capacity in timescales before day ahead and for hedging price risk between bidding zones: establish a framework for the calculation and allocation of interconnection capacity, and for cross-border trading, in forward markets (i.e. timeframes longer than day-ahead).

- *Validated by Member States, awaiting validation by European Parliament and Council:*

6. **Operational Security** (merged into the System Operation guideline [120]): The draft Regulation received a positive vote in comitology on 4 May 2016. The purpose is to set common rules for ensuring the operational security of the pan-European power system.
7. **Operational Planning & Scheduling** (merged into the System Operation guideline [120]): The draft Regulation received a positive vote in comitology on 4 May 2016. It sets requirements, ranging from the year ahead timeframe to real time, for assessing the adequacy and operational security of the interconnected power system and for planning outages required by TSO's and grid users when they have cross-border impacts on power flows.

8. **Load Frequency Control & Reserves** (merged into the System Operation guideline [120]): The draft Regulation received a positive vote in comitology on 4 May 2016. It sets out coordinated and clearly specified load frequency control processes and rules regarding the levels and location of reserves (back-up) which TSOs need to hold.
9. **Emergency and Restoration (ER)** [121]: The draft Regulation establishing a network code on emergency and restoration received a positive vote in comitology on 24 October. It deals with the procedures and remedial actions to be applied in the Emergency, Blackout and Restoration states. This involves preparation of system defence, system restoration and re-synchronization plans in advance, dealing with information exchange, procedures for operating when a system enters into one of these states and ad-hoc analysis of the incidents.

- *Awaiting validation by EU Member States:*

10. **Electricity Balancing (EB)** [122]: The draft Regulation sets out rules on the operation of balancing markets, i.e. those markets that Transmission System Operators (TSOs) use to procure energy and capacity to keep the system in balance in real time. The objectives of the guideline include increasing the opportunities for cross-border trading and the efficiency of balancing markets. An updated draft will be discussed in the next electricity cross-border committee.

Regarding the **Network Code on Requirements for Generators (NC RfG)**, we can say that it is seen as one of the main drivers for creating harmonized solutions and products necessary for an efficient pan-European (and global) market in generator technology.

This Regulation establishes a network code which lays down the requirements for grid connection of power-generating facilities, namely synchronous power-generating modules, power park modules and offshore power park modules, to the interconnected system. Technical requirements in RfG are addressed to new generators, arranged in four types A to D based on a user's connection voltage and MW capacity depending upon the "Synchronous area" they belong.

Table 24 shows the values for the "Continental Europe Area".

Type	Connection Voltage	Capacity <sup>15</sup>
Type A	<110kV	800W – 1MW
Type B	<110kV	1MW – 50MW
Type C	<110kV	50MW – 75MW
Type D	<110kV or >110kV	>75KW

Table 24 - Main national climate and energy targets [12]

---

<sup>15</sup> Thresholds must be set on a national basis by the designated Transmission System Operator (TSO). This threshold shall not be above the limits contained in Table 24.

Below some of the main network services required depending on the plant type are listed:

- *Control of the active power injected:*

The objective of the requirement is to automatically reduce or increase Active Power output of Power Generating Modules (Synchronous Generators and Power Park Modules) in case of over or under frequency.

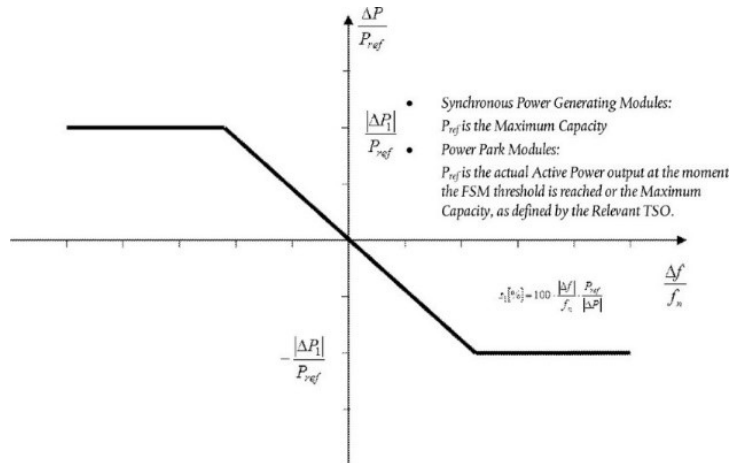


Figure 38 - Active power frequency response capability of power-generating modules [115]

- *Reactive Power Capability*

Reactive power is a key component in terms of voltage stability, which in turn is the foundation for cross-border trading. This requirement is focused on the provision of reactive power from Production Power Plants (Synchronous Power Generating Modules or Power Park Modules) in the steady state to allow the Relevant Network Operator having a sufficient reactive power reserve to keep voltages within the admissible limits in the power system operation.

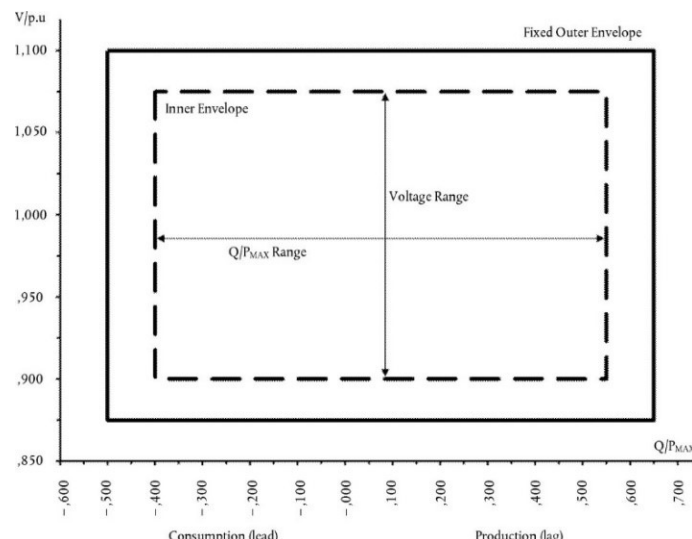


Figure 39 - U-Q/Pmax-profile of a synchronous power-generating module [115]

- **Fault Ride Through Capability of Generators**

The requirements aim at preventing power generating modules disconnection after a secured fault on the higher transmission level. The objective is to limit the potential loss of generation after a fault on the distribution or transmission system in order to avoid more severe disturbances.

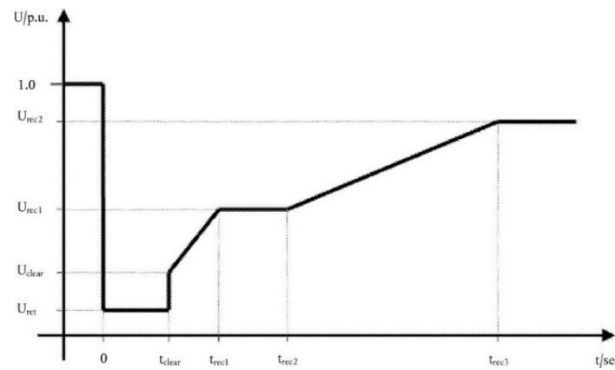


Figure 40 - Fault-ride-through profile of a power-generating module [115]

- **Capability to take part in isolated network operation**

This provision of NC RfG aims at setting requirements for power generating modules in order to enable them to operate in an isolated network after its disconnection from the interconnected system and control frequency and voltage in this isolated network. The objective is to guarantee the availability of such generating units able to operate in these specific conditions. The defined requirements consider frequency and voltage ranges and control features, e.g. the plant shall be able to operate in specific frequency and voltage ranges, and adjust its active power output automatically according to the actual frequency in the isolated network. The objective is to maintain supply in the isolated network and to be able to reconnect it to the interconnected system quickly.

### **2.2.1.1 Technical specifications regulating DG connections**

At European Committee for Electrotechnical Standardization (CENELEC) level, initiatives are currently being implemented to create a suitable set of European technical rules able to regulate the process of connection to the grids, both for what concerns operation (set of system rules) and for what concerns the machinery to connect to the networks (set of product rules). They would imply the collaboration of different Working Groups like for example TC8X/WG1 "Physical Characteristics of electric energy" and TC8X/WG3 "Requirements for connection of generators to distribution networks". Nevertheless owing to the presence of countries with different necessities in the different committees, the harmonization process of the rules relating to distribution networks is particularly critical [123].

Indeed, different national technical requirements are in force: they are generally prescriptions issued on a voluntary basis by each distribution company. In this respect, the attempt to converge on some specific advanced grid support requirements can be observed by the national peculiar rules; as for example:

- Germany: VDE-AR 4105:2011-08 "Power generation systems connected to the low-voltage distribution network";
- Germany: BDEWMV Guideline (2008) "Generating Plants Connected to the Medium-Voltage Network";
- Italy: CEI 0-21 "Reference technical standard for the connection for active and passive users at LV networks of the electric energy distributors";
- Italy: CEI 0-16 "Reference technical standard for the connection for active and passive users at MV networks of the electric energy distributors";
- Austria: TOR D4:2015 "Technical and organizational rules";
- France: ERDF-NOI-RES\_13E "Protections des installations de production raccordées au réseau public de distribution";
- France: Arrêté du 23 avril 2008 "Prescriptions techniques de conception et de fonctionnement pour le raccordement à un réseau public de distribution d'électricité en basse tension ou en moyenne tension d'une installation de production d'énergie électrique".

Recently at European level, 3 technical specifications have been developed by CENELEC for LV and MV connections [124]:

- CLC/EN 50438-1:2015 - Requirements for micro-generating plants to be connected in parallel with public low-voltage distribution networks;

- CLC/TS 50549-1:2015 - Requirements for generating plants to be connected in parallel with distribution networks - Part 1: Connection to a LV distribution network above 16 A;
- CLC/TS 50549-2:2015 - Requirements for generating plants to be connected in parallel with distribution networks - Part 2: Connection to a MV distribution network.

They substantially include Italian requirements (CEI 0-16 and CEI 0-21) [123].

Table 25 and Table 26 summarize the advanced functional requirements for Distributed Energy Resources (DER) required in the different European countries respectively for LV and MV distribution grids [125], where:

- **P at low f:** Active power feed-in at under frequency;
- **P(f):** Reduction of active power at over-frequency;
- **Q/cosφ:** Reactive power control mode;
- **Q(U):** Reactive power control mode;
- **P(U):** Limitation of active power at over-voltage;
- **Remote P:** Possibility for DSO to send setpoint values to generators;
- **Remote trip:** Disconnection on demand by grid operator;
- **LVRT:** Low Voltage Ride Through;
- **HVRT:** High Voltage Ride Through.

	Germany	Italy	Austria	France	Spain	Europe ( $\leq 16A$ )	Europe ( $> 16A$ )
<b>P at low f</b>	Yes (All)	Yes (All)	Yes (All)	No	No	Yes (All)	Yes (All)
<b>P(f)</b>	Yes (All)	Yes (All)	Yes (All)	Yes (All)	No	Yes (All)	Yes (All)
<b>Q/cosφ</b>	>3,68kVA	>3kVA	>3,68kVA	No	No	Yes (All)	Yes (All)
<b>Q(U)</b>	No	>6kVA	Yes (All)	No	No	Yes (All)	Yes (All)
<b>P(U)</b>	No	Option	Yes (All)	No	No	No	Option
<b>Remote P</b>	>100kW	>3kVA	>100kW	No	No	No	Yes (All)
<b>Remote trip</b>	No	Yes (All)	No	No	No	No	Yes (All)
<b>LVRT</b>	No	>6kVA	No	No	No	No	Yes (All)
<b>HVRT</b>	N/A	No	No	No	No	No	Yes (All)
<b>Reference</b>	VDE-AR 4105:2011-08	CEI 0-21	TOR D4:2015	ERDF-NOI-RES_13E	RD 1699/2011 UNE 206007-1 IN:2013	CLC/EN 50438-1:2015	CLC/TS 50549-1:2015

Table 25 - Functions required for LV connections in Europe [125]

	Germany	Italy	Austria	France	Spain	Europe	NC RfG
<b>P at low f</b>	Yes (All)	Yes (All)	Yes (All)	>5MW	No	Yes (All)	Yes (A,B,C,D)
<b>P(f)</b>	Yes (All)	Yes (All)	Yes (All)	No	>2/10MW	Yes (All)	Yes (A,B,C,D)
<b>Q/cosφ</b>	Yes (All)	Yes (All)	Yes (All)	Yes (All)	>2/10MW	Yes (All)	Yes (B,C,D)
<b>Q(U)</b>	Option	Yes (All)	Yes (All)	No	No	Yes (All)	Yes (B,C,D)
<b>Remote P</b>	>100kW	Yes (All)	Yes (All)	No	>2/10MW	Yes (All)	Yes (B,C,D)
<b>P(U)</b>	No	Option	Yes (All)	No	No	Option	No
<b>Remote trip</b>	Option	Yes (All)	No	No	No	Yes (All)	Yes (B,C,D)
<b>LVRT</b>	Yes (All)	Yes (All)	Yes (All)	>5MW	>2MW	Yes (All)	Yes (B,C,D)
<b>HVRT</b>	No	Yes (All)	No	No	No	Yes (All)	No
<b>Reference</b>	BDEWMV Guideline (2008)	CEI 0-16	TOR D4:2015	Arrêté du 23 avril 2008	P.O.12.3:201 16 P.O.12.2 RD1565:2010 UNE 206007-2 IN:2014	CLC/TS 50549-2:2015	RfG 2016

Table 26 - Functions required for MV connections in Europe [125]

## 2.2.2 Italian regulatory environment

### 2.2.2.1 Regulations for distribution networks

For what concerns LV distribution networks, till the publication of CEI 0-21 I edition – published in December 2011 - connections were regulated by technical standards of:

- Italian Electrotechnical Committee [126] (CEI 11-20 with variants V1 e V2 [127]) and;
- the main Italian DSO (Guide for the connections of ENEL Network [128]).

The standard CEI 0-16 III edition (CEI 0-16:2012-12) was published in December 2012. Until then, the connection to distribution networks with rated voltage greater than 1 kV, was regulated by the second edition [129] [130].

Generally speaking, all previous regulations for LV and MV did not contemplate specific arrangements in favour of the evolution towards Smart Grids (like for example the reactive power control of active users for voltage regulation). However, several needs have arisen for DSOs. The identified needs, shared by all the stakeholders that interacted in Working Groups, have materialized in paragraphs 3 and 4 of article 11 of DM 05/5/2011<sup>16</sup> [9] (Fourth Feed-in scheme):

*"3. The inverters used in photovoltaic plants that operate later than 31st December 2012 must consider the need of the electrical network providing the following services and protection:*

- a) to keep insensitivity when fast fluctuations occur;*
- b) to allow disconnection by means of a remote control;*
- c) to increase selectivity of protections in order to avoid sudden disconnections of the photovoltaic plant;*
- d) to allow the supply or the absorption of reactive energy;*
- e) to limit power injection into the network (in order to reduce the network voltage fluctuations);*
- f) to avoid the inverter may feed the electric network load when there is no voltage on the network station.*

*4. For the implementation of the provision of paragraph 3, , the Italian Electrotechnical Committee (CEI), consulted The Italian Authority for Electric Energy and Gas defines specific technical rules".*

Furthermore, on the 8th of March 2012 the deliberation AEEG 84/2012/R/eel [131] [132] has been issued "Urgent measures related to electric energy production plants with particular reference to distributed generation to guarantee the national electric system

---

<sup>16</sup> These requests are also confirmed in the subsequent Ministerial Decree 5 July 2012 ("Fifth feed-in scheme")

security". Such deliberation approves new attachments of the Grid Code (A68 [133], A69 [134] and A70 [135]), introducing particular requirements for production plants.

In the light of this, the Italian Electrotechnical Committee (CEI) [126] issued the new editions of the rules CEI 0-21 and CEI 0-16, which transpose the urgent requirements of Annex A.70 [135] and differently from previous rules consider new scenarios, like for example:

- active distribution networks with high penetration of DG;
- evolution of Smart Grids.

In the perspective of the evolution of the networks towards Smart Grids, one of the most important aspects introduced by CEI 0-21 and CEI 0-16 is the one referred to the Remote Control: the provisions state that by means of protocol IEC 61850 [104] active users can:

- provide network services by modulation of active and reactive power according to what required by the Distributor;
- to disconnect generators on reception of the related remote detachment signal;
- to enable/inhibit IPS frequency thresholds;
- to provide the measures of voltage, active and reactive power at the Point of Delivery.

In the past five years, the rules have undergone an adaptation and change process to take into account technical innovations and new legislation delineated both at national and European level.

The latest versions have been published in July 2016 in alignment with the European Standard CEI EN 50438 [136] on generators up to 16 A. Currently in Italy the requirements for the connection of DGs to distribution network are defined by:

- CEI 0-21:2016-07: "Reference technical rules for the connection of active and passive users to the LV electrical Utilities" [137];
- CEI 0-16;V2:2016-07: "Reference technical rules for the connection of active and passive consumers to the HV and MV electrical networks of distribution Company" [138].

Here below some of the main functions required are described:

- IPS in line with system requirements;
- taking part in defense plans;
- LVFRT (Low Voltage Fault Ride Through);
- voltage control;
- generated active power limitation.

### 2.2.2.1.1 Interface Protection System in line with system requirements

The problems to be minimized through the steps reported in such paragraph are:

1. instability of the electric system due to frequency transients because of events on the HV transmission network
2. formation of an undesired island

To favour network stability a shift from the restrictive frequency thresholds<sup>17</sup> to permissive frequency thresholds<sup>18</sup> is required so as to render the IPS less sensitive to frequency transients.

However, the enlargement of frequency thresholds favors the formation of the undesired island since the IPS is dramatically less sensitive also to frequency shifts recorded locally during the formation of the island.

Such problems may be definitively solved sending a signal which on the opening of the circuit breaker or of any other maneuvering switch along the MV line triggers the more restrictive threshold in respect to the more ordinary ones of the IPS production plants connected to the same line and placed downstream the opening maneuvering organ (Figure 41).

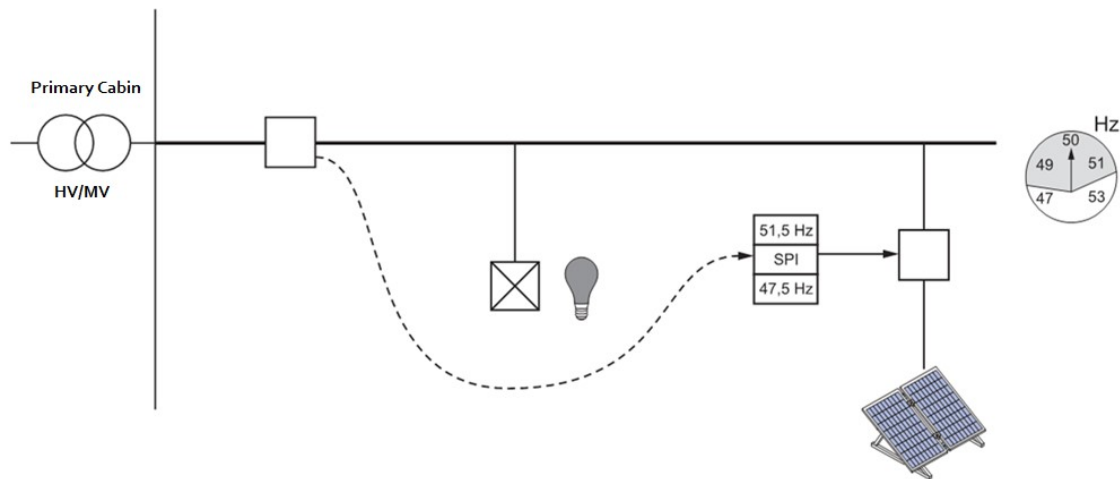


Figure 41 - Sending of the signal from the primary station to users [74]

---

<sup>17</sup> Restrictive frequency thresholds are equal to:

- 49,8 Hz - 50,2 Hz for MV
- 49,5 Hz - 50,5 Hz for LV

<sup>18</sup> Permissive frequency thresholds are equal to 47,5 Hz - 51,5 Hz both for MV and LV

Waiting for the opening remote signal, thanks to the full diffusion of Smart Grids, at present the IPS for DGs connected to MV<sup>19</sup> distribution networks is expected to be equipped with a voltmetric unlocking function able to recognize failures on the MV grid<sup>20</sup>. In that case it would trigger frequency restrictive threshold; vice versa if the phenomenon shows different features, the restrictive range frequency will have to remain inactive and the plant disconnection will occur exclusively according to the broad frequency range. The operation of the IPS can be summarized through the logic scheme of Figure 42.

The solution does not consider the case when the voltage required by load is equal to the power of distributed generators connected on the considered line. In the same way it does not take into consideration the man-acted opening of a circuit breaker of the Distributor when there is no failure [74] [139] [137] [138].

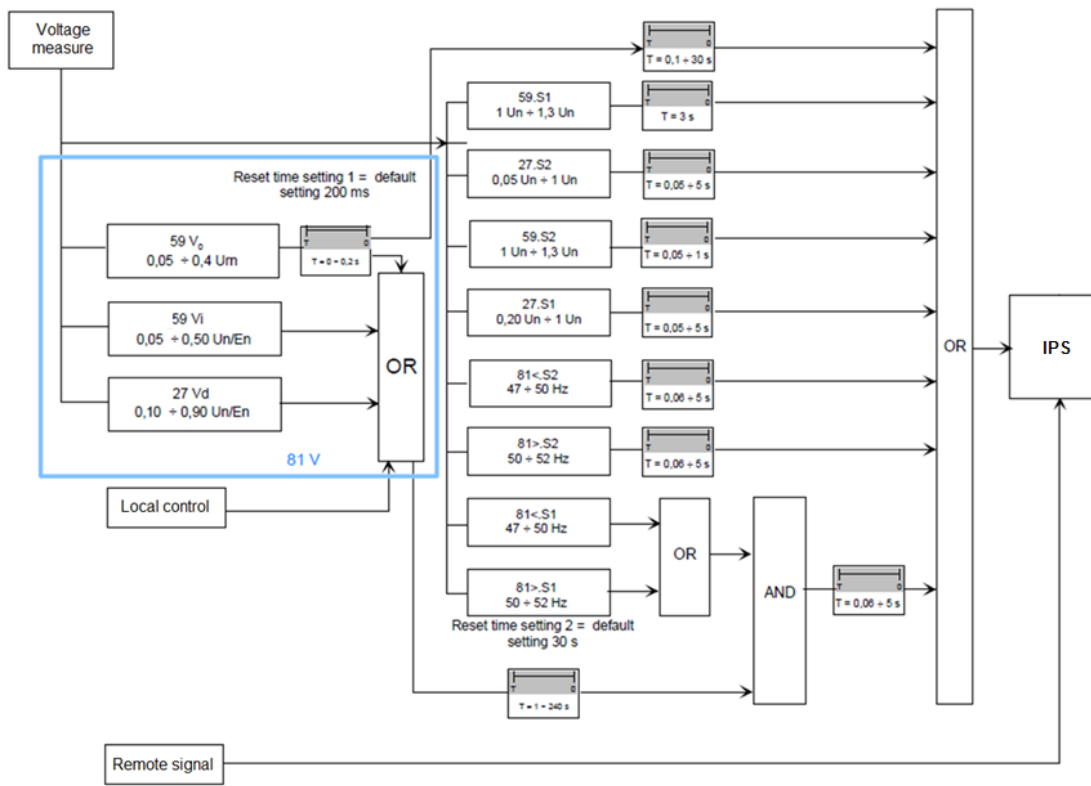


Figure 42 - Functioning logic for the activation of the threshold of relay [138]

<sup>19</sup> This function is not feasible in LV network; therefore, in this case, DSO chooses which thresholds to be set and these are set locally

<sup>20</sup> The presence of a ground fault on MV network is detected by the voltage homopolar value, while a fault between the phases is detected by the value of direct and indirect sequence voltages

### 2.2.2.1.2 Taking part in defense plans

From Figure 42 the indication of a remote detachment signal can be noted.

Indeed AEEG, with the Resolution 421/2014/R/EEL of 7 August 2014 approved the Annex A72 to the network code [140]. The adopted requirements are the ones of Appendix M of the CEI 0-16 III edition.

The service aims to solve critical issues arisen both in MV distribution networks and in HV transmission network.

The requirement is applied to wind and static generators of power higher or equal to 100 kW. At the request of the Distributor, the generators must allow remote detachment - with partial or total reduction of production - by means of remote signals sent from a remote center.

The remote detachment mode can be:

- planned (slow mode): essentially intended to handle over-voltage situations, insufficient regulating capacity of the National Electric Service or congestion on the transmission network
- with immediate action (quick mode): to resolve fast dynamic network events (frequency control and preventive actions to avoid network instability risks).

This process will be managed according to the logic flow shown in Figure 43.

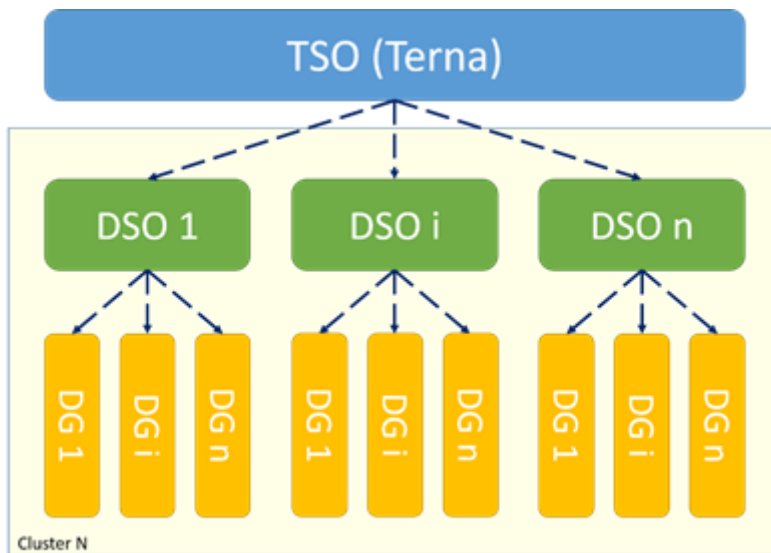


Figure 43 - Logic Flow [140]

In the Smart Grid perspective, the signal will be sent through an "always on" communication system.

During the transitional period, as the current remote control system of the distribution network is based on GSM / GPRS technology, in order to ensure the integration of Active

Users in the Defense Plans, the remote detachment command can also be activated through a GSM / GPRS system (Figure 44).

Such signal can also be used in order to avoid the undesired island phenomenon caused by a DSO intentional operation (for instance an opening of a Primary Station switchgear).

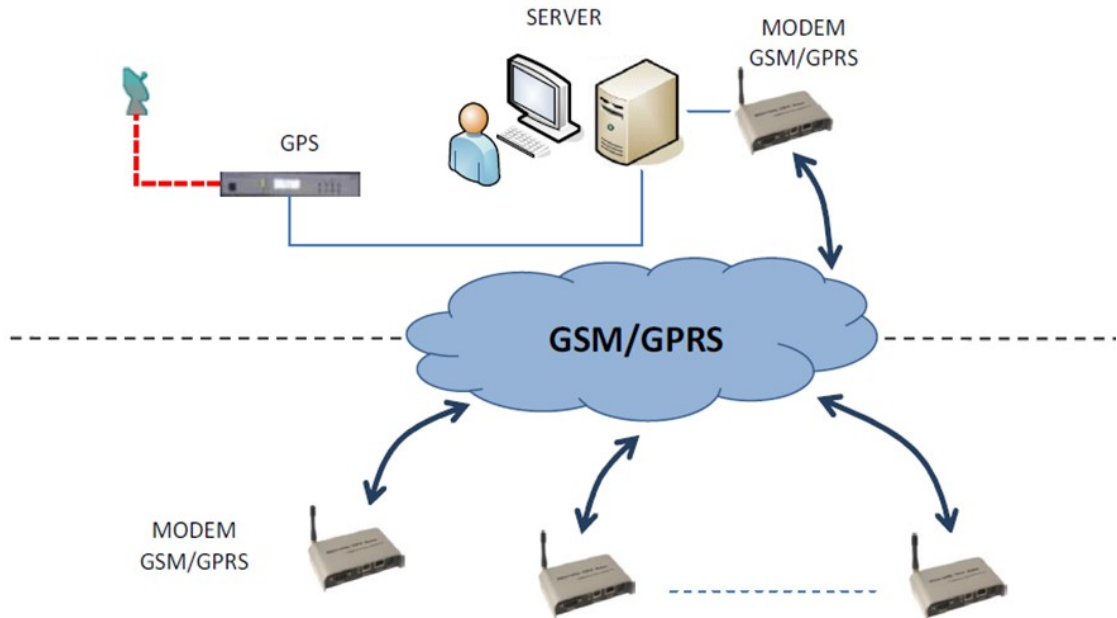


Figure 44 - System Architecture [140]

Therefore, the IPS must be able to receive signals on protocol IEC 61850 [104] but also to receive signals of detachment based on the GSM / GPRS technology.

### 2.2.2.1.3 LVFRT (Low Voltage Fault Ride Through)

Such function is introduced to tackle the problem of electric system instability due to undervoltage because of events on the HV transmission network.

All production plants and the related machinery and equipment must be designed, built and operated to remain in parallel even in emergency conditions.

In particular, the power plants have to be able to stay permanently connected to distribution networks for voltage values at the Point of Delivery included in the following range:  $85\% V_n \leq V \leq 110\% V_n$  [74].

In order to avoid the undo separation from the network in case of undervoltage events on the grid, the production plants connected through an electronic interface must be within certain limits immune from undervoltage. They must implement a LVFRT (Low Voltage Fault Ride Through).

Currently such function is required only for static converters since imposing a LVFRT (Figure 45) to synchronous generators is a complex problem. When a voltage dip occurs, the synchronous generator will tend to inject the same active power generated by prime mover while the passive load of the network (in island or not) lowers<sup>21</sup>, the result is a non-null accelerated power and frequency tends therefore to increase.

On fault elimination voltage goes back to nominal value (almost immediately) and therefore also the absorbed load returns to the values prior to voltage dip. The result is a strong deceleration couple that may create damage to generators, but especially prime movers (turbines in particular) [74] [139] [137] [138].

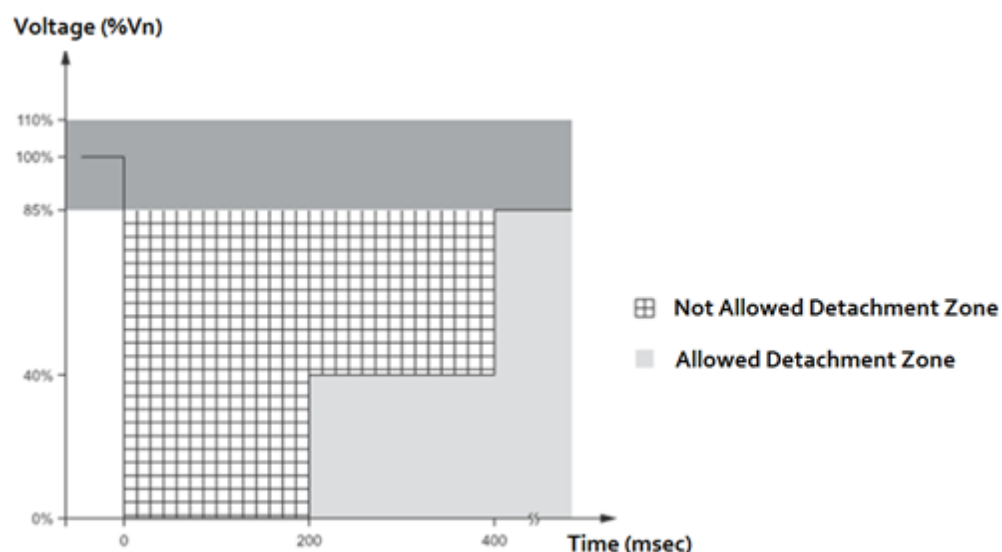


Figure 45 - LVFRT curve for LV distribution networks [137]

---

<sup>21</sup> It can be considered, on first approximation, proportional to voltage.

#### **2.2.2.1.4 Voltage control**

To mitigate the problem related to the change of the voltage profile that occurs in the presence of DG, the new rules CEI 0-16;V2 [138] e CEI 0-21 [137] (both updated in July 2016), require that:

- a) for voltage values higher than 115% of  $V_n$  for more than 0,2 s, DG units be detached from the network (task carried out by IPS);
- b) when the average voltage value measured on a 10 minutes temporal range in average mobile mode exceeds 110 % of  $V_n$ , DG units be detached from the network within 3 s (task carried out by IPS)

Furthermore it is required DGs with a whatever rated power<sup>22</sup> to take part in the voltage control through the absorption/injection of reactive power.

Participation to voltage control is required only for Synchronous Generators, Static Generators, Wind Full Converter and Wind Doubly Fed Induction Generators (DFIG), while Conventional Asynchronous Generators are exempted.

The supply of reactive power (absorption or injection) by active users must be in accordance with two local control logics – described in paragraph 3.2.6:

- based on a curve characteristic  $\cos\varphi = f(P)$ ;
- based on a curve characteristic  $Q = f(V)$ ;

or with a remote control logic through signal exchange according to protocol IEC61850<sup>23</sup> [74] [139] [137] [138] [104].

#### **2.2.2.1.5 Generated active power limitation**

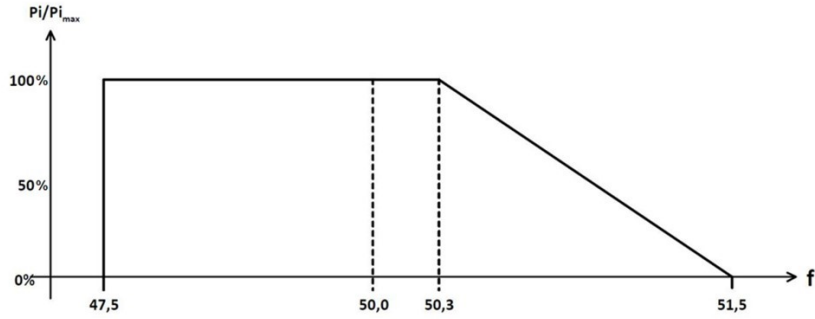
In order to avoid the disconnection of DG from the grid, generators can limit automatically their active power:

- if voltage is close to 110 % of  $V_n$ , according to a function chosen by the manufacturer;
- in case of over-frequency transients, according to a droop between 2 and 5 (it will be generally set at a value equal to 2,4) for frequencies between 50,3 Hz e 51,5 Hz (Figure 46).

---

<sup>22</sup> In alignment with the European Standard EN 50438 on generators up to 16 A, the field of application of the requirements for active users has been extended also to DG with a rated power lower than 1 kW

<sup>23</sup> For LV distribution network this function is only required for Static Generators with power higher than 11,08kW



$P_{i\max}$ : active power supplied at the time of exceeding 50,3Hz (stored value)  
 $P_{i\max}$ : active power supplied

**Figure 46 - Curve of active power reduction in over frequency for LV distribution networks [137]**

- as a consequence of a centralized logic: in the Smart Grid perspective a suitable signal of active power level to be limited by the DG unit (activated only in plants of total power exceeding 11,086kW) [74] [139] [137] [138].

### 2.2.2.2 Regulations for HV transmission network

With regard to Italy, for RES power plants connected to the HV network, the connection is regulated by the Grid Code [141] and its specific Annexes [133] [142] [143].

The main interesting regulations for photovoltaic and wind power plants are respectively Annex A.68 [133] and Annex A.17 [142] in virtue of which these power plants must be equipped with proper control systems in order to provide network services similar to those described for MV and LV networks:

- control of the active power injected;
- control of the reactive power injected or absorbed;
- Low Voltage Fault Ride Through functionality;
- remote disconnection functionality.

Below are described the main requirements of such attachments.

First of all, wind and photovoltaic power plants have to be able to stay permanently connected to distribution networks for voltage values at the point of delivery included in the following range:

$$85\% V_n \leq V \leq 110\% V_n$$

$$47,5 \text{ Hz} \leq f \leq 51,5 \text{ Hz}$$

- a) Remote disconnection functionality:

The service aims to solve critical issues arisen in the HV transmission network. Generators, at the request of TSO, must allow remote detachment - with partial or total reduction of production - by means of remote signals sent from a remote center or by means of procedures ensuring traceability of the request.

The detailed description of the application methods is described in Annex A.64 [143] and A.52 [144].

- b) Control of the active power injected

If transients are present on the transmission network, generated active power will be limited according to a droop between 2% and 5% (it will be generally set at a value equal to 2,4) for frequencies between 50,3 Hz e 51,5 Hz (Figure 47).

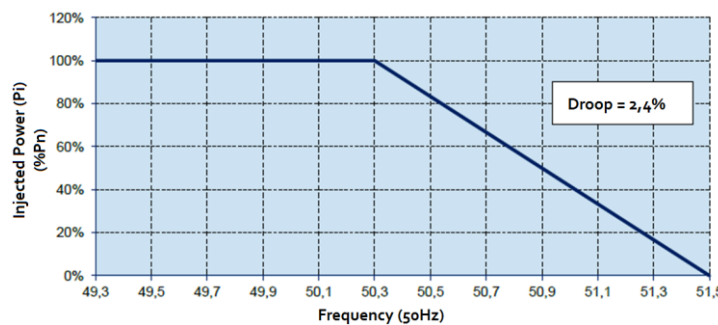


Figure 47 - Curve of active power reduction in over frequency [133]

### c) Low Voltage Fault Ride Through functionality

In order to avoid the undo separation from the network in case of undervoltage events on the grid, Wind and PV production plants must be within certain limits immune from undervoltage.

They must have a suitable LVFRT (Low Voltage Fault Ride Through) curve that is an adequate skill to overcome a voltage gap unscathed (Figure 48 and Figure 49).

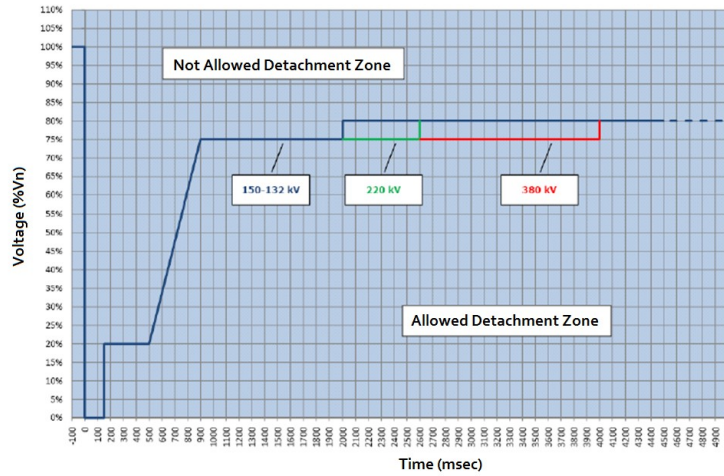


Figure 48 - LVFRT curve for PV power plants [133]

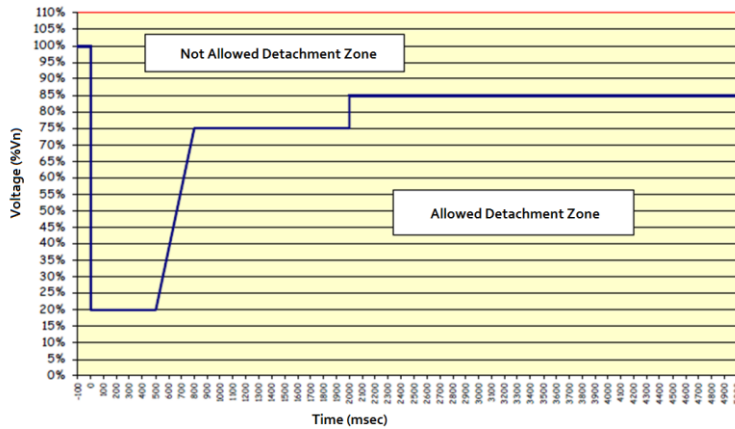


Figure 49 - LVFRT curve for wind power plants [142]

### d) Control of the reactive power injected or absorbed

Regarding the participation to the voltage regulation it is required that:

- wind power plants have to be able only to adjust the power factor in the range [0.95-1.00] both lagging and leading. The power factor can be maintained at a fixed value chosen in agreement between the Network Operator and the Owner of the plant; normally it is required to ensure the power factor equal to 1.
- PV power plants have to be able to control reactive power injection or absorption according to a local logic or to a remote control signal sent by the TSO [133].

The capability curve required for PV inverters is shown in Figure 50.

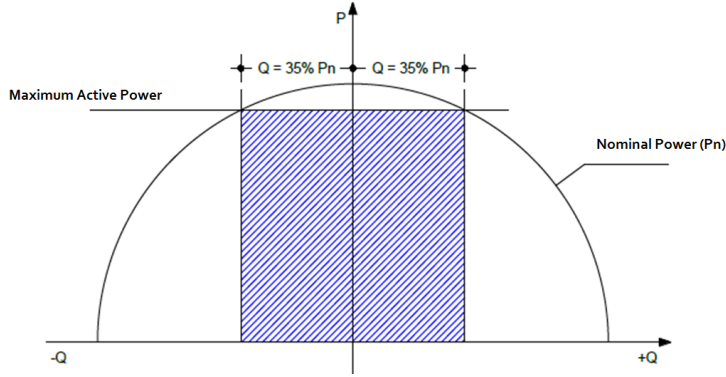


Figure 50 - Capability curve for PV inverters [133]

The value of the reference voltage will be notified by the Grid Operator and will have to be modified by the user, if necessary, in real time (local logic) following the curve  $Q=f(V)$ , represented in Figure 51.

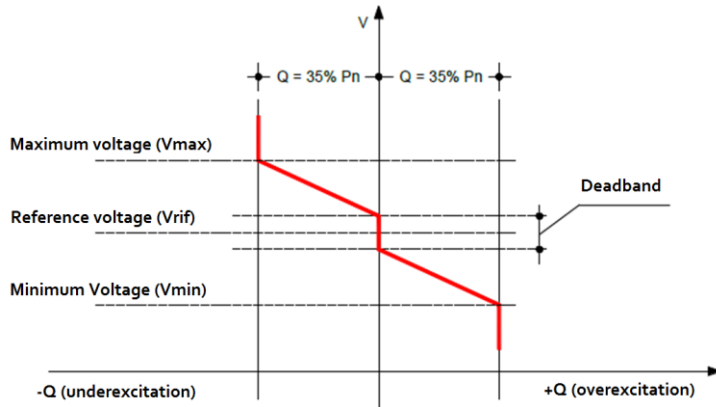


Figure 51 - Local logic  $Q=f(V)$  [133]

Furthermore, the control system must allow that the reactive power exchanged by the plant can be modulated by a remote adjustment signal sent from a remote center the Operating Company (centralized logic).



## Chapter 3.

# Voltage control of Distributed Generation

---

The user appliances work in the best conditions (performance, efficiency, lifetime) when they are fed at rated voltage or within small voltage deviations from the nominal value. As regards the components of production, transmission and distribution systems (generators, transformers, lines, reactors and shunt capacitors, etc.), it is equally appropriate to maintain the voltage within a limited range around the nominal value, to avoid various negative effects on the operation.

The voltage fluctuations at the network nodes are caused by the variations of the active and reactive power absorbed by different loads connected to the network: as a result of active and reactive load fluctuations, the upstream network components (lines, transformers, etc.) are crossed by a varying current. The voltage drops through network impedances vary proportionally and cause voltage changes in all network nodes, which must be drastically reduced or compensated.

In addition, voltage variations may be caused by temporary out of service of any network component (lines, transformers).

It is therefore necessary to undertake a complex of measures to achieve an adequate voltage regulation in the various nodes of transmission and distribution networks [145].

### 3.1 Qualitative considerations for different voltage levels

Let us consider a long symmetrical line under symmetrical three-phase sinusoidal regime, crossed by a balanced currents system and characterized by uniformly distributed fundamental constants  $r$  [ $\Omega/\text{km}$ ],  $l$  [ $\text{H}/\text{km}$ ],  $g$  [ $\text{S}/\text{km}$ ],  $c$  [ $\text{F}/\text{km}$ ].

The line can be represented by the single-phase equivalent model shown in Figure 52 [145].

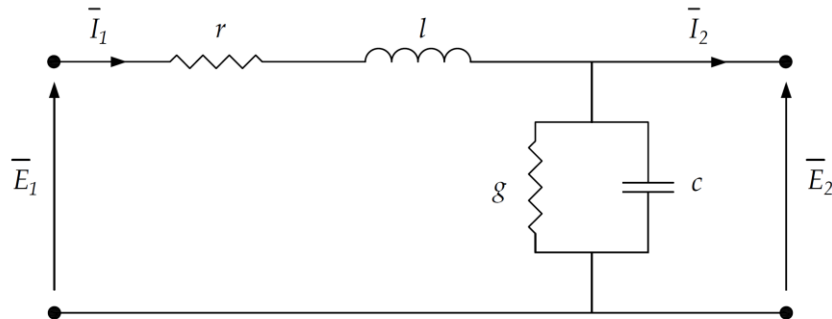


Figure 52 - Equivalent single-phase model

---

The fundamental equations governing the operation of such line are:

$$\begin{cases} \bar{E}_1 = \bar{E}_2 \cdot \cosh(\bar{K}L) + \bar{Z}_o \bar{I}_2 \cdot \operatorname{senh}(\bar{K}L) \\ \bar{I}_1 = \frac{\bar{E}_2}{\bar{Z}_o} \cdot \operatorname{senh}(\bar{K}L) + \bar{I}_2 \cdot \cosh(\bar{K}L) \end{cases} \quad (3.1)$$

with:

- $\bar{E}_1$  -> the voltage at the beginning of the line;
- $\bar{E}_2$  -> the voltage at the end of the line;
- $\bar{I}_1$  -> the current at the beginning of the line;
- $\bar{I}_2$  -> the current at the end of the line (it is  $\varphi$  phase shifted with respect to  $\bar{E}_2$ );
- $\bar{Z}_o = \sqrt{\frac{r+j\omega l}{g+j\omega c}}$  -> the characteristic impedance of the line;
- $\bar{K} = \sqrt{(r+j\omega l) \cdot (g+j\omega c)}$  -> the propagation constant;
- $L$  -> the line length.

Knowing the voltage and the current in a given point, it is possible to calculate the regimen at any other point [145].

Therefore, from (3.1) one can infer that the equivalent single-phase model can be represented by the equations of the double passive bipole in sinusoidal regime (Figure 53) [146]:

$$\begin{cases} \bar{E}_1 = \bar{A} \bar{E}_2 + \bar{B} \bar{I}_2 \\ \bar{I}_1 = \bar{C} \bar{E}_2 + \bar{D} \bar{I}_2 \end{cases} \quad (3.2)$$

with:

$$\begin{cases} \bar{A} = \bar{D} = \cosh(\bar{K}L) \\ \bar{B} = \bar{Z}_o \cdot \operatorname{senh}(\bar{K}L) \\ \bar{C} = \frac{\operatorname{senh}(\bar{K}L)}{\bar{Z}_o} \end{cases}$$

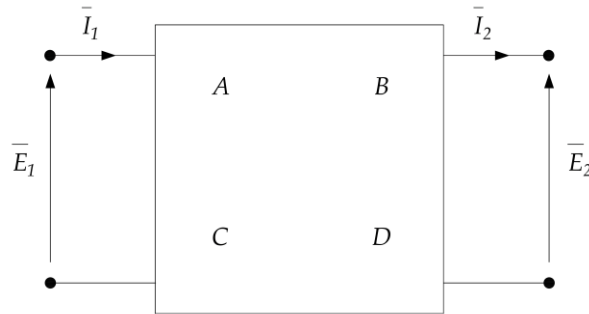


Figure 53 - Double Bipole Representation

### 3.1.1 HV transmission lines

In an HV transmission line with a length ( $L$ ) up to about 100 km, the coefficients typically assume the following values [145]:

- $\bar{A} = \bar{D} = 1$
- $\bar{B} = L \cdot (r + j\omega l) = R + jX_L$
- $\bar{C} = L \cdot (g + j\omega c) = G + jB_c$

The study is currently carried out with the numerical calculation applied to the general equations or by a graphic procedure. The Perrine-Baum diagram [147] [148] allows to easily examine the behaviour of an electric line to changes in its operating condition (active and reactive power at the end of the line).

Simply to notice that:

- $\bar{A} \cdot \bar{E}_2 = \bar{E}_{1,0}$  represents the voltage at the beginning of the line when  $\bar{I}_2 = 0$ ;
- $\bar{B} \cdot \bar{I}_2 = \bar{E}_1 - \bar{A} \cdot \bar{E}_2 = \Delta \bar{E}_2$  represents the voltage drop between the beginning and the end of the line.

Having set  $\bar{A} = 1$  will result  $\bar{E}_2 = \bar{A} \cdot \bar{E}_2 = \bar{E}_{1,0}$ . Furthermore being in HV, the total line reactance ( $X_L$ ) prevails over the total line resistance ( $R$ ), such that  $\beta \approx 90^\circ$  and then  $\bar{B} \cdot \bar{I}_2$  is almost vertical.

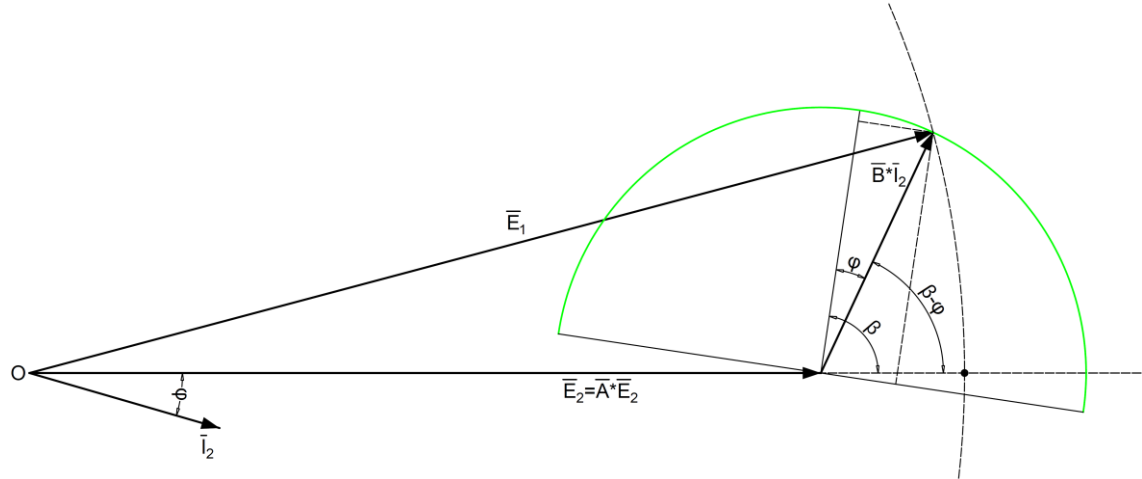


Figure 54 – Perrine-Baum Diagram for a HV network

The diagram highlights the cause of the voltage drop is mainly due to inductive reactive power. On equal apparent power absorbed by the load (points on the green semicircle) the higher the inductive component absorbed by the load (the higher is the power factor  $\varphi$ ) the more evident is the voltage drop.

### 3.1.2 MV and LV distribution lines

In MV and LV distribution networks, and also in short HV lines up to 150 kV, it is possible to neglect transverse admittance for the calculation of the voltage drops [145].

With this simplification, the line can be represented by the single-phase equivalent model shown in Figure 55.

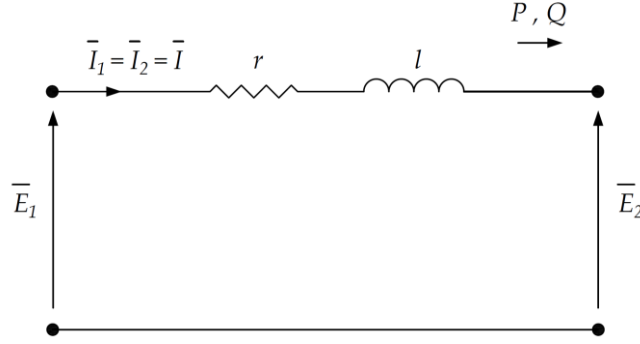


Figure 55 - Equivalent single-phase model for a MV or LV distribution network

The double bipole coefficients assume therefore the following typical values:

- $\bar{A} = \bar{D} = 1$
- $\bar{B} = L \cdot (r + j\omega l) = R + jX_L$
- $\bar{C} = 0$

where  $R$  and  $X_L$  are respectively the total line resistance and reactance.

In this case typically  $X_L$  is not  $\gg R$  and therefore  $\beta$  does not tend to  $90^\circ$ . Therefore the diagram will be much more inclined than the previous case (Figure 56).

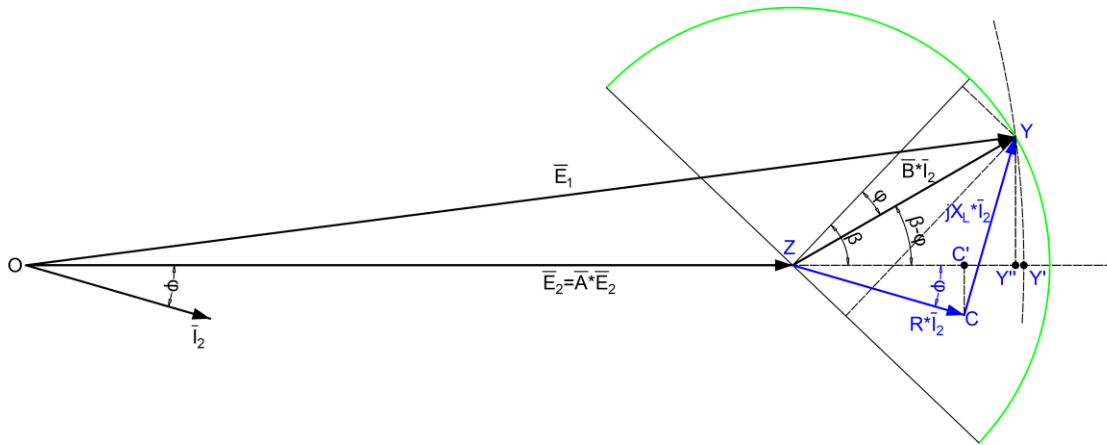


Figure 56 - Perrine-Baum Diagram for a MV or LV distribution network

The diagram in Figure 56 emphasizes that in this case the cause of voltage drop is not attributable to the inductive reactive power transport only. The resistive component produces a not negligible voltage drop on line [145].

The current  $\bar{I}$ ,  $\varphi$  phase shifted with respect to  $\bar{E}_2$ , causes [145]:

- a resistive voltage drop  $R \cdot \bar{I}$  in phase with  $\bar{I}$  (represented by the segment ZC);
- a reactive voltage drop  $jX_L \cdot \bar{I}$  in quadrature with  $\bar{I}$  (represented by the vector CY).

### 3.1.3 Quantitative considerations

The equivalent single-phase model of a MV or LV distribution network is considered.

From Figure 56, approximating the point Y' with Y'' and projecting Y on the x-axis, we obtain the following approximate expression:

$$\Delta E = E_1 - E_2 = \overline{OY} - \overline{OZ} = \overline{OY'} - \overline{OZ} \quad (3.3)$$

$$\approx \overline{OY''} - \overline{OZ} = \overline{ZC'} + \overline{CY''} \quad (3.4)$$

$$= \overline{ZC} \cdot \cos \varphi + \overline{YC} \cdot \sin \varphi \quad (3.5)$$

$$= R \cdot I \cdot \cos \varphi + X_L \cdot I \cdot \sin \varphi \quad (3.6)$$

Therefore, for a three-phase line with  $V$  the rated voltage of the system, the voltage drop  $\Delta V$  assumes the following expression:

$$\Delta V \approx \sqrt{3} \cdot (R \cdot I \cdot \cos \varphi + X_L \cdot I \cdot \sin \varphi) \quad (3.7)$$

$$\Delta V \approx \frac{\sqrt{3} \cdot (V \cdot R \cdot I \cdot \cos \varphi + V \cdot X_L \cdot I \cdot \sin \varphi)}{V} \quad (3.8)$$

$$\Delta V \approx \frac{(R \cdot P + X_L \cdot Q)}{V} \quad (3.9)$$

From which the voltage drop percentage follows:

$$\Delta V \% = \frac{\Delta V}{V} * 100 \approx \frac{(R \cdot P + X_L \cdot Q)}{V^2} * 100 \quad (3.10)$$

It is pointed out that in lines where transverse admittance is negligible, voltage drop percentage is inversely proportional to the square of the operating voltage.

It consists of two addends:

- the first is to be attributed to the active power transit through the line resistance;
- the second is to be attributed to the transit of reactive power through the line reactance.

▪ **NOTE:**

For an approximate calculation of the voltage variations at i-th node ( $\Delta V_i$ ), while maintaining the same conditions to all other nodes, equation (3.10) can be applied also to HV networks [145].

It should be taken into account that for HV networks the second term takes on greater importance, because the reactance of the line is normally much greater than resistance. Therefore you can neglect the term  $R \cdot P$ , and then the equation can be rewritten as follows:

$$\Delta V_i \approx \frac{(X_{Li} \cdot \Delta Q_i)}{V_{ni}} \quad (3.11)$$

$$\Delta V_i \% = \frac{\Delta V_i}{V_{ni}} * 100 \approx \frac{(X_{Li} \cdot \Delta Q_i)}{V_{ni}^2} * 100 \quad (3.12)$$

With:

- $V_{ni}$  -> the nominal phase-to-phase voltage at the node  $i$ ;
- $V_i$  -> the phase-to-phase voltage at the node  $i$ ;
- $X_{Li}$  -> the equivalent reactance of the grid seen from the i-th node;
- $\Delta Q_i$  -> the reactive power changes at the i-th node.

Assuming the equivalent impedance of the grid seen from the i-th node  $Z_i \cong X_{Li}$ , the short-circuit power at the node  $i$  is equal to:

$$P_{cc,i} \approx \frac{V_{ni}^2}{X_{Li}} \quad (3.13)$$

From equation (3.13) it can be written:

$$\Delta V_i \% = \frac{(X_{Li} \cdot \Delta Q_i)}{V_{ni}^2} * 100 \approx \frac{(X_{Li} \cdot \Delta Q_i)}{P_{cc,i} \cdot X_{Li}} * 100 \quad (3.14)$$

$$\Delta V_i \% \approx \frac{\Delta Q_i}{P_{cc,i}} * 100 = \Delta Q_i \% \quad (3.15)$$

From equation (3.15) it can be noticed that, with good approximation, the percentage voltage drop at node  $i$  is equal to the reactive power delivered/absorbed at the same node, expressed in percent of the short-circuit power of the same node [145].

It follows that the greater the short-circuit power in the considered node, the more the voltage at node will tend to remain unperturbed.

## 3.2 Voltage control techniques for DGs connected to MV and LV distribution networks

### 3.2.1 The voltage rise phenomenon in distribution networks

The present paragraph analyses the phenomenon of voltage profile variations in distribution networks.

On the basis of what described in previous paragraphs, one can infer that for the short line represented in Figure 57 voltage drop (at steady-state) between buses 1 and 2 when power  $P$  (active) and  $Q$  (reactive) flows from bus 1 to bus 2, is given by the following approximation (powers are assumed positive when absorbed by loads) [149] [150]:

$$V_1 - V_2 \approx \frac{(R \cdot P + X \cdot Q)}{V} \quad (3.16)$$

where:

- $V$  is the rated voltage of the line;
- $V_1, V_2$  are the voltages at buses 1 and 2 of the line;
- $R$  and  $X$  are the resistance and reactance of the line;
- $P$  and  $Q$  are active and reactive power flowing from bus 1 to bus 2.



Figure 57 - Line connecting two buses [151]

A relevant injection of active power generated by DGs into the distribution network can therefore change the sign of difference  $V_1 - V_2$ . This makes voltage profiles to rise, from the substation bus to the end of the network, instead of dropping, as normally expected.

This is exactly what happens when a distributed generator provides power in the related distribution network: voltage at the injection point increases. The phenomenon goes under the name of voltage rise [77].

In HV networks the voltage mainly depends on injections of reactive power, while in MV networks it depends both on active and reactive power since line resistance is not negligible in respect to line inductive reactance.

Voltage profile in passive networks (no local generator connected) decreases monotonously along the line, profile "a" of Figure 58. But if generators are connected to a line and inject power, voltage profile is no longer monotonous, profile "b" of Figure 58.

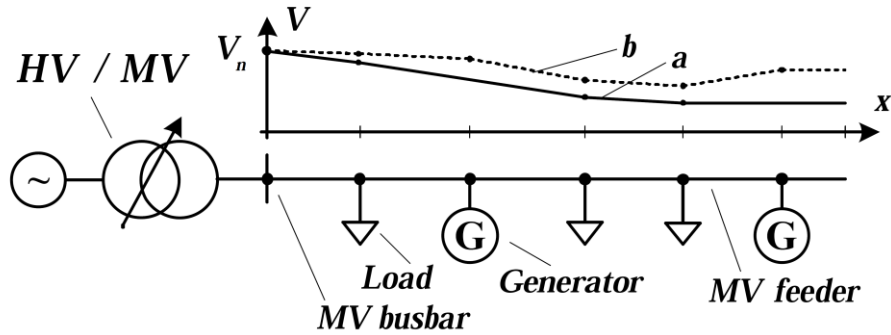


Figure 58 - Voltage profiles for a MT grid with and without DG [152]

The power is sometimes provided by generation plants fed by RES that, unfortunately, cannot be programmed. A large power input by non-programmable generators makes voltage in some points of the network exceed the allowed maximum value, especially in presence of a low load.

Below some possible solutions to mitigate the voltage rise phenomenon in distribution networks, proposed in literature and by connection rules, are shown. Finally the analysis of an original control technique proposed follows [149] [151].

### **3.2.2 Reduction of active power injected by DGs**

A possible means to avoid dangerous exceedances of the maximum value in distribution networks may be to act directly on the cause of the phenomenon; that is to ensure limitation of distributed generators active power [77].

Thus DG reduces its own operating income in order to provide voltage regulation service. It follows the DG willingness to limit its voltage output should be remunerated by the DSO asking for that service. The related remuneration should be comparable to the value of power not produced by the DG unit [153].

Even recent norms CEI 0-16 [138] and CEI 0-21 [137] (both updated to July 2016) provide the restriction of active power for voltage values of nearly 110% of nominal voltage in order to avoid generator disconnection.

### **3.2.3 Adaptation or reconfiguration of the distribution network**

A kind of adjustment consists in the increase of the sections of conductors (decrease of resistance). The updating and resizing of distribution lines allows a reduction of the equivalent longitudinal impedance of MV lines. It allows the provision of wider regulation adjustment margins and of a reduction of distribution losses. However, owing to what said so far, such a solution may incur in social, environmental and economic obstacles for the distribution company [153] [77].

### **3.2.4 Voltage reduction in primary substation**

In distribution networks voltage along the line decreases as a result of voltage drop along the same line. In order to face such drop one generally keeps voltage in primary substation a little higher than the nominal one, resorting to particular devices like OLTC (On-Load Tap Changer). Particular HV/MV transformers are installed, equipped with on OLTC which allows variation of transformer ratio with transformers in service<sup>24</sup>. Voltage control is carried out by means of a discrete tap regulation. However, such techniques, fundamentally based on the hypothesis of the passivity of the distribution network may not operate correctly in the presence of DG [153] [152]. For example, an uneven arrangement of local generators could cause the contemporary violation of eligible restrictions of maximum and minimum voltage. This happens especially in radial distribution lines and of rural type (with limited conductor section and very long traits) [153].

---

<sup>24</sup> Differently from an off circuit tap changer which is instead employed with a deactivated transformer

Some authors have proposed alternative solutions to control OLTC in presence of DG [154] [155], based on the knowledge of the network characteristics, the alleged trends of loads demand and some remote voltage and power measurements [156] [157] [158].

These techniques allow a better control of the voltage profiles. However, such a control mode may not be sufficient in the case of high non-uniformity of the generation plants and loads distribution [153].

### 3.2.5 DG reactive power regulation

From the equation (3.10) one can infer that if generators are able to regulate the provision or the absorption of reactive power in the network, then the change to voltage profile occurring because of active power input can be reduced (or even better cancelled).

Literature presents many works concerning techniques to make DGs exchanging reactive power in a controlled way. All proposed solutions can be classified as coordinated (centralized) [159] [160] [161] [162] or local strategies [163] [164] [165] [166]. In [167] a comparison of the two methods is presented. Simulations of local control strategies can be found in [164].

Local control is characterized by the fact that any local generator controls its own reactive power only on the basis of local measurements. On the contrary coordinated control requires a centralized controller (Power Control Unit) which exchanges data with all the nodes of the network linked to the control through appropriate communication infrastructure. In Figure 59 and Figure 60, the block diagrams for the two kinds of control considered can be seen [151].

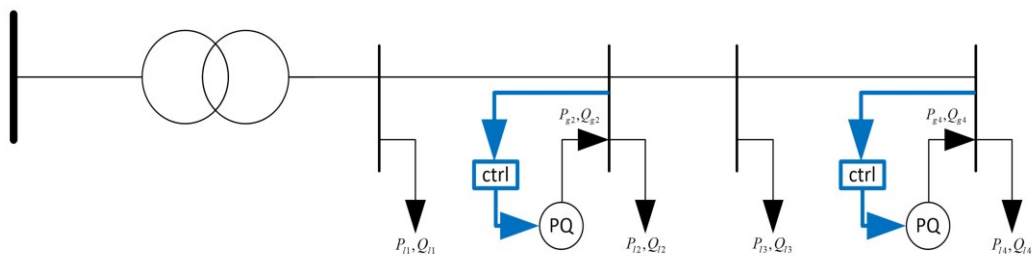


Figure 59 - Local Control [151]

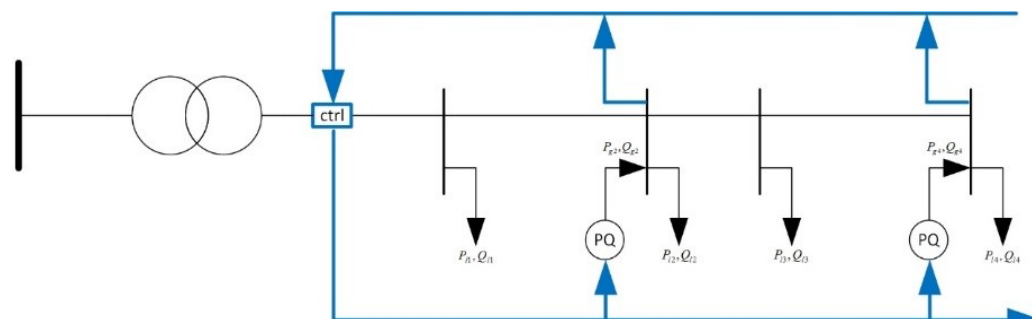


Figure 60 - Centralized control [151]

Most strategies require the on-line updates of the set-point of generators in order to absorb or inject reactive power. In [168], the voltage support is based on a multi-agent approach, while in [152] and [169] authors propose a voltage control based on sensitivity theory. Another type of centralized control can be achieved using a fuzzy logic for the determination of the reference power factor to be applied to the various DGs of the network, in function of the error voltage at the respective node, obtained as the difference between the measured voltage and the reference. The output of the fuzzy controller directly provides the reference power factor value for the various DGs. The participation factor of each generator to the system, is obtained from a sensitivity analysis of the i-th node voltage with respect to the injection of reactive power to the j-th node; that is on the basis of relations  $\frac{dV_i}{dQ_j}$  [159].

Other optimization criteria can be used together with the use of genetic algorithms, applied to a decentralized control of reactive power by the inverter. Each inverter regulates the reactive power on the basis of a local control of the reference voltage, wherein the data used for the calculation rule are generated with genetic algorithms. Such algorithms are typically suitable to solve optimization problems with multi parameters, which, in this case, represent the optimal values of reactive power production [166].

Some texts resume the idea of involving distributed generators for voltage regulation in the distribution networks, in combination with traditional regulation systems (capacitor banks, OLTC) aiming at the best coordination of the global action settlement, minimizing the total cost incurred by the distribution company to perform the voltage adjustment and the reactive power support [170]. Other authors point to reduce impact on the voltage of the transport system and mitigation of the voltage rise problems in distribution networks through the optimization of the OLTC position and power factor of DGs, through linear programming techniques [165]. A coordinated control strategy between OLTC and DGs may also consist of a coordinated action between a primary controller (centralized) to adjust the MV busbar voltage through the OLTC and a series of secondary controllers (one for each of the network supply line) to determine the reference control signal (power factor), which must be communicated to each local generator [161].

### 3.2.6 Control techniques proposed in Italy by the recent connection rules (CEI 0-16 CEI 0-21)

As discussed in paragraph 2.2.2.1.4 recent rules require DGs to take part in the voltage control through the absorption or injection of reactive power according with a local or centralized control logic.

More precisely for Static Generators, Wind Full Converter and Wind Doubly Fed Induction Generators (DFIG)<sup>25</sup> are defined two different local logics:

- ***Power factor control***

This control law requires an automatic adjustment of the reactive power according to a characteristic curve  $\cos \varphi = f(P)$ , where P is the generator active power. This control law provides the absorption of reactive power by distributed generators, only in order to limit the voltage rise caused by injection of active power by the same generator.

The control logic is as follows:

- for values of injected active power  $P/P_n < 0.5$  the inverter works at  $\cos \varphi = 1$
- on exceeding the working point  $P/P_n = 0.5$ , the inverter checks if the voltage at its terminals is greater than a critical value of lock-in, provided by the DSO according to CEI EN 50160 [171] (for example equal to  $1.05 V_n$ ) and in this case the reactive power regulation is activated, placing the working point P-Q according to the following expression according to Figure 61:  $\cos \varphi = -0.2 \frac{P}{P_n} + 1.1$

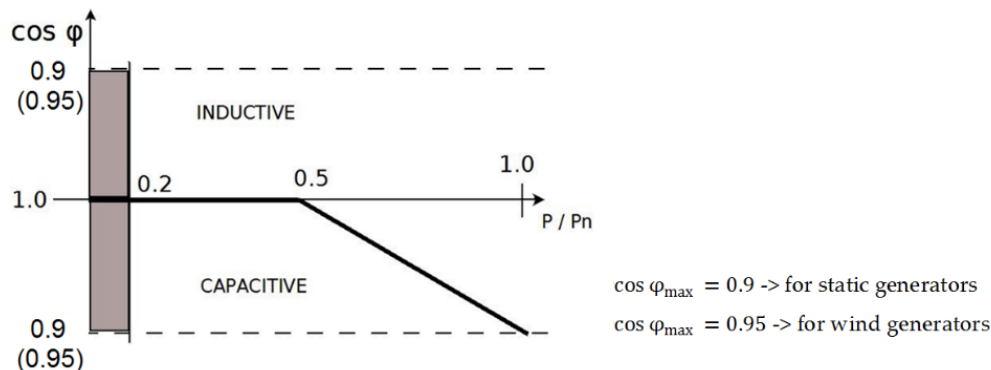


Figure 61 - Power factor control law [138]

Reactive power regulation is removed only when active power P falls below 50% of  $P_n$  (active power lock-out), independently from the voltage measured at the terminals, or if the voltage falls below a certain value (voltage lock-out) adjustable between  $0.9V_n$  and  $V_n$ .

---

<sup>25</sup> For Synchronous Generators prescriptions are being studied

#### ▪ *Reactive power control*

This control law requires an absorption or injection of reactive power in function of the voltage value at terminals in order to provide a network service: to limit voltage variations at node considered even if caused by other generators / loads of network.

To accomplish this, generators must be capable to absorb or inject reactive power automatically in a local control logic on the basis of a characteristic curve  $Q = f(V)$  shown in Figure 62.

Where  $V_{1i}$ ,  $V_{1s}$ ,  $V_{2i}$ ,  $V_{2s}$  are defined by DSO within these limits:

- $V_{1i} < V_n < V_{1s}$ ;
- $V_{2s} < V_{max}$  -> with  $V_{max} \leq 59.S1$  (default value:  $V_{max} = 1,1 V_n$ );
- $V_{2i} > V_{min}$  -> with  $V_{min} \geq 27.S1$  (default value:  $V_{min} = 0,9 V_n$ );
- $|Q_{min}| \text{ e } |Q_{max}| \geq 0,436 * S_n$ .

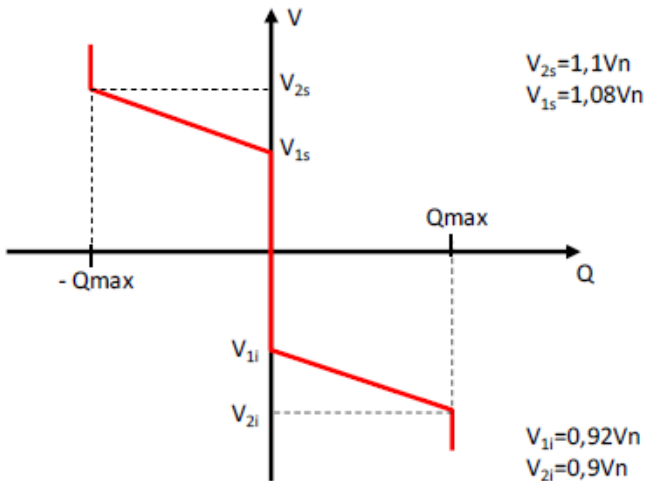


Figure 62 - Reactive power factor control [138]

Concerning centralized control, the connection rules contemplate the possibility of a remote control through signal exchange according to protocol IEC61850<sup>26</sup> [104], but they do not yet define a specific technique to control voltage through the absorption of reactive power.

The original technique described in the following section could be used for this purpose.

---

<sup>26</sup> For LV distribution network this function is only required for Static Generators with power higher than 11,08kW

### 3.2.7 A proposed control technique based on the network linearization

The proposed control technique contemplates the reactive power regulation provided by distributed generators, depending on the respective active power generated, in order to mitigate the voltage-rise phenomenon [149] [151].

This technique is based on the linearization<sup>27</sup> of the network around the operating point in which both reactive and active power generated by DGs are equal to zero (i.e. the distribution network in absence of DG).

For a given distribution network with a subset of  $N_G$  buses connecting generators, let chose a subset of  $M$  controlled buses. For small variations around the operating point, the vector of voltage variations at these buses  $[\Delta u_m]$ , can be represented by the following linear equation<sup>28</sup>:

$$[\Delta u_m] = [B][\Delta p] + [C][\Delta q] \quad (3.17)$$

Where:

- $[\Delta u_m]$  is the vector ( $M \times 1$ ) of the voltage variations at controlled buses, with respect to voltage values in absence of distributed generators;
- $[\Delta p]$  is the vector ( $N_G \times 1$ ) of the active power variations injected by distributed generators;
- $[\Delta q]$  is the vector ( $N_G \times 1$ ) of the reactive power variations injected by distributed generators;
- $[B]$  and  $[C]$  are ( $M \times N_G$ ) sensitivity matrices, in particular:
  - o  $[B]$  is the matrix of the partial derivatives of the voltages at the controlled nodes respect to the active power of the  $N_G$  generation nodes;
  - o  $[C]$  is the matrix of the partial derivatives of the voltages at the controlled nodes respect to the reactive powers of the  $N_G$  generation nodes.

$[B]$  and  $[C]$  matrices coefficients can be estimated by a series of power flow calculations, fixing all network parameters, incrementing respectively the active and the reactive power of each DG plant in turn and calculating the ratio between voltage variations and power injected [164].

Simply to notice that if the power flow calculation is carried out by using Newton-Raphson based methods, the voltage sensitivity coefficients can be derived directly from

<sup>27</sup> Linearization is needed because the equations describing the network - the power flow equations - are not linear.

<sup>28</sup> In the equation other voltage variations (i.e. those provoked by loads, network reconfigurations, disturbances coming from the transmission system, etc.) are not taken into account in respect to those provoked by DGs active and reactive power production.

the Jacobian matrix [172], proceeding to its inversion and extrapolating only items of interest.

The aim is to minimize the term  $[\Delta u_m]$  - due to active power variations injected into generation nodes  $[\Delta p]$  - acting on the reactive power production  $[\Delta q]$  of the DGs.

The reactive powers to be generated by DGs  $[\Delta q]$  are linearly linked to active powers fed into the network by the same set of generators, through the coefficients contained in the  $[A]$  matrix:

$$[\Delta q] = [A][\Delta p] \quad (3.18)$$

Substituting (3.18) in (3.17), we obtain that voltage variations for the chosen M buses results related to active power variations at the  $N_G$  generation nodes:

$$[\Delta u_b] = ([B] + [C][A])[\Delta p] \quad (3.19)$$

In this way, the problem becomes to find an  $[A]$  matrix, which minimizes voltage variations.

In particular, considering the hypotheses to have assumed  $M = N_G$  (in order to work with squared matrices) and  $[C]$  non-singular (this can always be achieved, by means of a proper selection of the M controlled buses), the analytical solution to eliminate voltage variations ( $[\Delta u_m] = 0$ ), is:

$$[A] = -[C]^{-1}[B] \quad (3.20)$$

with  $[A]$ ,  $[B]$  and  $[C]$  all squared matrices ( $N_G \times N_G$ ).

According to the mathematical formulation presented above, the proposed voltage rise mitigation strategy results applicable as a coordinated centralized control architecture: it requires to provide each reactive power generation control with active power information of all the other generators.

The application of the method described above can produce a solution vector  $[\Delta q]$  whose reactive powers can be, for some generators, beyond reactive power limits. In this case, those generators will be operated at their reactive power limits.

### 3.2.7.1 Choice of control nodes

In distribution networks, one of the adoptable strategies for the choice of the nodes on which to carry out the control of the voltage variations, can be conducted similarly to the transmission network. The nodes selected are the ones that for their connection features have a relevant influence on the voltages of an area of the electrical network considered. For example, the nodes in which the effect of voltage rise is more evident, dangerous and influential on the remaining nodes of network. The nodes chosen for voltage control then take on a role similar to the one of "pilot nodes" in the secondary regulation implemented for the transmission network [173] [174].

A quantity that represents the attitude of the  $j$ -th node to be disturbed by the  $i$ -th generator is represented by its sensitivity  $\frac{dv_j}{dP_i}$ , that is those nodes that show the greatest sensitivity of voltage with respect to the active power input by distributed generators. Such nodes correspond typically to the same generation nodes or in any case those close to them.

The voltage of these nodes is controlled by the actuators (power plants connected to the area of the node considered) which, in the case of the distribution network correspond to the same distributed generators.

### **3.3 Voltage control techniques for RES production power plants directly connected to HV transmission network**

There are several differences in how the voltage control service has been implemented by Transmission System Operators (TSOs) in different countries. As demonstrated in paragraph 3.1.1, HV voltage nodes are mainly affected by reactive power flows. Therefore, voltage control is typically performed through the control of reactive power flows using different reactive power resources: transformer tap changers, synchronous compensators, synchronous generators, static VAR compensators, capacitor banks, FACT devices and capacitance of lines and cables [73].

Several countries have implemented hierarchical systems to coordinate the production of reactive power resources based on conventional large power stations [175]:

- Spain: a hierarchical and automatic voltage control with a regional SVR [71] [176] has been designed but it seems not completely implemented at the moment.
- Switzerland: a centralized voltage/reactive power control is implemented [177].
- Belgium: a coordinate voltage control has been employed since 1998, a central control has been preferred to a secondary voltage control [178].
- Germany: each TSO is responsible for voltage control in its own controlled area, therefore a hierarchical system is not present. Each generating unit, if required, must be able to carry out voltage and reactive power control within the area of the respective network operator [179].
- France: a three level voltage control system has been implemented. Moreover a coordinated secondary voltage control has been designed and is active [70].
- In North America historically enhanced voltage control has not been used, although several examples of VAR support from RES power plants exists [180].
- Italy: Voltage hierarchical controls have been studied and developed in Italy starting from the 1980s and several power stations where equipped with local regulators, originally named REPORT and nowadays SART (Automatic System for Voltage Regulation). Specifications of the SART apparatus are given in the Italian Grid Code annex document A.16 [72] while in [181] a modern implementation is extensively reported.

In [182] the main benefits recognized to a coordinated control of reactive power resources are described.

Typically, voltage control is performed only on some pilot nodes of the network, the ones that can most influence the voltage nodes of the same area. Checking voltages of all selected HV nodes and acting simultaneously on all reactive power sources to maintain the voltages in those nodes constant is considered impracticable.

Therefore, a transmission power system is conveniently subdivided into subsets of nodes (named “pilot nodes”) whose voltage variations can depend (at small signals) on reactive power variations injected in the nodes. In a decentralized control scheme each subset of nodes is controlled independently [183] [184].

### 3.3.1 HV voltage control in Italy

Figure 63 represents the hierarchical structure of the Italian voltage control in HV transmission network.

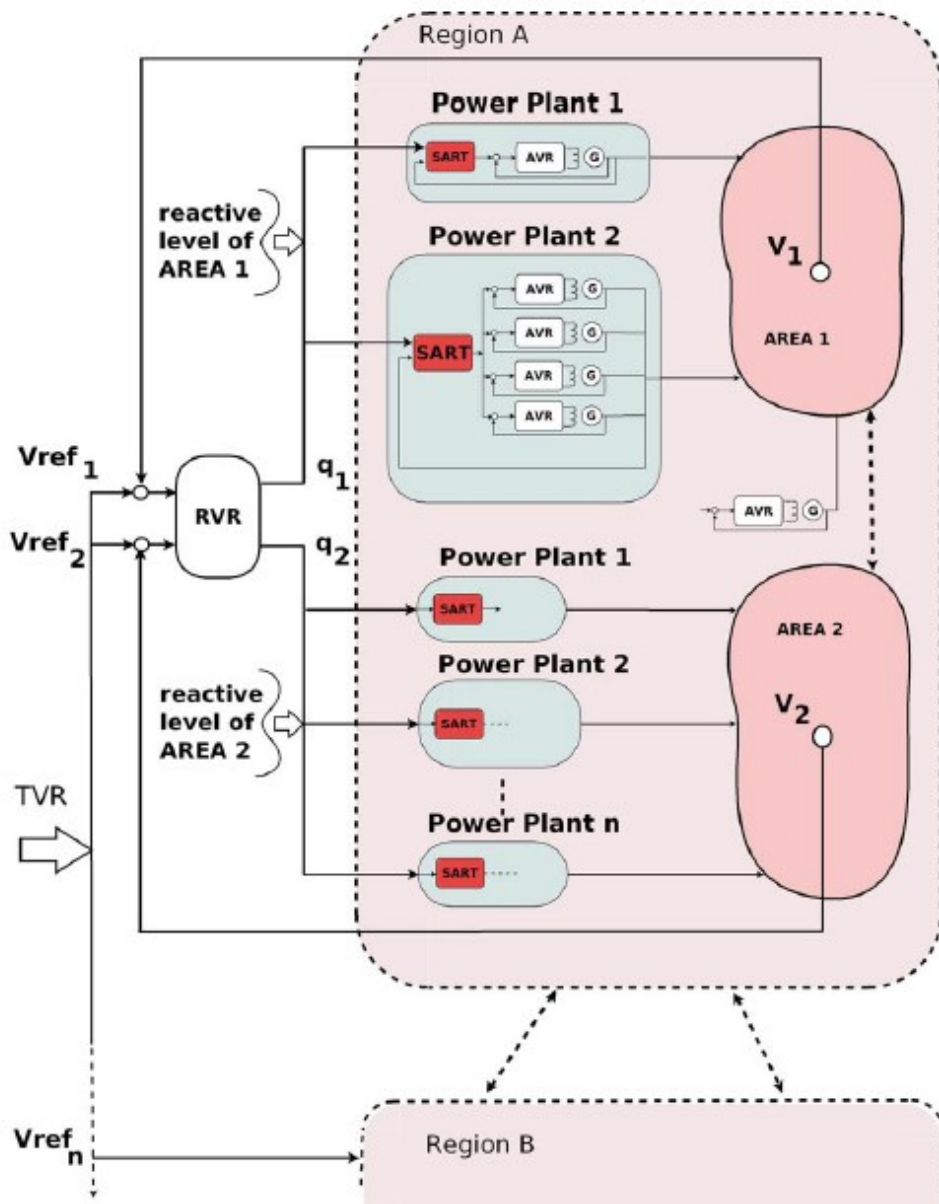


Figure 63 - Schematic diagram of the voltage control hierarchical system [73]

The Italian national transmission system was divided into three regions, each of which was divided into areas; each area is characterized by a pilot node<sup>29</sup> [183].



Figure 64 - Identification of pilot nodes in Italy [185]

The voltage control system is organized into a hierarchical structure, formed by three levels [72] [186]:

1. The first hierarchical level, the "Primary Voltage Regulation", is constituted by the Automatic Voltage Regulator (AVR) of each generator. It consists in the voltage control of each generation unit acting on its excitation system.
2. The second hierarchical level, the "Secondary Voltage Regulation", consists in the Regional Voltage Regulator (RVR) and in the various reactive power regulators (SART) of each power plant (Figure 63, Figure 65).

---

<sup>29</sup> Pilot nodes can be defined as the ones that for their connection features have a relevant influence on the voltages of an area of the electrical network considered

In particular:

- the RVR implements an outer voltage regulation loop: it regulates the voltage of the "pilot node" of its area, acting on the reactive power production of the controlled power plants of the same area.

Based on the voltage reference and the telemetry of the "pilot node", the RVR processes a reactive power level signal  $q_{liv}$  (in the range [-1; 1]) common to all the power plants of the area controlled. This level of reactive power signal is then sent to the SART of each power plant.

- the SART translate the  $q_{liv}$  required by the RVR (or by the Busbar Voltage Regulator BVR<sup>30</sup>), in a reactive power value to produce ( $Q_{ref}$ ) by each controlled group<sup>31</sup>. The Generator Reactive Power Regulators (GRPRs) implement a reactive power control loop for each of the controlled groups, external to the voltage control loop implemented by AVR. The reactive level  $q_{liv}$  is then obtained acting on the voltage reference ( $V_{ref}$ ) of AVRs.

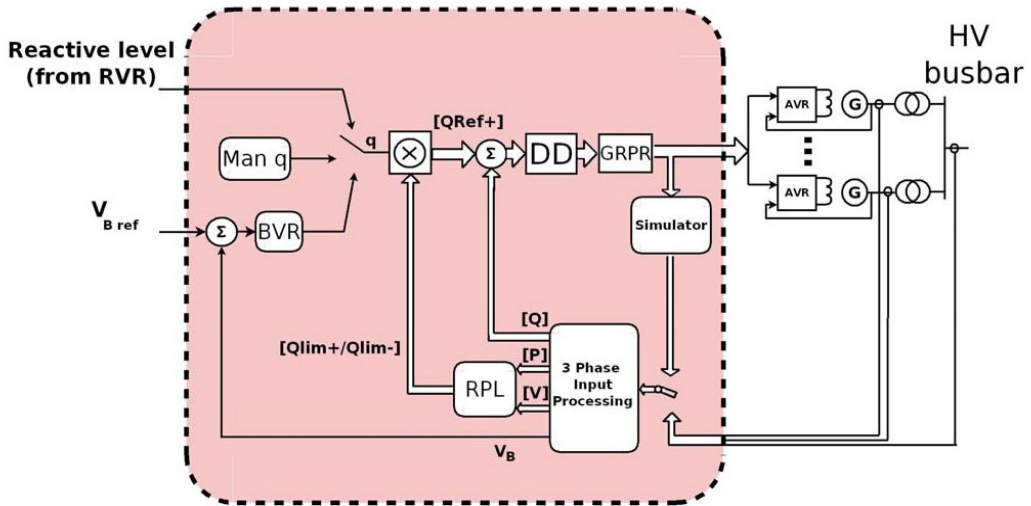


Figure 65 - Block Diagram of SART [73]

3. Lastly, Tertiary Voltage Regulator (TVR) establishes the pilot nodes voltage references on the basis of the algorithms aimed at maximizing the reactive power margins and minimizing the losses of the grid [183] [150] [73].

Each control cycle is dynamically decoupled.

---

<sup>30</sup> To cope with the unavailability of  $q_{liv}$  from the RVR, in addition to working in remote setting, the SART can also operate by adjusting the voltage of the local HV busbar or of a neighbouring network node.

<sup>31</sup> The  $q_{liv}$  signal is multiplied by each generator reactive power limit ( $Q_{lim}^+ / Q_{lim}^-$ ), calculated for each group in real time as a function of their capability curve and working point.

The Italian case is interesting for the presence of two important aspects: there is a strong penetration of not-dispatchable RES power plants (as described in paragraph 1.3.3) while TSO implements an automatic hierarchical voltage regulation using production plants as actuators.

Currently the SVR involves conventional power stations and hydroelectric power plants, while most of new renewable energy plants are not involved. Introduction of RES, regardless of their connection to MV or HV networks, can have consequences on voltage regulation. As noticed in [73], existing SVR based on reactive power sources offered by traditional fossil fuels power plants decreases its controlling capability when new RES generators replace equivalent amounts of power from traditional thermal and hydroelectric large plants.

It is therefore commonly accepted that RES power plants should not work at constant unitary power factor, regardless the fact that they are connected to the transmission network or to the distribution network.

Several proposal on the utilization of PV plants to voltage support are available: in [187], the authors propose to modulate the reactive power for voltage control functionality and bound the active power injected ramp whereas, in [188] authors propose to operate PV power plants as STATCOM devices. The possibility to use the connected PV units in the provision of the reactive power compensation ancillary service is shown in [189], which discusses the well-known dynamic reactive power compensation obtained through appropriate control scheme of power electronics devices [190].

Concerning Wind Farms, several voltage controls have been proposed in literature [191] [192] [193]. An example of voltage control for wind generators emulating hierarchical voltage control is shown in [194].

Furthermore, an interesting perspective is represented by "virtual power plants": a new methodology for the management and control of electrical networks. It consists of multiple generation facilities that are territorially distributed, connected and managed through a virtual smart network (therefore combined in a single "virtual center") that can be seen from the electrical grid as a single main service provider (energy and capacity) and auxiliary services (regulations, reserves, etc.) [195] [196] [197] [198].

### 3.3.2 Proposed control technique

As seen above, production plants based on RES are mainly connected to LV and MV distribution networks, but a considerable number of plants is connected directly to the HV national transmission grid.

Paragraph 2.2.2.2 shows that for RES power plants directly connected to the HV network a common technical specification for voltage control is not defined. A possible solution could be the application of a modified version of the hierarchical control strategy already used in the HV transmission network.

#### 3.3.2.1 Definition and calculation

Large RES production power plants connected at HV level are generally constituted of a cluster of multiple interconnected generators of medium or little size through an internal MV network and having a single point of delivery (POD), as represented in Figure 66. This topology is common for plants based on different RES (PV, wind, hydro, etc.) and with different types of generators (static, synchronous, asynchronous, etc.).

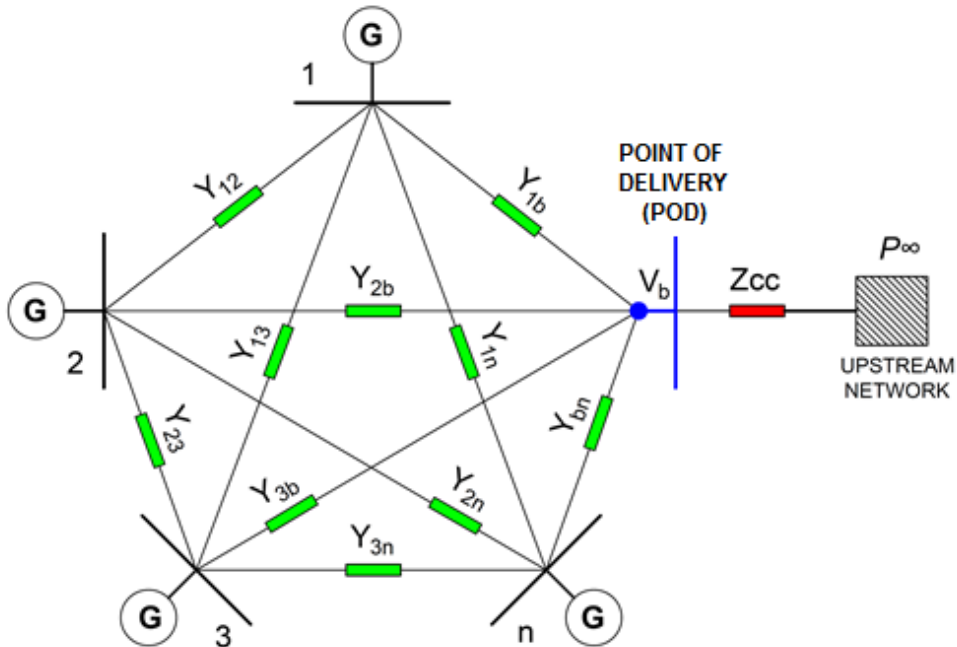


Figure 66 - Typical topology of a RES power plant connected to the HV level

The MV distribution network of the plant can be described, for the generic node k, by the well-known power flow equations, as follows:

$$\begin{cases} P_k = \sum_{i=1}^n V_k \cdot V_i \cdot Y_{ki} \cdot \cos(\theta_k - \theta_i - \gamma_{ki}) \\ Q_k = \sum_{i=1}^n V_k \cdot V_i \cdot Y_{ki} \cdot \sin(\theta_k - \theta_i - \gamma_{ki}) \end{cases} \quad (3.21)$$

Where:

$P$ : active power;

$Q$ : reactive power;

$V$ : voltage magnitude;

$Y$ : magnitude of admittance coefficients;

$\theta$ : phase angle of voltage;

$\gamma$ : phase angle of admittance coefficients;

$n$ : number of nodes of the network;

Linearizing (3.21) at a given operating point leads to the following matrix form in p.u.:

$$\begin{bmatrix} [\Delta p] \\ [\Delta q] \end{bmatrix} = \begin{bmatrix} \left[ \frac{dp}{d\theta} \right] & \left[ \frac{dp}{dv} \right] \\ \left[ \frac{dq}{d\theta} \right] & \left[ \frac{dq}{dv} \right] \end{bmatrix} \cdot \begin{bmatrix} [\Delta\theta] \\ [\Delta v] \end{bmatrix} \quad (3.22)$$

where the partial derivatives matrices  $\left[ \frac{dp}{dv} \right], \left[ \frac{dp}{d\theta} \right], \left[ \frac{dq}{dv} \right], \left[ \frac{dq}{d\theta} \right]$  constitute the Jacobian matrix and represent the link between the active and reactive power with the magnitude and the phase angle of voltage at buses around the operating point. Matrix coefficients embed information about the characteristic parameters of the lines of the network.

For the purposes of voltage control, active power variations are neglected ( $[\Delta p] = 0$ ) and only reactive power sources are utilized as actuators [172] thus equation (3.22) can be simplified as:

$$[\Delta q] = \left[ \left[ \frac{dq}{dv} \right] - \left[ \frac{dq}{d\theta} \right] \cdot \left[ \frac{dp}{d\theta} \right]^{-1} \cdot \left[ \frac{dp}{dv} \right] \right] [\Delta v] \quad (3.23)$$

Setting a working point of the system and solving the problem of power flow, it is possible to obtain the equations describing the linearized system:

$$[\Delta q] = [A] \cdot [\Delta v] \quad (3.24)$$

where  $[\Delta q]$  and  $[\Delta v]$  are the vectors  $(n,1)$  of the reactive power and voltage variations, respectively, and  $[A]$  is a  $(n,n)$  matrix that defines the electric coupling between reactive powers and voltage magnitudes.

Hence, generators are electrically coupled according to the matrix coefficients:

$$\left[ \frac{dq}{dv} \right] - \left[ \frac{dq}{d\theta} \right] \cdot \left[ \frac{dp}{d\theta} \right]^{-1} \cdot \left[ \frac{dp}{dv} \right] \quad (3.25)$$

Imposing a voltage variation at any network node, it causes a reactive power variation in all  $n$  nodes according to the coefficients of the matrix  $[A]$ :

$$\begin{bmatrix} \Delta q_1 \\ \Delta q_i \\ \Delta q_n \end{bmatrix} = \begin{bmatrix} a_{11} & a_{1i} & a_{1n} \\ a_{i1} & a_{ii} & a_{in} \\ a_{n1} & a_{ni} & a_{nn} \end{bmatrix} \cdot \begin{bmatrix} \Delta v_1 \\ \Delta v_i \\ \Delta v_n \end{bmatrix} \quad (3.26)$$

Note that we assume that  $[A]$  is full rank, as it is in most practical applications. The discussion of idiosyncratic cases where  $[A]$  is singular is out of the scope of this study.

Furthermore, the voltage at the point of delivery is determined by the following equation:

$$\Delta v_b = [S] \cdot [\Delta q] = \sum_{i=1}^n s_i * \Delta q_i \quad (3.27)$$

where  $[S]$  is the vector  $(1,n)$  of the sensitivity coefficients  $dv/dq$  that combine the point of delivery to all other nodes of the network.

That is, the reactive power variation achieved at different network nodes produces a voltage variation at the point of delivery, depending on the relative coefficients  $dv/dq$ .

Just to notice that the matrix  $[A]$   $(n,n)$  and the vector  $[S]$   $(1,n)$  can be also calculated through a numerical sensitivity analysis, by fixing all network parameters, incrementing the reactive power of each DG plant in turn and calculating the consequent voltage variation [164].

### 3.3.2.2 Voltage control scheme

The proposed control strategy is based on the hierarchical controller that has been successfully implemented in some countries in HV networks [70] [71]. Such a control scheme consists of an external and a cluster of internal controllers described below.

To control the voltage of a selected pilot bus (e.g. the point of connection with the transmission network), a central control unit (Reactive Power Regulator - RPR) coordinates the reactive power of each generator.

The control unit implements a reactive power regulation similar to the one of Secondary Voltage Regulation (SVR) of the transmission grid [181]. In the Italian Grid Code that device is called SART [72].

Figure 67 shows a synoptic scheme of the proposed control system.

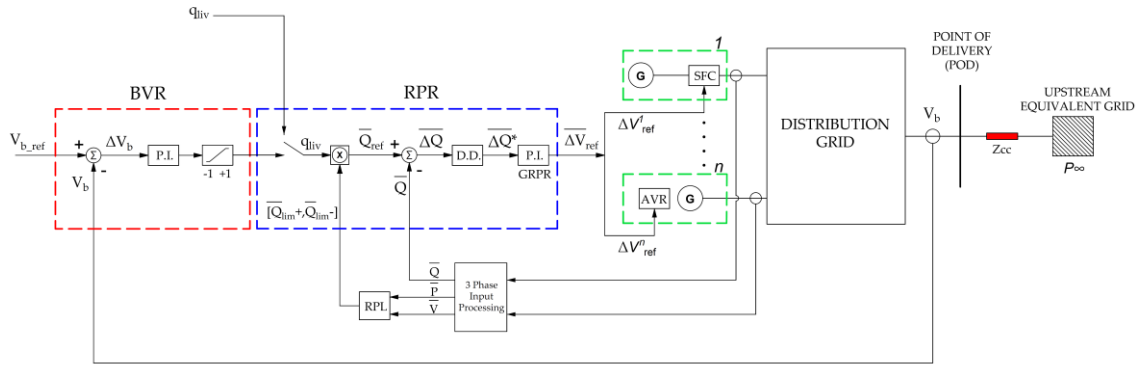


Figure 67 - Synoptic schema of Secondary Voltage Control

The control system receives the voltage reference from the network operator. The pilot bus (as defined in SVR) is the POD of the RES generation plant.

An external voltage control loop (with a time constant  $T_b$  of the order of tens of seconds), implemented by the Busbar Voltage Regulator (BVR) computes a reactive power level  $q_{liv}$  (between -1 and +1)<sup>32</sup> [181]. The BVR is of the proportional-integral type.

The  $q_{liv}$  signal is sent to the Reactive Power Regulator (RPR) and then multiplied by each generator reactive power limit. The result is the vector of reactive power references, namely  $\bar{Q}_{ref}$ . Every value of the vector is compared to the actual value of each generator reactive power  $\bar{Q}$ . The vector of errors  $\Delta \bar{Q}$  is multiplied by the Dynamic Decoupling (DD) matrix and sent to the Generator Reactive Power Regulators (GRPRs) [199].

The generator reactive power control loop is a Multiple-Input-Multiple-Output (MIMO) system, constituted of several regulators, one for each generator all of the same type (i.e.

---

<sup>32</sup> It is also possible to exclude the external voltage control loop and send a  $q_{liv}$  reference signal directly to the reactive power control loop.

---

proportional-integral). The time constant  $T_Q$  of the reactive power control loop is of the order of few seconds.

The GRPRs resulting control signals are the references of every generator  $\Delta V_{ref}$  (in Figure 67 these generators are represented as Static Frequency Converter SFC and Synchronous Generators AVR).

The BVR and RPR regulator parameters are chosen to ensure dynamic decoupling between the internal and external control cycle and also to obtain a time constant of the voltage regulation cycle equal to about 50 seconds, as normally required in the traditional production power plants connected in HV [72].

DGs have been modelled as “voltage actuators” in terms of a first order mathematical model in d and q-axis coordinates. Time constant  $T_v$  of voltage control loops is fast enough compared to that one of the outer reactive power loop  $T_Q$  (i.e. in the order of tenths of a second), so that it can be assumed that  $\Delta V_i = \Delta V_{i\_ref}$ .

This model is suitable to study the transient stability of the proposed hierarchical voltage control coupled with a simplified RES generator model (Figure 68) [200]. Several studies have been carried out on the possibility of controlling the reactive power of a Voltage Source Converter (VSC) independently from active power. In [201] the transient response of the reactive power to the change of reactive power reference is shown. The results show also P and Q injection decoupling. A fast response for the reactive power control can be found also in [202].

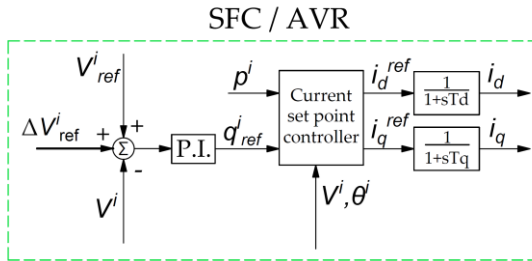


Figure 68 - Distributed Generator model

As demonstrated in [203] [204] [205], this control technique can be applied to different kinds of generation plants connected to HV networks (cluster of hydro power plants, wind and PV farms) coordinated by a TSO voltage regulation. Moreover, the application of a common control system for both traditional and RES power plants allow the standardization of the dynamic response of all types of generators of the network.

### 3.3.2.3 Dynamic Decoupling matrix

Starting from the inverse of the electric coupling matrix, it is possible to calculate the Dynamic Decoupling matrix as follows:

$$[DD] = [A]^{-1} \quad (3.28)$$

$[DD]$  is composed by the coefficients  $dv/dq$  and is defined by the following equation:

$$[\Delta v] = [DD] \cdot [\Delta q] \quad (3.29)$$

The insertion of Dynamic Decoupling matrix makes it possible to greatly simplify the control system: it compensate the mutual interactions, decoupling the MIMO reactive power control loop into  $n$  Single-Input-Single-Output (SISO) loops, one for each generator, all having the same transfer function [199].

Here after, some considerations focussing on the effect of the Dynamic Decoupling matrix follow [206]. With this aim, two networks are considered, each shows a different power plant topology and, hence a potentially different behaviour when coupled with the secondary voltage controller. The configurations under study are depicted in Figure 69 and Figure 70.

The notation of cable types is given in Table 27. Line length are indicated in Table 28 and Table 29 respectively for Plant A and Plant B. The characteristics of the generators are shown in Table 30 and Table 31.

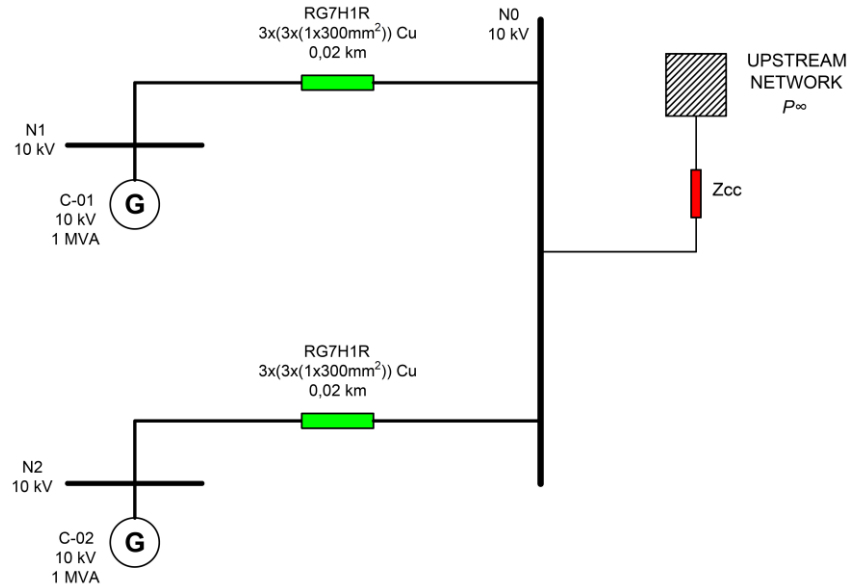
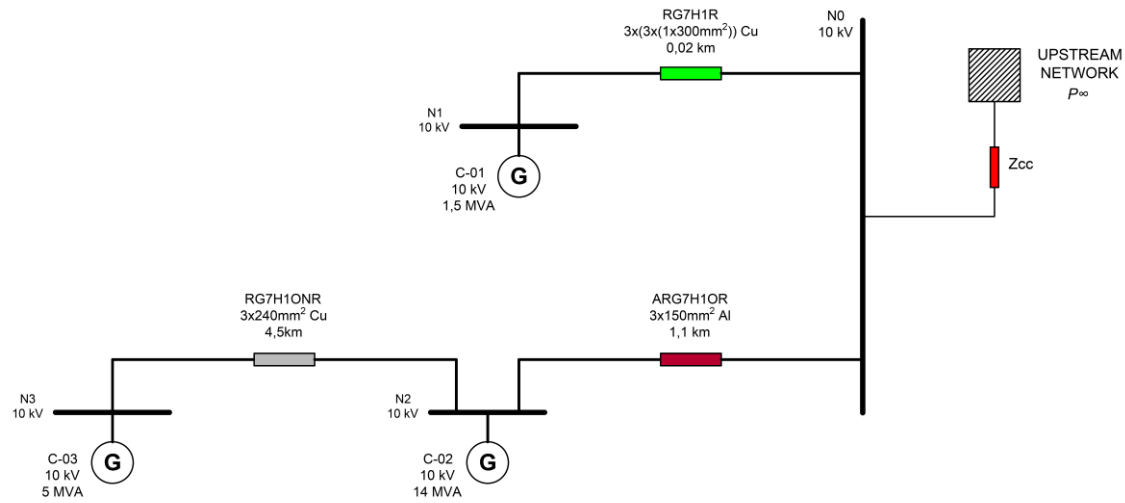


Figure 69 - Topology of plant A



**Figure 70 - Topology of plant B**

Line Type	Graphic symbol	R	X	c
		[Ohm/ Km]	[Ohm/ Km]	[μF/Km]
ARG7H1OR 3x150mmq		0,206	0,110	0,25
RG7H1R 3x(3x(1x300)mmq)		0,020	0,033	1,05
RG7H1ONR 3x240mmq		0,075	0,090	0,37

**Table 27 - Cable types**

From Node	To Node	Length L [km]
N0	N1	0,02
N0	N2	0,02

**Table 28 - Line lengths - Plant A**

From Node	To Node	Length L [km]
N0	N1	0,02
N0	N2	1,1
N2	N3	4,5

**Table 29 - Line lengths - Plant B**

Central	Node	P	V
		[MVA]	[kV]
C-01	N1	1	10
C-02	N2	1	10

**Table 30 - Characteristics of the generators - Plant A**

Central	Node	P	V
		[MVA]	[kV]
C-01	N1	1	10
C-02	N2	14	10
C-03	N3	5	10

Table 31 - Characteristics of the generators - Plant A

We first calculate the sensitivity coefficients  $dv/dq$  that correlate the POD (bus N0) to all the other nodes of the grid. For the two examples, Table 32 and Table 33 show, the influence on the voltage variations at POD of each generator. The higher the sensitivity, the more a generator participates in the voltage regulation. Clearly, if sensitivity values have similar magnitudes, then all the generators of a given power plant effectively participate in the voltage regulation proportionally to their capacity.

$dv/dq$	N0
C-01	0,777
C-02	0,777

Table 32 - Sensitivity Coefficients - Plant A

$dv/dq$	N0
C-01	0,6345
C-02	0,6103
C-03	0,5933

Table 33 - Sensitivity Coefficients - Plant B

The Dynamic Decoupling matrices are represented in Table 34 and Table 35 , constituted by the coefficients  $dv/dq$  that bind generation nodes to each other.

$dv/dq$	N1	N2
N1	0,7777	0,7770
N2	0,7770	0,7777

Table 34 - Dynamic Decoupling matrix - Plant A

$dv/dq$	N1	N2	N3
N1	0,6362	0,6103	0,5933
N2	0,6083	0,6775	0,6551
N3	0,5943	0,6619	0,9565

Table 35 - Dynamic Decoupling matrix - Plant B

For each power plant, regulator coefficients and time constants are chosen to ensure stability and a dynamic response with time scales comparable to those of traditional power plants.

The first simulation has been conducted considering the topology of plant A in Figure 69. In this case, two generators with same capacity are connected to a common bus bar and we assume that their reactive power production is different.

At time  $t = 50$  s, the control system is switched on. The purpose of the RPR is to balance the reactive power production of the two generators. Without the Dynamic Decoupling matrix, the RPR can introduce reactive power oscillations. Figure 71 shows such oscillations (all reactive power plots are in p.u. of 100 MVA), which are in antiphase, thus indicating a reactive power loop between the generators.

Note that reactive power loops should be avoided as they mechanically stress alternators, increase losses, interfere with voltage protections, and are seen as voltage disturbances by loads electrically close to the generators.

It should be noted that, although the topology of the network and starting conditions has been chosen to emphasize the coupling phenomenon, such asymmetric perturbations occur every time the system is started up or whenever a generator is inserted alone into the cluster. Figure 72 shows the effect of applying the same perturbation to the system but considering the effect of the proposed Dynamic Decoupling matrix. In this case, as expected, the transient evolution of reactive powers and, thus, bus voltages do not show oscillations.

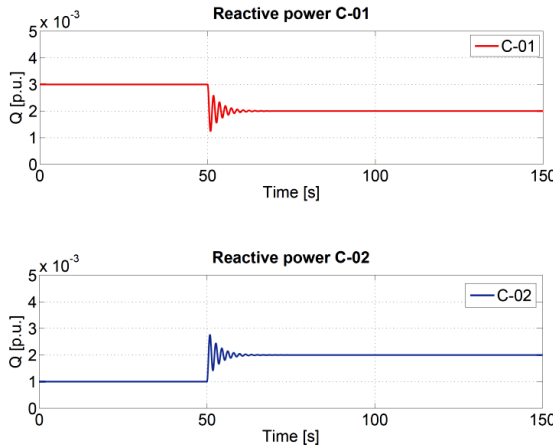


**Figure 71 - Reactive power response without Dynamic Decoupling matrix: network A**

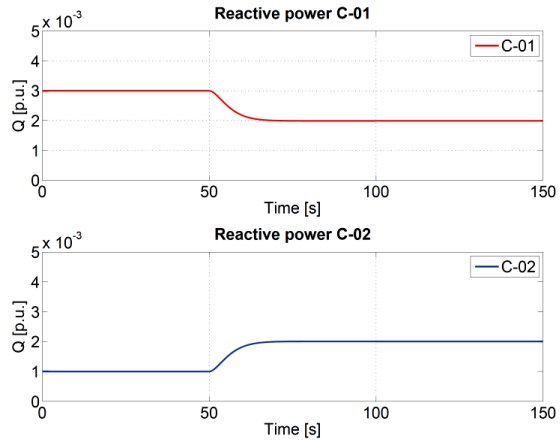


**Figure 72 - Reactive power response with Dynamic Decoupling matrix: network A**

Similar results are obtained with the power plant topology B. Figure 73 and Figure 74 show the response to a step of the voltage reference for network topology B respectively without and with the inclusion of the matrix  $[DD]$ .

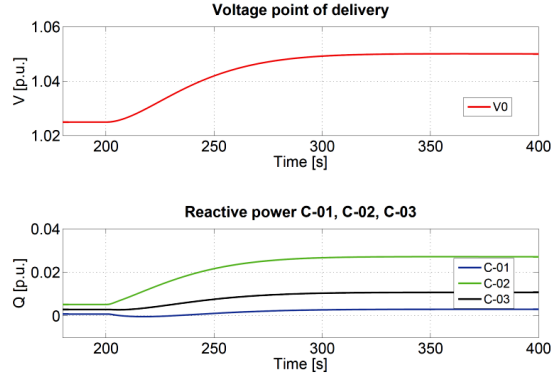


**Figure 73 - Voltage and reactive power response for a step in reference voltage without the Dynamic Decoupling matrix: network B**

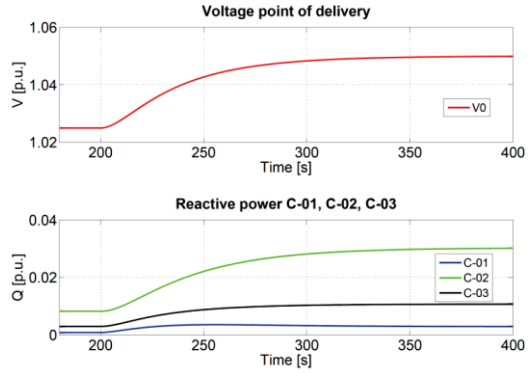


**Figure 74 - Voltage and reactive power response for a step in reference voltage with the Dynamic Decoupling matrix: network B**

The Dynamic Decoupling matrix provides positive effects on the robustness and the dynamic stability of the power system: thanks to the absence of cross-dynamics even in case of dissymmetrical conditions or disturbances, a stable operation is ensured [199]. Furthermore, at steady state each generator equally shares a quota of the reactive power requested by the coordinating unit [199] [206].

### 3.3.2.4 Traditional power plant

Figure 75 represents the network topology of a typical traditional power plant based on fossil fuel and Figure 76 shows the equivalent electrical model.

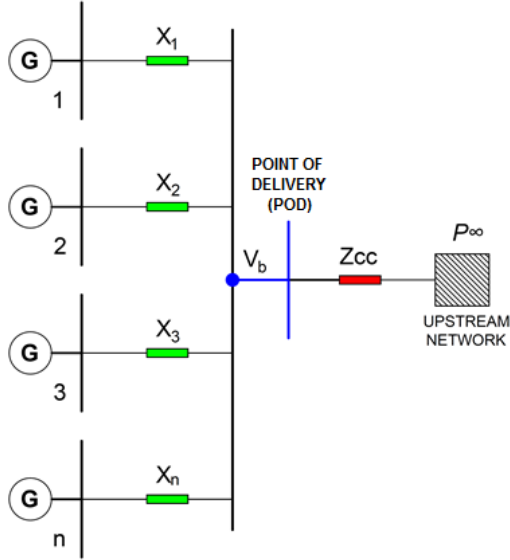


Figure 75 - Typical topology of a traditional power plant

Comparing the topology of RES power plants (Figure 66) with the one of traditional power plants (Figure 75), it is possible to note that the main difference is represented by the presence of an internal MV distribution network in the RES power plant case.

Indeed, in the traditional power plant case, every generator is connected to the main busbar, only through a transformer (named “generator transformer”), characterized by a reactance  $x_{ti}$ <sup>33</sup> [199].

So one can imagine that the traditional power plant is a subcase of the RES power plant case, in which the internal distribution network is merely constituted by the reactances of the generator transformers  $x_{ti}$ .

The electrical coupling of the generators is determined only by the reactances of the generator transformers  $x_{ti}$  and the equivalent reactance of the upstream network  $x_{cc}$ , as clarified in [199].

In these perspective, it is possible to say that the network topology represented in Figure 66 for the RES case and its mathematical model constitute the general case: they can describe a production power plant both based on RES and based on traditional fossil sources. Therefore, also the application of the control strategy to the traditional power plant results to be a particular case of the RES production power plant.

---

<sup>33</sup> Whereas no transformer connects the single alternator to the main busbar,  $X_{ti}$  is the equivalent reactance introduced by the compound action.

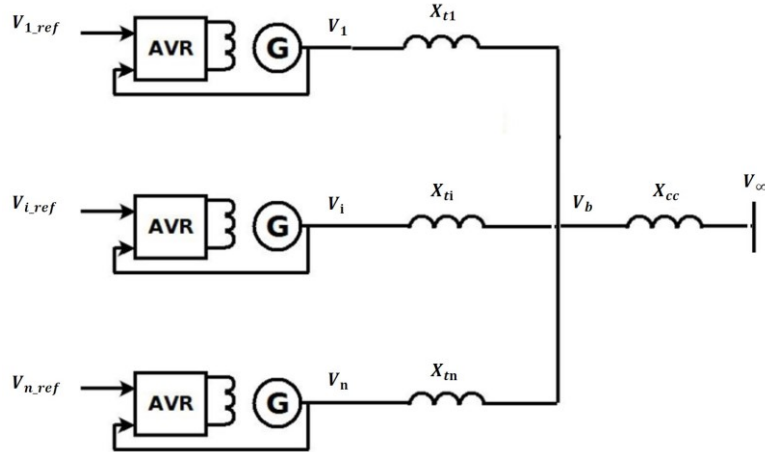


Figure 76 - Equivalent electrical model

In the traditional power plant case, referring to Figure 76, the relation between generator voltage variations and reactive power variations can be expressed with the following algebraic relations:

$$\begin{cases} \Delta v_1 = x_{t1} \cdot \Delta q_1 + x_{cc} \cdot \sum_{i=1}^n \Delta q_i \\ \vdots \\ \Delta v_i = x_{ti} \cdot \Delta q_i + x_{cc} \cdot \sum_{i=1}^n \Delta q_i \\ \vdots \\ \Delta v_n = x_{tn} \cdot \Delta q_n + x_{cc} \cdot \sum_{i=1}^n \Delta q_i \end{cases} \quad (3.30)$$

Where quantities are expressed in the common per unit system, and:

- $x_{ti}$  is the reactance of the i-th generator transformer;
- $x_{cc}$  is the equivalent reactance of the upstream network;
- $v_i$  is the voltage at the terminals of i-th generator;
- $q_i$  is the reactive power of the i-th generator;
- $v_b$  is the voltage at point of connection with the transmission network;

Expressed in matrix form, equation (3.30) becomes:

$$\begin{vmatrix} \Delta v_1 \\ \vdots \\ \Delta v_i \\ \vdots \\ \Delta v_n \end{vmatrix} = \begin{bmatrix} x_{t1} + x_{cc} & x_{cc} & x_{cc} \\ x_{cc} & x_{ti} + x_{cc} & x_{cc} \\ x_{cc} & x_{cc} & x_{tn} + x_{cc} \end{bmatrix} \begin{vmatrix} \Delta q_1 \\ \vdots \\ \Delta q_i \\ \vdots \\ \Delta q_n \end{vmatrix} \quad (3.31)$$

The result is that for a traditional electric plant the elements of the Dynamic Decoupling matrix are clearly defined by the reactances  $x_{ti}$  and  $x_{cc}$  [199], as follows:

$$DD_{i,j} = \begin{cases} x_{cc} & \text{if } i \neq j \\ x_{ti} + x_{cc} & \text{if } i = j \end{cases} \quad (3.32)$$

- **Steady state regime with and without Dynamic Decoupling matrix**

The traditional power plant case allows to understand more intuitively the effect of the Dynamic Decoupling matrix in the steady state regime.

Let us consider the following assumptions:

1. the power plant consists of two same size generators;
2. AVR's dynamic is fast enough comparing to that one of the outer control loop ( $\Delta v_i = \Delta v_{i\_ref}$ ).

The busbar voltage depends on voltage at the terminals of i-th generator  $v_i$ , through the following algebraic relation:

$$v_b = \frac{\frac{v_1}{x_{t1}} + \frac{v_2}{x_{t2}} + \frac{v_\infty}{x_{cc}}}{\frac{1}{x_{t1}} + \frac{1}{x_{t2}} + \frac{1}{x_{cc}}} \quad (3.33)$$

Written in terms of variations, (3.33) becomes:

$$\Delta v_b = \frac{\frac{\Delta v_1}{x_{t1}} + \frac{\Delta v_2}{x_{t2}}}{\frac{1}{x_{t1}} + \frac{1}{x_{t2}} + \frac{1}{x_{cc}}} \quad (3.34)$$

$$\Delta v_b = \Delta v_1 \cdot \left( \frac{x_{t2}x_{cc}}{x_{t1}x_{t2} + x_{t1}x_{cc} + x_{t2}x_{cc}} \right) + \Delta v_2 \cdot \left( \frac{x_{t1}x_{cc}}{x_{t1}x_{t2} + x_{t1}x_{cc} + x_{t2}x_{cc}} \right) \quad (3.35)$$

Neglecting resistive currents, the variation of reactive power generated by the i-th generator due to single node voltage variations  $\Delta v_i$ , can be expressed by the following simplified expression:

$$\Delta q_i \cong \frac{\Delta v_i - \Delta v_b}{x_{ti}} \quad (3.36)$$

For generator 1, equation (3.36) becomes:

$$\Delta q_1 \cong \frac{\Delta v_1 - \Delta v_b}{x_{t1}} \quad (3.37)$$

Then substituting (3.35) in (3.37), one obtains:

$$\Delta q_1 = \frac{\Delta v_1}{x_{t1}} \cdot \left( 1 - \frac{x_{t2}x_{cc}}{x_{t1}x_{t2} + x_{t1}x_{cc} + x_{t2}x_{cc}} \right) - \Delta v_2 \cdot \left( \frac{x_{cc}}{x_{t1}x_{t2} + x_{t1}x_{cc} + x_{t2}x_{cc}} \right) \quad (3.38)$$

$$\Delta q_1 = \Delta v_1 \cdot \left( \frac{x_{t2} + x_{cc}}{x_{t1}x_{t2} + x_{t1}x_{cc} + x_{t2}x_{cc}} \right) - \Delta v_2 \cdot \left( \frac{x_{cc}}{x_{t1}x_{t2} + x_{t1}x_{cc} + x_{t2}x_{cc}} \right) \quad (3.39)$$

Similarly, for generator 2:

$$\Delta q_2 = \Delta v_2 \cdot \left( \frac{x_{t1} + x_{cc}}{x_{t1}x_{t2} + x_{t1}x_{cc} + x_{t2}x_{cc}} \right) - \Delta v_1 \cdot \left( \frac{x_{cc}}{x_{t1}x_{t2} + x_{t1}x_{cc} + x_{t2}x_{cc}} \right) \quad (3.40)$$

Written in terms of matrices:

$$|\Delta q| = |A| \cdot |\Delta v| \quad (3.41)$$

Where:

$$|A| = \begin{bmatrix} \frac{x_{t2} + x_{cc}}{x_{t1}x_{t2} + x_{t1}x_{cc} + x_{t2}x_{cc}} & -\frac{x_{cc}}{x_{t1}x_{t2} + x_{t1}x_{cc} + x_{t2}x_{cc}} \\ -\frac{x_{cc}}{x_{t1}x_{t2} + x_{t1}x_{cc} + x_{t2}x_{cc}} & \frac{x_{t1} + x_{cc}}{x_{t1}x_{t2} + x_{t1}x_{cc} + x_{t2}x_{cc}} \end{bmatrix} \quad (3.42)$$

On the basis of the second hypothesis equation (3.41) can be written as:

$$\left\{ \begin{array}{l} |\Delta q| = |A| \cdot |\Delta v_{ref}| \\ \Delta q_1 = \frac{x_{t2} + x_{cc}}{x_{t1}x_{t2} + x_{t1}x_{cc} + x_{t2}x_{cc}} \Delta v_{1ref} - \frac{x_{cc}}{x_{t1}x_{t2} + x_{t1}x_{cc} + x_{t2}x_{cc}} \Delta v_{2ref} \\ \Delta q_2 = -\frac{x_{cc}}{x_{t1}x_{t2} + x_{t1}x_{cc} + x_{t2}x_{cc}} \Delta v_{1ref} + \frac{x_{t1} + x_{cc}}{x_{t1}x_{t2} + x_{t1}x_{cc} + x_{t2}x_{cc}} \Delta v_{2ref} \end{array} \right. \quad (3.43)$$

Without the matrix  $[DD]$ ,  $\Delta v_{1ref}$  and  $\Delta v_{2ref}$  will be the same, because the controller will divide equally (according to the generators capability) the total reactive power required.

$$\Delta v_{ref} = \Delta v_{1ref} = \Delta v_{2ref}$$

Equations (3.43) becomes:

$$\left\{ \begin{array}{l} \Delta q_1 = \frac{x_{t2}}{x_{t1}x_{t2} + x_{t1}x_{cc} + x_{t2}x_{cc}} \Delta v_{ref} \\ \Delta q_2 = \frac{x_{t1}}{x_{t1}x_{t2} + x_{t1}x_{cc} + x_{t2}x_{cc}} \Delta v_{ref} \end{array} \right. \quad (3.44)$$

Therefore, substituting the second equation in the first one of (3.44), it is obtained:

$$\Delta q_1 = \frac{x_{t2}}{x_{t1}x_{t2} + x_{t1}x_{cc} + x_{t2}x_{cc}} \cdot \Delta q_2 \cdot \frac{x_{t1}x_{t2} + x_{t1}x_{cc} + x_{t2}x_{cc}}{x_{t1}} \quad (3.45)$$

$$\Delta q_1 = \frac{x_{t2}}{x_{t1}} \cdot \Delta q_2 \quad (3.46)$$

It is clear that if  $x_{t1} \neq x_{t2}$ , than there will inevitably be  $\Delta q_1 \neq \Delta q_2$ . Therefore, in response to a variation of  $\Delta v_{ref}$ , the two groups will inject/absorb reactive power as a function of the reactance seen from their terminals.

Moreover, the system can be described by the following equations:

$$\begin{cases} \Delta v_1 = x_{t1} \cdot \Delta q_1 + x_{cc} \cdot (\Delta q_1 + \Delta q_2) \\ \Delta v_2 = x_{t2} \cdot \Delta q_2 + x_{cc} \cdot (\Delta q_1 + \Delta q_2) \end{cases} \quad (3.47)$$

On the basis of the second hypothesis equation (3.47) can be written as:

$$\begin{cases} \Delta v_{1ref} = (x_{t1} + x_{cc}) \cdot \Delta q_1 + x_{cc} \cdot \Delta q_2 \\ \Delta v_{2ref} = x_{cc} \cdot \Delta q_1 + (x_{t2} + x_{cc}) \cdot \Delta q_2 \end{cases} \quad (3.48)$$

$$|\Delta v_{ref}| = |DD| \cdot |\Delta q| \quad (3.49)$$

With:

$$|DD| = \begin{bmatrix} x_{t1} + x_{cc} & x_{cc} \\ x_{cc} & x_{t2} + x_{cc} \end{bmatrix} \quad (3.50)$$

Comparing (3.42) with (3.50), it results that:

$$|DD| = |A|^{-1}$$

Therefore, it is evident that introducing matrix [DD], a compensation of the AVR's voltage references ( $\Delta v_{1ref}$  and  $\Delta v_{2ref}$ ) is implemented, ensuring that  $\Delta q_1 = \Delta q_2$  independently of their electrically coupling.

# Chapter 4.

## Case studies and results

---

This chapter presents the simulation results carried out on some electrical testing networks, implementing the control techniques described in the previous chapter.

### 4.1 Case studies for power generation plants connected to the MV and LV distribution networks

#### 4.1.1 Application of control techniques proposed in Italy by the recent connection rules (CEI 0-16 CEI 0-21)

##### 4.1.1.1 IEEE 37-bus

A modified version of the IEEE 37-bus distribution system [207] is used for testing the effects of the voltage control logics of DGs described in paragraph 3.2.6. Figure 77 shows the topology of the IEEE 37-bus network. The same network has been already used to test voltage control strategies in [151] [149].

The IEEE 37-bus network includes four types of cables whose data are based on [208]. The line styles used in Figure 77 refer to the four cable types illustrated in Table 36. Line lengths have been augmented from the original ones described in [207] in such a way the technical rules about voltage control are actively applied (i.e. at least a voltage of  $1.05 V_n$  is reached). All line length changes are indicated in Table 37.

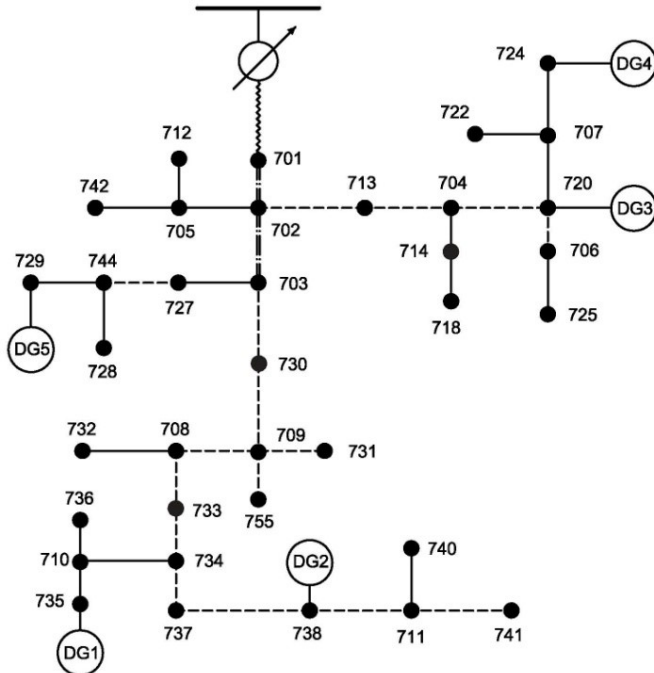


Figure 77 - IEEE 37-bus MV test system [207]

---

Line code	R [Ω/km]	L [mH/km]	Rate [A]
~~~~~ (721)	0,065	0,567	698
(722)	0,128	0,637	483
--- (723)	0,478	0,783	230
— (724)	0,957	0,853	200

Table 36 - Cable data for the IEEE 37-bus network

From bus	To bus	Original L [km]	Modified L [km]
701	702	0,293	1,0
702	705	0,122	0,122
702	713	0,110	1,0
702	703	0,402	1,0
703	727	0,073	0,073
703	730	0,183	1,0
704	714	0,024	0,024
704	720	0,244	0,244
705	742	0,098	0,098
705	712	0,073	0,073
706	725	0,085	0,085
707	724	0,232	1,0
707	722	0,037	0,037
708	733	0,098	0,098
708	732	0,098	0,098
709	731	0,183	0,183
709	708	0,098	0,098
710	735	0,061	1,0
710	736	0,390	0,390
711	741	0,122	0,122
711	740	0,061	0,061
713	704	0,158	1,0
714	718	0,158	0,158
720	707	0,280	1,0
720	706	0,183	0,183
727	744	0,085	0,085
730	709	0,061	1,0
733	734	0,171	0,171
734	737	0,195	0,195
734	710	0,158	0,159
737	738	0,122	1,0
738	711	0,122	0,122
744	728	0,061	0,061
744	729	0,085	2,0
799	701	0,564	3,0

Table 37 - Cable lengths

Loads have been expressed using static PQ constant models. DGs have been connected to selected buses as proposed in [209].

The rated capacity of the DGs is shown in Table 38. Without loss of generality all DGs are assumed to be solar photovoltaic (PV) energy resources.

DG unit	Bus	Rated Capacity [MW]
DG1	735	0,70
DG2	738	1,40
DG3	720	0,60
DG4	724	1,00
DG5	729	1,40

Table 38 - MV test network DGs data

There are various models for inverter-based generators. The model adopted in this case study is a simplified d-q axis current control based on first order lag transfer functions as proposed in [210] and [211].

The qualitative control scheme of DGs is shown in Figure 78. The control scheme has been completed with the inclusion of the voltage control logics discussed in paragraph 3.2.6. The logics are basically if-then loops that allow the definition of the value of  $Q_{ref}$  based in the current value of  $P_{ref}$ . We assume that  $P_{ref}$  is the available active power production resulting from the MPPT control of PV generators. We also assume that there are no restrictions on the active power output of DGs.

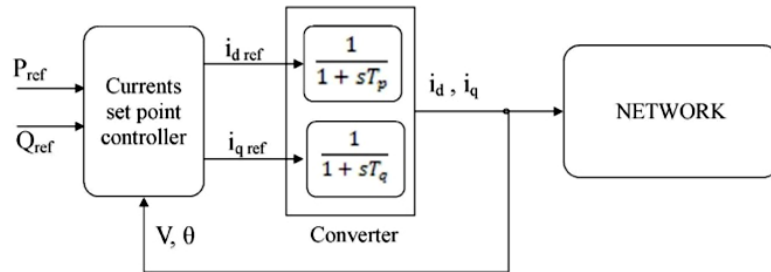
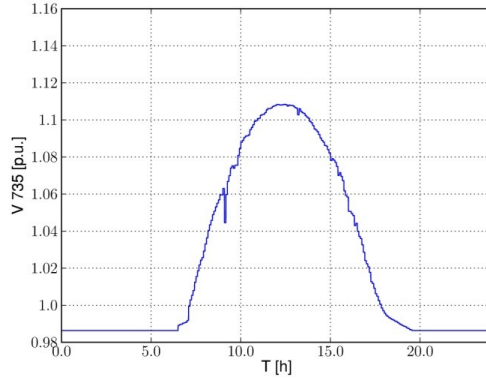
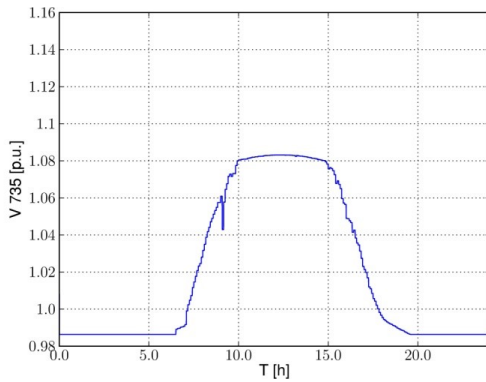


Figure 78 - Model used for PV energy resources [210]

Active power profiles have been obtained from experimental data of some PV panels located on the roof of some buildings of the University of Trieste, Italy. Figure 79, Figure 80 and Figure 81 show a typical daily voltage profile of the point of connection of a PV device and refer to the voltage at bus 735 of the proposed case study. In particular, Figure 79 shows the profile resulting by not applying any control, i.e., imposing a unity power factor, whereas Figure 80 shows the effect of the reactive power control. Figure 81 shows the effects of the application of the power factor control law.



**Figure 79 - Daily voltage profile at node 735 with unity power factor**



**Figure 80 - Daily voltage profile at node 735 with reactive power control**

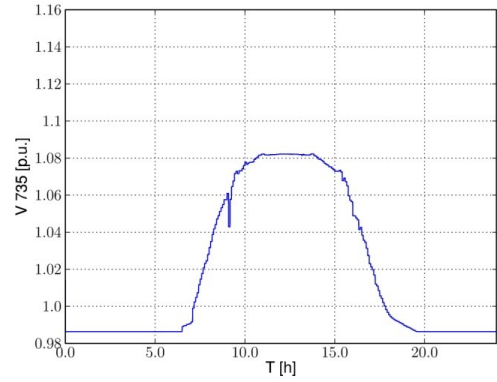


**Figure 81 - Daily voltage profile at node 735 with power factor control**

In Figure 82 three different voltage profiles for the network are shown. The red line is obtained with the produced maximum active power injection in the five DGs operating without any voltage control. The cyan dot-dashed line is obtained applying the reactive power control, while the green dashed line is with the power factor control.

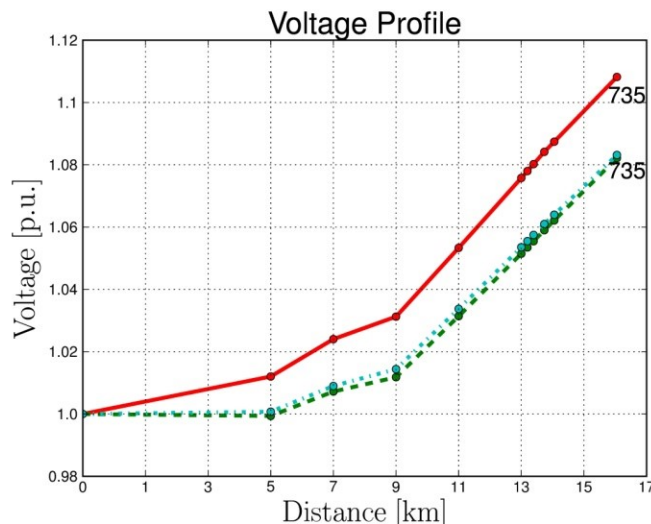


**Figure 82 - Voltage profile for the test network IEEE 37-bus: radial branch to node 735 (DG1)**

For all three cases the load has been kept at the constant value reported in [207] and the active power considered is at the maximal irradiation time during the day. There is no node that exceeds the value of  $1.1 V_n$ . The voltage level is beyond the standard contractual limits agreed for all load buses. Moreover, DGs should automatically disconnect from the grid if the voltage exceeds  $1.1 V_n$  (i.e. loosing active power production). Both control strategies avoid overvoltage keeping voltage in the limits and show very similar effects on the bus voltage profile.

All simulations have been carried out using DOME [88] - described in Appendix A1.2.

#### 4.1.1.2 Actual real-world distribution network

In this paragraph, an actual real-world distribution network is used to analyze the application of the local rules described in paragraph 3.2.6 [212]. The network topology is depicted in Figure 83. This network has been chosen in the present work mainly because of the high penetration of currently installed and planned DGs.

Moreover, the considered grid shows several voltage levels, i.e., 10, 20, 110, and 132 kV.

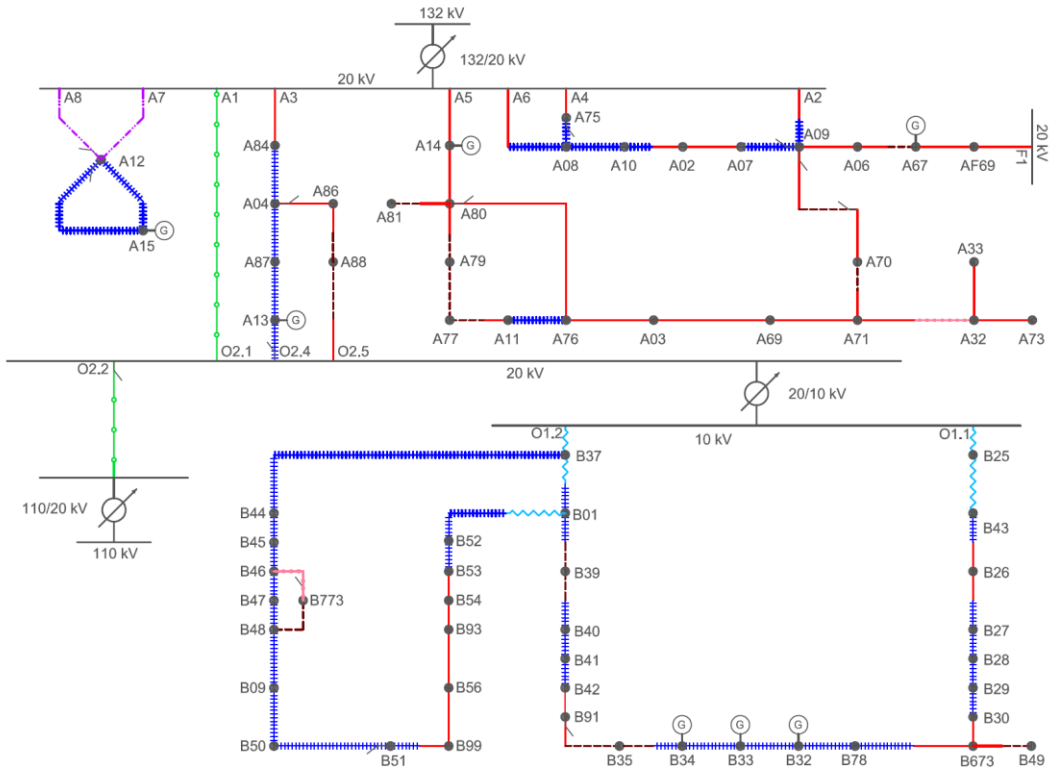


Figure 83 - Real-world grid used in the case study

The line styles used in Figure 83 refer to the seven cable types illustrated in Table 39.

Line Type	Graphic symbol	R	1	C
		[Ohm/Km]	[mH/Km]	[ $\mu$ F/Km]
Type 1	—●—●—●—	0,047	0,315	0,390
Type 2	—○—○—○—	0,075	0,350	0,320
Type 3	—■—■—■—	0,124	0,350	0,270
Type 4		0,125	0,318	0,330
Type 5	~~~~~	0,206	0,350	0,270
Type 6	—·—·—·—	0,387	0,413	0,180
Type 7	—■—■—■—	0,524	0,446	0,170

Table 39 - Cable data for the Actual Real-World distribution network

- **Scenario I: low power generation**

Network has been simulated in a typical operating condition in 3 different cases:

- not applying controls, i.e., imposing a unity power factor to installed generators;
- applying the power factor control;
- applying the reactive power control.

DGs data are shown in Table 40. Active and reactive nominal load powers for each node of the network are shown in Table 41: this can be considered as maximum load for the network. Minimum load conditions have been chosen as 10% of the nominal power.

Bus	P gen [kW]
A13	780
A14	321
A15	137
A67	0
B32	997
B33	1566
B34	999

Table 40 - DGs data for Scenario I

Results of the simulations are shown in Figure 84, three branches with DG have been chosen: the blue line is the voltage profile for branch B25 to B35; the red line is the voltage profile for branch A84 to A13; finally, the green line is the voltage profile of branch A09 to AF69. Two different conditions have been simulated: dashed line is without DG and minimal load, while solid line is with nominal DG and minimal load.

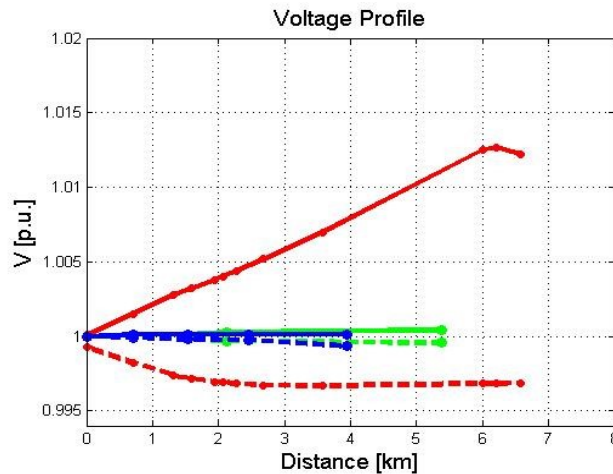


Figure 84 - Voltage profiles for three branches: solid line (with DG), dashed lines (without DG)

It is worth noting that voltage profiles do not change even if the power factor control or the reactive power control are implemented. This is due to the fact that the lock-in voltages (i.e., the thresholds to trigger the controls) in this particular case are never reached: the values of the voltages do not exceed the permissible limits. The most critical

branch is line B25-B35, where there are three generators. According to previous simulation results, cables appear well dimensioned for the actual level of DG penetration as voltage rise is relatively low (i.e., less than 1.5%).

The direct consequence is that the application of reactive power control produces no appreciable results and in addition, voltage rise is so small that the application of reactive power control is not enabled.

Bus	P load	Q load
	[kW]	[kVAR]
A02	53	26
A03	72	36
A04	48	24
A06	1	0
A07	7	4
A08	70	35
A09	100	50
A10	1	0
A11	0	0
A12	6.880	3.440
A32	15	8
A33	3	1
A67	0	0
A69	57	29
A70	5	3
A71	84	42
A73	1	0
A75	190	95
A76	8	4
A77	7	3
A79	16	8
A80	104	52
A81	56	28
A84	3	2
A86	54	27
A87	1	0
A88	26	13
AF69	10	6

Bus	P load	Q load
	[kW]	[kVAR]
B01	89	45
B09	72	36
B25	57	29
B26	56	28
B27	151	76
B28	0	0
B29	11	5
B30	96	48
B35	5	3
B37	41	20
B39	80	40
B40	56	28
B41	30	15
B42	97	48
B43	110	55
B44	54	27
B45	85	43
B46	124	62
B47	171	86
B48	80	40
B49	53	27
B50	29	15
B51	22	11
B52	37	19
B53	49	24
B54	56	28
B56	17	9
B673	78	5
B773	1.000	600
B78	33	17
B91	10	5
B93	40	20
B99	31	16
F1	0	0

Table 41 - Loads data

It can be shown that if  $V_t$  is the threshold (expressed in percentage of the nominal voltage) that has to be exceeded for the control to be activated, then there is a minimal length of the line:

$$l_{min} = V_t \frac{V_n}{I_{max}\sqrt{3}} \frac{1}{R} \quad (4.1)$$

Where:

- $V_n$  is the nominal voltage of the line;
- $I_{max}$  the ampacity of the line (maximum current);
- $R$  the resistance, in Ohms/km.

If the length of the line is lower than  $l_{min}$ , constraints on the maximum current transportable intervene before the constraints on the line voltage. As an example for line A05-A14, of Type 3 as in Table 39 (150 mm<sup>2</sup> copper), for a threshold of 5% the length of the cable should be of at least 14 km.

#### ▪ *Sensitivity matrix*

Based on sensitivity analysis, one can observe that voltages of nodes Axx do not depend on generators on nodes Bxx and vice-versa. Moreover, for each generator, one can define the nodes with maximum sensitivity to the power production of that generator. The results of sensitivity analysis are summarized in the following matrix, which shows the most sensitive nodes to the active power of each generator:

$$\begin{bmatrix} \Delta v_{A15} \\ \Delta v_{A67} \\ \Delta v_{B34} \\ \Delta v_{B33} \\ \Delta v_{B32} \\ \Delta v_{A13} \\ \Delta v_{A14} \end{bmatrix} = \begin{bmatrix} 0.0564 & 0 & 0 & 0 & 0 & 0 \\ 0 & 0.2299 & 0 & 0 & 0 & 0 \\ 0 & 0 & 0.8725 & 0.8287 & 0 & 0 \\ 0 & 0 & 0.8279 & 0.8290 & 0 & 0 \\ 0 & 0 & 0.8043 & 0.8054 & 0 & 0 \\ 0 & 0 & 0 & 0 & 0.1229 & 0 \\ 0 & 0 & 0 & 0 & 0 & 0.0179 \end{bmatrix} * \begin{bmatrix} \Delta p_{A15} \\ \Delta p_{A67} \\ \Delta p_{B34} \\ \Delta p_{B33} \\ \Delta p_{B32} \\ \Delta p_{A13} \\ \Delta p_{A14} \end{bmatrix}$$

As expected, the most critical generators are the ones connected to nodes B34, B33 and B32. Generators at nodes A14 and A15 have very little impact on voltages being very short to the bus bar.

#### ▪ *Scenario II: high power generation*

The study of sensitive matrices highlights most of the critical nodes of the network. In particular, DGs that contribute mostly to voltage rise phenomenon on different nodes can be recognized.

According to such considerations, we impose a substantial increase of the active power produced by installed DGs. With this aim, all generators powers have been multiplied by 5 (DGs data are indicated in Table 42). However, as discussed above, the power increase does not affect the voltage rise of most generators.

Simulations results are shown in Figure 85: the voltage profiles of the three branches B25-B35 (red line), A84-A13(blue line) and A09-F69 (green line) are shown without any voltage control (solid line) and with power factor and reactive power regulation (respectively dash-dot and dashed lines: almost unnoticeable as shown also in [89]). Increasing the active power injected by DGs, voltage rise becomes remarkable only for those generators far from the bus-bar. For branches A84-A13 and A09-F69 none of the voltage control logic functions are activated.

Bus	P gen [kW]
A13	3900
A14	1605
A15	6865
A67	0
B32	4985
B33	7830
B34	4995

Table 42 - DGs data for Scenario II

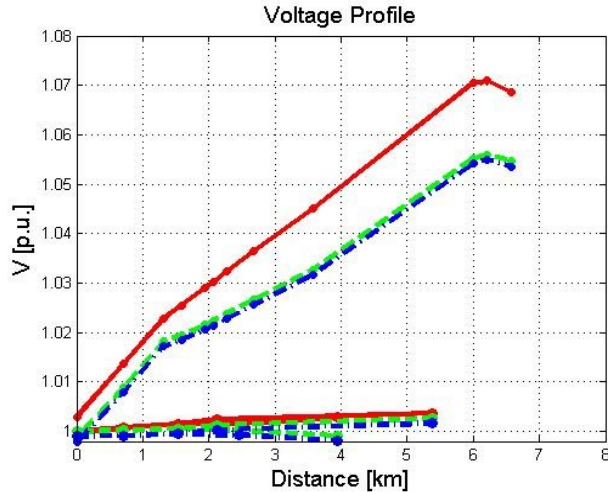


Figure 85 - Voltage profile for maximum DG

#### 4.1.2 Application of the centralized control technique proposed

This section shows the beneficial effects obtained by implementing an adequate adjustment of reactive power supplied by generators according to the control technique proposed in paragraph 3.2.7.

All simulations have been carried out using PSAT [213] [214] - described in Appendix A1.1. In particular, tests were conducted on a MV radial distribution network, consisting of 17 nodes [149]. Its topology is represented in Figure 86.

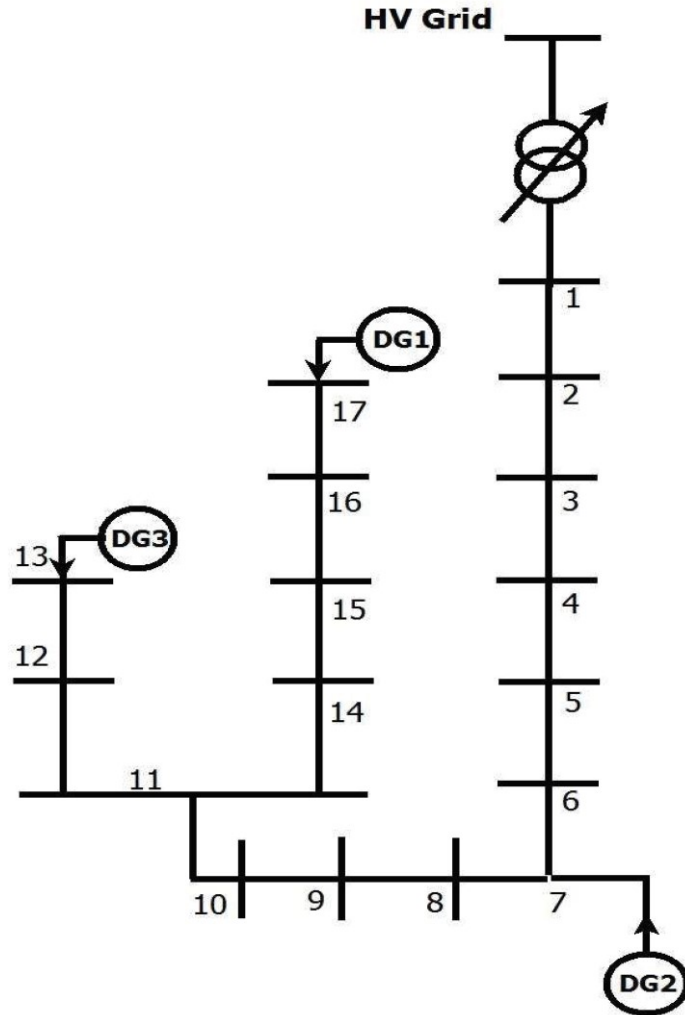


Figure 86 - Diagram of the test network

Generators: The network has three DG units (listed in Table 43).

DG unit	Node	Active power [MW]
DG1	17	5
DG2	7	2,2
DG3	13	2

Table 43 - Generators data

The data of the electrical lines are presented in Table 44.

From bus	To bus	Length [km]	Resistance [ $\Omega/\text{km}$ ]	Inductance [ $\text{mH}/\text{km}$ ]
1	2	0,942	0,125	0,493
2	3	0,810	0,125	0,493
3	4	0,266	0,125	0,493
4	5	0,642	0,125	0,493
5	6	0,809	0,206	0,608
6	7	0,266	0,206	0,608
7	8	1,000	0,125	0,493
8	9	1,200	0,125	0,493
9	10	1,126	0,206	0,608
10	11	0,378	0,125	0,493
11	12	0,935	0,519	1,957
12	13	0,595	0,519	1,957
11	14	0,640	0,206	0,608
14	15	0,400	0,206	0,608
15	16	1,500	0,519	1,957
16	17	2,000	0,519	1,957

Table 44 – Cable data

Loads: All loads are equal and absorb 400 kVA each with an inductive power factor equal to 0.85.

Control nodes: The nodes chosen for voltage control are nodes 7, 11, 17 and therefore with  $M = N_G = 3$  (number of nodes equal to the number of generators).

Network sensitivity matrices: as already described in paragraph 3.2.7., in order to cancel the gap between the two voltage profiles, the proposed control technique provides for the calculation of two matrices of sensitivity [B] and [C]. With reference to equation (3.20) one can obtain the matrix [A].

The matrices are shown below:

$$[B] = \begin{bmatrix} 0.152 & 0.169 & 0.162 \\ 0.303 & 0.171 & 0.324 \\ 0.874 & 0.171 & 0.325 \end{bmatrix}$$

$$[C] = \begin{bmatrix} 0.372 & 0.392 & 0.382 \\ 0.743 & 0.395 & 0.764 \\ 2.078 & 0.397 & 0.767 \end{bmatrix}$$

$$[A] = \begin{bmatrix} -0.428 & 0.001 & 0.000 \\ 0.020 & -0.430 & 0.000 \\ -0.020 & 0.003 & -0.424 \end{bmatrix}$$

- *Voltage Profile Analysis*

Through power flow calculations, the steady-state network profiles have been analysed. The results are reported in Figure 87.

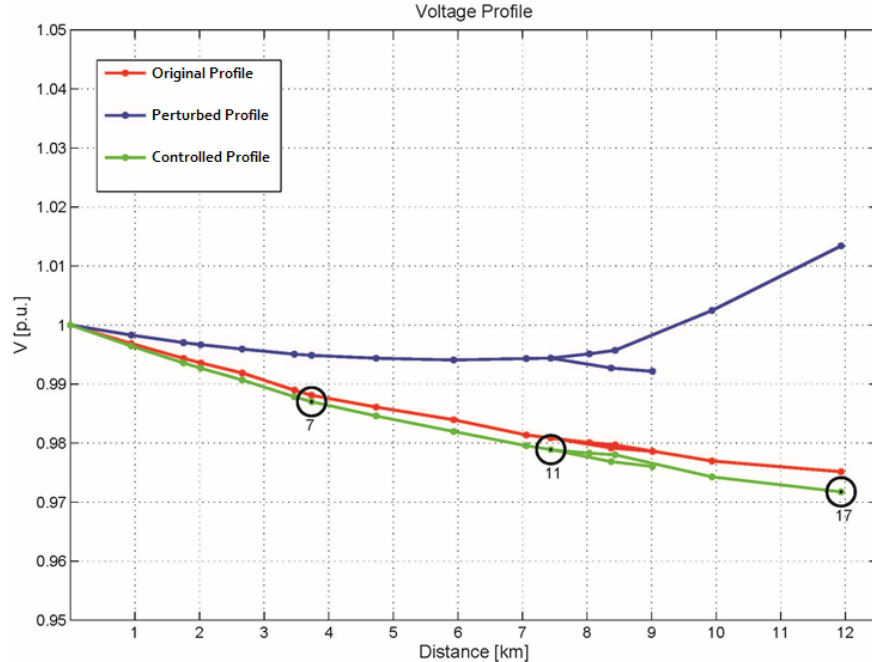


Figure 87 - Voltage profile

The black circles represent the nodes selected for the control (7, 11 17).

The red line represents the profile of the voltage to its original condition, that is in the absence of DG (Table 45). The values of the voltages at the nodes of the network decreases as one moves away from node 1 (representing the primary station), due to the voltage drops caused by the active power absorbed by the loads.

DG unit	Bus	Active Power [MW]	Reactive Power [MVAR]
DG1	17	0	0
DG2	7	0	0
DG3	13	0	0

Table 45 - Original Condition

The blue line represents the profile of the voltage under the conditions disturbed by the increase of active power of DGs, as shown in Table 46.

DG unit	Bus	Active Power [MW]	Reactive Power [MVAR]
DG1	17	5	0
DG2	7	2,2	0
DG3	13	2	0

Table 46 - Perturbed Condition

Finally, the green line represents the voltage profile under controlled conditions, applying the proposed control strategy: the various generators on the network are required to produce or absorb a certain reactive power for the mitigation of the voltage rise. Such values are given in Table 47.

DG unit	Bus	Active Power [MW]	Reactive Power [MVAR]
DG1	17	5	-2,134
DG2	7	2,2	-0,948
DG3	13	2	-0,813

**Table 47 - Controlled Condition**

#### **4.1.3 Concluding considerations on voltage control techniques for DGs connected to MV and LV distribution networks**

From previous simulations, it can be inferred that voltage control techniques based on Reactive Power Regulation allow the reduction of the typical voltage rise experimented by radial networks, that were not planned to include active power generation.

It can be seen that the voltage control logics proposed in Italy by the recent connection rules are effective. With this regards, the power factor control logic ( $\cos \varphi = f(P)$ ) and the reactive power control logic ( $Q = f(V)$ ) show very similar effects on the bus voltage profile.

In the particular case of the real-world distribution network analyzed in paragraph 4.1.1.2, the lock-in voltages (i.e., the thresholds to trigger the controls) are never reached. Cables appear well dimensioned for the actual and futurable level of DG penetration as the voltage rise is relatively low.

Control logics reported on new regulations can be never activated (while the installation is mandatory) and in some cases it concerns only DGs positioned in weak areas. Therefore, it can be considered in someway unfair.

The logics can be classified as local strategies. On the other side, the proposed control technique can be applied together with a coordinated communication architecture: its implementation requires the development of hardware and software platforms in distribution networks (a strong interaction with the ICT world is essential).

One can infer that the presented algorithm is effective and simple to be realized.

Matrix [A] strongly depends on the R/X ratio of the cables in the feeder: too high values of R/X ratio determines very high values in [A] coefficients and thus high values of reactive power to be injected/absorbed by DGs. In this case to mitigate voltage rise a network reinforcement is needed (i.e. an increase in conductor size to reduce the resistance).

## 4.2 Case studies of power generation plants directly connected to the HV transmission network

This section presents the simulation results performed on some real-world RES distributed generation plants, directly connected to HV transmission system, based on different primary sources (PV, wind, hydro, etc.) and with different types of generators (static, synchronous, asynchronous).

DG plants based on RES are typically constituted by a cluster of multiple interconnected generators. The generators form a local MV network that is connected to the transmission system through a single point of delivery (POD).

For these particular RES configurations, the study analyses the application of the hierarchical control strategy described in paragraph 3.3.2.

All simulations have been carried out using DOME [88] - described in Appendix A1.2 - and network components have been modelled as in [89].

Table 48 provides a legend of the symbols used in the schemes.

Graphic symbols	Description
	Short-circuit impedance of the upstream network
	Generator
	Transformer
	Three-Winding Transformer
	Load
	Line/Cable
	Bus
	Capacitor

Table 48 - Legend of symbols used

#### 4.2.1 Photovoltaic case

The proposed regulator is applied to a real-world PV power plant with a nominal peak power of 46,8 MWp, connected to the HV transmission grid [205]. The topology of the power plant is represented in Figure 88 and the line styles used refer to the two cable types illustrated in Table 49.

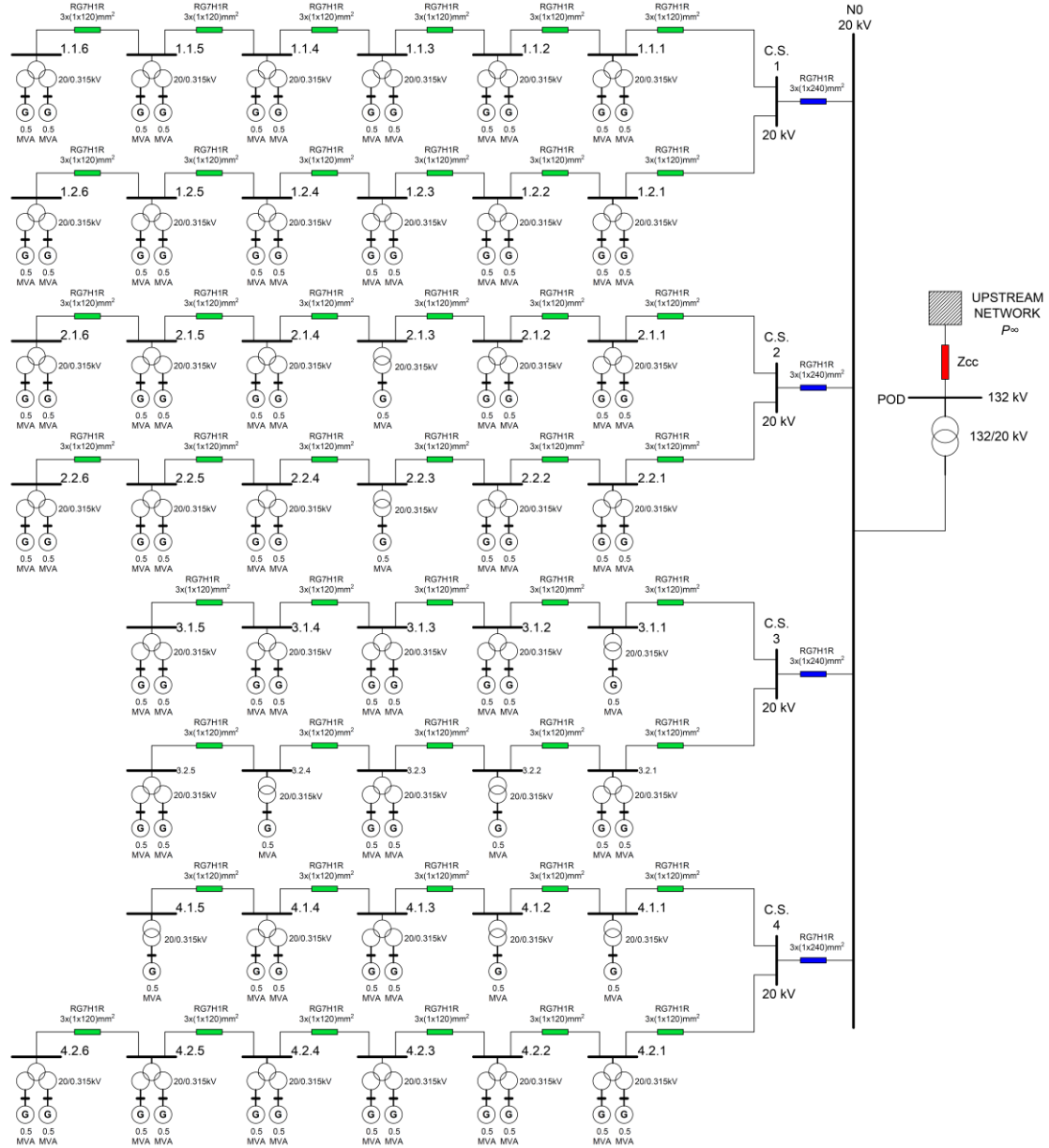


Figure 88 - Plant topology

The plant consists of 82 photovoltaic fields, connected to a same number of centralized (i.e. equipped with a unique MPPT) inverters. The LV inverter outputs are raised to 20kV via transformers, installed in 45 “inverter stations” (Table 50).

Line Type	Graphic symbol	R	X	c
		[Ohm/ Km]	[Ohm/ Km]	[μF/Km]
RG7H1R 3x1x240mmq		0,075	0,11	0,32
RG7H1R 3x1x120mmq		0,153	0,12	0,25

Table 49 - Cable types

Inverter Station	Pn Inverter [kVA]	Pn PV modules [kWp]
1.1.1	2 x 500	1143
1.1.2	2 x 500	1143
1.1.3	2 x 500	1143
1.1.4	2 x 500	1143
1.1.5	2 x 500	1143
1.1.6	2 x 500	1143
2.1.1	2 x 500	1143
2.1.2	2 x 500	1143
2.1.3	500	549
2.1.4	2 x 500	1143
2.1.5	2 x 500	1143
2.1.6	2 x 500	1143
3.1.1	500	567
3.1.2	2 x 500	1143
3.1.3	2 x 500	1143
3.1.4	2 x 500	1143
3.1.5	2 x 500	1143
4.1.1	500	567
4.1.2	500	567
4.1.3	2 x 500	1143
4.1.4	2 x 500	1143
4.1.5	500	567

Inverter Station	Pn Inverter [kVA]	Pn PV modules [kWp]
1.2.1	2 x 500	1143
1.2.2	2 x 500	1143
1.2.3	2 x 500	1143
1.2.4	2 x 500	1143
1.2.5	2 x 500	1143
1.2.6	2 x 500	1143
2.2.1	2 x 500	1143
2.2.2	2 x 500	1143
2.2.3	500	567
2.2.4	2 x 500	1143
2.2.5	2 x 500	1143
2.2.6	2 x 500	1143
3.2.1	2 x 500	1143
3.2.2	500	567
3.2.3	2 x 500	1143
3.2.4	500	567
3.2.5	2 x 500	1143
4.2.1	2 x 500	1143
4.2.2	2 x 500	1143
4.2.3	2 x 500	1143
4.2.4	2 x 500	1143
4.2.5	2 x 500	1143
4.2.6	2 x 500	1143

Table 50 - Inverter Stations

The output of each inverter station is parallel connected with the output of the nearby station forming four groups which are connected to a “central station” from where four MV circuits are sent to a “transforming station”. All line lengths are indicated in Table 51.

From Node	To Node	Length L [m]
N0	C.S.1	1416
C.S.1	1.1.1	358
1.1.1	1.1.2	394
1.1.2	1.1.3	175
1.1.3	1.1.4	175
1.1.4	1.1.5	175
1.1.5	1.1.6	608
C.S.1	1.2.1	358
1.2.1	1.2.2	484
1.2.2	1.2.3	175
1.2.3	1.2.4	175
1.2.4	1.2.5	160
1.2.5	1.2.6	209
N0	C.S.2	876
C.S.2	2.1.1	224
2.1.1	2.1.2	160
2.1.2	2.1.3	397
2.1.3	2.1.4	175
2.1.4	2.1.5	175
2.1.5	2.1.6	402
C.S.2	2.2.1	155
2.2.1	2.2.2	175
2.2.2	2.2.3	368
2.2.3	2.2.4	237
2.2.4	2.2.5	180
2.2.5	2.2.6	263

From Node	To Node	Length L [m]
N0	C.S.3	142
C.S.3	3.1.1	397
3.1.1	3.1.2	317
3.1.2	3.1.3	314
3.1.3	3.1.4	409
3.1.4	3.1.5	1040
C.S.3	3.2.1	340
3.2.1	3.2.2	175
3.2.2	3.2.3	412
3.2.3	3.2.4	201
3.2.4	3.2.5	72
N0	C.S.4	185
C.S.4	4.1.1	214
4.1.1	4.1.2	245
4.1.2	4.1.3	98
4.1.3	4.1.4	270
4.1.4	4.1.5	582
C.S.4	4.2.1	59
4.2.1	4.2.2	90
4.2.2	4.2.3	98
4.2.3	4.2.4	278
4.2.4	4.2.5	98
4.2.5	4.2.6	206

Table 51 - Line lengths

In the transforming station the four circuits are parallel connected to the MV side of a transformer that raises the voltage up to 132kV, that is the nominal voltage of the transmission line where the PV plant is connected. The equivalent inductance of the upstream network ( $x_{cc}$ ) is equal to 0.222 p.u. (having set the voltage base  $V_{bn}$  equal to 132kV and the power base  $A_{bn}$  equal to 100MVA).

Based on sensitivity analysis, it appears that the influence of different generators on voltage variations at the point of delivery is almost alike: the coefficients  $dv/dq$  that combine the POD to the other nodes of the network are approximately equal to 0.236.

Therefore, this case study is similar to the classical case of the application of SART in conventional power plants (single busbar). In other words, all generators participate in voltage regulation.

- **Simulation results**

Simulations have been carried out assuming an initial POD busbar reference voltage ( $v_{Bref}$ ) equal to 1.001 p.u. and same reactive power injections from all generators. At time  $t=500$ s a step to the reference voltage is applied (the new value set for  $v_{Bref}$  is equal to 1.03 p.u); consequently, the regulator imposes a new value of reactive power to be supplied by generators.

Figure 89 shows the voltage profile in p.u. at the point of delivery. Figure 90 reports the trend of the reactive power delivered by the generators expressed in p.u. of their nominal power.

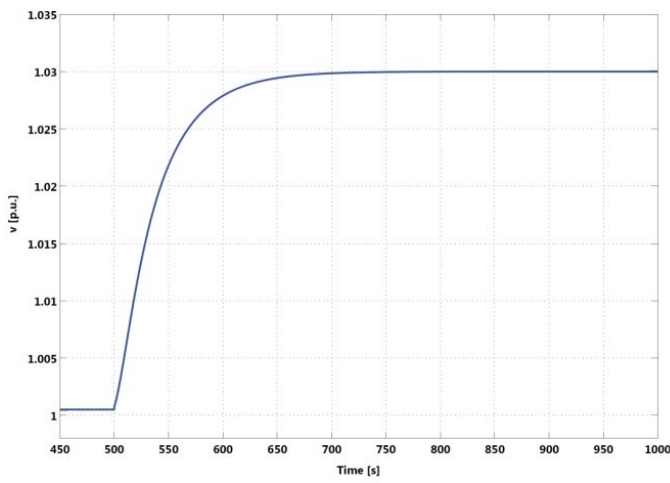


Figure 89 - Voltage profile at the point of delivery (in p.u.)

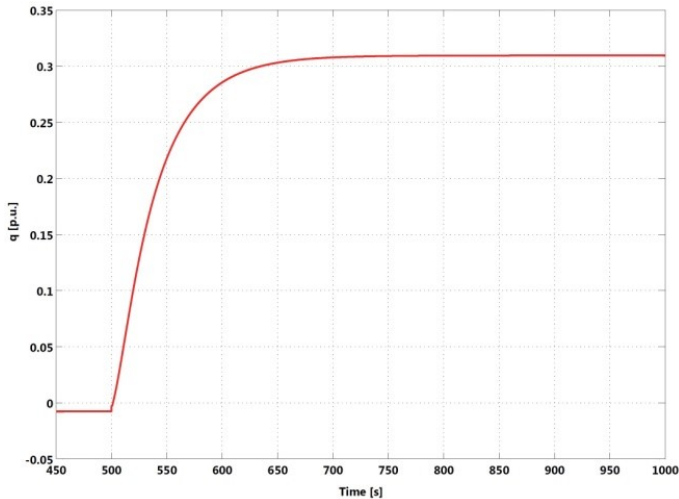


Figure 90 - Reactive power profile of generators (in p.u.)

#### 4.2.2 Wind farm case

The wind farm considered in this paragraph is a 28 MW plant composed of the following main elements [204]:

- 14 wind turbines of 2 MW rated power, constituted by asynchronous generators interfaced each one with a frequency converter. The output voltage is 690 V;
- 14 transformers (0,69/20kV) placed inside wind towers;
- a distribution network, realized with cable ARE4H1R 12/20 and
- a transformer substation (20/150kV), which is the point of connection to the HV grid.

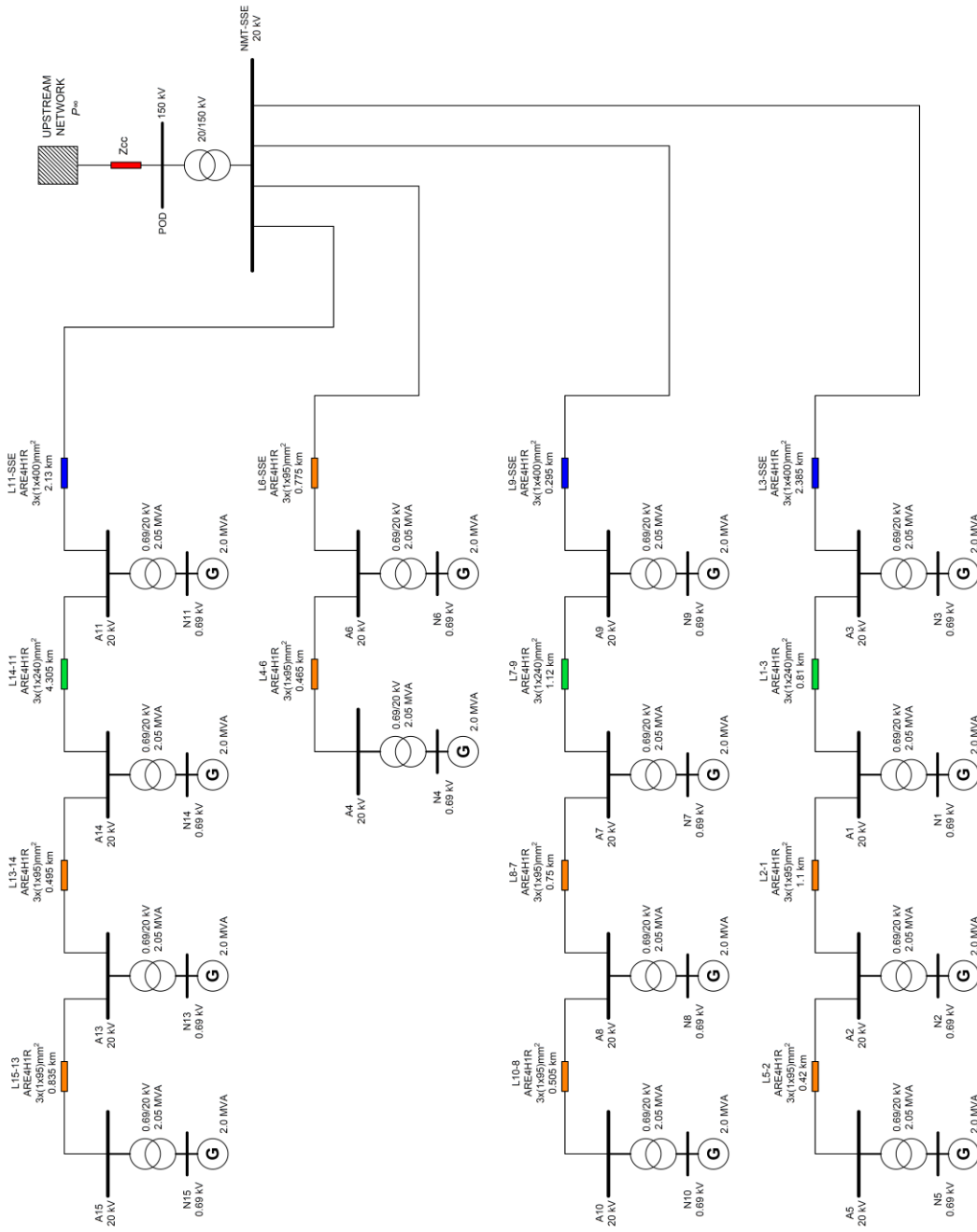


Figure 91 - Plant topology

The network topology is depicted in Figure 91. The turbines are divided into 4 groups connected by 4 lines:

- Group 1 (line 1): wind turbines (T15, T13, T14, T11).
- Group 2 (line 2): wind turbines (T5, T2, T1, T3).
- Group 3 (line 3): wind turbines (T10, T8, T7, T9).
- Group 4 (line 4): wind turbines (T4, T6).

The line styles used in Figure 91 refer to the three cable types illustrated in Table 52 and all line lengths are indicated in Table 53. The characteristics of the transformers are shown in Table 54.

Line Type	Graphic symbol	R	X	C
		[Ohm/Km]	[Ohm/Km]	[μF/Km]
ARE4H1R 3x(1x95)mmq		0,319	0,12	0,23
ARE4H1R 3x(1x240)mmq		0,127	0,11	0,33
ARE4H1R 3x(1x400)mmq		0,083	0,098	0,40

Table 52 - Cable types

From Node	To Node	Length L [km]
NMT-SSE	N11	2,13
N11	N14	4,305
N14	N13	0,495
N13	N15	0,835
NMT-SSE	N6	0,775
N6	N4	0,465
NMT-SSE	N9	0,295
N9	N7	1,12
N7	N8	0,75
N8	N10	0,505
NMT-SSE	N3	2,385
N3	N1	0,81
N1	N2	1,1
N2	N5	0,42

Table 53 - Line lengths

Type	P	V1	V2	Vk	Vr
	[MVA]	[kV]	[kV]	[%]	[%]
MT/AT	33	20	150	17,6	0,394
BT/MT	2,05	0,69	20	7	0,87

Table 54 - Characteristics of the transformers

The equivalent inductance of the upstream network ( $x_{cc}$ ) is equal to 0.0513 p.u. (having set the voltage base  $V_{bn}$  equal to 150kV and the power base  $A_{bn}$  equal to 100MVA).

Coefficients  $dv/dq$  that combine the POD to all other nodes of the network are expressed in Table 55. The Dynamic Decoupling matrix is represented in Table 56.

Node	$dv/dq$
N1	0.0515
N2	0.0515
N3	0.0515
N4	0.0515
N5	0.0515
N6	0.0515
N7	0.0515
N8	0.0515
N9	0.0515
N10	0.0515
N11	0.0515
N12	0.0515
N13	0.0515
N14	0.0515

Table 55 - Sensitivity Coefficients  $dv/dq$

DD	N1	N2	N3	N4	N5	N6	N7	N8	N9	N10	N11	N12	N13	N14
N1	3.553	0.298	0.277	0.221	0.298	0.221	0.221	0.221	0.221	0.221	0.221	0.221	0.221	0.221
N2	0.297	3.573	0.276	0.220	0.328	0.220	0.220	0.220	0.220	0.220	0.220	0.220	0.220	0.220
N3	0.277	0.277	3.537	0.221	0.277	0.221	0.221	0.221	0.221	0.221	0.221	0.221	0.221	0.221
N4	0.221	0.221	0.221	3.520	0.221	0.243	0.221	0.221	0.221	0.221	0.221	0.221	0.221	0.221
N5	0.297	0.328	0.276	0.220	3.583	0.220	0.220	0.220	0.220	0.220	0.220	0.220	0.220	0.220
N6	0.221	0.221	0.221	0.244	0.221	3.509	0.221	0.221	0.221	0.221	0.221	0.221	0.221	0.221
N7	0.221	0.221	0.221	0.221	0.221	0.221	3.522	0.258	0.228	0.258	0.221	0.221	0.221	0.221
N8	0.221	0.221	0.221	0.221	0.221	0.221	0.257	3.536	0.228	0.279	0.221	0.221	0.221	0.221
N9	0.222	0.222	0.222	0.222	0.222	0.222	0.229	0.229	3.500	0.229	0.222	0.222	0.222	0.222
N10	0.221	0.221	0.221	0.221	0.221	0.221	0.257	0.279	0.228	3.548	0.221	0.221	0.221	0.221
N11	0.221	0.221	0.221	0.221	0.221	0.221	0.221	0.221	0.221	3.532	0.271	0.271	0.271	0.271
N12	0.220	0.220	0.220	0.220	0.220	0.220	0.220	0.220	0.220	0.220	0.269	3.627	0.381	0.395
N13	0.220	0.220	0.220	0.220	0.220	0.220	0.220	0.220	0.220	0.220	0.270	0.382	3.618	0.382
N14	0.219	0.219	0.219	0.219	0.219	0.219	0.219	0.219	0.219	0.219	0.269	0.395	0.381	3.646

Table 56 - Dynamic Decoupling matrix

Starting from an operating condition in which all generators are working at the same state (same reactive power injected equal to 0.1 p.u.) and voltage at the point of delivery is equal to 1.0254 p.u., a first simulation has been conducted applying a step to the POD busbar reference voltage ( $v_{Bref}$ ): the new value set for  $v_{Bref}$  is equal to 1.03 p.u..

The results of the simulations are shown in Figure 92 and Figure 93. The trends of the reactive power delivered by the generators are expressed in p.u. in respect to their nominal power.

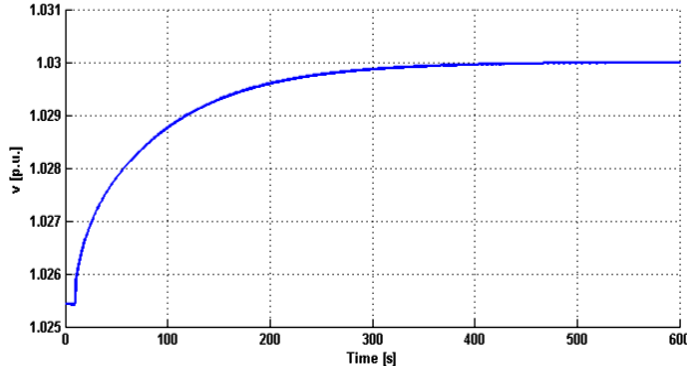


Figure 92 - Voltage profile at the point of delivery (in p.u.)

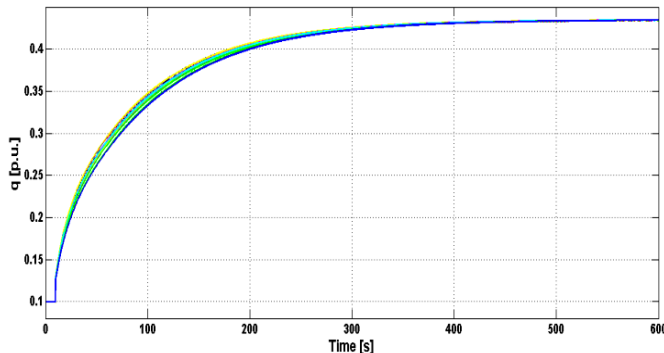


Figure 93 - Reactive power profile of generators (in p.u.)

Afterwards, starting from a hypothetical situation, in which all the generators are under different conditions (different reactive power injected), the intervention of the regulator was simulated. From Figure 94 one can appreciate how the control system brings all generators to produce the same level of reactive power, without mutual interference.

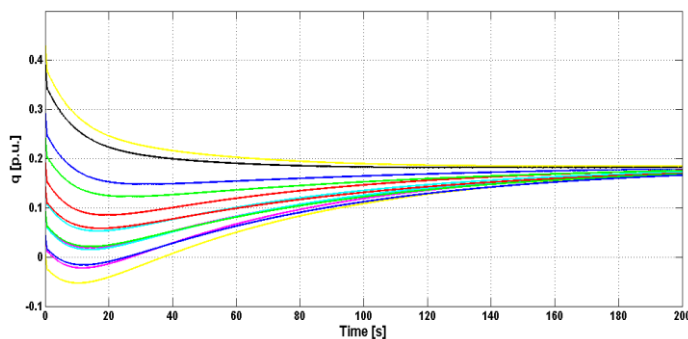


Figure 94 - Reactive power profile of generators - second simulation (in p.u.)

### 4.2.3 Hydroelectric case

The topology of the considered network is depicted in Figure 95 and it consists of a cluster of hydro power plants composed by 11 synchronous generators for a total power of 46,87 MVA [203].

The characteristics of each generator are shown respectively in Table 57 while those of transformers in Table 58. The line styles used in Figure 95 refer to the six cable types illustrated in Table 59 and all line lengths are indicated in Table 60.

Generator	Node	P	V
		[MVA]	[kV]
GEN 1	N2	10,14	6
GEN 2	N3	1,5	6
GEN 3	N4.1	14	11
GEN 4	N5.1	7,5	10
GEN 5	N5.1	7,5	10
GEN 6	N6	4,4	6
GEN 7	N7	1,83	6

Table 57 - Characteristics of the generators

Type	P	V1	V2	Vcc
	[MVA]	[kV]	[kV]	[%]
TR1	42	132	55	13
TR2	7	55	6	7,46
TR3	7	55	6	7,37
TR4	0,16	6	0,4	4
TR5	0,10	6	0,4	4
TR6	16	55	11	10,28
TR7	0,10	11	0,4	4
TR8	0,30	55	0,4	6
TR9	7,5	55	10	9,68
TR10	7,5	55	10	9,68
TR11	8,75	55	11	9,26
TR12	0,10	11	0,4	6
TR13	2,5	11	6	5,94

Table 58 - Characteristics of the transformers

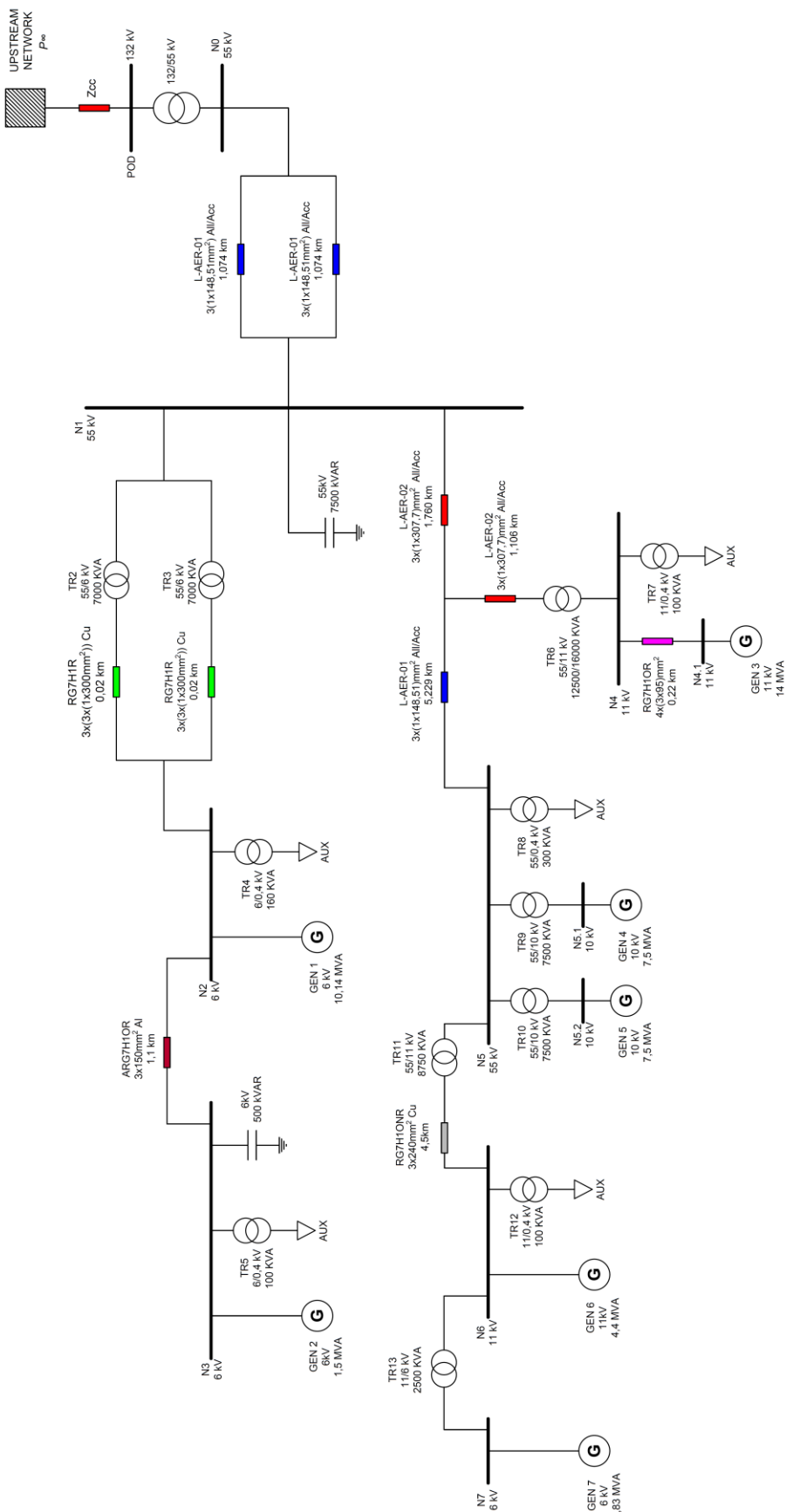


**Figure 95 - Plant topology**

Line Type	Graphic symbol	R	X	c
		[Ohm/ Km]	[Ohm/ Km]	[μF/Km]
L-AER-01 3x(1x148,51)mmq		0,219	0,339	0,010
L-AER-02 3x(1x307,7)mmq		0,106	0,316	0,011
ARG7H1OR 3x150mmq		0,206	0,110	0,25
RG7H1R 3x(3x(1x300))mmq		0,020	0,033	1,05
RG7H1OR 3x240mmq		0,075	0,090	0,37
RG7H1OR 4x(3x95)mmq		0,048	0,025	1,04

Table 59 - Cable types

From Node	To Node	Length L [km]
N0	N1	1,074
N1	N2	0,02
N2	N3	1,1
N1	N4	2,866
N4	N4.1	0,22
N1	N5	6,989
N5	N6	4,5

Table 60 - Line lengths

The equivalent inductance of the upstream network ( $x_{cc}$ ) is equal to 0.0938 p.u. (having set the voltage base  $V_{bn}$  equal to 132kV and the power base  $A_{bn}$  equal to 100MVA).

Based on sensitivity analysis, it can be noticed that the influence of the various generators on voltage variations at the point of delivery is almost equal and therefore it can be seen that all generators can participate in voltage regulation.

Coefficients  $dv/dq$  that combine the POD to all other nodes of the network are expressed in Table 61.

Node	Generator	$dv/dq$
N2	GEN 1	0.0983
N3	GEN 2	0.0984
N4.1	GEN 3	0.0981
N5.1	GEN 4	0.0981
N5.2	GEN 5	0.0981
N6	GEN 6	0.0985
N7	GEN 7	0.0975

Table 61 - Sensitivity Coefficients  $dv/dq$

The Dynamic Decoupling matrix is represented in Table 62, constituted by the coefficients  $dv/dq$  that bind generation nodes to each other.

DD	N2	N3	N4.1	N5.1	N5.2	N6	N7
N2	0.9220	0.9217	0.4208	0.4207	0.4207	0.4225	0.4179
N3	0.9152	1.2275	0.4177	0.4176	0.4176	0.4194	0.4148
N4.1	0.4205	0.4208	1.2193	0.4368	0.4368	0.4386	0.4339
N5.1	0.4178	0.4181	0.4341	1.6800	0.4895	0.4914	0.4861
N5.2	0.4178	0.4181	0.4341	0.4895	1.6886	0.4914	0.4861
N6	0.4127	0.4130	0.4288	0.4835	0.4835	1.7821	1.7629
N7	0.4107	0.4110	0.4267	0.4812	0.4812	1.7736	3.9239

Table 62 - Dynamic Decoupling matrix

#### ▪ Simulation results

The response to a step variation of the reference voltage is simulated to show the correct design and the behaviour of the control.

Starting from a steady state situation characterized by a POD busbar reference voltage ( $v_{Bref}$ ) equal to 1.003 p.u., at time t=500s a step to the reference voltage  $v_{Bref}$  is applied (the new value set is 1.01 p.u.). Figure 96 shows the voltage profile at the point of delivery. Figure 97 shows voltages at the different nodes of generation.

In Figure 98 the trends of the reactive power delivered by the generators are reported and expressed in p.u. in respect to their nominal power; whereas in Figure 99 the same variables are expressed in MVAr. In Figure 99 the profile related to GEN 4 and GEN 5 coincide because the two generation groups have the same nominal power.

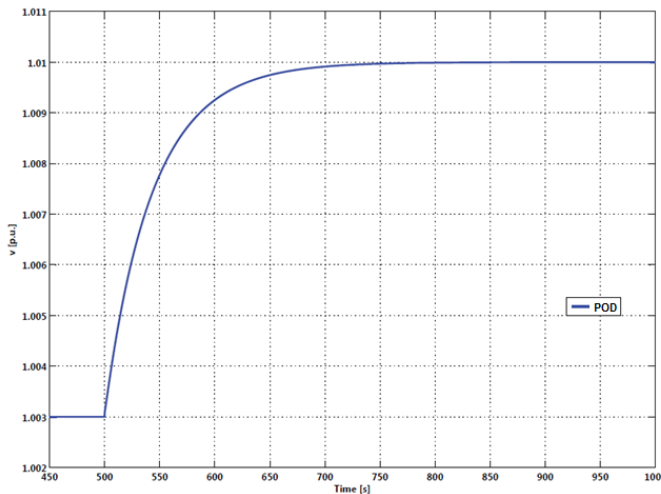


Figure 96 - Voltage profile at the point of delivery (in p.u.)

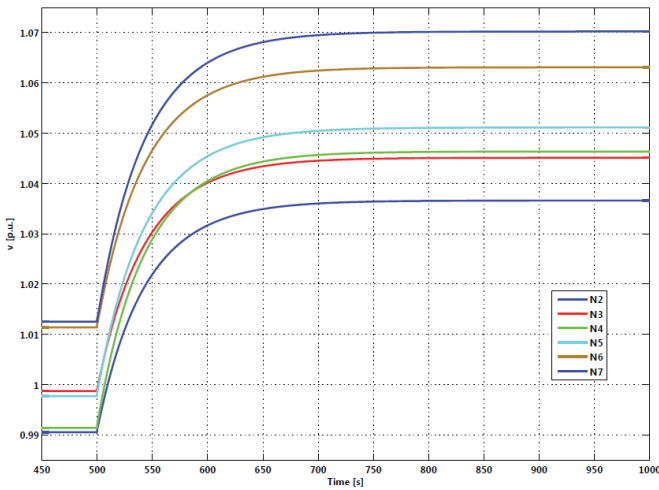


Figure 97 - Voltage profile at the different nodes of generation (in p.u.)

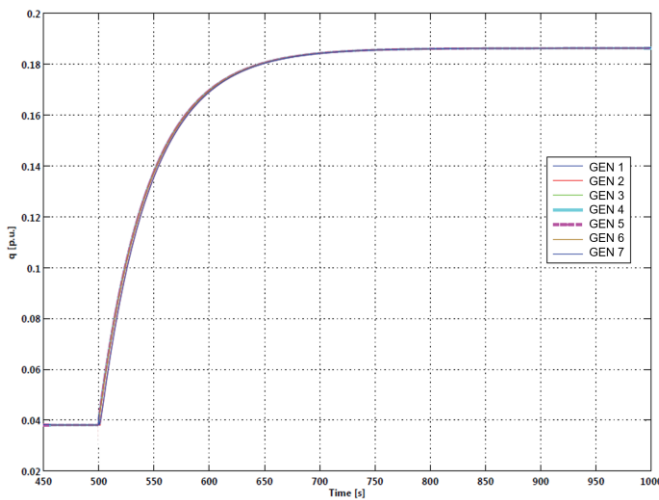


Figure 98 - Reactive power profile of generators (in p.u.)

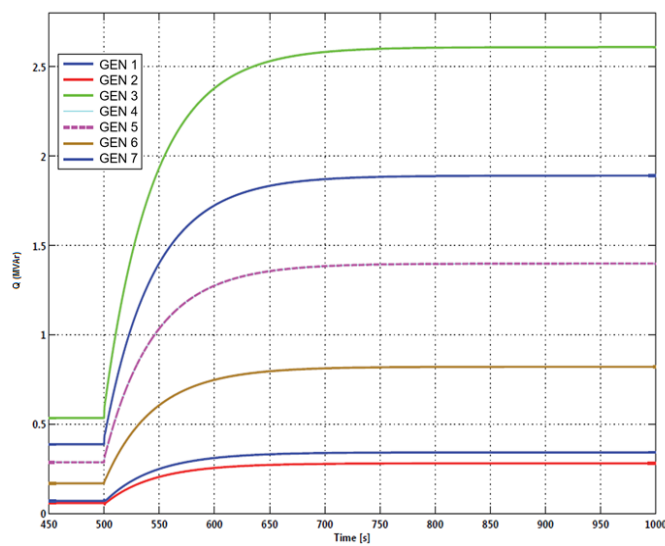


Figure 99 - Reactive power profile of generators (MVAr)

The results of simulations carried out in order to underline the effect of the matrix  $[DD]$ , are shown in Figure 100 and Figure 101 [206]. They show the response to a step of the voltage reference respectively without and with the inclusion of the Dynamic Decoupling matrix (all reactive power plots are in p.u. of 100 MVA).

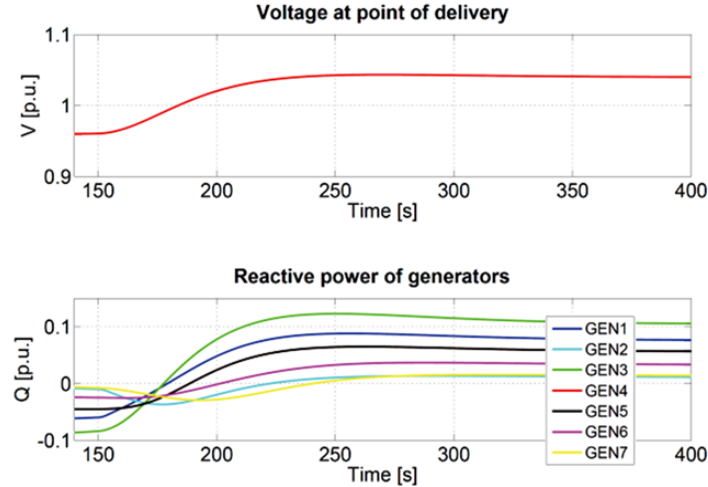


Figure 100 - Reactive power profile of generators and voltage response at the point of delivery without Dynamic Decoupling matrix

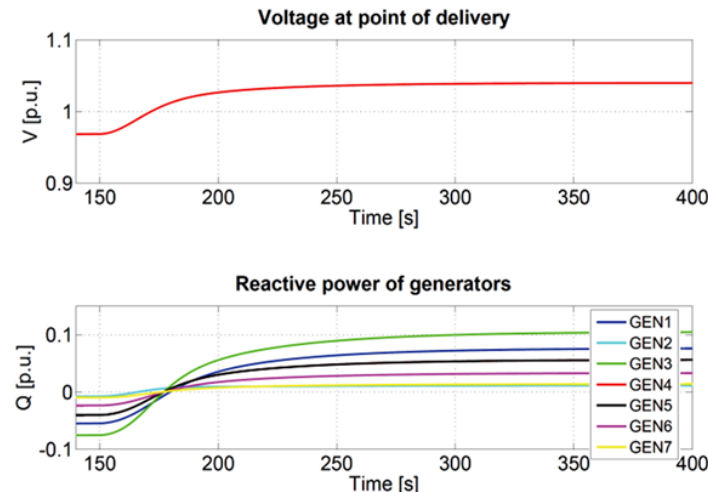


Figure 101 - Reactive power profile of generators and voltage response at the point of delivery with Dynamic Decoupling matrix

The transient evolution of reactive powers in Figure 101 confirms the expected stabilizing effect of the proposed decoupled control scheme: no reactive power loop occurs among generators. It is worth noting that such phenomenon does not appear merely observing the dynamic evolution of bus voltage magnitude alone. As results measurement and control of the reactive powers are necessary.

#### 4.2.4 Virtual Power Plant case: a MV distribution network with several generators types

A local DSO of a mountain area ( $170 \text{ km}^2$ ) in Italy produces and distributes electricity through 75 km of MV lines, 120 km of LV lines and 86 transformers, feeding about 5.500 users.

The power plants owned by the DSO are essentially five hydroelectric power plants with a total installed power of 10,8 MW that generate approximately 44.000 MWh per year. In addition, there are other power plants which, although operated by third parties, are connected to the DSO distribution networks. The energy produced fully satisfies the annual needs of “internal” users, providing also an electricity surplus of about 24.000 MWh.

The DSO network has a single point of connection (POC) to the HV national transmission network. Moreover, from the point of view of the national TSO, it turns out to be an active user (for most of the year). Therefore, the set of generators afferent to the DSO distribution network can be seen as a single VPP which can participate in the secondary voltage regulation (and possibly be remunerated for this service). The idea presented in this section is to control the voltage at the point of connection with the transmission network using the proposed control technique and acting co-ordinately on the reactive power of each DG unit constituting the VPP.

- ***Network model***

The considered network has been modelled with the software PSAT [214] and its graphical representation is depicted in Figure 103.

The connection to HV national transmission network at 132 kV is carried out in the primary substation. Figure 102 shows a detail of the external reactance (up to the infinite power node of the HV network), the HV busbar (132 kV), the HV/MV transformer and the MV busbar (20 kV). Eight main distribution lines depart from the MV busbar and they supply all the network users (generators or loads) - directly or by means of secondary transformation cabins (MV/LV).

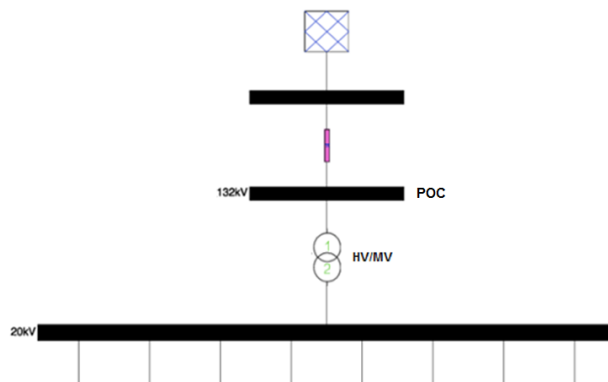


Figure 102 - Primary substation

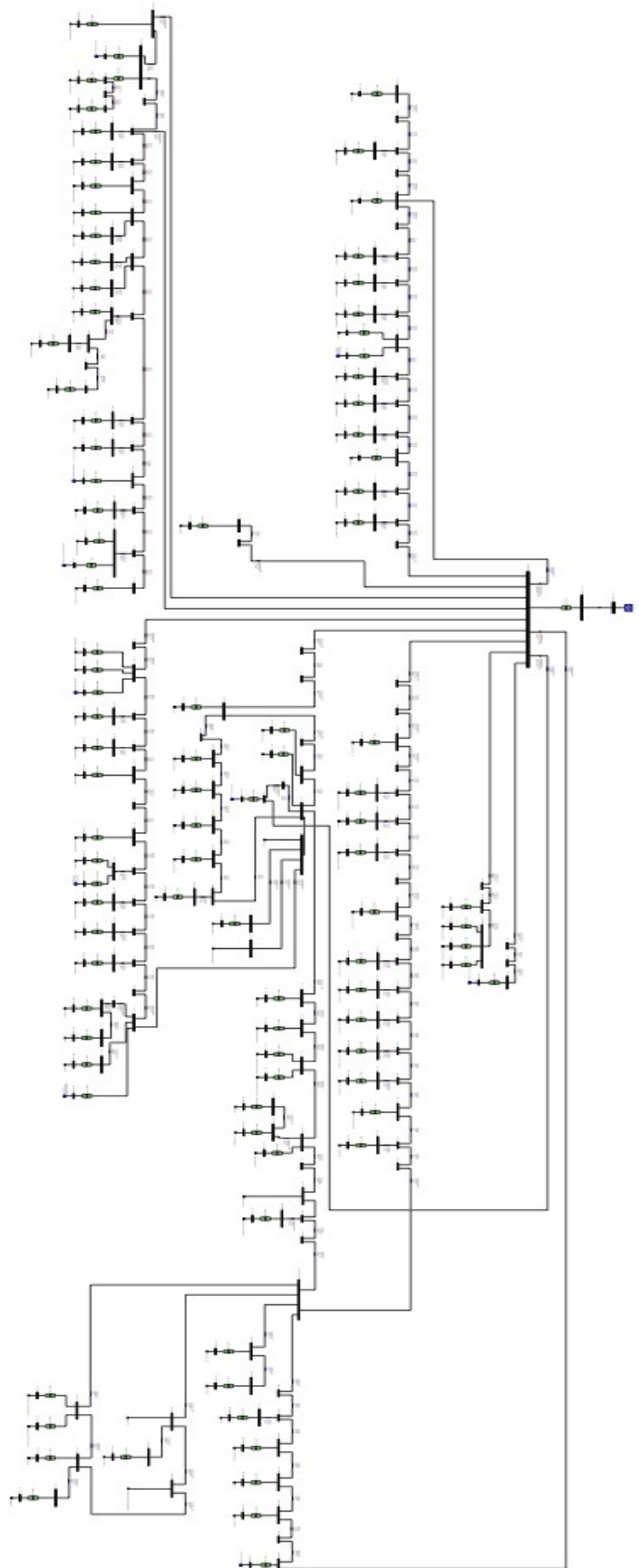


Figure 103 - Network topology

The characteristics of the generators are shown in Table 63. Given the large number of PV plants, most of them have been grouped taking into account the area of plants location in order to make their division balanced.

Generator Type	Nominal Power
Hydroelectric	2870 kVA
Hydroelectric	132 kVA
Hydroelectric	275 kVA
Hydroelectric	2250 kVA
Hydroelectric	2700 kVA
Hydroelectric	1850 kVA
Hydroelectric	2270 kVA
Hydroelectric	1000 kVA
Hydroelectric	590 kVA
Hydroelectric	230 kVA
Thermoelectric	560 kVA
Thermoelectric	999 kVA
PV	599,32 kWp
PV	157,92 kWp
PV	967 kWp

Table 63 - Characteristics of the generators

The characteristics of the transformers and cable types are illustrated in [215].

#### ▪ *Simulation Results*

Starting from a steady state condition characterized by a POC busbar reference voltage ( $v_{Bref}$ ) of about 1.0005 p.u., the simulation has been carried out applying at time  $t=20$ s a step to the POC busbar reference voltage (the new value for  $v_{Bref}$  is set equal to 1.005 p.u.). The results are shown in Figure 104 and Figure 105.

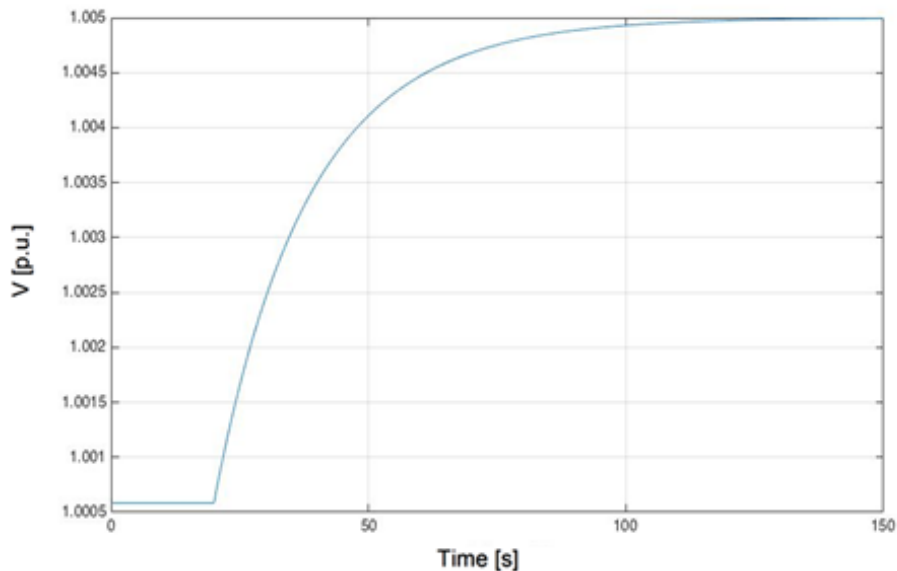


Figure 104 - Voltage profile at the point of connection (in p.u.)

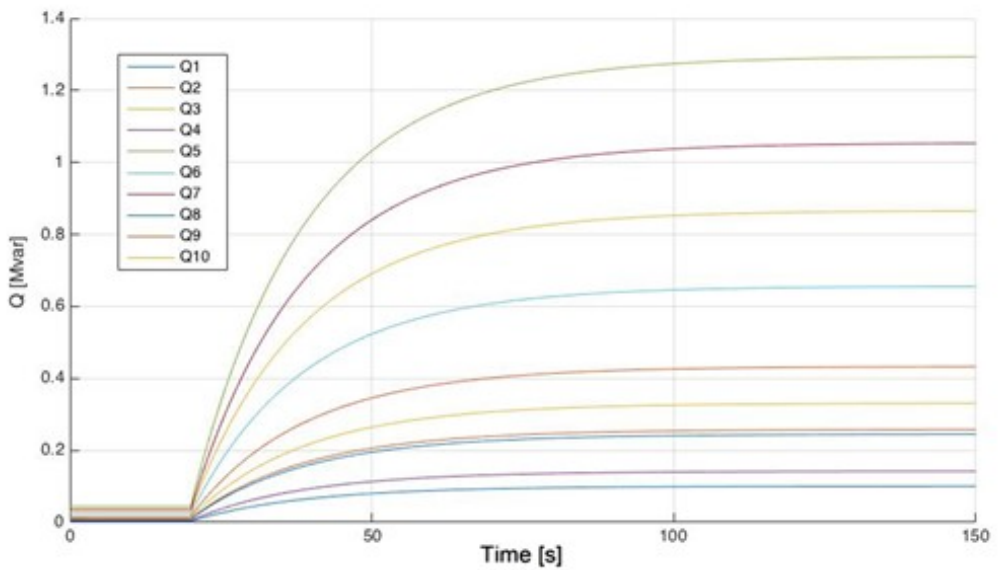


Figure 105 - Reactive power profile of generators (MVAr)

From the previous figures it is possible to notice how generators regulate their reactive power to ensure that the delivery node assumes the required voltage. This regulation takes place in a coordinated manner: each generator intervenes depending on its capability.

#### **4.2.5 Propaedeutic studies for the experimental implementation of the proposed control technique to a 72,6 MWp PV power plant**

Recently, our research group has started to study the implementation of the proposed control technique to a large PV power plant.

The PV plant is among the largest in Europe: it has a nominal peak power of 72,6 MWp, consisting of 281.724 ground-mounted photovoltaic panels (it occupies an area of about 85 hectares).

The system is constituted by sixty "sub-fields" each one characterized by an inverter; in particular:

- thirty inverters with  $P_n = 1.000\text{ kW}$  and  $V_n = 300\text{ V}$ ;
- thirty inverters with  $P_n = 1.000\text{ kW}$  and  $V_n = 275\text{ V}$ ;
- one inverter with  $P_n = 500\text{ kW}$  and  $V_n = 275\text{ V}$ .

The LV outputs of the inverters are raised to 20kV via LV/MV elevator transformers.



**Figure 106 - Aerial view of the PV plant [216]**

The electrical infrastructure of the plant is composed of the following main parts (Figure 107):

- a point of delivery (POD) at 132 kV voltage level: the plant is directly connected to the HV national transmission network;
- a transforming station with three HV/MV transformers that do not operate in parallel (bus-tie breakers normally open): only transformers TR1 and TR3 are normally in operation, while TR2 performs a backup function (redundancy in case TR1 or TR3 may fail);

- an internal MV distribution network at 20 kV voltage level, consisting of eight main sections operated in an open-loop configuration, to which the various inverters are connected (Figure 108).

The open-loop configuration provides flexibility and redundancy in case of failure or maintenance of one of the loop nodes.

A complete description of the characteristics of network components can be found in [217].

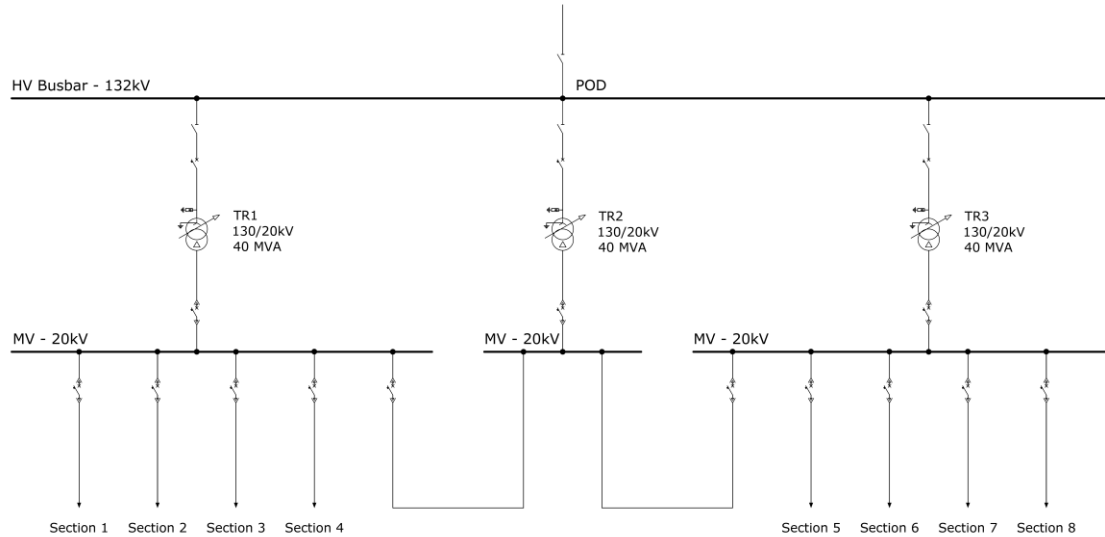


**Figure 107 - General layout of the electrical system infrastructure**

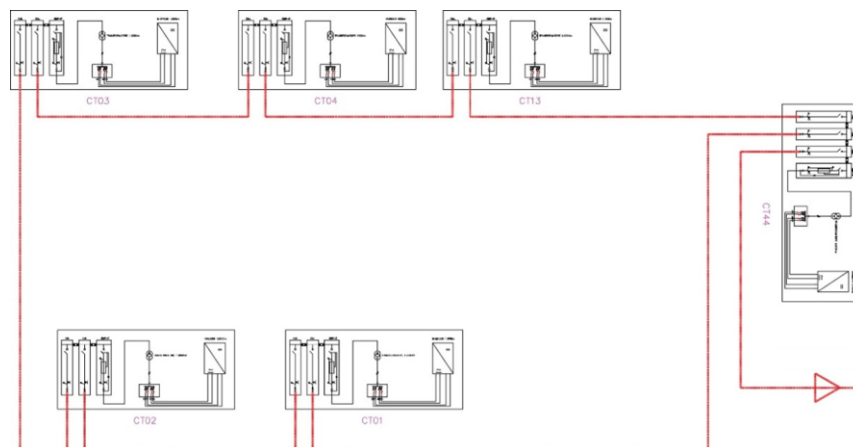


**Figure 108 - Detail of a MV section [217]**

Before proceeding with the implementation of the proposed control system, we have carried out simulations to verify the actual applicability. The network has been modelled with the software PSAT [214] and its graphical representation is depicted in Figure 109.

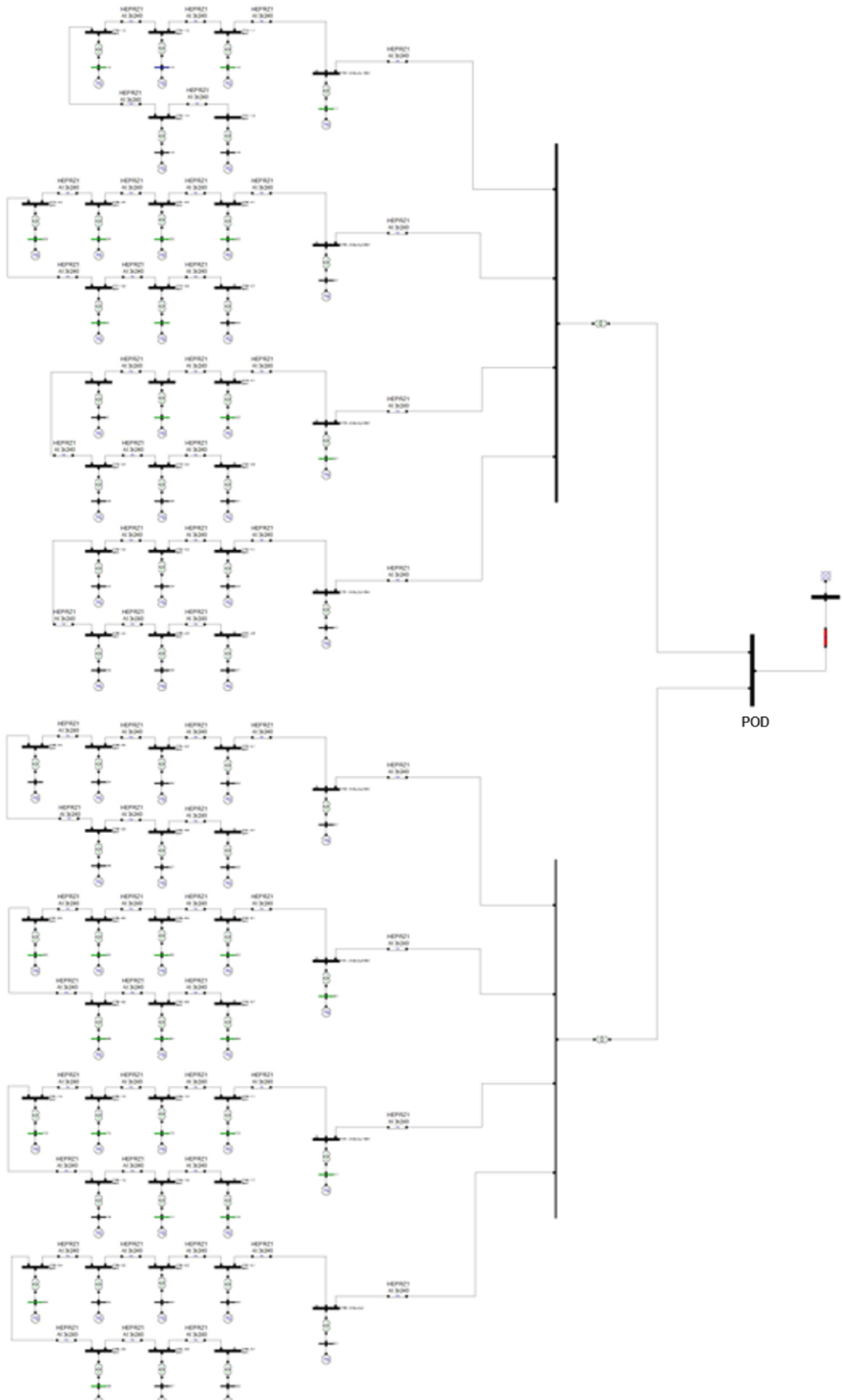


**Figure 109 - Plant topology**

- ***Simulation Results***

Using the proposed control, the voltage at the point of delivery is controlled acting on the reactive power of each inverter. Starting from the model of Figure 109, the response to a step variation of the POD busbar reference voltage ( $v_{Bref}$ ) is simulated.

In particular, three main scenarios have been considered:

- scenario 1: without the Dynamic Decoupling matrix [DD] (Figure 110 and Figure 111);
- scenario 2: with the Dynamic Decoupling matrix [DD] (Figure 112 and Figure 113);
- scenario 3: with the Dynamic Decoupling matrix [DD], considering also the current communication infrastructure latency (Figure 116 and Figure 117): the communication of the references from the controller to the inverters requires about 5 seconds.

All reactive power plots are in p.u. of 100 MVA.

For every scenario two different simulations were carried out:

- simulation 1: starting from a steady state situation, at time t=20 s a step to the reference voltage  $v_{Bref}$  equal to +0.005 p.u. is applied;
- simulation 2: starting from a steady state situation, at time t=20 s a step to the reference voltage  $v_{Bref}$  equal to -0.005 p.u. is applied.

All simulations have been carried out using DOME [88] - described in Appendix A1.2 - and network components have been modelled as in [89].

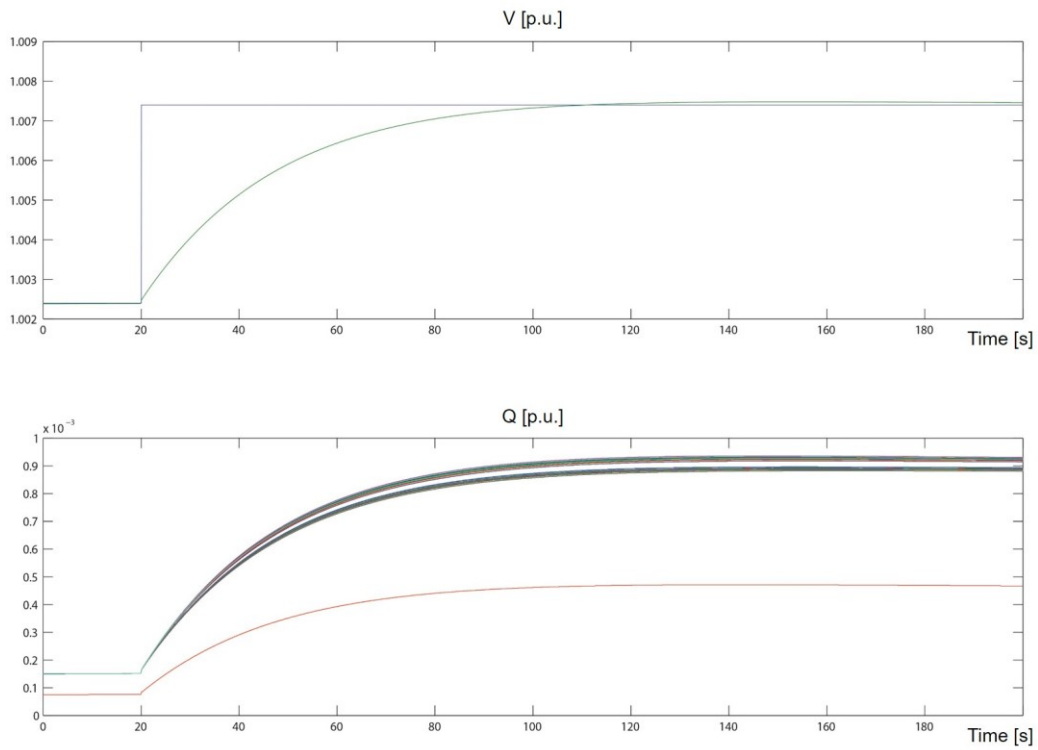


**Figure 110 - Scenario 1, Simulation 1: Voltage profile at the point of delivery and Reactive power profile of generators (in p.u.)**

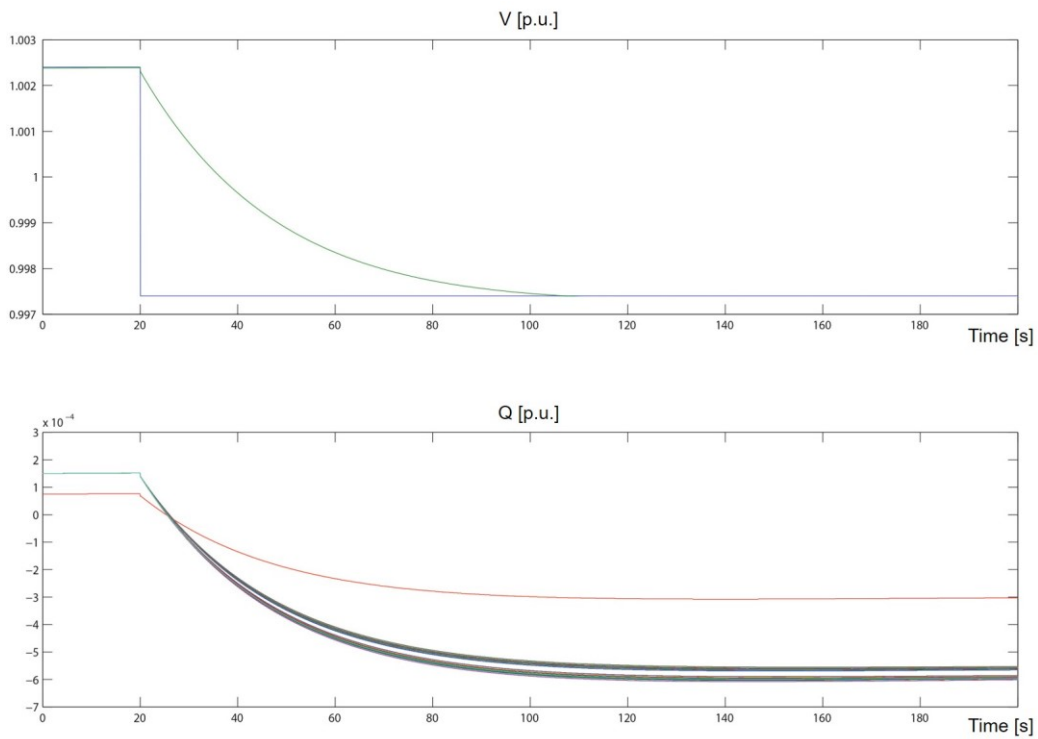


**Figure 111 - Scenario 1, Simulation 2: Voltage profile at the point of delivery and Reactive power profile of generators (in p.u.)**

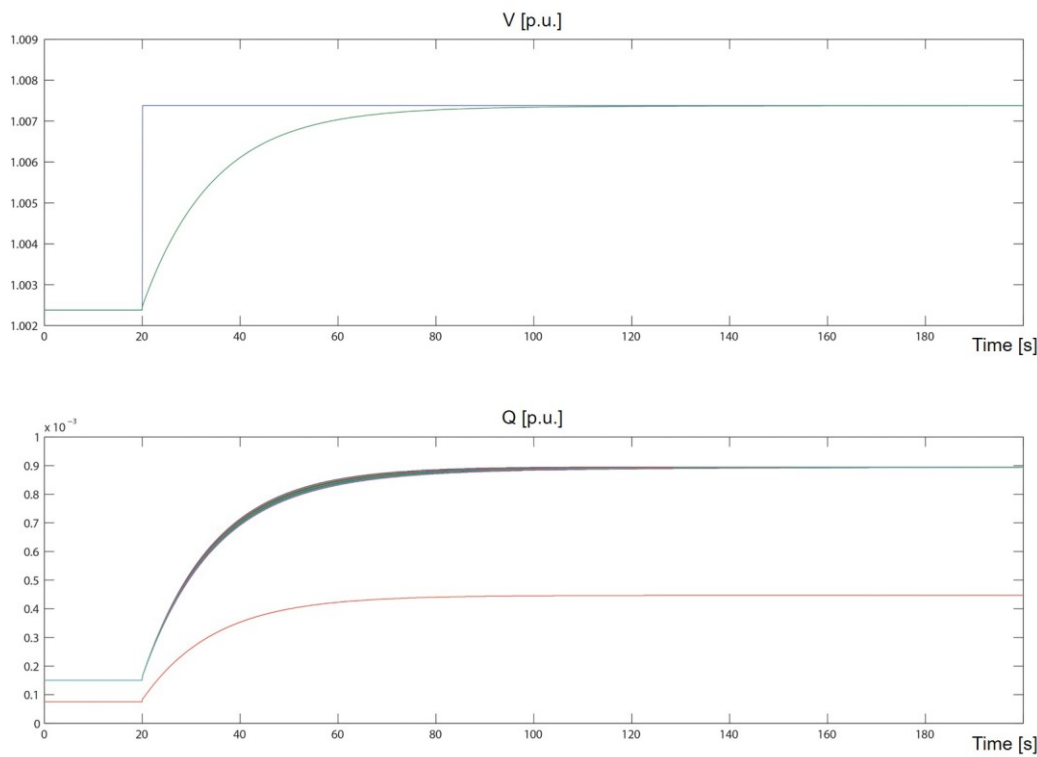


**Figure 112 - Scenario 2, Simulation 1: Voltage profile at the point of delivery and Reactive power profile of generators (in p.u.)**

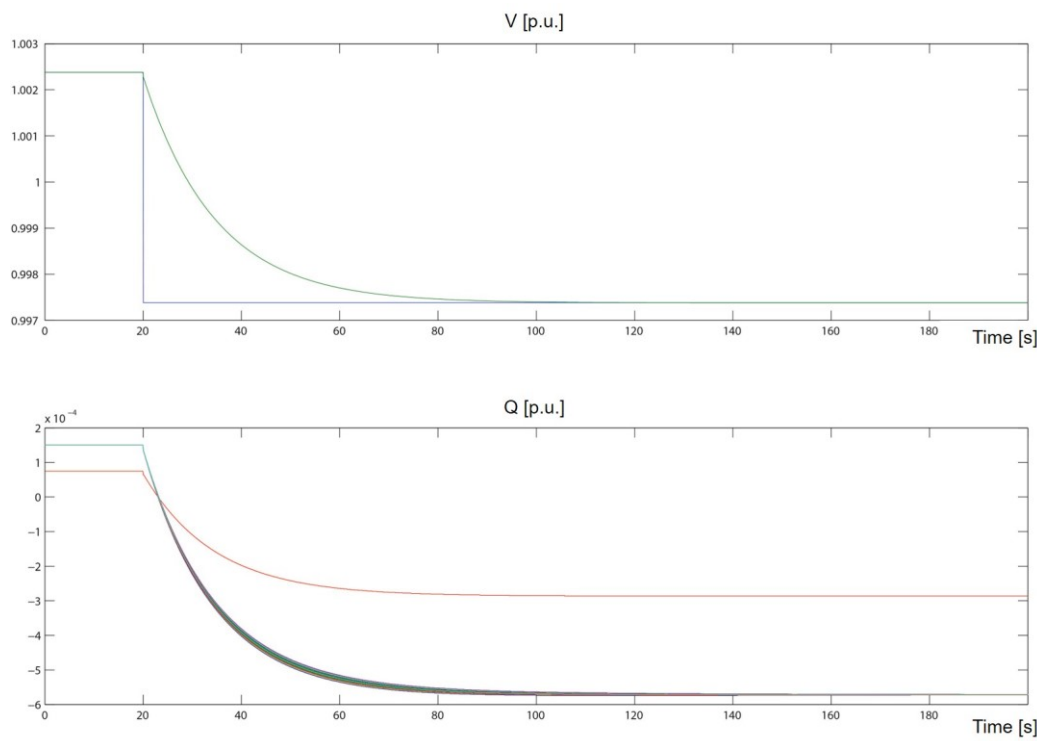


**Figure 113 - Scenario 2, Simulation 2: Voltage profile at the point of delivery and Reactive power profile of generators (in p.u.)**

Comparing results of Scenario 1 and Scenario 2, one can note that voltage response is almost equal, while the response of the reactive power supplied by each inverter is different:

- in Figure 110 and Figure 111 two distinct groups of reactive power responses can be noticed, according to the different reactances seen from the two main branches of the MV network;
- in Figure 112 and Figure 113, there is a unique group of reactive power curves, i.e. all generators equally take part in voltage regulation.

To highlight these differences, in Figure 114 and Figure 115 a detail of the reactive power profile of the generators is reported, without and with the Dynamic Decoupling matrix respectively.

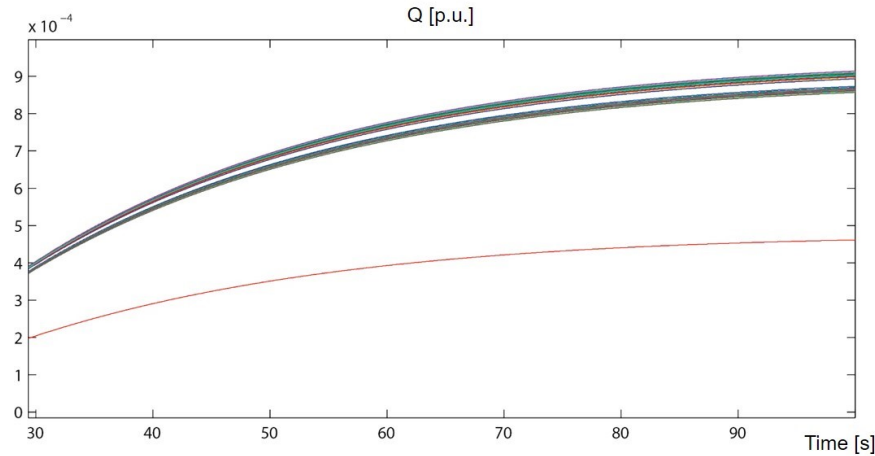


**Figure 114 – Detail of reactive power profile of generators (in p.u.): without Dynamic Decoupling matrix (in p.u.)**

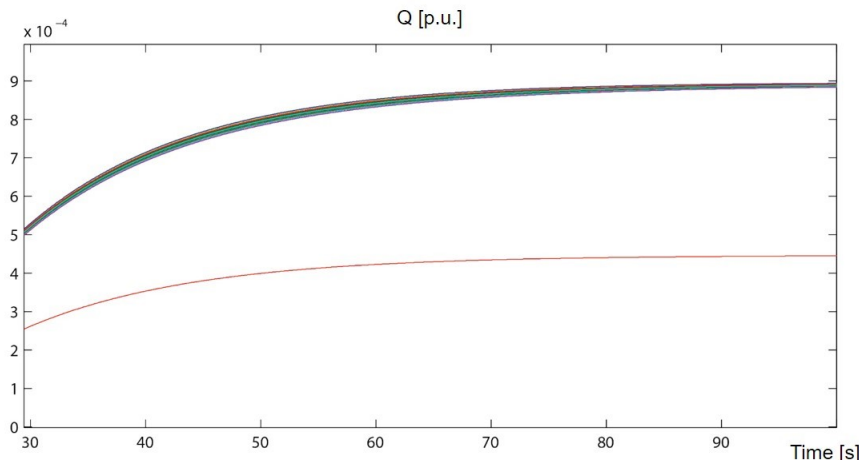


**Figure 115 – Detail of reactive power profile of generators (in p.u.): with Dynamic Decoupling matrix (in p.u.)**

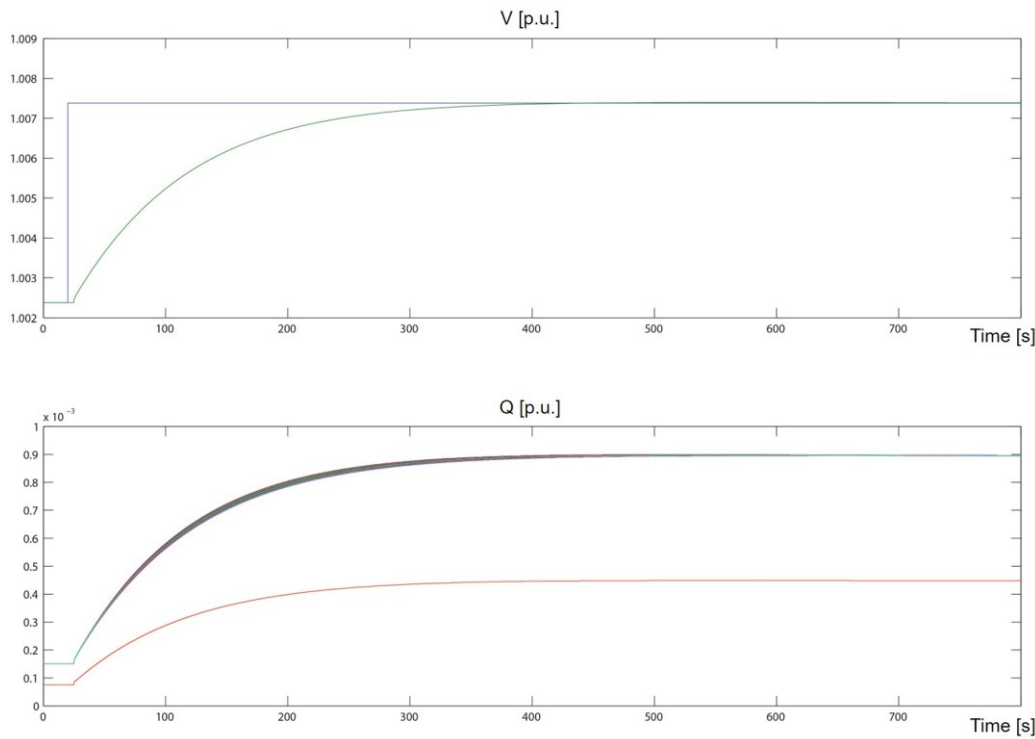


**Figure 116 - Scenario 3, Simulation 1: Voltage profile at the point of delivery and Reactive power profile of generators (in p.u.)**

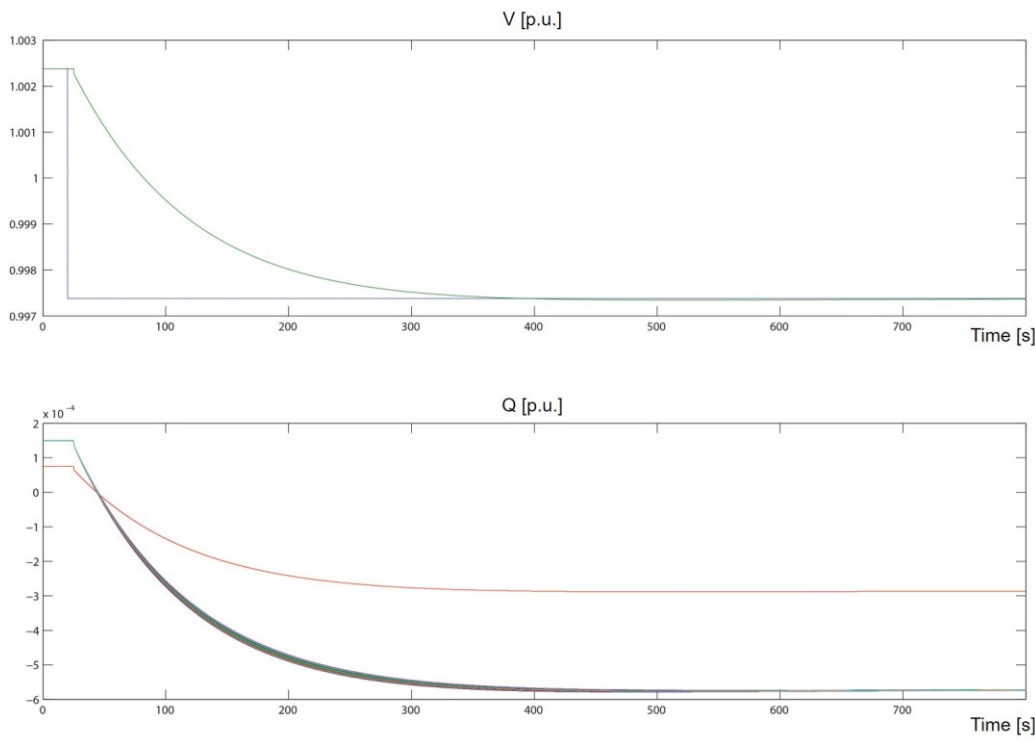


**Figure 117 - Scenario 3, Simulation 2: Voltage profile at the point of delivery and Reactive power profile of generators (in p.u.)**

From Figure 116 and Figure 117 it can be seen that implementation of the proposed control strategy is possible also maintaining the current communication infrastructure of the plant. In this case, in order to still achieve a response of the first order (to guarantee a dynamic decoupling between the control loops), the external voltage regulation loop has been slowed down, setting its time constant equal to about 200 s.

#### **4.2.6 Concluding considerations on the proposed voltage control technique for RES production power plants directly connected to HV transmission network**

Simulation results, based on different power plant topologies (five different real cases have been studied), show that the proposed control system allows to equally distribute the reactive power among the various generators of the power plant.

Furthermore there is no steady-state error, the dynamic of the system does not show oscillations and it appears to be similar to the typical one of a first order system and fully comparable to that of a SART installed in conventional power plants [181]

Even in case of dissymmetrical disturbances, the control ensures a stable operation, thanks to the decoupling action implemented by the matrix  $[DD]$ . Each generator equally shares a quota of the reactive power requested by the coordinating unit.

Moreover, the proposed control strategy is easy to implement, as it is based only on a single  $q_{liv}$  signal, and has already been successfully implemented for conventional power plants. The latter feature makes it attractive for TSOs.

## **Chapter 5.**

### **Conclusions**

---

The constant increase of DG collides with the current configuration of electrical systems, resulting in a change of the electrical energy production paradigm. The new architecture of generation and distribution of electrical energy is no longer based on big centralized power plants, it is rather characterized by a geographically distributed generation with small and medium sized generators often based on non-programmable RES.

The radical on-going transformation, involves new problems in the management of electrical distribution networks as well as a possible negative impact on the security and stability of the overall electrical system.

A change in the exercise of networks and a strong integration of electrical systems with ICT is therefore essential.

The present thesis has examined the voltage regulation in presence of strong penetration of DG based on RES, which is one of the most crucial aspects related to the increase of DG in electrical systems.

The two main issues considered in the present work are:

- the voltage rise phenomenon in distribution networks due to active power flow inversion;
- the weakening process of reactive power capability needed for secondary voltage regulation in HV transmission networks due to the decrease of operating conventional power plants.

The above mentioned issues have been explored through the analysis of causes and effects in traditional regulation systems.

A review of voltage control techniques proposed in literature for distribution networks with a strong presence of non-programmable DG is presented. New voltage control techniques based on reactive power regulation are studied and extensively simulated. In particular, the new connection rules introduced in Italy and a proposed coordinated strategy have been applied to some test electrical networks and to some actual electrical grids.

The results have highlighted that the voltage control strategies based on reactive power regulation can mitigate the voltage rise phenomenon, but their effect is strongly dependent on the cable characteristics of the network and in particular on R/X ratio.

For the power plants connected to the HV transmission grid, a voltage control technique derived from the hierarchical secondary voltage control has been proposed. The

---

technique has been adapted to the power plants based on RES consisting of several generators connected to a MV internal network and having a single point of connection to the HV grid. The technique can be applied to synchronous generators as well static generators (any kind of RES with an inverter as active front end).

Several simulations were carried out and some actual cases were examined to outline the specific behaviour of the control technique in real cases.

In all the studies the results of the simulations show that the proposed control allows to equally distribute reactive power among the various generators of the power plant. In addition, no steady-state error was recorded and the system shows the desired dynamic behaviour avoiding oscillations.

The proposed control strategy has been already successfully implemented and applied in conventional power plants in the secondary voltage control and its extension to distribution grids does not present particular implementation problems.

The study of the proposed controls on real cases has also pointed out some issues that should provide the basis for further investigations.

All the techniques illustrated so far require a communication infrastructure among generators. The requirements highlighted by the study seem to be met by various technologies that can cover both plants with limited geographic extent and installations on very large scale.

For the implementation of the proposed control technique to the photovoltaic power plant described at paragraph 4.2.5 some field tests are needed. In this context, studies on the existing ICT architecture will be carried out to identify the suitable interventions needed to reduce the related communication latency.

While the implementation of the control technique in the cases of synchronous generators is clear (using standard functionality of AVR), the way to implement it on static generators is yet to be studied.

Such implementation issues are out of the scope of the present work and should represent the object of further research work.

## **Appendix A1.**

### **Software tools used**

---

Simulations described in Chapter 4 have been carried out mainly through the combined use of two software tools (PSAT and DOME) recently released by prof. Federico Milano (Dublin University), with whom our research group has started a collaboration .

Such software has been chosen because it presents distinguished and original elements, as for example:

- the possibility to execute power-flow calculations of electrical networks inside scripts;
- the possibility to carry out time domain analysis of the same networks with original mathematical models;
- a dedicated graphical interface and specific Simulink libraries, making it possible to model electrical networks in an intuitive way;
- the possibility to implement innovative and complex control systems as simple scripts in modern and high level programming languages.

During the research activity new building blocks representing new mathematical models of the proposed control systems have been developed in collaboration with the author of the tools.

The following sections provide a description of the two software tools used.

#### **A1.1 PSAT - Power System Analysis Toolbox**

PSAT is a toolbox of MatLab for static and dynamic analysis of electrical power systems and allows power flow calculations, optimal power flow, stability analysis for small signals and analysis in time domain (time domain simulation) [213] [214] [218] [219].

There are also functional libraries of Simulink that allow easy drawing of the electricity grid, with its components (Figure 118). The parameters of each component used can be properly set through the related interface masks (Figure 119) both in physical terms and in terms of p.u..

Prior to performing any type of simulation the initial screen of PSAT has to be set properly with the correct values of frequency, tolerance, resolution method etc. (Figure 120).

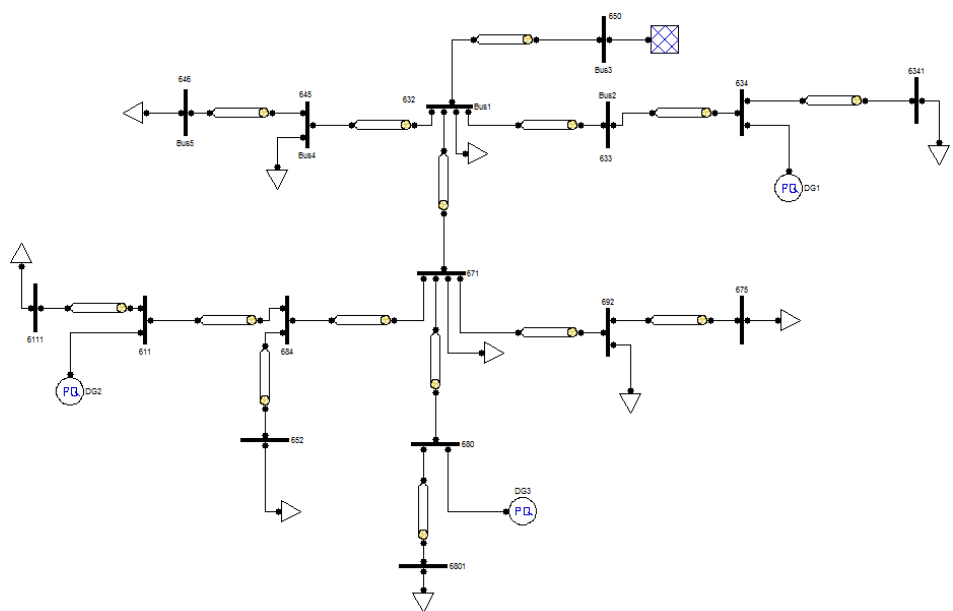
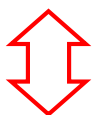
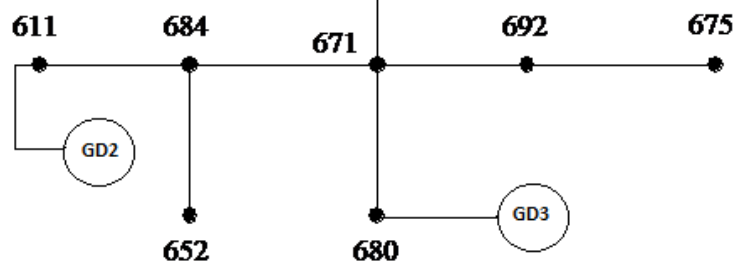
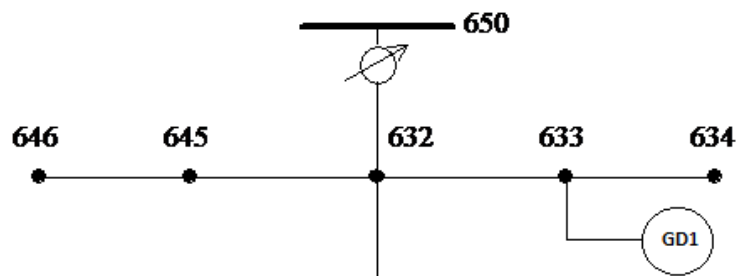


**Figure 118 - Electric network and its modelization in PSAT**

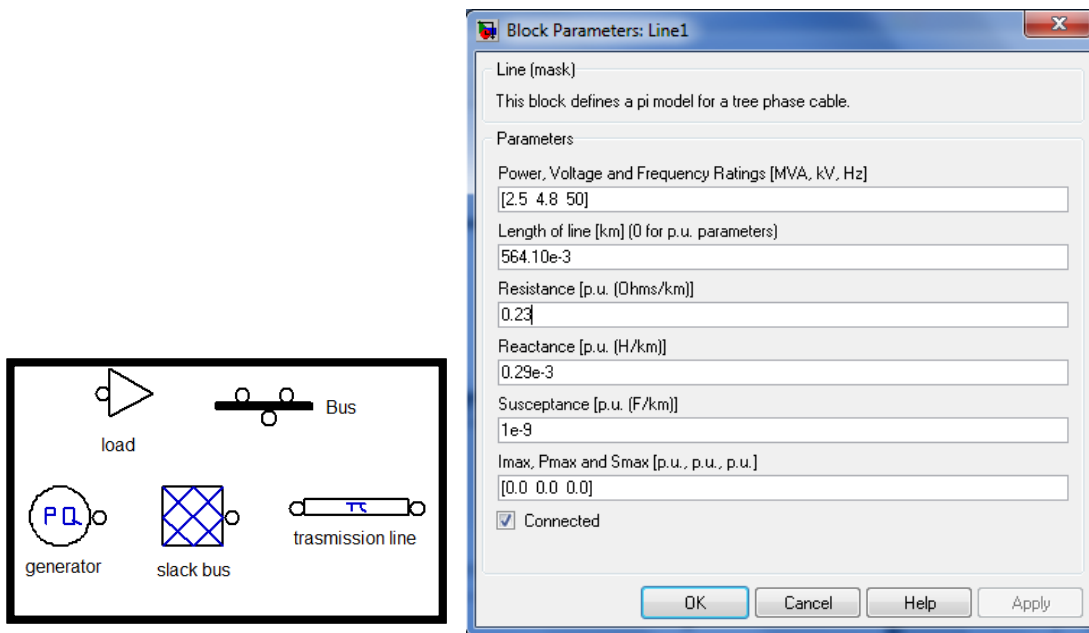


Figure 119 - Simulink blocks used and example of setting mask for conductors

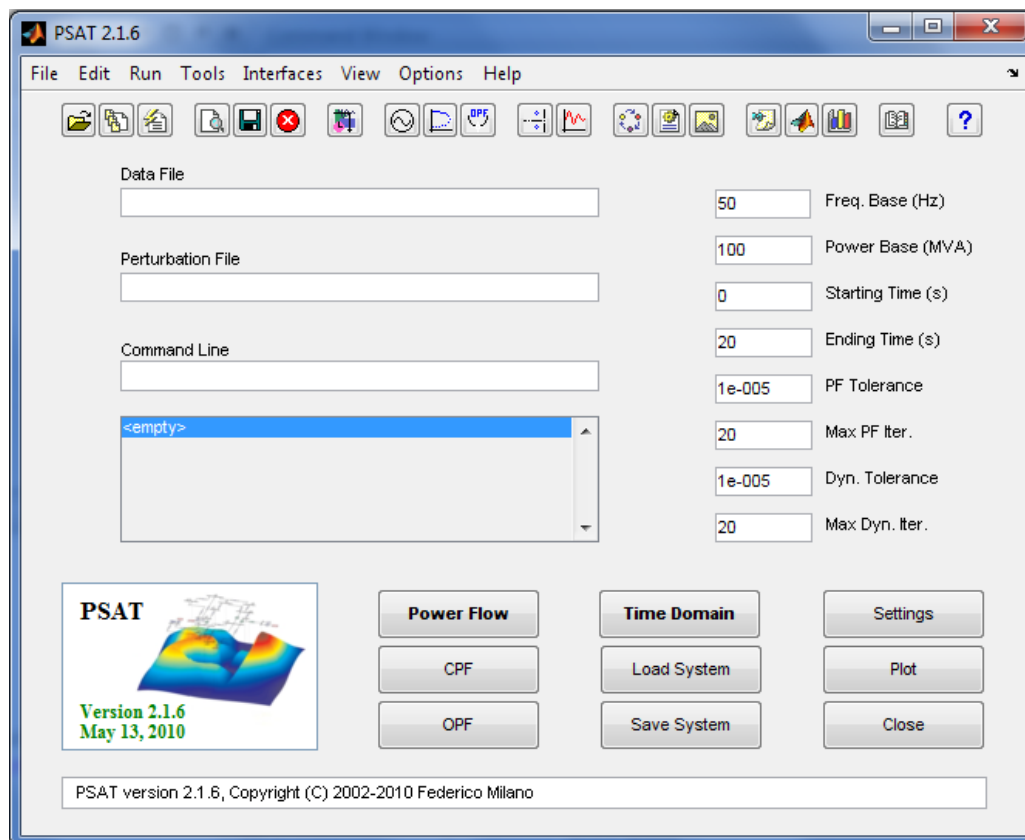


Figure 120 - Main graphical interface

After physically drawing the electrical network and assigning all the known start values, the calculations of the unknown quantities can be performed through the power flow, and later the results from a graphical interface or from the workspace of Matlab can be visualised such as:

- voltage vector (magnitude and phase) of the bus,
- admittance network matrix,
- vectors of active and reactive power of generators injected to bus [213],
- Jacobian matrix

The results can then be saved in a .m MatLab file.

The evolution over time of the electrical network parameters can be also evaluated (time domain simulation), against variations assigned through a "perturbation file": such file, with .m extension, must be written in Matlab language with a structure of the type:

```
\function Perturbation(t)
global global_variable_name1 global_variable_name2 ...
if ... % criterion
% actions
elseif ... %% criterion
% actions
else
% actions
end
```

Also in time domain simulations, one can visualize the results directly from a graphical interface Figure 121, or by exporting the results to a Matlab figures or array of values.

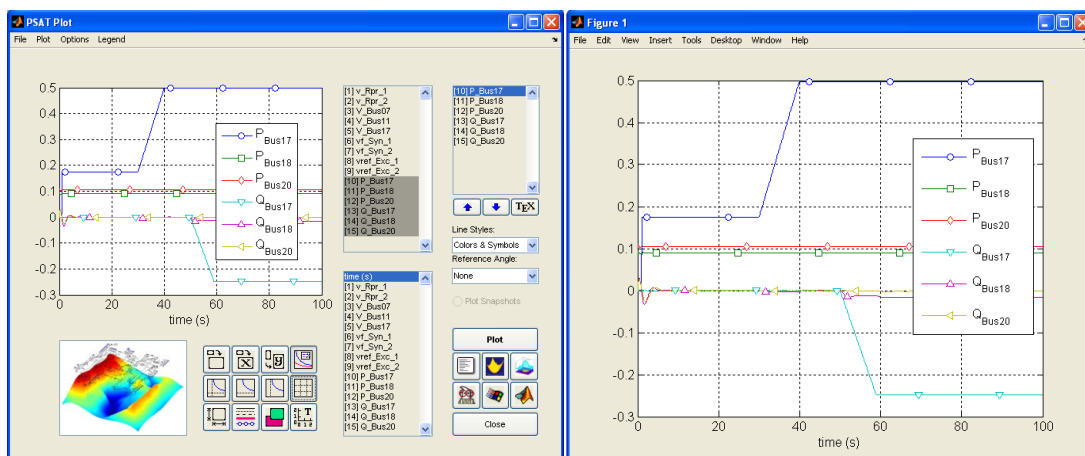


**Figure 121 - Visualization of time domain simulation results**

## A1.2 DOME

DOME is a Python-based software [88] that permits to represent and solve electrical grids through python scripts. Although using the interpreted programming language Python, the computations are very fast (being solved by external linked routines).

The tool is founded on two main principles: modularity and reusability of the code. Basically no part of the code, except for a tiny kernel, is really necessary. The code is based on four main blocks, as follows:

- Parsing the data file and initializing device models.
- Solving the power flow analysis.
- Solving other analyses, e.g., time domain simulation.
- Dumping data to adequate output files.

The user can also provide custom modules. Figure 122 sketches the structure of the software.

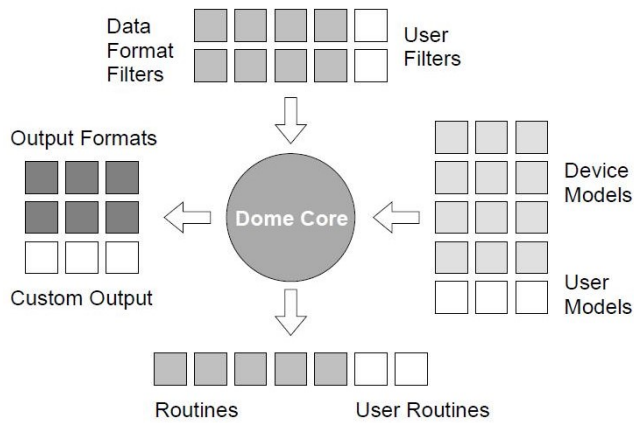


Figure 122 - Representation of the structure of Dome

Currently, DOME provides about 50 parsers for input data, including most popular power system formats such as PSS/E and GE and SIMPOW formats; about 350 devices ranging from standard power flow models, synchronous machines, AVRs and other basic controllers to a variety of wind turbines, energy storage devices and distributed energy sources; 10 analysis tools including standard power flow analysis as well as three-phase unbalanced power flow, continuation power flow, OPF, time domain simulation, electromagnetic transients, eigenvalue analysis, short circuit analysis, equivalence procedures and load admission control strategies for smart grids; and 10 output formats, including Latex, Excel, and 2D and 3D visualization tools.

Despite the vastness of the tools and models provided, DOME remains a light tool. Required modules are loaded at run-time. These are generally less than 1% of available modules. Hence, the project can grow indefinitely without affecting performance.

Modularity has also the advantage of allowing parallel development of new modules: if a beta-version of a new function is broken, all users that are not using such function can continue using DOME smoothly. Moreover, no forking is necessary as different versions of the same module can coexist.

# Bibliography

---

- [1] THE EUROPEAN PARLIAMENT AND THE COUNCIL OF THE EUROPEAN UNION, "Directive 2009/28/EC of the European Parliament and of the Council of 23 April 2009 on the promotion of the use of energy from renewable sources and amending and subsequently repealing Directives 2001/77/EC and 2003/30/EC," Official Journal of the European Union, 2009.
- [2] European Commission. Effort Sharing Decision. [Online].  
[https://ec.europa.eu/clima/policies/effort\\_en](https://ec.europa.eu/clima/policies/effort_en)
- [3] Gestore dei Servizi Energetici (GSE), "Monitoraggio statistico degli obiettivi nazionali e regionali sulle fonti rinnovabili di energia," 2016.
- [4] Gestore dei Servizi Energetici (GSE). Certificati verdi. [Online].  
<http://www.gse.it/it/Qualifiche%20e%20certificati/Certificati%20Verdi/Pages/default.aspx>
- [5] D.M. 28/07/2005: Criteri per l'incentivazione della produzione di energia elettrica mediante conversione fotovoltaica della fonte solare (alias "First feed-in scheme").
- [6] D.M. 6/2/2006: Criteri per l'incentivazione della produzione di energia elettrica mediante conversione fotovoltaica della fonte solare (alias "First feed-in scheme").
- [7] D.M. 19/02/2007: Criteri e modalita' per incentivare la produzione di energia elettrica mediante conversione fotovoltaica della fonte solare, in attuazione dell'articolo 7 del decreto legislativo 29 dicembre 2003 (alias "Second feed-in scheme").
- [8] D.M. 6/8/2010: Incentivazione della produzione di energia elettrica mediante conversione fotovoltaica della fonte solare (alias "Third feed-in scheme").
- [9] D.M. 05/05/2011: Incentivazione della produzione di energia elettrica da impianti solari fotovoltaici (alias "Fourth feed-in scheme").
- [10] D.M. 5/7/2012: Attuazione dell'art. 25 del decreto legislativo 3 marzo 2011, n. 28, recante incentivazione della produzione di energia (alias "Fifth feed-in scheme").
- [11] Gestore dei Servizi Energetici (GSE). Certificati Bianchi. [Online].  
<http://www.gse.it/it/CertificatiBianchi/Pages/default.aspx>

- [12] European Environment Agency (EEA), "Trends and projections in Europe 2015 - Tracking progress towards Europe's climate and energy targets," Publications Office of the European Union, Luxembourg, 2015.
- [13] Gilbert M. Masters, *Renewable and Efficient Electric Power Systems*. Hoboken, New Jersey: John Wiley & Sons, Inc., 2004.
- [14] International Energy Agency (IEA), "Distributed Generation in Liberalised Electricity Markets," IEA PUBLICATIONS, Paris, 26 June 2002.
- [15] Ministero dello Sviluppo Economico Italiano, "Sintesi piano di azione nazionale per le energie rinnovabili (direttiva 2009/28/ce)," 11/06/2010.
- [16] NETANIR. Introduction to Distributed Generation (DG). [Online]. <http://www.netanir.ir/VisitorPages/show.aspx?IsDetailList=true&ItemID=638,1>
- [17] M. Delfanti et al., "Smart Grid: i primi progetti pilota in Italia," in *AEIT Annual Conference - Prospettive economiche e strategiche industriali*, Milano, 2011.
- [18] Bravo Projects. Power Transmission & Distribution Solution. [Online]. <http://www.bravoprojects.co.in/transmission.php>
- [19] TERNA. [Online]. [www.terna.it](http://www.terna.it)
- [20] TERNA, "Piano di riaccensione del sistema elettrico nazionale," Annex A10 to the National Grid Code.
- [21] ENTSO-E. ENTSO-E Grid Map. [Online]. <https://www.entsoe.eu/publications/order-maps-and-publications/electronic-grid-maps/Pages/default.aspx>
- [22] G. Mauri, "L'evoluzione delle reti di distribuzione verso le Smart Grid," in *AEIT Giornata di Studio - Smart Grid: prospettive per i clienti finali e distributori*, Milano, 19/04/2012.
- [23] T. Ackermann, G. Anderson, and L. Soder, "Distributed generation: a definition," *ELSEVIER - Electric Power System Research*, vol. 57, no. 3, pp. 195-204, December 2001.
- [24] Autorità per l'energia elettrica, il gas ed il sistema idrico (AEEGSI), "Stato di utilizzo e di integrazione degli impianti di produzione alimentati dalle fonti rinnovabili e degli impianti di cogenerazione ad alto rendimento," 339/2016/I/EFR, 24/06/2016.
- [25] TERNA, "Piano di Sviluppo 2016,".

- [26] European Commission, "EU Energy in figures - Statistical Pocketbook 2016," Luxembourg, 2016.
- [27] Gestore dei Servizi Energetici (GSE), "Energia da fonti rinnovabili in Italia - Dati preliminari 2015," 10/03/2016.
- [28] Gestore dei Servizi Energetici (GSE), "Rapporto Statistico: Energia da Fonti Rinnovabili in Italia - Anno 2014," 21/12/2015.
- [29] Gestore dei Servizi Energetici (GSE), "Rapporto statistico 2011 - Impianti a Fonti Rinnovabili," 09/10/2012.
- [30] EPIA (European Photovoltaic Industry Association), "Global Market Outlook for Photovoltaics 2013-2017," 2013.
- [31] Gestore dei Servizi Energetici (GSE), "Solare Fotovoltaico - Rapporto Statistico 2015," 10/08/2016.
- [32] Gestore dei Servizi Energetici (GSE), "Solare Fotovoltaico - Rapporto Statistico 2011," 14/05/2012.
- [33] R. Campaner, M. Chiandone, V. Lugh, A. Massi Pavan, and G. Sulligoi, "Assessment of photovoltaic systems for electric power generation using EROEI (energy return on energy investment)," in *IEEE AEIT Annual Conference - From Research to Industry: The Need for a More Effective Technology Transfer (AEIT)*, Trieste, 2014, pp. 1-4.
- [34] D. Weißbach et al., "Energy intensities, EROIs (energy returned on invested), and energy payback times of electricity generating power plants," *ELSEVIER - Energy*, vol. 52, no. 1, pp. 210–221, April 2013.
- [35] F. Cucchiella and I. D'Adamo, "Estimation of the energetic and environmental impacts of a roof-mounted building-integrated photovoltaic systems," *ELSEVIER - Renewable and Sustainable Energy Reviews*, vol. 16, no. 7, pp. 5245–5259, September 2012.
- [36] U. Desideri, S. Proietti, F. Zepparelli, P. Sdringola, and S. Bini, "Life Cycle Assessment of a ground-mounted 1778 kWp photovoltaic plant," *ELSEVIER - Applied Energy*, vol. 97, pp. 930–943, September 2012.
- [37] M. Raugei, P. Fullana-i-Palmer, and V. Fthenakis, "The energy return on energy investment (EROI) of photovoltaics: Methodology and comparisons with fossil fuel life cycles," *ELSEVIER - Energy Policy*, vol. 45, pp. 576–582, June 2012.
- [38] F. Almonacid, P. Pérez-Higueras, and L. Hontoria, "Calculation of the energy provided by a PV generator. Comparative study: Conventional methods vs.

- artificial neural networks," *ELSEVIER - Energy*, vol. 36, no. 1, pp. 375–384, January 2011 2011.
- [39] G.Notton, V. Lazarov, and L. Stoyanov, "Optimal sizing of a grid-connected PV system for various PV module technologies and inclinations, inverter efficiency characteristics and locations," *ELSEVIER - Renewable Energy*, vol. 35, no. 2, pp. 541–554, February 2010.
- [40] B. Herteleer, J. Cappelle, and J. Driesen, "Quantifying Low-Light Behaviour of Photovoltaic Modules by Identifying Their Irradiance-Dependent Efficiency from Data Sheets," in *27th European Photovoltaic Solar Energy Conference and Exhibition*, Frankfurt, 23-28 September 2012, pp. 3714 - 3719.
- [41] E. Kaplani, "Design and performance considerations in stand alone PV powered Telecommunication Systems," *IEEE Latin America Transactions*, vol. 10, no. 3, pp. 1723-1729, April 2012.
- [42] A. Massi Pavan, "Progettazione dell'impianto fotovoltaico connesso in rete," in *Manuale di energia solare.: Tecniche Nuove*, 2009, p. 721.
- [43] A. Schumann, "Irradiance level characteristics of PV modules and the need for improved data quality," in *24th European Photovoltaic Solar Energy Conference*, Hamburg, Germany, 21-25 September 2009, pp. 3468 - 3470.
- [44] Angel A. Bayod-Rújula, A. Ortego-Bielsa, and A. Martínez-Gracia, "Photovoltaics on flat roofs: Energy considerations," *ELSEVIER - Energy*, vol. 36, no. 4, pp. 1996–2010, April 2011.
- [45] J. Riley Caron and Bodo Littmann, "Direct Monitoring of Energy Lost Due to Soiling on First Solar Modules in California," *IEEE Journal of Photovoltaics*, vol. 3, no. 1, pp. 336-340, June 2013.
- [46] A. Massi Pavan, A. Mellit, and D. De Pieri, "The effect of soiling on energy production for large-scale photovoltaic plants," *ELSEVIER - Solar Energy*, vol. 85, no. 5, pp. 1128–1136, May 2011.
- [47] E. Skoplaki and J.A. Palyvos, "Operating temperature of photovoltaic modules: A survey of pertinent correlations," *ELSEVIER - Renewable Energy*, vol. 34, no. 1, pp. 23–29, January 2009.
- [48] E. Skoplaki, A.G. Boudouvis, and J.A. Palyvos, "A simple correlation for the operating temperature of photovoltaic modules of arbitrary mounting," *ELSEVIER - Solar Energy Materials & Solar Cells*, vol. 92, no. 11, pp. 1393–1402, November 2008.

- [49] A. Chel and G.N. Tiwari, "A case study of a typical 2.32 kWp stand-alone photovoltaic (SAPV) in composite climate of New Delhi (India)," *ELSEVIER - Applied Energy*, vol. 88, no. 4, pp. 1415–1426, April 2011.
- [50] Angel A. Bayod-Rújula, Ana M. Lorente-Lafuente, and F. Cirez-Oto, "Environmental assessment of grid connected photovoltaic plants with 2-axis tracking versus fixed modules systems," *ELSEVIER - Energy*, vol. 36, no. 5, pp. 3148–3158, May 2011.
- [51] L. Lu and H.X. Yang, "Environmental payback time analysis of a roof-mounted building-integrated photovoltaic (BIPV) system in Hong Kong," *ELSEVIER - Applied Energy*, vol. 87, no. 12, pp. 3625–3631, December 2010.
- [52] V. Lughì and A. Massi Pavan, "Photovoltaics in Italy: Toward grid parity in the residential electricity market," in *24th International Conference on Microelectronics (ICM)*, Algiers, Algeria, 2012, pp. 1-4.
- [53] A. Massi Pavan, R. Campaner, M. Chiandone, V. Lughì, and G. Sulligoi, "Evolution of the main economic parameters for photovoltaic plants installed in Italy," in *IEEE AEIT Annual Conference - From Research to Industry: The Need for a More Effective Technology Transfer (AEIT)*, Trieste, 2014, pp. 1-5.
- [54] D.M. 16/03/2001: Programma Tetti Fotovoltaici.
- [55] V. Lughì, A. Massi Pavan, S. Quaia, and G. Sulligoi, "Economical analysis and innovative solutions for grid connected PV plants," in *International Symposium on Power Electronics, Electrical Drives, Automation and Motion*, Ischia, 2008, pp. 211-216.
- [56] Energy Strategy Group - Politecnico di Milano, "Solar Energy Report - Il sistema industriale italiano nel business dell'energia solare," April 2014.
- [57] TERNA. Dati Statistici. [Online]. <https://www.terna.it/it-it/sistemalettrico/statisticheprevisioni/datistatistici.aspx>
- [58] A. Massi Pavan, M. Chiandone, V. Lughì, and G. Sulligoi, "Despite the attainment of grid parity, the Italian PV market does not take off. An analysis," in *3rd Renewable Power Generation Conference (RPG 2014)*, Naples, 2014, pp. 1-6.
- [59] A. Massi Pavan and V. Lughì, "Grid parity in the Italian and industrial electricity market," in *International Conference on Clean Electrical Power (ICCEP)*, Alghero, 2013, pp. 332-335.
- [60] L. 27/12/2013, n. 147: Disposizioni per la formazione del bilancio annuale e pluriennale dello Stato (Legge di stabilità 2014).

- [61] Redazione Soldionline. (2013, Nov.) Andamento dei rendimenti dei Btp decennali dal 1997. [Online]. <http://www.soldionline.it/infografiche/andamento-dei-rendimenti-dei-btp-decennali-dal-1997>
- [62] Acquirente Unico (AU). [Online]. <http://www.acquirenteunico.it/>
- [63] Gestore dei Servizi Energetici (GSE). [Online]. <http://www.gse.it/>
- [64] Hanwha QCELLS. [Online]. [http://www.soltis.be/files/uploaded/documents/Hanwha\\_Q\\_CELLS\\_Data\\_sheet\\_QPRO-G3\\_250-265\\_2013-03\\_Rev02\\_EN\\_04.pdf](http://www.soltis.be/files/uploaded/documents/Hanwha_Q_CELLS_Data_sheet_QPRO-G3_250-265_2013-03_Rev02_EN_04.pdf)
- [65] Autorità per l'energia elettrica, il gas ed il sistema idrico (AEEGSI), "Ridefinizione dei prezzi minimi garantiti per impianti di produzione di energia elettrica fino a 1 MW alimentati da fonti rinnovabili," 486/2013/R/EFR, 31/10/2013.
- [66] Stefano Bracco, Federico Delfino, Fabio Pampararo, Michela Robba, and Mansueto Rossi, "Planning and Management of Sustainable Microgrids: the test-bed facilities at the University of Genoa," in *Africon*, Pointe-Aux-Piments, 2013, pp. 1-5.
- [67] Mohammad Shahidehpour and Mohammad Khodayar, "Cutting Campus Energy Costs with Hierarchical Control: The Economical and Reliable Operation of a Microgrid," *IEEE Electrification Magazine*, vol. 1, no. 1, pp. 40 - 56, September 2013.
- [68] A. Galliani, "Stato di utilizzo e di integrazione degli impianti di produzione alimentati dalle fonti rinnovabili e degli impianti di cogenerazione ad alto rendimento," 25 giugno 2015.
- [69] A. Galliani, "L'integrazione degli impianti alimentati da fonti rinnovabili non programmabili nelle reti elettriche," in *Convegno eleMeNS*, Milano, 15 maggio 2012.
- [70] J.C. Sabonnadiére, J.Y. Léost, J.P. Paul, and P. Lagonotte, "Structural analysis of the electrical system: application to Secondary Voltage Control in France," *IEEE Transactions on Power Systems*, vol. 4, no. 2, pp. 479-486, May 1989.
- [71] J. L. Sancha, J. L. Femhdez, F. Martinez, and C. Sall, "Spanish Practices in Reactive Power Management and Voltage Control," in *IEEE Colloquium on International Practices in Reactive Power Control*, London, 1993, pp. 3/1-3/4.

- [72] TERNA, "Sistema Automatico per la Regolazione di Tensione (SART) per Centrali Elettriche di Produzione," Annex A16 to the National Grid Code.
- [73] M. Chiandone, G. Sulligoi, S. Massucco, and F. Silvestro, "Hierarchical Voltage Regulation of Transmission Systems with Renewable Power Plants: an overview of the Italian case," in *3rd Renewable Power Generation Conference (RPG 2014)*, Naples, 2014, pp. 1-5.
- [74] A. Cerretti and M. Delfanti, "Smart Grid: Cosa sono e a cosa servono," *TuttoNormel*, no. 5, pp. 3-9, Maggio 2012.
- [75] Stefania Conti, "Analysis of distribution network protection issues in presence of dispersed generation," *ELSEVIER - Electric Power Systems Research*, vol. 79, no. 1, pp. 49–56, 2009 January.
- [76] A. Cerretti, G. DiLembo, R. Lama, I. Misesti, and G. Valtorta, "Ruolo del distributore, problematiche aperte, soluzioni," in *AEIT Giornata di Studio - Smart Grid: prospettive per i clienti finali e distributori*, Milano, 19/04/2012.
- [77] C.L. Masters, "Voltage rise: the big issue when connecting embedded generation to long 11 kV overhead lines," *Power Engineering Journal*, vol. 16, no. 1, pp. 5-12, 2002 Feb.
- [78] F. Polidoro, C. Bossi, C. Casale, M. Marzoli, E. Micolano, F. Paletta, O. Perego, M. Benini e P. Bresesti - CESI, "Monitoraggio degli impianti di generazione distribuita e microgenerazione," Dicembre 2006.
- [79] K. Kauhaniemi and L. Kumpulainen, "Impact of distributed generation on the protection of distribution networks," in *Eighth IEE International Conference on Developments in Power System Protection*, Amsterdam, 2004, pp. 315-318.
- [80] H. Li, S. Ge, and H. Liu, "Analysis of the Effect of Distributed Generation on Power Grid," in *Asia-Pacific Power and Energy Engineering Conference (APPEEC)*, Shanghai, 2012, pp. 1-5.
- [81] S. Wang, "Distributed generation and its effect on distribution network system," in *20th International Conference and Exhibition on Electricity Distribution - CIRED*, Prague, Czech Republic, 2009., pp. 1-4.
- [82] K. Dang, J. Yu, T. Dang, and B. Han, "Benefit of distributed generation on line loss reduction," in *International Conference on Electrical and Control Engineering (ICECE)*, Yichang, 2011, pp. 2042-2045.

- [83] P.A. Daly and J. Morrison, "Understanding the potential benefits of distributed generation on power delivery systems," in *Rural Electric Power Conference, Papers Presented at the 45th Annual Conference*, Little Rock, AR, 2001, pp. A2/1-A213.
- [84] D. Q. Hung and N. Mithulanthan, "A simple approach for distributed generation integration considering benefits for DNO," in *IEEE International Conference on Power System Technology (POWERCON)*, Auckland, 2012, pp. 1-6.
- [85] P. Chiradeja, "Benefit of Distributed Generation: A Line Loss Reduction Analysis," in *IEEE/PES Transmission & Distribution Conference & Exposition: Asia and Pacific*, Dalian, 2005, pp. 1-5.
- [86] M. Chiandone, R. Campaner, A. Massi Pavan, G. Sulligoi, P. Mania and G. Piccoli, "Impact of Distributed Generation on power losses on an actual distribution network," in *IEEE International Conference on Renewable Energy Research and Application (ICRERA)*, Milwaukee, WI, 2014, pp. 1007-1011.
- [87] Autorità per l'energia elettrica, il gas ed il sistema idrico (AEEGSI). [Online]. <http://www.autorita.energia.it>
- [88] F. Milano, "A Python-based Software Tool for Power System Analysis," in *IEEE Power & Energy Society General Meeting*, Vancouver, BC, 2013, pp. 1-5.
- [89] R. Campaner, M. Chiandone, F. Milano, and G. Sulligoi, "New rules to employ distributed generators in voltage control: assessment and numerical validation using DOME," in *IEEE International Conference on Clean Electrical Power (ICCEP)*, Alghero, 2013, pp. 128-132.
- [90] N. Acharya, P. Mahat, and N. Mithulanthan, "An analytical approach for DG allocation in primary distribution network," *ELSEVIER - International Journal of Electrical Power & Energy Systems*, vol. 28, no. 10, pp. 669–678, December 2006.
- [91] C. Wang and M.H. Nehri, "Analytical approaches for optimal placement of distributed generation sources in power systems," *IEEE Transactions on Power Systems*, vol. 19, no. 4, pp. 2068-2076, Nov. 2004.
- [92] European Electricity Grid Initiative (EEGI), "The European Electricity Grid Initiative (EEGI): a joint TSO-DSO contribution to the European Industrial Initiative (EII) on Electricity Networks," in *The Contribution of Network Operators to the European Electricity Grid Initiative*, 2009.
- [93] Nur Asyik Hidayatullah, Blagojce Stojcevski, and Akhtar Kalam, "Analysis of Distributed Generation Systems, Smart Grid Technologies and Future

- Motivators Influencing Change in the Electricity Sector," *Smart Grid and Renewable Energy*, vol. 2, no. 3, 2011.
- [94] EU Commission Task Force for Smart Grids, "Expert Group 1: Functionalities of smart grids and smart meters," December 2010.
  - [95] M. Gallanti, "Smart Grids, passaggio obbligatorio per l'integrazioni delle rinnovabili in rete," in *KeyEnergy 2011*, Pavia, 16/11/2011.
  - [96] S. J. Young, *Real Time Languages: Design and Development.*: Ellis Horwood, 1982.
  - [97] V. Cagri Gungor et al., "A Survey on Smart Grid Potential Applications and Communication Requirements," *IEEE Transactions on Industrial Informatics*, vol. 9, no. 1, pp. 28-42, Feb. 2013.
  - [98] M. Kuzlu and M. Pipattanasomporn, "Assessment of communication technologies and network requirements for different smart grid applications," in *IEEE PES Innovative Smart Grid Technologies Conference (ISGT)*, Washington, DC, 2013 IEEE PES Innovative Smart Grid Technologies Conference (ISGT), Washington, DC, 2013, pp. 1-6., pp. 1-6.
  - [99] X. Lu, Z. Lu, W. Wang, and J. Ma, "On Network Performance Evaluation toward the Smart Grid: A Case Study of DNP3 over TCP/IP," in *IEEE Global Telecommunications Conference - GLOBECOM 2011*, Houston, TX, USA, 2011, pp. 1-6.
  - [100] Rami Amiri and Omar Elkeelany, "An embedded TCP/IP hard core for Smart Grid information and communication networks," in *Proceedings of the 2012 44th Southeastern Symposium on System Theory (SSST)*, Jacksonville, FL, 2012, pp. 185-189.
  - [101] Andrea Angioni et al., "Coordinated voltage control in distribution grids with LTE based communication infrastructure," in *IEEE 15th International Conference on Environment and Electrical Engineering (EEEIC)*, Rome, 2090-2095, p. 2015.
  - [102] P. Scalera and A. De Bellis, "Reti di distribuzione intelligenti nel nuovo contesto," in *AEIT Giornata di Studio - Smart Grid: prospettive per i clienti finali e distributori*, Milano, 19/04/2012.
  - [103] F. Zanellini, "Il dispacciatore locale: strumenti e procedure per la gestione dello Smart Distibution System," in *AEIT Giornata di Studio - Smart Grid: prospettive per i clienti finali e distributori*, Milano, 14/04/2012.
  - [104] International Electrotechnical Commission (IEC), "Communication networks and systems for power utility automation," IEC 61850:2016 SER.

- [105] I. Martinez de Alegria, J. Andreua, P. Ibanez, J. Villate Luis, and H. Camblong, "Connection requirements for wind farms: A survey on technical requierements and regulation," *ELSEVIER - Renewable and Sustainable Energy Reviews*, vol. 11, no. 8, pp. 1858–1872, October 2007.
- [106] M. Tsili and S. Papathanassiou, "A review of grid code technical requirements for wind farms," *IET Renewable Power Generation*, vol. 3, no. 3, pp. 308-332, Sept. 2009.
- [107] B. Singh and S.N. Singh, "Wind Power Interconnection into the Power System: A Review of Grid Code Requirements," *ELSEVIER - The Electricity Journal*, vol. 22, no. 5, pp. 54–63, June 2009.
- [108] ENTSO-E. European Network of Transmission System Operators for Electricity (ENTSOE). [Online]. <https://www.entsoe.eu>
- [109] ACER. Agency for the Cooperation of Energy Regulators (ACER). [Online]. <http://www.acer.europa.eu>
- [110] A. Cerretti, "Evoluzione delle reti di distribuzione: nuove tecnologie e nuove regole," in *Convegno AEIT SMART GRID: Sviluppo delle reti elettriche di distribuzione, SEL*, Bolzano, 2012.
- [111] THE EUROPEAN PARLIAMENT AND THE COUNCIL OF THE EUROPEAN UNION, "Regulation (EC) No 714/2009 of the European Parliament and of the Council of 13 July 2009 on conditions for access to the network for cross-border exchanges in electricity and repealing Regulation (EC) No 1228/2003," Official Journal of the European Union, 2009.
- [112] ENTSO-E. Network Code Overview. [Online]. <https://www.entsoe.eu/major-projects/network-code-development/Pages/default.aspx>
- [113] THE EUROPEAN COMMISSION, "Commission Regulation (EU) 2015/1222 of 24 July 2015 establishing a guideline on capacity allocation and congestion management," Official Journal of the European Union, 2015.
- [114] ENTSO-E, IMPLEMENTATION GUIDELINE FOR NETWORK CODE "Requirements for Grid Connection Applicable to all Generators", 16 October 2013.
- [115] THE EUROPEAN COMMISSION, "Commission Regulation (EU) 2016/631 of 14 April 2016 establishing a network code on requirements for grid connection of generators," Official Journal of the European Union, 2016.

- [116] THE EUROPEAN COMMISSION, "Commission Regulation (EU) 2016/1388 of 17 August 2016 establishing a Network Code on Demand Connection," Official Journal of the European Union, 2016.
- [117] ENTSO-E, IMPLEMENTATION GUIDELINE FOR NETWORK CODE "Demand Connection", 16 October 2013.
- [118] THE EUROPEAN COMMISSION, "Commission Regulation (EU) 2016/1447 of 26 August 2016 establishing a network code on requirements for grid connection of high voltage direct current systems and direct current-connected power park modules," Official Journal of the European Union, 2016.
- [119] THE EUROPEAN COMMISSION, "Commission Regulation (EU) 2016/1719 of 26 September 2016 establishing a guideline on forward capacity allocation," Official Journal of the European Union, 2016.
- [120] ENTSO-E. System Operation. [Online]. <https://www.entsoe.eu/major-projects/network-code-development/system-operation/Pages/default.aspx>
- [121] ENTSO-E. Network Code on Emergency and Restoration (ER). [Online]. <https://www.entsoe.eu/major-projects/network-code-development/emergency-and-restoration/Pages/default.aspx>
- [122] ENTSO-E. Network Code on Electricity Balancing (EB). [Online]. <https://www.entsoe.eu/major-projects/network-code-development/electricity-balancing/Pages/default.aspx>
- [123] Alberto Cerretti, "Standards evolution Impact of the requirements on the operation of the distribution network," in *Enel Distribuzione Study day: Uncontrolled islanding on distribution network*, Rome.
- [124] Ralph Pfeiffer - ENTSO-E, "Brief status on CENELEC standardsrelated to Connection Network Code," in *3rd Grid Connection Stakeholder Committee meeting*, 8th September 2016.
- [125] Roland Bründlinger, "Advanced smart inverter and DER functions Requirements in latest European Grid Codes and future trends," in *Solar Canada 2015 Conference*, Toronto, Ontario, Canada, 2015.
- [126] Comitato Elettrotecnico Italiano (CEI). [Online]. <http://www.ceinorme.it/it>
- [127] Comitato Elettrotecnico Italiano (CEI), "Impianti di produzione di energia elettrica collegati a reti di I e II categoria," CEI 11-20.
- [128] Enel Distribuzione S.p.A., "Guida per le connessioni alla rete elettrica di Enel Distribuzione".

- [129] Comitato Elettrotecnico Italiano (CEI), "Regole Tecniche di Connessione (RTC) per Utenti attivi ed Utenti passivi alle reti AT ed MT delle imprese distributrici di energia elettrica," CEI 0-16 Ed.II:2008.
- [130] Comitato Elettrotecnico Italiano (CEI), "Foglio di interpretazione F1. Regola tecnica di riferimento per la connessione di Utenti attivi e passivi alle reti AT e MT delle imprese distributrici di energia elettrica," CEI 0-16 Ed.II; V2:2009-04.
- [131] Autorità per l'energia elettrica, il gas ed il sistema idrico (AEEGSI), "Interventi urgenti relativi agli impianti di produzione di energia elettrica, con particolare riferimento alla generazione distribuita, per garantire la sicurezza del sistema elettrico nazionale," 84/2012/r/eel, 08/03/2012.
- [132] Alessandro Arena, Gervasio Ciaccia, Andrea Galliani, and Maurizio Delfanti, "GD e sicurezza del sistema: le novità introdotte dalla deliberazione n. 84/2012/R/eel e dall'allegato A.70," *L'Energia Elettrica*, vol. 89, no. 2, pp. 19-32, 2012.
- [133] TERNA, "Impianti di produzione fotovoltaica requisiti minimi per la connessione e l'esercizio in parallelo con la rete AT," Annex A68 to the National Grid Code.
- [134] TERNA, "Criteri di connessione degli impianti di produzione al sistema di difesa di Terna," Annex A69 to the National Grid Code.
- [135] TERNA, "Regolazione tecnica dei requisiti di Sistema della generazione distribuita," Annex A70 to the National Grid Code.
- [136] Comitato Elettrotecnico Italiano (CEI), "Requirements for micro-generating plants to be connected in parallel with public," CEI EN 50438.
- [137] Comitato Elettrotecnico Italiano (CEI), "Regola tecnica di riferimento per la connessione di Utenti attivi e passivi alle reti BT delle imprese distributrici di energia elettrica," CEI 0-21:2016-07.
- [138] Comitato Elettrotecnico Italiano (CEI), "Regola tecnica di riferimento per la connessione di Utenti attivi e passivi alle reti AT ed MT delle imprese distributrici di energia elettrica," CEI 0-16;V2:2016-07.
- [139] TuttoNormel, "Nuove regole di connessione alla rete: per i nuovi impianti e per quelli esistenti," *TuttoNormel*, no. 4 Aprile, pp. 3-12, 2012.
- [140] TERNA, "Procedura per la riduzione della generazione distribuita in condizioni di emergenza del Sistema Elettrico Nazionale (RIGEDI)," Annex A72 to the National Grid Code.

- [141] TERNA. Code for transmission, dispatching, development and security of the grid. [Online]. <https://www.terna.it/en-gb/sistemalettrico/codicedirete.aspx>
- [142] TERNA, "Sistemi di controllo e protezione delle centrali eoliche (Prescrizioni tecniche per la connessione)," Annex A17 to the National Grid Code.
- [143] TERNA, "Modalità di utilizzo del teledistacco applicato ad impianti di produzione da fonte eolica," Annex A64 to the National Grid Code.
- [144] TERNA, "Unità periferica dei sistemi di difesa e monitoraggio specifiche funzionali e di comunicazione," Annex A52 to the National Grid Code.
- [145] Francesco Iliceto, *Impianti elettrici*. Bologna: Patron, 1984.
- [146] Vincenzo Cataliotti, *Impianti elettrici Vol.2.*: Flaccovio, 2004.
- [147] C. H. Holladay, "A graphic method for the exact solution of transmission lines," *Journal of the American Institute of Electrical Engineers*, vol. 41, no. 44, pp. 807-810, Nov. 1992.
- [148] R. Horta-Bernús and M. Rosas-Casals, "Modification of the Perrine–Baum Diagram to Improve the Calculation of High-Voltage Transmission Lines," *IEEE Transactions on Education*, vol. 56, no. 3, pp. 274-279, Aug. 2013.
- [149] V. Arcidiacono, M. Chiandone, and G. Sulligoi, "Voltage control in distribution networks using smart control devices of the distributed generators," in *International Conference on Clean Electrical Power (ICCEP)*, Ischia, 2011, pp. 738-743.
- [150] Roberto Marconato, *Electric power systems*, II ed. Milano: CEI - Italian Electrotechnical Committee, 2004.
- [151] G. Sulligoi and M. Chiandone, "Voltage Rise Mitigation in Distribution Networks using Generators Automatic Reactive Power Controls," in *IEEE Power and Energy Society General Meeting*, San Diego, CA, 22-26 July 2012, pp. 1-5.
- [152] Morris Brenna, Ettore De Bernardinis, Federica Foiadelli, Gianluca Sapienza, and Dario Zaninelli, "Voltage Control in Smart Grids: An Approach Based on Sensitivity Theory," *Journal of Electromagnetic Analysis and Applications*, vol. 2, no. 8, pp. 467-474, August 2010.
- [153] Fabio Bignucolo, "Il controllo delle reti attive di distribuzione," PhD thesis, Università degli Studi di Padova, 2009.
- [154] Ferry A. Viawan, Ambra Sannino, and Jaap Daalder, "Voltage control with on-load tap changers in medium voltage feeders in presence of distributed

generation," *Electric Power Systems Research*, vol. 77, no. 10, pp. 1314–1322, August 2007.

- [155] A. Casavola, G. Franze, D. Menniti, and N. Sorrentino, "A command governor approach to the voltage regulation problem in MV/LV networks with renewable generation units," in *International Conference on Clean Electrical Power*, Capri, 2009, pp. 304-309.
- [156] S. K. Salman and Z. G. Wan, "Voltage control of distribution network with distributed/embedded generation using fuzzy logic-based AVC relay," in *42nd International Universities Power Engineering Conference*, Brighton, 2007, pp. 576-579.
- [157] Ruey-Hsun Liang and Chen-Kuo Cheng, "Dispatch of main transformer ULTC and capacitors in a distribution system," *IEEE Transactions on Power Delivery*, vol. 16, no. 4, pp. 625-630, Oct. 2001.
- [158] F.A. Viawan and D. Karlsson, "Coordinated Voltage and Reactive Power Control in the Presence of Distributed Generation," in *Power and Energy Society General Meeting - Conversion and Delivery of Electrical Energy in the 21st Century, 2008 IEEE*, Pittsburgh, Pennsylvania (USA), 2008, pp. 1-6.
- [159] D.N. Gaonkar and G.N. Pillai, "Fuzzy logic based coordinated voltage regulation method for distribution system with multiple synchronous generators," in *IEEE PES Transmission and Distribution Conference and Exposition*, New Orleans, LA, USA, 2010, pp. 1-5.
- [160] A. G. Madureira and J. A. Pecas Lopes, "Coordinated voltage support in distribution networks with distributed generation and microgrids," *IET Renewable Power Generation*, vol. 3, no. 4, pp. 439-454, December 2009.
- [161] R. Caldon, S. Spelta, V. Prandoni, and R. Turri, "Co-ordinated Voltage Regulation in distributed Networks with Embedded Generation," in *CIRED 2005 - 18th International Conference and Exhibition on Electricity Distribution*, Turin, Italy, 2005, pp. 1-4.
- [162] M. Fila, G. A. Taylor, J. Hiscock, M. R. Irving, and P. Lang, "Flexible voltage control to support Distributed Generation in distribution networks , " in *43rd International Universities Power Engineering Conference*, Padova, 2008, pp. 1-5.
- [163] T. Sansawatt, L.F. Ochoa, and G.P. Harrison, "Integrating distributed generation using decentralised voltage regulation," in *IEEE PES General Meeting*, Minneapolis, MN, 2010, pp. 1-6.

- [164] P.M. Carvalho, P. F. Correia, and L.A.F.M. Ferreira, "Distributed Reactive Power Generation Control for Voltage Rise Mitigation in Distribution Networks," *IEEE Transactions on Power Systems*, vol. 23, no. 2, pp. 766-772, May 2008.
- [165] A. Keane, L.F. Ochoa, E. Vittal, C.J. Dent, and G.P. Harrison, "Enhanced Utilization of Voltage Control Resources With Distributed Generation," *IEEE Transactions on Power Systems*, vol. 26, no. 1, pp. 252-260, February 2011.
- [166] K. Tanaka et al., "Decentralised control of voltage in distribution systems by distributed generators," *IET Generation, Transmission & Distribution*, vol. 4, no. 11, pp. 1252-1260, November 2010.
- [167] P.N. Vovos, A.E. Kiprakis, A.R. Wallace, and G.P. Harrison, "Centralized and Distributed Voltage Control: Impact on Distributed Generation Penetration," *IEEE Trans. on Power Systems*, vol. 22, no. 1, pp. 476-483, 2007.
- [168] F. Berthold, M. Carpita, A. Monti, and F. Ponci, "A multi-agent approach to radial feeder voltage control of PEBB-based converter: A real time simulation test," in *IEEE Energy Conversion Congress and Exposition (ECCE)*, Raleigh, NC, 2012, pp. 1990-1997.
- [169] Morris Brenna et al., "Automatic Distributed Voltage Control Algorithm in Smart Grids Applications," *IEEE Transactions on Smart Grid*, vol. 4, no. 2, pp. 877-885, June 2013.
- [170] R. Caldon, F. Rossetto, and A. Scala, "Reactive power control in distribution networks with dispersed generators: a cost based method," *ELSEVIER - Electric Power Systems Research*, vol. 64, no. 3, pp. 209-217, March 2003.
- [171] Comitato Elettrotecnico Italiano (CEI), "Caratteristiche della tensione fornita dalle reti pubbliche di distribuzione dell'energia elettrica," CEI EN 50160.
- [172] B. Gao, G. K. Morison, and P. Kundur, "Voltage Stability Evaluation Using Modal Analysis," *IEEE Transactions on Power Systems*, vol. 7, no. 4, pp. 1529-1542, November 1992.
- [173] V. Arcidiacono, S. Corsi, A. Garzillo, and M. Mocenigo, "Studies on area voltage and reactive power control at ENEL," in *IEE Colloquium on International Practices in Reactive Power Control*, London (UK), 1993.
- [174] V. Arcidiacono, "Automatic Voltage and Reactive Power Control in Transmission Systems," in *CIGRE-IFAC Symposium*, Florence, 1983.

- [175] O. A. Mousavi and R. Cherkaoui, "Literature Survey on Fundamental Issues of Voltage and Reactive Power Control," in *EPF - École polytechnique fédérale de Lausanne*, Lausanne, 2011.
- [176] J.L. Sancha, J.L. Fernandez, A. Cortes, and J.T. Abarca, "Secondary voltage control: analysis, solutions and simulation results for the Spanish transmission system," *IEEE Transactions on Power Systems*, vol. 11, no. 2, pp. 630-638, May 1996.
- [177] M. Geidl, "Implementation of coordinated voltage control for the Swiss transmission system," in *Melecon 2010 - 15th IEEE Mediterranean Electrotechnical Conference*, Valletta, 2010, pp. 230-236.
- [178] J. Van Hecke, N. Janssens, J. Deuse, and F. Promel, "Coordinatedd Voltage Control Experience in Belgium," in *CIGRE*, Paris, 2000.
- [179] Verband der Netzbetreiber - VDN – e.V. beim VDEW, "TransmissionCode 2007 - Network and System Rules of the German Transmission System Operators," 2007.
- [180] H. Romanowitz, E. Muljadi, and R. Yinger, "VAR Support from Distributed Wind Energy Resources," in *World Renewable Energy Congress*, Denver, 2004.
- [181] G. Sulligoi, M. Chiandone, and V. Arcidiacono, "New SART Automatic Voltage and Reactive Power Regulator for Secondary Voltage Regulation: Design and Application," in *IEEE Power and Energy Society General Meeting*, San Diego, CA, 2011, pp. 1-7.
- [182] B. Fardanesh, "Future Trends in Power System Control," *IEEE C. A. in Power*, vol. 15, pp. 24-31, July 2002.
- [183] S. Corsi, M. Pozzi, C. Sabelli, and A. Serrani, "The coordinated automatic voltage control of the Italian transmission Grid-part I: reasons of the choice and overview of the consolidated hierarchical system," *IEEE Transactions on Power Systems*, vol. 19, no. 4, pp. 1723-1732, Nov. 2004.
- [184] S. Corsi, M. Pozzi, M. Sforza, and G. Dell'Olio, "The coordinated automatic voltage control of the Italian transmission Grid-part II: control apparatuses and field performance of the consolidated hierarchical system," *IEEE Transactions on Power Systems*, vol. 19, no. 4, pp. 1733-1741, Nov. 2004.
- [185] Sandro Corsi, "The Secondary Voltage Regulation in Italy," in *Power Engineering Society Summer Meeting*, Seattle, WA, USA, 2000, pp. 296-304.
- [186] TERNA, "Partecipazione alla regolazione di tensione," Annex A14 to the National Grid Code.

- [187] J. Arrinda, J. A. Barrena, M. A. Rodríguez, and A. Guerrero, "Analysis of massive integration of renewable power plants under new regulatory frameworks," in *International Conference on Renewable Energy Research and Application (ICRERA)*, Milwaukee, WI, 2014, pp. 462-467.
- [188] R. K. Varma and M. Salama, "Large-scale photovoltaic solar power integration in transmission and distribution networks," in *IEEE Power and Energy Society General Meeting*, Detroit, MI, USA, 2011, pp. 1-4.
- [189] F. Delfino, R. Procopio, M. Rossi, and G. Ronda, "Integration of large-size photovoltaic systems into the distribution grids: a P–Q chart approach to assess reactive support capability," *IET Renewable Power Generation*, vol. 4, no. 4, pp. 329-340, July 2010.
- [190] H. K. Tyll and F. Schettle, "Historical overview on dynamic reactive power compensation solutions from the begin of AC power transmission towards present applications," in *IEEE/PES Power Systems Conference and Exposition*, Seattle, WA, 2009, pp. 1-7.
- [191] H. S. Ko, S. Bruey, J. Jatskevich, G. Dumont, and A. Moshref, "A PI Control of DFIG-Based Wind Farm for Voltage Regulation at Remote Location," in *IEEE Power Engineering Society General Meeting*, Tampa, FL, 2007, pp. 1-6.
- [192] F. Baalbergen, M. Gibescu, and L. Van Der Sluis, "Voltage stability consequences of decentralized generation and possibilities for intelligent control," in *IEEE PES Innovative Smart Grid Technologies Conference Europe (ISGT Europe)*, Gothenburg, 2010, pp. 1-8.
- [193] T. H. M. El-Fouly, E. F. El-Saadany, and M. M. A. Salama, "Voltage Regulation of Wind Farms Equipped with Variable-Speed Doubly-Fed Induction Generators Wind Turbines," in *IEEE Power Engineering Society General Meeting*, Tampa, FL, 2007, pp. 1-8.
- [194] R. A. Mastromauro, N. A. Orlando, D. Ricchiuto, M. Liserre, and A. Dell'Aquila, "Hierarchical Control of a Small Wind Turbine System for Active Integration in LV Distribution Network," in *International Conference on Clean Electrical Power (ICCEP)*, Alghero, 2013, pp. 426-433.
- [195] D. Unger, L. Spitalny, and J. M. A. Myrzik, "Voltage control by small hydro power plants integrated into a virtual power plant," in *IEEE Energytech*, Cleveland, OH, 2012, pp. 1-6.
- [196] K. Dielmann and A. Van der Velden, "Virtual power plants (VPP) - a new perspective for energy generation," in *Proceedings of the 9th International Scientific*

*and Practical Conference of Students, Post-graduates Modern Techniques and Technologies (MTT 2003)*, 2003, pp. 18-20.

- [197] D. Pudjianto, C. Ramsay, and G. Strbac, "Virtual power plant and system integration of distributed energy resources," *IET Renewable Power Generation*, vol. 1, no. 1, pp. 10-16, March 2007.
- [198] Ricerca Sistema Energetico (RSE), "Definizione dei concetti e delle architetture di gestione, controllo e comunicazione di microreti e Virtual Power Plant," RSE 06007061, 2006.
- [199] V. Arcidiacono, R. Menis, and G. Sulligoi, "Improving Power Quality in All Electric Ships Using a Voltage and VAR Integrated Regulator," in *IEEE Electric Ship Technologies Symposium*, Arlington, VA, 2007, pp. 322-327.
- [200] B. Tamimi, C. Cañizares, and K. Bhattacharya, "Modeling and performance analysis of large solar photo-voltaic generation on voltage stability and inter-area oscillations," in *IEEE Power and Energy Society General Meeting*, San Diego, CA, 2011, pp. 1-6.
- [201] J. C. Vasquez, R. A. Mastromauro, J. M. Guerrero, and M. Liserre, "Voltage Support Provided by a Droop-Controlled Multifunctional Inverter," *IEEE Transactions on Industrial Electronics*, vol. 56, no. 11, pp. 4510-4519, Nov. 2009.
- [202] A. Cagnano, E. De Tuglie, M. Liserre, and R. A. Mastromauro, "Online Optimal Reactive Power Control Strategy of PV Inverters," *IEEE Transactions on Industrial Electronics*, vol. 58, no. 10, pp. 4549-4558, Oct. 2011.
- [203] R. Campaner, M. Chiandone, V. Arcidiacono, G. Sulligoi, and F. Milano, "Automatic Voltage Control of a Cluster of Hydro Power Plants to Operate as a Virtual Power Plant," in *IEEE 15th International Conference on Environment and Electrical Engineering (EEEIC)*, Rome, 2015, pp. 2153-2158.
- [204] M. Chiandone, R. Campaner, V. Arcidiacono, G. Sulligoi, and F. Milano, "Automatic Voltage and Reactive Power Regulator for Wind Farms participating to TSO Voltage Regulation," in *IEEE Eindhoven PowerTech*, Eindhoven, 2015, pp. 1-5.
- [205] M. Chiandone, R. Campaner; A. Massi Pavan, V. Arcidiacono; F. Milano and G. Sulligoi, "Coordinated Voltage Control of Multi-Converter power plants operating in Transmission System. The case of Photovoltaics," in *IEEE International Conference on Clean Electrical Power (ICCEP)*, Taormina, 2015, pp. 506-510.

- [206] R. Campaner, M. Chiandone, G. Sulligoi, and F. Milano, "Automatic voltage and reactive power control in distribution systems: Dynamic coupling analysis," in *IEEE International Conference on Renewable Energy Research and Applications (ICRERA)*, Birmingham, United Kingdom, 2016, pp. 934-939.
- [207] IEEE - Institute of Electrical and Electronics Engineers. Distribution System Analysis Subcommittee Report: Radial Distribution Test Feeders. [Online]. <http://ewh.ieee.org/soc/pes/dsacom/testfeeders/index.html>
- [208] W. H. Kersting, "Radial Distribution Test Feeders," *IEEE Transactions on Power Systems*, vol. 6, no. 3, pp. 975 - 985, Aug. 1991.
- [209] M. Shahidehpour and Y. Wang, *Communication and Control in Electric Power Systems: Applications of Parallel and Distributed Processing*, I ed. Hoboken, New Jersey: John Wiley & Sons, IEEE Press, 2003.
- [210] B. Tamimi, C. Canizares, and K. Bhattacharya, "System Stability Impact of Large-Scale and Distributed Solar Photovoltaic Generation: The Case of Ontario, Canada," *IEEE Transactions on Sustainable Energy*, vol. 4, no. 3, pp. 680-688, July 2013.
- [211] F. Fernandez-Bernal, L. Rouco, P. Centeno, M. Gonzalez, and M. Alonso, "Modelling of photovoltaic plants for power system dynamic studies," in *Fifth International Conference on Power System Management and Control Conference*, London, UK, 2002, pp. 341-346.
- [212] R. Campaner, M. Chiandone, G. Sulligoi, P. Mania, and F. Milano, "Application of new voltage control rules in distribution networks," in *IEEE International Conference on Renewable Energy Research and Applications (ICRERA)*, Madrid, 2013, pp. 1206-1211.
- [213] F. Milano, *Power System Analysis Toolbox: Documentation for PSAT version 2.1.6.*, May 13, 2010.
- [214] F. Milano, "An Open Source Power System Analysis Toolbox," *IEEE Transactions on Power Systems*, vol. 3, no. 20, pp. 1199-1206, Aug. 2005.
- [215] Christian Tam, "Aspetti di gestione e controllo di una microgrid in ambito alpino," Graduate Thesis, Università degli Studi di Trieste, 2016.
- [216] Fotovoltaico Nord Italia. [Online]. [www.fotovoltaiconorditalia.it](http://www.fotovoltaiconorditalia.it)
- [217] Marco Dalle Feste, "Analisi delle architetture di regolazione della tensione di grandi impianti fotovoltaici per la produzione dell'energia elettrica," Graduate Thesis, Università degli Studi di Trieste, 2016.

- [218] Federico Milano, Luigi Vanfretti, and Carlos Morataya-Juan, "An Open Source Power System Virtual Laboratory: The PSAT," *IEEE Transactions on Education*, vol. 51, no. 1, pp. 17 - 23 , Feb. 2008.
- [219] F. Milano, *Power system modelling and scripting*, I ed.: Springer-Verlag Berlin Heidelberg, 2010.

